AD_____

Award Number: DAMD17-98-1-8614

TITLE: Mechanisms Involved in Virus-Induced Neural Cell Death

PRINCIPAL INVESTIGATOR: Kenneth L. Tyler, M.D.

CONTRACTING ORGANIZATION: University of Colorado
Health Sciences Center
Denver, Colorado 802626

REPORT DATE: September 2001

TYPE OF REPORT: Annual

PREPARED FOR: U.S. Army Medical Research and Materiel Command
Fort Detrick, Maryland 21702-5012

REPORT DOCUMENTATION PAGE

Form Approved
OMB No. 074-0188

1. AGENCY USE ONLY (Leave blank)	2. REPORT DATE	3. REPORT TYPE AND DATES COVERED
	September 2001	Annual (15 Aug 00 - 14 Aug 01)

4. TITLE AND SUBTITLE
Mechanisms Involved in Virus-Induced Neural Cell Death

5. FUNDING NUMBERS
DAMD17-98-1-8614

6. AUTHOR(S)
Kenneth L. Tyler, M.D.

7. PERFORMING ORGANIZATION NAME(S) AND ADDRESS(ES)
University of Colorado Health Sciences Center
Denver, Colorado 80262

E-Mail: Ken.Tyler@uchsc.edu

8. PERFORMING ORGANIZATION REPORT NUMBER

9. SPONSORING / MONITORING AGENCY NAME(S) AND ADDRESS(ES)
U.S. Army Medical Research and Materiel Command
Fort Detrick, Maryland 21702-5012

10. SPONSORING / MONITORING AGENCY REPORT NUMBER

11. SUPPLEMENTARY NOTES
Report contains color

12a. DISTRIBUTION / AVAILABILITY STATEMENT
Approved for Public Release; Distribution Unlimited

12b. DISTRIBUTION CODE

13. Abstract *(Maximum 200 Words) (abstract should contain no proprietary or confidential information)*

We are using experimental infection with reoviruses as a model to study how viruses induce cell death (apoptosis) and cause dysregulation of the cell cycle, and the significance of these events on viral pathogenesis in vivo. We have developed this into one of the most fully characterized systems for understanding viral and cellular mechanisms of both apoptosis and cell cycle dysregulation. We have shown that apoptosis is a critical part of tissue injury in vivo in both experimental models of virus-induced CNS injury (encephalitis) and cardiac injury (myocarditis). Our in vitro studies indicate that reovirus-induced apoptosis involves the tumor necrosis factor receptor (TNFR) superfamily and specifically death receptors 4 and 5 (DR4, DR5) and their ligand (TRAIL). Apoptosis involves both death-receptor (DR) and mitochondrial-associated cell death pathways, and leads to the early activation of initiator caspases 8 and 9, followed by activation of effector caspase 3 and cleavage of caspase-dependent cellular substrates. Caspase-8 dependent cleavage of the pro-apoptotic Bcl-2 family protein Bid is required for cytosolic release of cytochrome *c* and the subsequent apoptosome-mediated activation of caspase 9. Reovirus-induced DR-initiated apoptosis requires participation of the mitochondrial signaling pathways for its optimal expression. In addition to inducing apoptosis, infection results in dysregulation of the normal cell cycle. This results from a G2/M phase arrest which requires the viral σ1s protein and is associated with inhibition of the activity of the key G2 to M checkpoint transition kinase p34cdc2.

14. Subject Terms (keywords previously assigned to proposal abstract or terms which apply to this award)
Apoptosis, caspases, cell cycle, reoviruses, calpain, neurons, NF-KB, C-JUN.

15. NUMBER OF PAGES
200

16. PRICE CODE

17. SECURITY CLASSIFICATION OF REPORT	18. SECURITY CLASSIFICATION OF THIS PAGE	19. SECURITY CLASSIFICATION OF ABSTRACT	20. LIMITATION OF ABSTRACT
Unclassified	Unclassified	Unclassified	Unlimited

TABLE OF CONTENTS

INTRODUCTION (Subject, Purpose, Scope of the Research):

The clinical manifestations of viral injury result from the capacity of viruses to damage or kill cells in different organs. Two distinct patterns of cell death, necrosis and apoptosis, have been recognized and can be distinguished based on a variety of morphological criteria. Apoptotic cell death is characterized by diminution in cell size, membrane blebbing, and compaction, margination and fragmentation of nuclear DNA. DNA fragmentation occurs predominantly at internucleosomal regions resulting in the generation of pathognomonic DNA 'ladders' when DNA from apoptotic cells is subjected to agarose gel electrophoresis. The subject and purpose of this research project is to study the cellular mechanisms by which viruses induce apoptotic cell death.

This is the third annual progress report on this research project. Six papers have been published or accepted for publication during the current reporting period, and three additional papers are currently under review. (see Reportable Outcomes). In accordance with the format requirements for preparing this progress report, we have included reprints of all published papers and copies of all accepted papers in an appendix. The technical reporting requirements for this grant specify that journal publications can be substituted for detailed descriptions of specific aspects of the research. However, to facilitate review of this report, we have also briefly summarized the key points in these papers in the text (see Research Accomplishments) with detailed references to particular figures in individual papers. Accomplishments are reviewed below and keyed to the specific aims as outlined in the original research application.

RESEARCH ACCOMPLISHMENTS

(Keyed to individual specific aims in the original Statement of Work)

Specific Aim 1: Is apoptosis a general feature of human viral encephalitis?

As previously noted we have identified and collected a substantial number of brain tissue specimens from autopsy and surgical pathology cases of patients with identified forms of viral encephalitis from the Pathology Department of the of the University of Colorado Health Sciences Center and its affiliated medical institutions. As suggested by previous reviewers we have elected to initially focus on the subset of cases involving immunocompetent individuals. We have also decided to initially focus on those cases with herpesvirus infections, particularly those due to herpes simplex virus (HSV, ten cases), and cytomegalovirus (CMV, three cases of congenital CMV in immunocompetent individuals).

We have tested a variety of staining techniques on this material in order to facilitate identification of apoptotic cells. Based on our experience with infected mouse brain tissue (Oberhaus et al., J Virol 71:2100-06, 1997), we initially utilized TUNEL staining to search for apoptosis in human brain material. Our initial experience with this technique was disappointing. Although TUNEL positive areas were identified in infected brain sections, it was difficult to characterize the nature of the infected cells, and the nature of the positive staining was such that we felt it was critical to develop an independent method to support the presence of apoptotic injury. We have therefore performed additional studies using reovirus-infected mouse brain tissue to identify promising techniques that could be used to supplement results obtained with TUNEL staining. We have achieved excellent results in mouse brain tissue using monoclonal antibodies specific for the activated form of caspase-3 (Appendix, Figure 1), and antibodies specific for the caspase-3 specific cleavage product of PARP (poly-ADP-ribose polymerase). Caspase 3 is an effector caspase that is activated in

virtually all known forms of neuronal apoptosis. PARP is a well characterized cellular substrate for caspase-3 and other effector caspases, and its cleavage into specific fragments is a reliable indicator of effector caspase activation. We have had excellent results staining human brain material for the presence of activated caspase 3. An example of positive caspase 3 staining, indicative of apoptosis, is shown in a brain tissue specimen from a child with congenital CMV infection (note also the characteristic CMV-infected multinucleated cells)(Appendix, Figure 1). We believe this is the first clear demonstration that CMV encephalitis is associated with apoptotic cell death. We are currently screening all our non-HIV associated CMV cases, confirming the results obtained with caspase 3 staining with TUNEL and co-staining for viral antigen, and with cell specific markers (e.g. lymphocyte markers for infiltrating cells). Similar studies are underway in the HSV brain material. We are extremely encouraged by these recent results, and anticipate submitting a paper describing apoptosis in human non-HIV encephalitis during the next reporting period. As part of our analysis of the cases with herpesvirus infections we have published a paper, supported by this grant, reviewing the use of polymerase chain reaction techniques in the diagnosis of herpesvirus infections of the CNS (Kleinschmidt-DeMasters et al. Brain Pathology 11:452-64, 2001).

Specific Aim 2: Is the ceramide-sphingomyelin pathway involved in reovirus-induced apoptosis? We have made substantial progress in accomplishing the goals of this specific aim, and, as outlined in earlier annual reports, have expanded this aim to identify cellular pathways involved in reovirus-induced apoptosis. During the current reporting period three papers have been published or accepted by the **Journal of Virology** (the leading journal in the field), and an additional paper by **Oncogene**. An additional paper is currently under revision at the **Journal of** Virology. Two additional papers are currently under review by the **Journal of Virology** and by the **Journal of Neuroscience**. (Copies of all published and in press papers referred to below are included in the appendix). Unless otherwise noted, figures referred to in the text are from these papers. We have previously shown, in work supported by this grant, that reovirus infection of HeLa cells is associated with a dramatic increase in NF-κB activity, and that inhibition of this activity inhibits apoptosis (see Connolly et al., J Virol 74:2981-89, 2000). We have now extended this observation by showing that reovirus infection is also associated with activation of the transcription factor c-Jun and identifying viral factors and cellular pathways involved in this process (Clarke et al. J Virol in press, 2001).

c-Jun activation results from its phosphorylation by specific kinases. Activated c-Jun can homo- or hetero-dimerize with related proteins to form the Ap-1 transcription factor complex. Activated c-Jun/Ap-1 is translocated to the nucleus where it activates the transcription of specific sets of cellular genes with AP-1 specific promoters. We have shown that reovirus infection is associated with selective activation of specific mitogen activated protein kinases (MAPKs) (Clarke et al. J Virol, in press, 2001). Reovirus infection activates c-Jun amino-terminal kinase (JNK) (also known as stress activated protein kinase, SAPK) and extracellular response kinase (ERK) (Clarke et al J Virol, 2001: Fig. 1, Fig. 5), but does not activate p38 MAPK or Akt kinase (*ibid*, Fig.5). Activation of JNK occurs as early as 10-12 hrs post-infection (*ibid*, Fig. 1, Fig. 2). Specific patterns of MAPK activation have been associated with apoptosis, with JNK activation often being associated with pro-apoptotic phenomena. We have shown that there is a strong correlation between the capacity of the

prototypic reovirus strains T1L, T3D, and T3A to activate JNK and to induce apoptosis (*ibid*, Figure 3). Because of differences in the capacity of reovirus strains to activate JNK we have been able to use reassortant viruses containing different combinations of genes derived from T1L (a poor JNK inducer) and T3D (a potent JNK inducer) to identify viral genes that played a key role in this process. Using a panel of T1L x T3D reassortant viruses we have shown that two reovirus genes (S1, M2) were associated with differences in the capacity of reovirus reassortants to activate JNK (*ibid*, Table 1). Unfortunately the nature of the reassortant pool tested did not permit us to initially distinguish the relative contributions of these two gene segments.

One of the principal substrates for JNK is the transcription factor c-Jun. Consistent with our finding that reovirus infection can activate JNK, we have also shown that reovirus infection is associated with significant increases in the amount of phosphorylated (active) c-Jun in infected cells (*ibid*, Figure 2). We now have preliminary data that differences in the capacity of reovirus strains to induce c-Jun phosphorylation is determined by the viral S1 gene. The reassortant pool used for these experiments enabled us to identify just the S1 gene, rather than the S1 and M2 genes, as the key determinant in strain-specific differences in c-Jun activation.

The S1 gene is bicistronic and encodes both the virion structural protein σ1 and a small non-structural protein, σ1s. We have shown, in work supported by this grant (see Specific Aim 3) that the S1-encoded σ1s protein plays a critical role in virus-induced perturbation of cell cycle regulation. We have measured c-Jun activity in cells stably transfected with σ1s under the control of a cadmium inducible promoter. Preliminary studies suggest that there is substantially more c-Jun activation in cells expressing σ1s as compared to control cells (cadmium treated cells stably transfected with a plasmid that lacks σ1s). Supporting these results, we have also recently found that a reovirus σ1s null mutant (T3C84-MA, gift of Dr. T. Dermody, Vanderbilt University) induces substantially less c-Jun activation than its wild-type (σ1s-positive) parent (T3C84). **These results indicate that reovirus infection is associated with selective activation of the JNK MAPK cascade and its associated transcription factor c-Jun. Activation of both c-Jun and JNK correlates with the capacity of viruses to induce apoptosis, and is determined by the viral S1 gene (a gene we have previously shown is a key determinant of both apoptosis and cell cycle perturbation).**

Our work, supported by this grant, indicates that reovirus infection is associated with activation of transcription factors including NF-κB and c-Jun. We have shown that inhibition of NF-κB activation inhibits reovirus-induced apoptosis (see Connolly et al. J Virol 74:2981-9, 2000). We have also shown that there is a strong correlation between the capacity of reoviruses to activate JNK and c-Jun and their capacity to induce apoptosis (Clarke et al. J Virol, in press 2001). These studies form the basis for our studies, supported by a supplement to this grant, of the pattern of reovirus-induced gene expression in target cells (Poggioli G et al. J Virol, under revision, 2001).

We have used large-scale oligonucleotide microarray technology to examine the pattern of gene expression in cells infected with apoptosis-inducing (T3A) and non-inducing (T1L) strains of reovirus. For our initial studies we elected to look at infection of HEK293 cells, a human embryonic kidney epithelial line. These cells were selected because of our extensive previous work in this line identifying apoptotic signaling pathways (see below).

Total cellular RNA was extracted from duplicate sets of infected (T1L, T3A) and mock-infected cells at 6, 12, and 24 hrs post-infection. Total RNA was reversed transcribed into cDNA then in vitro transcribed and biotin labeled to yield biotin-labeled cRNAs. These cRNAs were fragmented (60-300 base-pair size) and hybridized to Affymetrix Hu95A Genechips. These chips contain oligonucleotides probe sets corresponding to ~12,000 human genes (the largest chip currently available). Binding of cRNAs was detected following streptavidin-phycoerythrin staining. Chips were analyzed according to standard protocols (see Poggioli et al. J Virol, under revision, 2001 for additional details).

We utilized stringent criteria for analysis of virus-induced changes in gene expression. In order to consider a gene up-regulated we required that levels of expression of the target gene in each of the independent duplicate sets of infected cells differed by $\geq$2-fold as compared to expression in independent duplicate sets of mock-infected cells (4-way analysis). Using these criteria we found that 18 of the 12,000 genes analyzed were up-regulated and none down-regulated in T3D infected cells at 6 hrs. By 12 hrs the numbers had increased to 29 up-regulated and 57 down-regulated genes, and by 24 hrs there were 215 up-regulated and 94 down-regulated genes. The majority of the genes involved encode proteins involved in signal transduction, transcription, apoptosis and DNA damage and repair, and cell cycle regulation. An initial manuscript describing reovirus-induced transcriptional alteration of genes related to cell cycle is under revision (Poggioli et al. J Virol, under revision, 2001) (see Aim 3 research results).

Pilot studies of genes expression using multiprobe ribonuclease protection assays suggested that cell surface death receptors belonging to the TNF receptor superfamily, and specifically death receptors 4 & 5 (DR4, DR5) and their apoptosis-inducing ligand (TRAIL) might play an important role in reovirus-induced apoptosis. We have now confirmed these results (Clarke et al. J Virol 74:8135-9, 2000). Antibodies against TRAIL, but not against other TNF family death ligands (FasL, TNF) inhibited reovirus induced apoptosis in both HEK293 cells and mouse L929 fibroblasts (Clarke et al. J Virol 74:8135-9, 2000: Fig. 1). In order to confirm these results, cells were also pre-treated with soluble forms of the DR4 and DR5 receptor. These soluble receptors bind TRAIL, and inhibit its binding to functional cell-surface receptors. Pre-treatment of cells with soluble DR4 and DR5 receptors, but not with soluble TNF-receptor, inhibited reovirus apoptosis in a dose-dependent manner (Clarke et al., J Virol 74:8135-9, 2000: Fig.1).

There has recently been intense interest in the potential utility of TRAIL as a cancer chemotherapeutic agent. We have recently shown, in work supported by this grant, that reovirus infection induces apoptosis in a variety of cancer cell lines including those derived from lung, breast, and cervical cancers (Clarke et al., Oncogene, in press, 2001). In addition, reovirus infection can sensitize cells to killing by TRAIL, and can make previously resistant cells susceptible to TRAIL-induced apoptosis (Clarke et al. Oncogene, in press, 2001). The mechanism of reovirus-induced sensitization of cancer cells to killing involves the capacity of TRAIL and reovirus to induce synergistic activation of the key initiator protease, caspase 8, and can can be inhibited by cell permeable peptide inhibitors of caspase 8 (Clarke et al., Oncogene, in press 2001).

Our previous in vivo studies (Oberhaus et al., J Virol 71:2100-06, 1997) demonstrated that in addition to the capacity to induce apoptosis in a variety of cultured cells in vitro, that reovirus infection also induced apoptosis in vivo in the mouse CNS. In an effort to better understand whether the cellular pathways involved in neuronal apoptosis differed

from those in epithelial and cancer cells, we have examined the capacity of reoviruses to induce apoptosis in both neuroblastomas and primary mouse cortical neuronal cultures (Richardson-Burns et al., J Neuroscience, submitted, 2001). We have shown that reovirus does induce apoptosis in neuronal cultures (primary and continuous) as determined by a variety of techniques including nuclear morphology using dye staining assays, TUNEL staining, annexin staining, and the presence of oligonucleosomal DNA ladders. Infection is associated with activation of caspase 3, and can be inhibited by cell permeable pancaspase and caspase-3 specific peptide inhibitors. Studies are currently underway to determine whether neuronal apoptosis involves the DR4/DR5/TRAIL system, and whether the caspase activation pathways are similar to those encountered in epithelial and cancer cells.

Interaction of specific apoptosis-inducing ligands with their cognate death receptor results in oligomerization of receptors. This allows cytoplasmic death domains (DDs) of these receptors to interact. Apposition of these DDs is followed by their interaction with adapter proteins (exemplified by TNF Receptor associated death domain protein, TRADD and Fas associated death domain protein, FADD). These proteins contain death effector domain (DED) sequences that interact with initiator caspases (e.g. caspase-8). Initiator caspases in turn interact with other caspases in an ordered cascade that leads ultimately to the activation of effector caspases (e.g. caspase 3) and apoptosis. Additional proteases, including the calcium-activated neutral protease, calpain, are also involved in this process.

We have now completed a detailed characterization of the caspase cascades activated following reovirus infection. Reovirus-induced apoptosis requires a FADD-like adapter protein, and is inhibited by over-expression of a dominant-negative form of FADD (Clarke et al., J Virol 74:8135-9, 2000: Fig. 5). Caspase 8 is activated as an early event following reovirus infection (Kominsky et al., J Virol, submitted, 2001), and this activation is inhibited in cells stably expressing DN-FADD. Caspase 8 activation is followed by cleavage of Bid (Kominsky et al., J Virol, submitted, 2001: Fig 4), a pro-apoptotic member of the Bcl-2 family of proteins. Cleaved Bid translocates to the mitochondrion where it interacts with other Bcl-2 family members including Bak and Bax to facilitate release of cytochrome *c* into the cytoplasm, where it forms part of the apoptosome that activates caspase 9. We have shown that reovirus infection is associated with cytosolic release of cytochrome *c* as early as 6 hrs post-infection, and subsequently with activation of caspase 9 (Kominsky et al., J Virol, submitted, 2001: Fig. 2 & 3). Activation of the death-receptor associated effector caspase (caspase 8) and the mitochondrial effector caspase (caspase 9) is associated with subsequent activation of caspase 3 and the cleavage of caspase-3 related cellular substrates including poly-ADP ribosyl polymerase (PARP) (Kominsky et al., J Virol, submitted, 2001: Fig 5). As would be predicted from these results, we have also shown that cell permeable peptide inhibitors specific for caspases including caspases 3, 8 and 9, but not for other caspases (e.g. caspase 1) inhibit reovirus-induced apoptosis (Kominsky et al., J Virol, submitted, 2001: Fig. 9).

We have previously shown that over-expression of the anti-apoptotic protein Bcl-2 in MDCK cells inhibits reovirus-induced apoptosis (Rodgers et al. J Virol 71:2540-46, 1997). We have now shown that stable over-expression of Bcl-2 inhibits both cytosolic release of cytochrome *c* and activation of caspase 9. Inhibition of caspase 8 activation by stable over-expression of FADD-DN prevents Bid cleavage and subsequent mitochondrial cytochrome *c* release (Kominsky et al., J Virol, submitted, 2001: Fig. 7). Taken together these results

indicate that reovirus-induced apoptosis is initiated by death-receptor activation and that this process is augmented and amplified by mitochondrial factors.

In previously published work, supported by this grant, we have shown that calpain is activated following reovirus infection and that inhibition of this activation with either active site or calcium-binding site inhibitors of calpain will inhibit reovirus apoptosis in vitro (DeBiasi et al. J Virol 73:695-701, 1999). We have extended these studies by testing calpain inhibitors for their capacity to inhibit reovirus-induced apoptosis in a murine model (DeBiasi et al., J Virol 75:351-61, 2001). We have shown that myocarditis induced in mice following intramuscular injection of reovirus strain 8B is due to apoptosis. Hearts from reovirus-infected mice showed morphological changes consistent with apoptosis, TUNEL+ staining of myocardiocytes, and a laddering pattern of fragmentation of DNA (extracted from whole hearts) (DeBiasi et al, J Virol 75:351-61, 2001: Fig. 1 & 2). Treatment of mice with CTX295, a calpain inhibitor, resulted in dramatic reduction in morphological evidence of cardiac pathology, reduction in serum levels of cardiac-specific enzymes (a marker of the severity of cardiac injury), and marked inhibition in apoptosis (as demonstrated by reduction in TUNEL staining) (DeBiasi et al., J Virol 75:351-61, 2001: Fig. 5,6,7). Similar results were also seen in primary myocardiocyte cultures. **These studies clearly indicate that pathways of apoptosis identified as potentially significant in vitro, are also operative in vivo, and can be targeted as the basis for antiviral therapy.**

Specific Aim 3: Is reovirus apoptosis associated with aberrant regulation of cell cycle progression and does this dysregulation occur in post-mitotic neurons?

During the current reporting period two papers related to this aim have been published in the Journal of Virology and a third paper is currently under revision at that journal.

Reovirus infection is associated with an inhibition of cellular proliferation, and different strains of virus differ in this capacity (Poggioli et al., J Virol 74:9562-70, 2000, Fig. 1). We have used flow cytometry to analyze DNA content in infected cells permeabilized and stained with propidium iodine. These studies indicate that reovirus strains that inhibit cellular proliferation cause a progressive accumulation of cells in the G2M phase of the cell cycle (Poggioli et al., J Virol 74:9562-70, 2000: Fig. 2). Studies using reassortant viruses containing different combinations of genes derived from the G2M arrest-inducing T3D and non-inducing T1L viral strains indicate that the viral S1 gene is the primary determinant of this process (Poggioli et al., 2000, Table 1).

As noted earlier, the S1 gene is bicistronic, encoding two non-homologous viral proteins (σ1, σ1s) from over-lapping but out-of-sequence open reading frames (ORFs). A σ1s null mutant reovirus (T3C84-MA) remains able to induce apoptosis but does not induce G2M arrest (Poggioli et al. J Virol 74:9562-70, 2000: Fig. 6). C127 cells expressing σ1s under the control of a cadmium inducible promoter, show an increased accumulation of cells in the G2M phase of the cell cycle following cadmium treatment when compared to either non-induced cells or to cadmium treated C127 cells containing a control plasmid lacking σ1s (Poggioli et al., J Virol 74:9562-70, 2000: Fig. 7).

We have now made additional progress in identifying the exact cellular pathways by which reovirus-induced G2M arrest is mediated (Poggioli et al. J Virol 75:7429-34, 2000). Progression of the cell cycle from G2 into mitosis (M) requires the activity of the G2/M checkpoint transition kinase, $p34^{cdc2}$. Reovirus infection is associated with decrease in the

activity of this kinase (*ibid* Figure 2), and its associated inhibitory phosphorylation (*ibid* Figure 3). Inhibitory phosphorylation of $p34^{cdc2}$ also occurs following induced expression of σ1s, and fails to occur in cells infected with a reovirus σ1s null mutant (T3C84-MA)(*ibid* Figure 5). As noted, activity of p34cdc2 is regulated by phosphorylation. Kinases including chk1 and wee1 contribute to the inhibitory phosphorylation of $p34^{cdc2}$, and this effect is counterbalanced by removal of inhibitory phosphate groups by phosphatases including cdc25c. Cdc25c is itself regulated by inhibitory phosphorylation. Reovirus infection is associated with enhanced inhibitory phosphorylation of cdc25C (*ibid*, Figure 6).

A paper describing our analysis of virus-induced alterations in expression of genes encoding proteins involved in cell cycle regulation is currently under revision at the **Journal of Virology** (Poggioli et al., J Virol, under revision, 2001). Reovirus T3 infection results in differential expression of ten genes encoding G1/S-related proteins, 11 genes encoding G2/M proteins, and 4 proteins involved in the mitotic spindle checkpoint. The results with T1L infection, which does not induce cell cycle arrest in infected cells, were dramatically different , resulting in altered expression of only 4 G1/S genes, 3 G2/M genes, and no mitotic spindle checkpoint genes. Of particular interest, was the fact that two of the identified genes were those encoding chk 1 and wee1. Reovirus T3 infection, but not infection with T1L, increased expression of both these genes. As noted earlier these are two of the key kinases that inhibit the activity of the G2/M transition kinase $p34^{cdc2}$.

We have previously shown that the capacity of reoviruses to inhibit cellular proliferation and to induce apoptosis are closely associated (Tyler et al. J Virol 70:7984-91, 1996). We have now tested the capacity of several inhibitors of reovirus-induced apoptosis to also inhibit reovirus-induced G2M arrest. Inhibition of calpain activation, blockade of caspase-3 activation, inhibition of TRAIL binding to DR4/DR5, and inhibition of NF-κB activation all inhibit reovirus-induced apoptosis, yet none of these interventions prevents virus-induced G2M arrest in susceptible cells (Poggioli et al., J Virol 74:9562-70, 2000: Fig. 8). These results clearly indicate that reovirus-induced perturbation of cell cycle regulation is not simply the result of DNA damage occurring during apoptosis.

KEY RESEARCH ACCOMPLISHMENTS

*Human congenital CMV encephalitis is associated with evidence of apoptosis as evidenced by both positive TUNEL staining and staining for activated caspase 3.

*Reovirus infection is associated with selective activation of mitogen activated protein kinase (MAPK) cascades including those involving c-Jun amino-terminal kinase (JNK).

*Differences in the capacity of reovirus strains to activate JNK are determined by the S1 and M2 genome segments.

*Reovirus infection is associated with phosphorylation and activation of the transcription factor c-Jun.

*Reovirus-induced apoptosis in a variety of epithelial cell lines involves the TNF receptor superfamily of cell surface death receptors specifically death receptors 4 & 5 (DR4, DR5) and their apoptosis-inducing ligand, TRAIL.

*Reovirus infection can induce apoptotic cell death in cancer cell lines derived from human cervical, breast and lung cancers. This process involves the TRAIL/DR4/DR5 system and can sensitize cells to killing by TRAIL.

*Reovirus can induce caspase 3-dependent apoptosis in both neuroblastomas cell lines and primary cortical neuronal cultures.

*Reovirus infection is associated with activation of the death receptor-associated initiator caspase, caspase 8.

*Reovirus-induced sensitization of cancer cells to TRAIL killing involves synergistic activation of the death-receptor associated initiator caspase, caspase 8, and can be blocked by cell permeable peptide inhibitors of caspase 8.

*Reovirus-induced caspase 8 activation is associated with cleavage of the pro-apoptotic Bcl-2 family protein Bid.

*Reovirus infection results in release of the mitochondrial protein cytochrome *c* into the cytosol, and subsequent activation of the mitochondrial-associated initiator caspase, caspase 9.

*Reovirus infection is associated with activation of the effector caspase, caspase 3, and cleavage of the caspase 3 cellular substrate PARP (poly-ADP ribose polymerase).

*Cell permeable peptide inhibitors of caspases 3, 8, and 9 all inhibit reovirus-induced apoptosis.

*Reovirus infection is associated with alteration in the expression of a limited subset of cellular genes. These genes encode proteins involved in signal transduction, transcription, DNA damage and repair, and apoptosis.

*Reovirus induces apoptosis in the heart following infection of mice with strain 8B. This is associated with myocardial calpain activation, and can be inhibited by in vivo treatment of infected mice with calpain inhibitor.

*Reovirus-induced inhibition of cellular proliferation is associated with arrest of cells in the G2M phase of the cell cycle.

*The reovirus S1 gene is the primary determinant of differences in the capacity of reovirus strains to induce G2M arrest.

* The reovirus σ1s protein, which is encoded by the S1 gene, is necessary for reovirus-induced G2M arrest, and over-expression of this protein in susceptible cells results in increased accumulation of cells in the G2M phase of the cell cycle.

*Although the capacity of reovirus strains to induce apoptosis and G2M are closely associated, apoptosis can be inhibited without preventing the capacity of reoviruses to induce G2M arrest, indicating that G2M arrest is not simply the result of apoptosis-associated cellular DNA damage.

*Reovirus-induced G2M arrest is associated with inhibition of the activity of the G2M transition kinase $p34^{cdc2}$.

*Reovirus infection is associated with inhibitory phosphorylation of the $p34^{cdc2}$ phosphatase, cdc25C.

REPORTABLE OUTCOMES (Annual Reporting Period Only)
Peer-reviewed publications

Clarke P, Meintzer SM, Gibson S, Widmann C, Garrington TP, Johnson GL, **Tyler KL**. Reovirus-induced apoptosis is mediated by TRAIL. J Virol 74: 8135-39, 2000.

Poggioli GJ, Keefer C, Connolly JL, Dermody TS, **Tyler KL**. Reovirus-induced G_2/M arrest Requires σ1s and occurs in the absence of apoptosis. J Virol 74:9562-70, 2000.

DeBiasi R, Edelstein C, Sherry B, **Tyler KL**. Calpain inhibition protects against virus induced apoptotic myocardial injury J Virol 75:351-361, 2001.

Poggioli GJ, Dermody TS, **Tyler KL**. Reovirus-induced σ1s-dependent G2/M cell cycle arrest is associated with inhibition of $p34^{cdc2}$. J Virol 75:7429-34, 2001.

Clarke P, Meintzer SM, Widmann C, Johnson GL, **Tyler KL.** Reovirus infection activates JNK and the JNK-dependent transcription factor c-Jun. J. Virol 75:(In press, December, 2001.)

DeMasters BK, DeBiasi R, **Tyler KL.** Polymerase chain reaction as a diagnostic adjunct in herpesvirus infections of the nervous system. Brain Pathol 11:452-64, 2001.

Clarke P, Meintzer SM, Spalding AC, Johnson GL, **Tyler KL.** Caspase-8 dependent sensitization of cancer cells to TRAIL-induced apoptosis following reovirus infection. Oncogene (in press, December), 2001.

Tyler KL, Clarke P, DeBisai RL, Kominsky D, Poggioli GJ. Reoviruses and the host cell. Trends in Microbiology, (in press), 2001.

Poggioli GJ, DeBiasi RL, Bickel R, Jotte R, Spalding A, Johnson GL, **Tyler KL**. Reovirus-Induced transcriptional alteration of genes related to cell cycle regulation. J. Virol. (Under revision, #1317-01), 2001.

Kominsky D, Bickel RJ, Meintzer SM, Clarke P, **Tyler KL**. Reovirus infection induces both Death receptor- and mitochondrial-mediated caspase-dependent pathways of cell death. J. Virol. (Submitted, #987-01), 2001.

Richardson-Burns S, **Tyler KL.** Reovirus induces apoptosis in primary neuronal cultures and neuroblastoma-derived cell lines. J. Neurosci. (Submitted, #JN1660-01).

Abstracts (Annual reporting period only)

*Poggioli GJ, Connolly JL, Dermody TS, **Tyler KL**. Reovirus-induced sigma 1s-dependent G2/M cell cycle arrest results from inhibition of p34cdc2. (7th International Symposium on Double-stranded RNA viruses, Palm Beach, Aruba, December 2-7, 2000).

***DeBiasi RL**, Clarke P, Jotte R, Johnson GL, **Tyler KL**. Analysis of gene expression following reovirus T3 Abney infection using high density oligonucleotide microarrays. (7th International Symposium on Double-stranded RNA viruses, Palm Beach, Aruba, December 2-7, 2000).

*Richardson-Burns, S, Clarke P, **Tyler KL.** Reovirus induces apoptosis in neural cell lines and primary neuronal cultures. (7th International Symposium on Double-stranded RNA viruses, Palm Beach, Aruba, December 2-7, 2000).

*Hoyt CC, **Tyler KL**. Use of the yeast-2-hybrid system to investigate interaction of sigma 1 with host cell receptors. (7th International Symposium on Double-stranded RNA viruses, Palm Beach, Aruba, December 2-7, 2000).

*Clarke P, Meintzer SM, **Tyler KL.** Reovirus sensitizes cancer cells to TRAIL-induced apoptosis. (7th International Symposium on Double-stranded RNA viruses, Palm Beach, Aruba, December 2-7, 2000).

*Kominsky D, Clarke P, Bickel R, Meintzer S, **Tyler KL**. Reovirus-induced apoptosis involves both death-receptor and mitochondrial-mediated pathways of cell death. (7th International Symposium on Double-stranded RNA viruses, Palm Beach, Aruba, December 2-7, 2000).

*Kominsky D, Bickel R, **Tyler KL**. Reovirus infection induces both extrinsic death receptor- and intrinsic mitochondrial-mediated pathways of apoptosis. (American Society for Virology, 20th Annual Meeting, Madison, WI, July 21-5, 2001.)

*Clarke P, Meintzer SM, Widmann C, Johnson GL, **Tyler KL.** Reovirus infection results in the activation of c-Jun N-terminal kinase (JNK) and the JNK-stimulated transcription factor c-Jun. (American Society for Virology, 20th Annual Meeting, Madison, WI, July 21-5, 2001.)

***DeBiasi RL**, Poggioli GJ, Bickel R, Kominsky D, Jotte RM, Johnson GJ, **Tyler KL**. Reovirus infection results in altered transcription of genes related to cell cycle, apoptosis and DNA repair including BRCA-1, GADD45 and regulators of Bcl-2. (American Society for Virology, 20th Annual Meeting, Madison, WI, July 21-5, 2001.)

*Richardson-Burns S, Clarke P, **Tyler KL**. Reovirus infection induces neuronal apoptosis. . (American Society for Virology, 20th Annual Meeting, Madison, WI, July 21-5, 2001.)

***DeBiasi RL,** Jotte R, Poggioli G, Johnson G, Tyler KL. Analysis of cellular gene expression following reovirus (T3 Abney) infection using high density oligonucleotide arrays. (American Academy of Neurology, 53rd Annual Meeting, Philadelphia, PA May 6-11, 2001.

***Tyler KL**, Kominsky D, Richardson-Burns S, Clarke P. Mechanisms of virus-induced cell death. (American Neurological Association, 126th Annual Meeting, Chicago, IL, September 30-October 3, 2001).

Richardson-Burns S, **Tyler KL.** Reovirus induces apoptosis in primary neuronal cultures and neuroblastoma-derived cell lines. (Society for Neuroscience 31st Annual Meeting, San Diego, CA, Nov. 10-15, 2001)

Presentations (selected, Annual reporting period only)

Mechanisms of virus-induced apoptosis in vitro and in vivo: insights from the reovirus system. Department of Virology, Institut Pasteur, Paris, France

Mechanisms of reovirus-induced apoptosis *in vitro* and *in vivo*
4th semi-annual FASEB summer conference on Microbial Pathogenesis, Snowmass, CO.

Cellular mechanisms of virus-induced apoptosis: Role of the TRAIL/DR4/DR5 death receptor system. 3rd International Symposium on Neurovirology, San Francisco, CA.

7th International Symposium on Double-Stranded RNA Viruses. Reovirus apoptosis and cell signaling pathways (plenary talk). Palm Beach, Aruba.

Dept. of Neurology, UCSF. Frontiers in Neurology & Neuroscience (Neurology Grand Rounds). Update on herpes simplex virus infections of the CNS and Mechanisms of viral pathogenesis and cell death (2 talks)

Western Regional Meeting American Federation for Medical Research,
Western Association of Physicians, Western Society for Clinical Investigation, Carmel, CA.
State of the Art Lecture. Mechanisms of virus-induced apoptosis in vitro and in vivo-lessons from the reovirus system

Microbiology, Immunology, and Cancer Biology Seminar Series, University of Minnesota: Mechanisms of virus-induced cell death *in vitro* and *in vivo*.

Neurology Grand Rounds. Dartmouth University Medical School, Dartmouth, NH.

Gordon Conference: Animal Cells and Viruses, Mechanisms of virus-induced

apoptosis *in vitro* and *in* vivo-lessons from the reovirus system. Tilton, N.H..

Patents and Licenses

None

Degrees obtained

George Poggioli, Ph.D. degree (Department of Microbiology) (Thesis: Reovirus induced σ1s-dependent G2/M cell cycle arrest is associated with inhibition of $p34^{cdc2}$.

CONCLUSIONS

The work performed during the first three years of this grant award have made reovirus infection one of the best characterized models of virus-induced apoptosis available. We now know that apoptosis is an essential feature of virus-induced tissue injury in at least two reovirus models of major human infections- encephalitis and myocarditis. Our studies indicate that once apoptotic pathways are identified in vitro, that these results can be translated to in vivo models, and these pathways can suggest novel targets for antiviral therapy.

Reovirus infection, in a variety of cell lines is associated with the TNF receptor superfamily of cell surface death receptors, specifically death receptors 4 and 5 (DR4, DR5) and their apoptosis-inducing ligand, TRAIL. Inhibition of TRAIL binding to its receptors inhibits reovirus-induced apoptosis. Apoptosis involves both the death-receptor and mitochondrial-associated apoptotic pathways leading to the activation of both caspase 8 and caspase 9. Activation of initiator caspases leads to the subsequent activation of caspase 3 and other effector caspases and the cleavage of cellular substrates of these caspases including PARP. Inhibition of activation of caspases 3, 8, and 9 all inhibit reovirus-induced apoptosis.

In addition to inducing apoptosis, reovirus infection is associated with perturbation of host cell cycle regulation. Many viruses perturb cell cycle regulation as a consequence of their interaction with host cells. Based on results obtained as part of the research supported by this grant, we now understand the mechanisms by which reoviruses perturb host cell cycle with a degree of detail that equals or exceeds that available for any other viral system. Reovirus infection is associated with a G2/M cell cycle arrest. Differences in the capacity of reovirus strains to induce G2/M arrest are determined by the reovirus S1 genome segment. The S1-encoded σ1s protein is the key determinant of reovirus-induced G2/M arrest. Induced over-expression of this protein causes cells to accumulate in the G2/M phase of the cell cycle, and a mutant virus lacking this protein fails to induce G2/M arrest in infected cells. The transition between the G2 and M phases of the cell cycle is controlled by the G2/M transition checkpoint kinase p34cdc2. Reovirus infection is associated with inhibition of p34cdc2, resulting from its inhibitory phosphorylation. The phosphorylation of p34cdc2 is regulated by kinases (chk 1, wee1) and by phosphatases (cdc25C). We have shown that reovirus infection is associated with increased expression of both chk1 and wee1 and with inhibition of cdc25C.

In addition to its capacity to cause apoptosis in epithelial cells, we have recently shown that reovirus infection can also cause apoptotic cell death in a variety of cell lines derived from human cervical, breast, and lung cancers. Apoptosis in these cells also involves

the TRAIL/DR4/DR5 system, and sensitizes tumor cells to killing by TRAIL. The mechanism of reovirus-induced sensitization of cancer cells to TRAIL killing involves synergistic activation of caspase 8 and can be prevented by caspase 8 inhibitors.

Viruses belonging to virtually all viral families have the capacity to kill target cells by apoptosis. We have now developed one of the most comprehensive systems for evaluating the mechanisms of virus-induced cell death both in vitro and in vivo. In addition, the capacity of viruses to perturb cell cycle regulation is a fundamental feature of many diverse viral infections. We have now provided one of the most detailed characterizations by which a virus induces one form of cell cycle dysregulation (G2/M arrest).

Apoptosis as Indicated by Caspase 3 Activation in Virus-Infected CNS Tissue

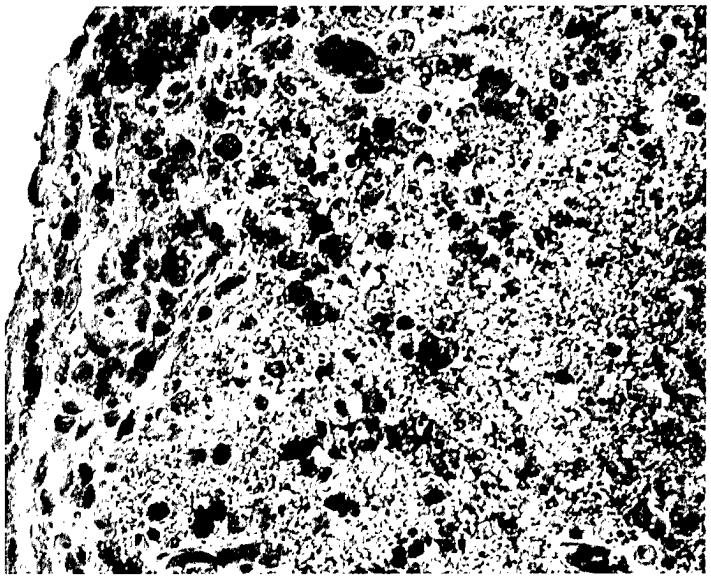

T3 Reovirus-Infected Neonatal Mouse Cortex

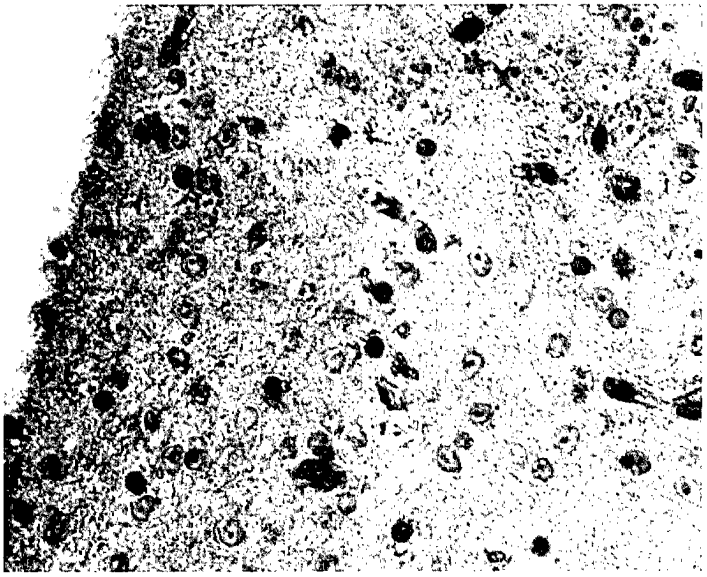

Un-Infected Neonatal Mouse Cortex

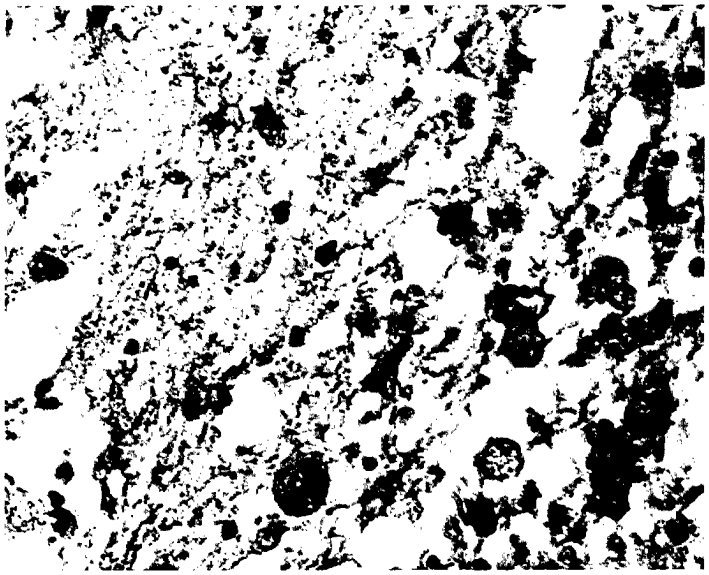

CMV-Infected Neonatal Human Midbrain

JOURNAL OF VIROLOGY, Sept. 2000, p. 8135–8139
0022-538X/00/$04.00+0

Vol. 74, No. 17

Reovirus-Induced Apoptosis Is Mediated by TRAIL

PENNY CLARKE,[1] SUZANNE M. MEINTZER,[1] SPENCER GIBSON,[2,3] CHRISTIAN WIDMANN,[2,3] TIMOTHY P. GARRINGTON,[2,3] GARY L. JOHNSON,[2,3,4] AND KENNETH L. TYLER[1,5,6]*

Departments of Neurology,[1] Pharmacology,[4] and Medicine, Microbiology and Immunology,[5] University of Colorado Health Sciences Center, and Denver Veteran's Affairs Medical Center,[6] Denver, Colorado 80262, and Program in Molecular Signal Transduction[2] and Division of Basic Sciences,[3] National Jewish Center for Immunology and Respiratory Medicine, Denver, Colorado 80206

Received 13 April 2000/Accepted 9 June 2000

Members of the tumor necrosis factor (TNF) receptor superfamily and their activating ligands transmit apoptotic signals in a variety of systems. We now show that the binding of TNF-related, apoptosis-inducing ligand (TRAIL) to its cellular receptors DR5 (TRAILR2) and DR4 (TRAILR1) mediates reovirus-induced apoptosis. Anti-TRAIL antibody and soluble TRAIL receptors block reovirus-induced apoptosis by preventing TRAIL-receptor binding. In addition, reovirus induces both TRAIL release and an increase in the expression of DR5 and DR4 in infected cells. Reovirus-induced apoptosis is also blocked following inhibition of the death receptor-associated, apoptosis-inducing molecules FADD (for FAS-associated death domain) and caspase 8. We propose that reovirus infection promotes apoptosis via the expression of DR5 and the release of TRAIL from infected cells. Virus-induced regulation of the TRAIL apoptotic pathway defines a novel mechanism for virus-induced apoptosis.

Studies using mammalian reoviruses have provided fundamental insights into the molecular and genetic basis of viral pathogenesis and virus-induced cell death. Reovirus infection induces apoptosis in cultured cells in vitro (13, 15, 26) and in target tissues in vivo, including the central nervous system, heart, and liver (12, 13). Reovirus induces apoptosis by a p53-independent mechanism that involves cellular proteases including calpains (4), is dependent on reovirus-induced NF-κB activation (3), and is inhibited by overexpression of Bcl-2 (15). Strain-specific differences in the capacity of reoviruses to induce apoptosis are determined by the viral S1 gene (26) and require viral binding to cell surface receptors but not completion of the full viral replication cycle (15). Reovirus-induced apoptosis correlates with pathology in vivo and is a critical mechanism by which disease is triggered in the host (12). Inhibition of apoptosis in vivo reduces the extent of tissue injury (R. L. Debiasi et al., Am. Soc. Virol. Sci. Program Abstr., abstr. W52-1, 1999), emphasizing the importance of apoptosis in reovirus pathogenesis. We have thus used reovirus infection to study mechanisms of virus-induced apoptosis.

Cellular death receptors (DRs) transmit apoptosis-inducing signals initiated by specific death ligands, most of which are primarily expressed as biologically active type II membrane proteins that are cleaved into soluble forms. Fas ligand (FasL) activates Fas/CD95/Apo1, tumor necrosis factor (TNF) activates TNFR1 (TNF receptor 1), Apo 3L/TWEAK activates DR3, and TRAIL (for TNF-related apoptosis-inducing ligand; also called Apo2L) activates DR4 (TRAILR1) and DR5 (TRAILR2/TRICK2). Ligand-mediated activation triggers a cascade of events that begins with DR oligomerization and the close association of their cytoplasmic death domains (DDs). This is followed by DD-associated interaction with adapter molecules and cellular proteases critical to DR-induced apoptosis (reviewed in reference 1). In this paper we describe a novel mechanism for virus-induced cell death involving the upregulation of DR5, the release of TRAIL from infected cells, and subsequent TRAIL-mediated apoptosis.

MATERIALS AND METHODS

Cells, virus, and inhibitors. HEK293 cells (ATCC CRL1573) were grown in Dulbecco's modified Eagle's medium supplemented with 100 U each of penicillin and streptomycin per ml and containing 10% fetal bovine serum. HeLa cells (ATCC CCL2) were grown in Eagle's minimal essential medium supplemented with 2.4 mM L-glutamine, nonessential amino acids, 60 U each of penicillin and streptomycin per ml, and containing 10% fetal bovine serum (Gibco BRL, Gaithersburg, Md.). FADD-DN cells express amino acids 80 to 208 of the Fas-associated DD (FADD) cDNA (with the addition of an AU1 epitope tag at the N terminus), from the cytomegalovirus promoter from pcDNA3 (Invitrogen, Carlsbad, Calif.). Reovirus (type 3 Abney [T3A]) is a laboratory stock which has been plaque purified and passaged (twice) in L929 (ATCC CCL1) cells to generate working stocks (27). Virus growth was determined by plaque assay as previously described (25).

Western blot analysis and antibodies. Twenty-four hours following infection with reovirus, cells were pelleted by centrifugation, washed twice with ice-cold phosphate-buffered saline, and lysed by sonication in 200 μl of a buffer containing 15 mM Tris (pH 7.5), 2 mM EDTA, 10 mM EGTA, 20% glycerol, 0.1% NP-40, 50 mM β-mercaptoethanol, 100 μg of leupeptin and 2 μg of aprotinin per ml, 40 μM Z-D-DCB, and 1 mM phenylmethylsulfonyl fluoride. The lysates were then cleared by centrifugation at 16,000 × *g* for 5 min, normalized for protein amount, mixed 1:1 with sodium dodecyl sulfate (SDS) sample buffer (100 mM Tris [pH 6.8], 2% SDS, 300 mM β-mercaptoethanol, 30% glycerol, 5% pyronine Y), boiled for 5 min, and stored at −70°C. Proteins were electrophoresed by SDS–10% polyacrylamide gels and probed with polyclonal antibodies directed against DR4 (366891N [PharMingen, San Diego, Calif.] and sc-6823 [Santa Cruz Biotechnology, Santa Cruz, Calif.]), DR5 (210-730-C100 [Alexis Corporation, Pittsburgh, Pa.] and sc-7191 [Santa Cruz Biotechnology]), DCR-2 (33060-100; Biovision, Palo Alto, Calif.), Fas (sc-714-G; Santa Cruz Biotechnology), and actin (CP01; Oncogene, Cambridge, Mass.). Additional antibodies directed against FasL (sc-834-G; Santa Cruz Biotechnology) and TRAIL (3210-732-R100 [Alexis Corporation] and antibody from Affinity Bioreagents, Golden, Color.) were used for antibody blocking experiments. Autoradiographs were quantitated by densitometric analysis using ImageQuant (Amersham Pharmacia Biotech, Inc., Piscataway, N.J.).

Apoptosis assays and reagents. Forty-eight hours after infection with reovirus, cells were harvested and stained with acridine orange, for determination of nuclear morphology, and ethidium bromide, to distinguish cell viability, at a final concentration of 1 μg/ml each (5). Following staining, cells were examined by epifluorescence microscopy (Nikon Labophot-2; B-2A filter; excitation, 450 to 490 nm; barrier, 520 nm; dichroic mirror, 505 nm). The percentage of cells containing condensed nuclei and/or marginated chromatin in a population of 100 cells was recorded. The specificity of this assay has been previously established in

* Corresponding author. Mailing address: Department of Neurology (127), Denver VA Medical Center, 1066 Clermont St., Denver, CO 80220. Phone: (303) 393-2874. Fax: (303) 393-4686. E-mail: Ken.Tyler@uchsc.edu.

† Present address: Institute de Biologie Cellulaire et de Morphologie, Lausanne, Switzerland.

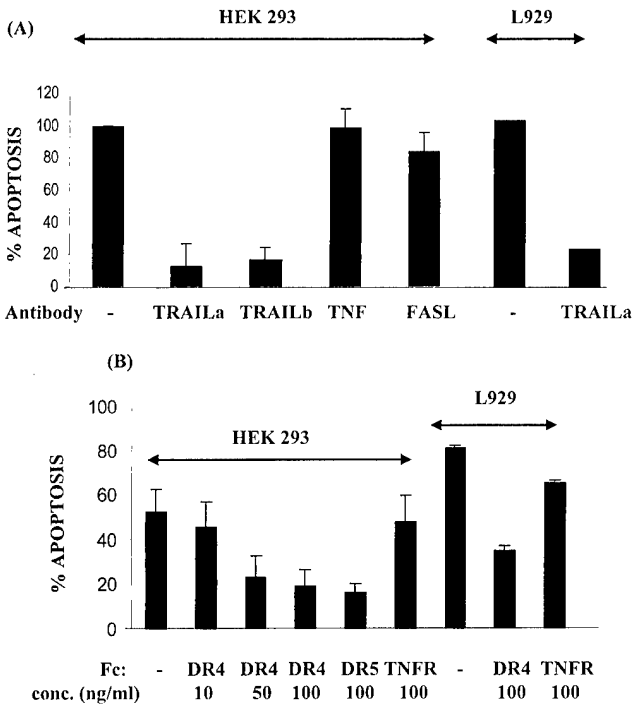

FIG. 1. TRAIL mediates reovirus-induced apoptosis. Anti-TRAIL antibodies and soluble TRAIL receptors (Fc:DR4 and Fc:DR5) specifically inhibit reovirus-induced apoptosis. HEK293 and L929 cells were pretreated for 1 h with two different anti-TRAIL (TRAILa and TRAILb) antibodies (A) or increasing concentrations of soluble TRAIL receptors (B) before being infected with reovirus (MOIs of 10 and 50, respectively, for antibody and receptor experiments). After infection cells were incubated in media containing antibody or receptor for 48 h before cells were harvested and the percentage of apoptotic cells was determined. The graphs show percent apoptosis compared to untreated cells in reovirus-infected minus mock-infected cells (A) and the actual percent apoptosis in reovirus-infected minus mock-infected cells (B). Error bars represent standard error of the mean. Antibodies directed against TNF and FasL were used as controls in the antibody blocking experiments. Soluble TNFR (Fc:TNFR) was used as a control in the receptor experiments.

reovirus-infected cells using DNA laddering techniques and electron microscopy (26). Soluble TRAIL was obtained from Upstate Biotechnology, Lake Placid, N.Y. Soluble DRs Fc:DR4, Fc:DR5, and Fc:TNFR were obtained from Alexis Corporation. Z-IETD-FMK (granzyme B inhibitor III), a specific inhibitor of caspase 8 activity, was obtained from Clontech, Palo Alto, Calif.

RESULTS

Reovirus-induced apoptosis is mediated by TRAIL. We investigated the role of ligand-mediated apoptosis in reovirus-induced cell death using two separate polyclonal antibodies directed against TRAIL and antibodies directed against FasL and TNF to block ligand binding during reovirus infection. HEK293 cells were pretreated with antiligand antibodies (30 μg/ml) for 1 h before viral infection (multiplicity of infection [MOI] of 10) and were maintained in antibody-containing media following infection with reovirus. Antibody was not present during viral infection. The percentage of apoptotic cells was determined at 48 h postinfection. Anti-TRAIL antibodies, but not antibodies directed against FasL (TRAIL versus FasL, $P = 0.008$) or TNF (TRAIL versus TNF, $P = 0.003$) significantly inhibit reovirus-induced apoptosis (Fig. 1A). Thus, anti-TRAIL antibodies specifically inhibit reovirus-induced apoptosis. Anti-TRAIL antibody also inhibits reovirus-induced apoptosis in L929 cells (Fig. 1A), indicating that TRAIL-mediated apoptosis is likely to be a general feature of reovirus-induced apoptosis. Both anti-TRAIL antibodies bound soluble ligand in Western blot analysis (results not shown).

TRAIL binding was further shown to be essential for reovirus-induced apoptosis using the soluble TRAIL receptors Fc:DR4 and Fc:DR5 (Fig. 1B). These molecules contain the extracellular domain of DR4 or DR5 fused to the Fc portion of human immunoglobulin G and inhibit TRAIL-induced apoptosis by preventing TRAIL binding to DR4 and DR5 present on the cell surface (7). Cells were pretreated with soluble receptor for 1 h before virus infection (MOI of 50) and were maintained in receptor-containing media following infection. Soluble receptor was not present during viral infection. Treatment of cells with Fc:DR4 or Fc:DR5 (not shown) produces a dose-dependent inhibitory effect on reovirus-induced apoptosis (Fig. 1B). Thus, Fc:DR4 and Fc:DR5 appear to be similar in potency for TRAIL binding. Fc:DR4 (100 ng/ml) and Fc:DR5 (100 ng/ml) reduced reovirus-induced apoptosis by 65% (from 54% to 19%, $P = 0.048$) and by 70% (from 54% to 16%), respectively. Soluble TNFR (Fc:TNFR; 100 ng/ml) does not significantly inhibit reovirus-induced apoptosis, indicating that the inhibition is specific for the TRAIL-associated receptors DR4 and DR5. In L929 cells, Fc:DR4, but not Fc:TNFR, also significantly inhibited reovirus-induced apoptosis by 57% (from 81% to 35% [Fig. 1B]), again indicating that TRAIL-mediated apoptosis is likely to be a general feature of reovirus-induced apoptosis. To confirm that antibody or soluble receptor-mediated inhibition of apoptosis was not due to any effect of these reagents on viral replication, we measured viral yield in anti-TRAIL and soluble receptor-treated cells and found no significant difference compared with untreated cells (results not shown).

TRAIL is released from cells following infection with reovirus. Having shown that TRAIL is required for reovirus-induced apoptosis, we next wanted to determine whether cleaved, soluble TRAIL is released from in reovirus-infected cells.

Following infection of HEK293 cells with reovirus (MOI of 100), the supernatant was collected and transferred onto HeLa cells, which are sensitive to TRAIL-induced apoptosis (Fig. 2). Supernatants collected from virus-infected HEK293 cells 24, 36, and 48 h postinfection induce apoptosis (18, 30, and 68%, respectively) when transferred onto HeLa cells. Apoptotic

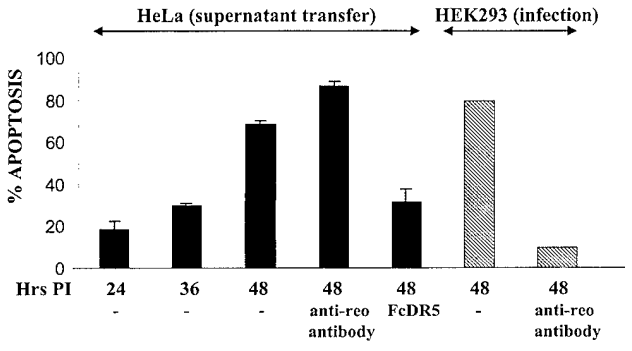

FIG. 2. TRAIL is released from reovirus-infected cells. HEK293 cells were either mock infected or infected with reovirus (MOI of 100). At various times postinfection (PI), supernatant from infected HEK293 cells was transferred onto TRAIL-sensitive HeLa cells. Apoptosis was assayed in HeLa cells 24 h following supernatant transfer. The graph shows the percent increase of apoptotic nuclei in HeLa cells following treatment with supernatants taken from reovirus-infected, compared to mock-infected, HEK293 cells. Error bars represent standard errors of the mean. Soluble DR5 (Fc:DR5) and an antireovirus (anti-reo) antibody were used as TRAIL specificity controls. The shaded bars demonstrate that reovirus-induced (MOI of 100) apoptosis is blocked by the antireovirus antibody in HEK293 cells.

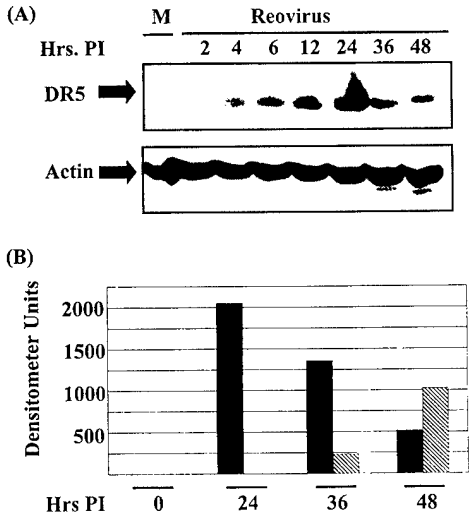

FIG. 3. DR5 is up-regulated during reovirus-induced apoptosis. Cell lysates were prepared and examined by Western blotting using antibodies directed against DR5 and actin (A). Following autoradiography, densitometric analysis was performed (B). The graph shows the increase in signal observed in reovirus-infected compared to mock-infected cells for DR5 (black columns) and DR4 (shaded columns). M, mock infection; PI, postinfection.

HeLa nuclei were assayed 24 h following treatment with supernatant from reovirus-infected HEK293 cells. Supernatant-induced apoptosis of HeLa cells is inhibited 64% (from 68% to 31%, $P = 0.001$) by soluble DR5 (Fc:DR5; 100 ng/ml [Fig. 2]) and by soluble DR4 (Fc:DR4; 100 ng/ml [results not shown]), indicating that the apoptosis seen in the HeLa cells following supernatant transfer is TRAIL specific. TRAIL is thus released from reovirus-infected cells and induces apoptosis in HeLa cells. The apoptotic effects of infected cell supernatants are not due to the presence of infectious virus in the transferred supernatant since addition of a neutralizing polyclonal antireovirus antiserum that blocks apoptosis induced by infectious virus (26) does not block apoptosis induced in HeLa cells by supernatant transfer (Fig. 2). This antibody inhibits reovirus (MOI of 100)-induced apoptosis in HEK293 cells (Fig. 2).

Expression of DR5 is up-regulated following infection with reovirus. Reovirus-induced apoptosis thus requires TRAIL binding, and TRAIL is released from reovirus-infected cells. We next investigated the expression of TRAIL receptors in reovirus-infected cells. HEK293 cells were infected with reovirus (MOI of 100), harvested at various times postinfection, and examined by Western blot analysis. DR5 is detected in lysates extracted from reovirus-infected but not mock-infected HEK293 cells. DR5 expression is first detected at 4 h postinfection. Expression peaks at 24 h postinfection and then declines (Fig. 3). The expression of DR4 also increases in reovirus-infected cells, but with much less magnitude and only at late times after infection (Fig. 3B). DR5 thus appears to be the TRAIL receptor that is predominantly up-regulated following reovirus infection.

Decoy receptor 1 (DcR-1; also called TRAILR3/TRID/LIT) and DcR-2 (TRAILR4) compete with DR4 and DR5 for TRAIL binding. These decoy receptors do not contain active intracellular DDs do not transduse apoptotic signals, and have antiapoptotic effects (6, 17). Neither DcR-1 nor DcR-2 expression is significantly altered in reovirus-infected cells (results not shown).

Reovirus infection sensitizes cells to TRAIL-induced apoptosis. TRAIL-induced apoptosis is enhanced in cells demonstrating an increase in the surface expression of DR4 and DR5 (7). Having shown that reovirus infection results in increased expression of DR5 and to a lesser extent DR4, we next wished to determine whether these increases occur at the cell surface by demonstrating that reovirus sensitizes cells to TRAIL-induced apoptosis. Cells were infected with reovirus (MOI of 10), treated with TRAIL (200 ng/ml) at various times postinfection and assayed for apoptosis 24 h later. Mock-infected HEK293 cells do not undergo apoptosis when treated with TRAIL. However, following infection with reovirus, HEK293 cells become sensitive to TRAIL-induced apoptosis (Fig. 4), and the percentage of apoptotic nuclei in TRAIL-treated, reovirus-infected cells is greater than that in cells treated with reovirus alone (Fig. 4). At 12, 24, 30, and 48 h after infection with reovirus, TRAIL-treated cells demonstrated 2.4-, 3.7-, 3.3-, and 1.8-fold increases in apoptosis, respectively, compared to TRAIL-treated mock-infected cells. Since TRAIL-induced apoptosis is apparent 12 h following infection with

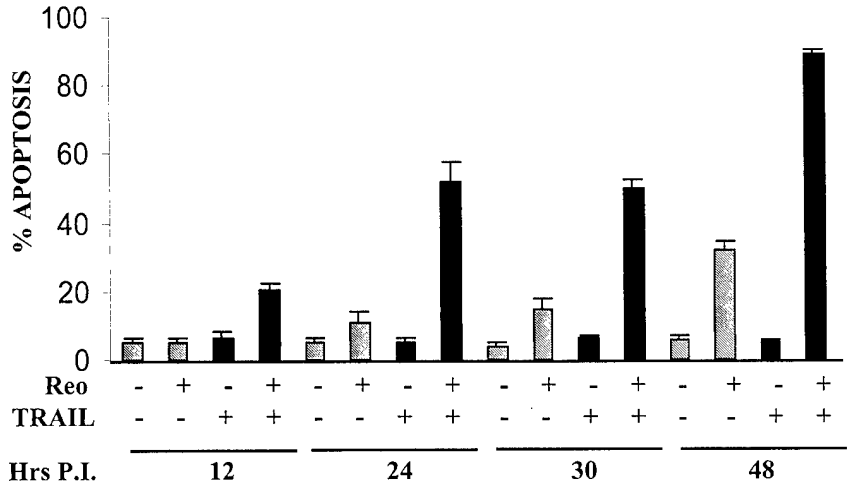

FIG. 4. Reovirus infection sensitizes cells to TRAIL-induced apoptosis. The effectiveness of TRAIL (200 ng/ml)-induced apoptosis was assayed in mock (−)- or reovirus (+; MOI of 10)-infected cells. Cells were treated with TRAIL (black bars) or left untreated (shaded bars). At various times postinfection (P.I.), cells were assayed for the presence of apoptotic nuclei. The graph shows the mean percentage of apoptotic nuclei. Error bars represent standard errors of the mean.

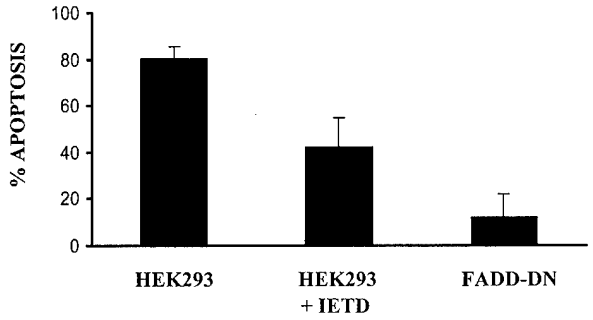

FIG. 5. Reovirus-induced apoptosis involves FADD and caspase 8 activity. HEK293 cells expressing FADD-DN or HEK293 cells treated with a specific inhibitor of caspase 8 (IETD) were infected with reovirus (MOI of 50). Apoptosis was assayed 48 h postinfection. The graph shows the mean percentage of apoptotic nuclei. Error bars represent standard errors of the mean.

reovirus and since the up-regulation of DR4 is not seen until 24 h postinfection, this again suggests that it is the increased expression of DR5 rather than DR4 that is the primary TRAIL receptor involved in reovirus-induced apoptosis.

FADD and caspase 8 are involved in reovirus-induced apoptosis. DRs mediate apoptosis through receptor-associated DD containing adapter proteins, exemplified by FADD (also called Mort 1). These adapter molecules contain their own DDs that bind to the clustered receptor DDs, resulting from receptor-ligand binding (reviewed in reference 1). Studies with dominant negative (DN) mutants of FADD (28) and cells derived from FADD gene knockout mice (31) indicate that FADD is necessary for apoptosis mediated by Fas, TNFR1, and DR3 (1, 9, 28). Apoptotic signals induced by DR4 and DR5 also appear to be mediated either by FADD or a FADD-like adapter molecule (1, 29). We constructed a HEK293 cell line expressing DN FADD (FADD-DN) in order to inhibit FADD and therefore DR-mediated apoptosis. Reovirus-induced apoptosis in HEK293 cells (and in HEK293 cells expressing vector alone [not shown]) is reduced by 85% (from 80.3% to 12%, $P = 0.0012$) in reovirus-infected HEK293 cells expressing FADD-DN (Fig. 5). These results confirm our findings that reovirus-induced apoptosis involves cellular DRs.

DR-induced, FADD-mediated apoptosis requires the activity of caspase 8. Activation of caspase 8 requires association of its death effector domains with those of FADD. Activated caspase 8 then activates the downstream effector caspases, including caspase 3 (reviewed in references 16 and 23). To further support the role of the TRAIL/DR pathway in reovirus-induced apoptosis, we demonstrate that IETD-fmk (50 μM), a specific inhibitor of caspase 8, reduces reovirus-induced apoptosis by 48% (from 80.3% to 42%, $P = 0.372$), indicating that caspase 8 is involved in reovirus-induced apoptosis (Fig. 5).

DISCUSSION

We have shown that reovirus-induced apoptosis requires TRAIL binding to its apoptosis-inducing receptors DR5 and/or DR4. However, exogenous TRAIL (200 ng/ml) does not induce apoptosis in uninfected HEK293 cells since these cells do not express sufficient cell surface DR4 or DR5. To induce apoptosis, reovirus must therefore up-regulate both TRAIL and a death-associated TRAIL receptor. We therefore determined that there is both an increase in the release of TRAIL and an increase in the expression of DR5, and to a lesser extent DR4, in reovirus-infected cells. It seems unlikely that the up-regulation of both DR4 and DR5 is required for TRAIL-mediated expression in reovirus-infected cells. The quicker and more dramatic increase in DR5 expression compared to DR4 expression suggests that DR5 is the major receptor involved in triggering apoptosis. Furthermore, the increased sensitivity of reovirus-infected HEK293 cells to TRAIL-induced apoptosis is detectable 12 h following infection, whereas the alteration in expression of DR4 does not occur until 24 h postinfection. These results suggest that the contribution of DR4 to reovirus-induced apoptosis may be a secondary event and that its up-regulation in reovirus-infected cells may function to amplify the effects of TRAIL/DR5 regulation.

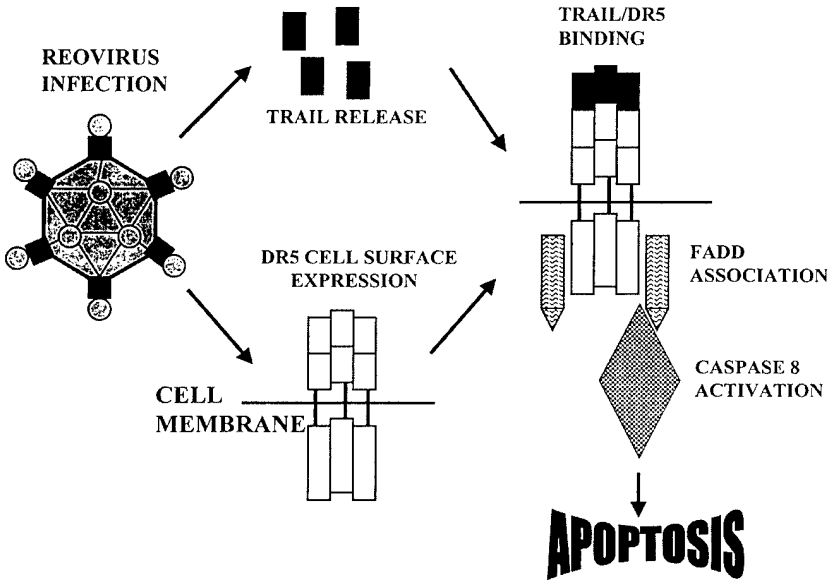

FIG. 6. Reovirus induces the TRAIL apoptotic pathway in infected cells by inducing the release of TRAIL and the up-regulation of DR5. The consequent binding of TRAIL to DR5 then promotes FADD association and the activation of caspase 8.

We propose a model in which reovirus infection results in the up-regulation of DR5 and the release of TRAIL, thereby activating the TRAIL pathway of cell death (Fig. 6). Similar to other DR-mediated apoptotic pathways, reovirus-induced apoptosis requires the participation of an adapter molecule (FADD) and the activation of the caspase cascade since it is reduced in the presence of inhibitors of FADD or caspase 8 activity. We have recently shown that reovirus-induced apoptosis requires the transcription factor NF-κB (3). Future studies will be directed at examining the role of NF-κB in the up-regulation of TRAIL and DR5 in reovirus-infected cells.

Our results demonstrate the involvement of the TRAIL apoptotic pathway in reovirus-induced cell death and provide the first direct evidence for the involvement of this pathway in virus-induced apoptosis. Additional support for the potential role of DR4 and DR5 in virus-induced apoptosis comes from studies suggesting that human immunodeficiency virus (HIV) infection increases the expression of TRAIL and sensitizes T cells to TRAIL-mediated apoptosis (10). Previous studies have suggested that other members of the TNFR DR superfamily may also be involved in apoptosis induced in cells infected with a variety of viruses. Alteration of the cell surface expression of Fas may be involved in virus-induced, or viral regulation of, apoptosis in cells infected with influenza virus (21, 22), herpes simplex virus type 2 (19), bovine herpesvirus 4 (30), adenovirus (24), and HIV type 1 (2, 11). Similarly, apoptosis induced by hepatitis B virus (20), HIV type 1 (8), bovine herpesvirus 4 (30), and parvovirus H-1 (14) may involve the TNFR signaling pathway. TRAIL and TRAIL receptor expression have been shown to mediate gamma interferon-induced antiviral activity (18), although the mechanism by which this occurs is unknown.

We propose that the regulation of TRAIL and its death-promoting receptors is a primary mediator of apoptosis that is induced not only following viral infection but also as a component of apoptosis-inducing stress responses, including chemotherapy (7).

ACKNOWLEDGMENTS

This work was supported by Public Health Service grants 1RO1AG14071 and GM30324 from the National Institutes of Health, Merit and REAP grants from the Department of Veterans Affairs, and U.S. Army Medical Research and Material Command grant USAMRMC98293015 (K.L.T.) S.G. is a Leukemia Society fellow. The University of Colorado Cancer Center provided core tissue culture and media facilities.

We thank Terrence S. Dermody and Jodi L. Connelly for helpful advice during the development of this project.

REFERENCES

1. **Ashkenazi, A., and V. M. Dixit.** 1998. Death receptors: signaling and modulation. Science **281:**1305–1308.
2. **Conaldi, P. G., L. Biancone, A. Bottelli, A. Wade-Evans, L. C. Racusen, M. Boccellino, V. Orlandi, C. Serra, G. Camussi, and A. Toniolo.** 1998. HIV-1 kills renal tubular epithelial cells in vitro by triggering an apoptotic pathway involving caspase activation and Fas up regulation. J. Clin. Investig. **102:** 2041–2049.
3. **Connolly, J. L., S. E. Rodgers, P. Clarke, D. W. Ballard, L. D. Kerr, K. L. Tyler, and T. S. Dermody.** 2000. Reovirus-induced apoptosis requires activation of transcription factor NF-κB. J. Virol. **74:**2981–2989.
4. **Debiasi, R. L., M. K. T. Squier, B. Pike, M. Wynes, T. S. Dermody, J. J. Cohen, and K. L. Tyler.** 1999. Reovirus-induced apoptosis is preceded by increased cellular calpain activity and is blocked by calpain inhibitors. J. Virol. **73:**695–701.
5. **Duke, R. C., and J. J. Cohen.** 1992. Morphological and biochemical assays of apoptosis, p. 3.17.1–3.17.16. *In* J. E. Coligan et al. (ed.), Current protocols in immunology. John Wiley & Sons, New York, N.Y.
6. **French, L. E., and J. Tschopp.** 1999. The TRAIL to selective tumor death. Nat. Med. **5:**146–147.
7. **Gibson, S. B., R. Oyer, A. C. Spalding, S. M. Anderson, and G. L. Johnson.** 2000. Increased expression of death receptors 4 and 5 synergizes the apoptosis response to combined treatment with etopiside and TRAIL. Mol. Cell. Biol. **20:**205–212.
8. **Herbein, G., U. Mahlknecht, F. Batliwalla, P. Gregerson, T. Pappas, J. Butler, W. A. O'Brian, and E. Verdin.** 1999. Apoptosis of CD8+ T cells is mediated by macrophages through interaction of gp120 with chemokine receptor CXCR4. Nature **395:**189–194.
9. **Hu, S., C. Vincenz, M. Buller, and V. M. Dixit.** 1997. A novel family member of viral death effector domain-containing molecules that inhibit both CD-95- and tumor necrosis factor receptor-1-induced apoptosis. J. Biol. Chem. **272:** 9621–9624.
10. **Jeremias, I., I. Herr, T. Boehler, and K.-M. Debatin.** 1998. TRAIL/Apo-2-ligand-induced apoptosis in human T cells. Eur. J. Immunol. **28:**143–152.
11. **Kaplan, D., and S. Sieg.** 1998. Role of the Fas/Fas ligand apoptotic pathway in human immunodeficiency virus type 1 disease. J. Virol. **72:**6279–6282.
12. **Oberhaus, S. M., R. L. Smith, G. H. Clayton, T. S. Dermody, and K. L. Tyler.** 1997. Reovirus infection and tissue injury in mouse central nervous system are associated with apoptosis. J. Virol. **71:**2100–2106.
13. **Oberhaus, S. M., T. S. Dermody, and K. L. Tyler.** 1998. Apoptosis and the cytopathic effects of reovirus. Curr. Top. Microbiol. Immunol. **233:**23–49.
14. **Rayet, B., J.-A. Lopez-Guerrero, J. Rommelaere, and C. Dinsart.** 1998. Induction of programmed cell death by parvovirus H-1 in U937 cells: connection with the tumor necrosis factor alpha-signaling pathway. J. Virol. **72:**8893–8903.
15. **Rodgers, S. E., E. S. Barton, S. M. Oberhaus, B. Pike, C. A. Gibson, K. L. Tyler, and T. S. Dermody.** 1997. Reovirus-induced apoptosis of MDCK cells is not linked to viral yield and is blocked by Bcl-2. J. Virol. **71:**2540–2546.
16. **Salvesen, G., and V. M. Dixit.** 1997. Caspases: intracellular signaling by proteolysis. Cell **91:**443–446.
17. **Schneider, P., J. L. Bodmer, M. Thome, K. Hofmann, T. Kataoka, N. Holler, and J. Tschopp.** 1997. Characterization of two receptors for TRAIL. FEBS Lett. **416:**329–334.
18. **Sedger, L. M., D. M. Shows, R. A. Blanton, J. J. Peschon, R. G. Goodwin, D. Cosman, and S. R. Wiley.** 1999. IFN-γ mediates a novel antiviral activity through dynamic expression of TRAIL and TRAIL receptor expression. J. Immunol. **163:**920–926.
19. **Sieg, S., Z. Yildirim, D. Smith, N. Kayagaki, H. Yagita, Y. Huang, and D. Kaplan.** 1996. Herpes simplex virus type 2 inhibition of Fas ligand expression. J. Virol. **70:**8747–8751.
20. **Su, F., and R. J. Schneider.** 1997. Hepatitis B virus HBx protein sensitizes cells to apoptotic killing by tumor necrosis factor α. Proc. Natl. Acad. Sci. USA **94:**8744–8749.
21. **Takizawa, T., S. Matsukawa, Y. Higuchi, S. Nakamura, Y. Nakanishi, and R. Fukuda.** 1993. Induction of programmed cell death (apoptosis) by influenza virus infection in tissue culture cells. J. Gen. Virol. **74:**2347–2355.
22. **Takizawa, T., R. Fukuda, T. Miyawaki, K. Ohashi, and Y. Nakanishi.** 1995. Activation of the apoptotic Fas antigen-encoding gene upon influenza virus infection involving spontaneously produced beta-interferon. Virology **209:** 288–296.
23. **Thornberry, N. A., and Y. Lazebnik.** 1998. Caspases: enemies within. Science **281:**1312–1316.
24. **Tollefson, A. E., T. W. Hermiston, D. L. Lichtenstein, C. F. Colle, R. A. Tripp, T. Dimitrov, K. Toth, C. E. Wells, P. C. Doherty, and W. S. Wold.** 1998. Forced degradation of Fas inhibits apoptosis in adenovirus-infected cells. Nature **392:**726–730.
25. **Tyler, K. L., R. T. Bronson, K. B. Byers, and B. N. Fields.** 1985. Molecular basis of viral neurotropism: experimental reovirus infection. Neurology **35:** 88–92.
26. **Tyler, K. L., M. K. T. Squier, S. E. Rodgers, B. E. Schneider, S. M. Oberhaus, T. A. Grdina, J. J. Cohen, and T. S. Dermody.** 1995. Differences in the capacity of reovirus strains to induce apoptosis are determined by the viral attachment protein sigma 1. J. Virol. **69:**6972–6979.
27. **Tyler, K. L., M. K. T. Squier, A. L. Brown, B. Pike, D. Willis, S. M. Oberhaus, T. S. Dermody, and J. J. Cohen.** 1996. Linkage between reovirus-induced apoptosis and inhibition of cellular DNA synthesis: role of the S1 and M2 genes. J. Virol. **70:**7984–7991.
28. **Wajant, H., F. J. Johannes, E. Haas, K. Siemienski, R. Schwenzer, G. Schubert, T. Weiss, M. Grell, and P. Scheurich.** 1998. Dominant-negative FADD inhibits TNFR60-, Fas/Apo-1- and TRAIL-R/Apo2-mediated cell death but not gene induction. Curr. Biol. **8:**113–116.
29. **Walczak, H., M. A. Degli-Esposti, R. S. Johnson, P. J. Smolak, J. Y. Waugh, N. Boiani, M. S. Timour, M. J. Gerhart, K. A. Schooley, C. A. Smith, R. G. Goodwin, and C. T. Rauch.** 1997. TRAIL-R2: a novel apoptosis-mediating receptor for TRAIL. EMBO J. **16:**5386–5397.
30. **Wang, G. H., J. Bertin, Y. Wang, D. A. Martin, J. Wang, K. J. Tomaselli, R. C. Armstrong, and J. I. Cohen.** 1997. Bovine herpesvirus 4 BORFE2 protein inhibits Fas- and tumor necrosis factor receptor 1-induced apoptosis and contains death effector domains shared with other gamma-2-herpesviruses. J. Virol. **71:**8928–8932.
31. **Zhang, J., D. Cado, A. Chen, N. H. Kabra, and A. Winoto.** 1998. Fas-mediated apoptosis and activation-induced T-cell proliferation are defective in mice lacking FADD/Mort1. Nature **392:**296–299.

JOURNAL OF VIROLOGY, Oct. 2000, p. 9562–9570 Vol. 74, No. 20
0022-538X/00/$04.00+0

Reovirus-Induced G_2/M Cell Cycle Arrest Requires σ1s and Occurs in the Absence of Apoptosis

GEORGE J. POGGIOLI,[1] CHRISTOPHER KEEFER,[2] JODI L. CONNOLLY,[3,4] TERENCE S. DERMODY,[2,3,4] AND KENNETH L. TYLER[1,5,6,7,8]*

Departments of Neurology,[5] Medicine,[6] Microbiology,[1] and Immunology,[7] University of Colorado Health Sciences Center, and Neurology Service, Denver Veterans Affairs Medical Center,[8] Denver, Colorado 80220, and Departments of Pediatrics[2] and Microbiology and Immunology[3] and Elizabeth B. Lamb Center for Pediatric Research,[4] Vanderbilt University School of Medicine, Nashville, Tennessee 37232

Received 1 May 2000/Accepted 18 July 2000

Serotype-specific differences in the capacity of reovirus strains to inhibit proliferation of murine L929 cells correlate with the capacity to induce apoptosis. The prototype serotype 3 reovirus strains Abney (T3A) and Dearing (T3D) inhibit cellular proliferation and induce apoptosis to a greater extent than the prototype serotype 1 reovirus strain Lang (T1L). We now show that reovirus-induced inhibition of cellular proliferation results from a G_2/M cell cycle arrest. Using T1L × T3D reassortant viruses, we found that strain-specific differences in the capacity to induce G_2/M arrest, like the differences in the capacity to induce apoptosis, are determined by the viral S1 gene. The S1 gene is bicistronic, encoding the viral attachment protein σ1 and the nonstructural protein σ1s. A σ1s-deficient reovirus strain, T3C84-MA, fails to induce G_2/M arrest, yet retains the capacity to induce apoptosis, indicating that σ1s is required for reovirus-induced G_2/M arrest. Expression of σ1s in C127 cells increases the percentage of cells in the G_2/M phase of the cell cycle, supporting a role for this protein in reovirus-induced G_2/M arrest. Inhibition of reovirus-induced apoptosis failed to prevent virus-induced G_2/M arrest, indicating that G_2/M arrest is not the result of apoptosis related DNA damage and suggests that these two processes occur through distinct pathways.

Reovirus infection of cultured cells results in inhibition of cellular proliferation (10, 17–19, 21, 24–27, 38, 40, 41, 44). Serotype 3 prototype strains type 3 Abney (T3A) and type 3 Dearing (T3D) inhibit cellular DNA synthesis to a greater extent than the serotype 1 prototype strain type 1 Lang (T1L) (40, 44). Studies using T1L × T3A and T1L × T3D reassortant viruses indicate that the S1 gene is the primary determinant of DNA synthesis inhibition (40, 44). Earlier studies suggested that reovirus-induced inhibition of cellular proliferation results from inhibition of the initiation of DNA synthesis, consistent with a G_1-S transition block (10, 19, 26, 27, 38).

Reovirus infection also results in apoptosis (11, 36, 37, 44, 45). Reovirus strains T3A and T3D induce apoptosis to substantially greater extent than T1L (44, 45). A significant correlation exists between the capacities of both T1L × T3A (r = 0.937) and T1L × T3D (r = 0.772) reassortant viruses and reovirus field isolate strains (r = 0.851) to inhibit cellular proliferation and induce apoptosis (44). Like strain-specific differences in DNA synthesis inhibition, strain-specific differences in apoptosis induction also segregate with the S1 gene (36, 44, 45).

The viral S1 gene segment is bicistronic, encoding the viral attachment protein, σ1, and a non-virion-associated protein with no known function, σ1s, from overlapping reading frames (20, 30, 39). Using a σ1s-deficient virus strain, it was shown that σ1s is not required for reovirus growth in cell culture and is dispensable for the induction of apoptosis (37). These observations in conjunction with the genetic mapping studies suggest that σ1 is the primary determinant of strain-specific differences in apoptosis induction. The S1 gene product associated with reovirus-induced inhibition of cellular DNA synthesis has not been identified.

We conducted experiments to further investigate the relationship between reovirus-induced cellular DNA synthesis inhibition and apoptosis. We found that inhibition of cellular proliferation in response to reovirus infection is caused by an arrest in the G_2/M phase of the cell cycle. Reovirus strains differ in the capacity to induce G_2/M arrest, and we used reassortant viruses to demonstrate that these differences segregate with the S1 gene. A reovirus σ1s mutant fails to induce G_2/M arrest but retains the capacity to induce apoptosis. Inducible expression of σ1s results in the accumulation of cells in G_2/M phase. Inhibition of reovirus-induced apoptosis does not affect reovirus-induced G_2/M arrest. These results indicate that the σ1s protein is required for reovirus-induced G_2/M arrest and suggest that reovirus-induced inhibition of cellular proliferation and induction of apoptosis involve independent pathways.

MATERIALS AND METHODS

Cells and viruses. Spinner-adapted mouse L929 cells (ATCC CCL1) were grown in Joklik's modified Eagle's minimal essential medium (JMEM) supplemented to contain 5% heat-inactivated fetal bovine serum (Gibco BRL, Gaithersburg, Md.) and 2 mM L-glutamine (Gibco). Human embryonic kidney (HEK293) cells (ATCC CRL1573), Madin-Darby canine kidney (MDCK) cells (ATCC CCL34), C127 cells (ATCC CRL1616), and HeLa cells (ATCC CCL2) were grown in Dulbecco's modified Eagle's medium (DMEM) supplemented to contain 10% heat-inactivated fetal bovine serum (HEK293, MDCK, and C127) or 10% non-heat-inactivated fetal bovine serum (HeLa), 2 mM L-glutamine, and 100 U of penicillin and 100 μg of streptomycin per ml (Gibco). IκB-ΔN2 cells are HEK293 cells expressing a strong dominant-negative IκB mutant lacking the phosphorylation sites that regulate signal-dependent activation of NF-κB (7).

Reovirus strains T1L, T3A, and T3D are laboratory stocks. T1L × T3D reassortant viruses were grown from stocks originally isolated by Kevin Coombs, Bernard Fields, and Max Nibert (4, 9). The reovirus field-isolate strain type 3 clone 84 (T3C84) was isolated from a human host, and T3C84-MA was isolated

* Corresponding author. Mailing address: Department of Neurology (B-182), University of Colorado Health Sciences Center, 4200 E. 9th Ave., Denver, CO 80262. Phone: (303) 393-2874. Fax: (303) 393-4686. E-mail: Ken.Tyler@UCHSC.edu.

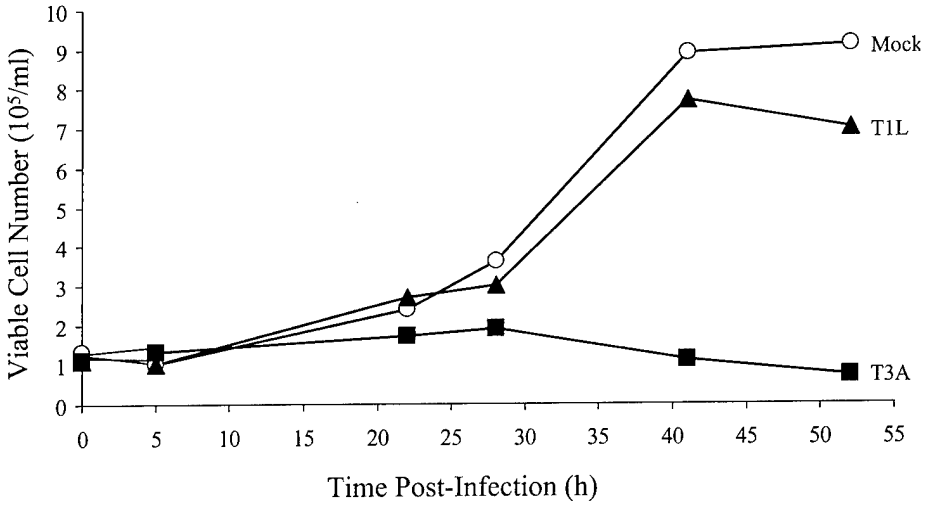

FIG. 1. Reovirus inhibits cellular proliferation. Asynchronous, subconfluent monolayers of L929 cells were either mock infected (circles) or infected with T1L (triangles) or T3A (squares) at an MOI of 100 PFU per cell. Cells were harvested at the indicated times postinfection and counted. Cells that excluded trypan blue were scored as viable. Results are presented as the number of viable cells $\times 10^5$ per ml. The results from a representative experiment of three independent experiments are shown.

as previously described (6, 12). Viral strains were plaque purified and passaged two to three times in L929 cells to generate working stocks as previously described (43).

Isolation and characterization of T3C84-MA/σ1s+. T3C84-MA/σ1s+ was isolated following serial passage of T3C84 in MEL cells as previously described (6). To isolate a sialic acid binding MEL cell-adapted variant derived from T3C84 that retains the capacity to express σ1s, virus isolates from a fifth-passage murine erythroleukemia (MEL) cell lysate stock were plaque purified twice on L929 cell monolayers. Plaques were amplified twice in L929 cell cultures and used to infect L929 cells (10^7) at a multiplicity of infection (MOI) of 10 PFU per cell. Cytoplasmic extracts were prepared 24 h following infection as previously described (8). Protein (100 μg) was electrophoresed in a 14% sodium dodecyl sulfate-polyacrylamide gel and transferred to a nitrocellulose membrane. An immunoblot for σ1s was performed as previously described (37). The S1 gene of a fifth-passage isolate that expresses σ1s, termed T3C84-MA/σ1s+, was sequenced as previously described (6). T3C84-MA/σ1s+ contains the mutation at nucleotide 616 that results in a tryptophan-to-arginine substitution at residue 202 of the σ1 protein, which is also present in the S1 gene of T3C84-MA and confers the capacity to bind sialic acid but does not contain the mutation that results in the introduction of a stop codon following amino acid six in the σ1s protein.

Cellular proliferation. L929 cells were seeded in six-well plates (Costar, Cambridge, Mass.) at 10^5 cells per well in a volume of 2.5 ml in JMEM supplemented to contain nonessential amino acids, 5% fetal bovine serum, 2 mM L-glutamine, 100 U of penicillin per ml, and 100 μg of streptomycin per ml. After 24 h of incubation, when cells were 10 to 20% confluent, the medium was removed, and cells were infected with viral strains at an MOI of 100 PFU per cell in a volume of 100 μl at 37°C for 1 h. After viral infection, 2.5 ml of fresh medium was added to each well. At various times postinfection, cells were harvested, resuspended in 2 ml of phosphate-buffered saline (PBS), and counted using a hemacytometer. Cell viability was determined by trypan blue exclusion. Results are presented as the viable cell numbers per milliliter.

Flow cytometry. L929, HEK293, MDCK, and HeLa cells were seeded in either 12-well plates (Costar) at 10^5 cells per well in a volume of 1 ml per well or 24-well plates (Costar) at 3.7×10^4 cells per well in a volume of 0.5 ml per well and then infected with reovirus as described above. Cells were harvested, washed once with PBS, and stained at 4°C overnight with Krishan's stain containing 3.8 mM trisodium citrate (Sigma Chemical Co., St. Louis, Mo.), 70 μM propidium iodide (Sigma), 0.01% Nonidet P-40 (Sigma), and 0.01 mg of RNase A (Boehringer Mannheim Co., Indianapolis, Ind.) per ml (33). Cell cycle analysis was performed using a Coulter Epics XL flow cytometer (Beckman-Coulter, Hialeah, Fla.). Alignment of the instrument was verified daily using DNA check beads (Coulter). Peak versus integral gating was used to exclude doublet events from the analysis. Data were collected for 10,000 events. The Modfit LT program (Verity Software House, Topsham, Maine) was used for cell cycle modeling.

Cell synchronization. L929 cells were seeded in 24-well plates at 3.7×10^4 cells per well in a volume of 0.5 ml per well. After 24 h, cells were treated with 1 μM amethopterin (methotrexate) (Sigma) and 50 μM adenosine (Sigma) for 16 h. Cells were washed twice with PBS, infected with reovirus, and incubated with fresh JMEM supplemented to contain 5% heat-inactivated fetal bovine serum, 2 mM L-glutamine, and 2 mg of thymidine (Sigma) per ml. At various times after infection, cells were harvested, washed once with PBS, and stained at 4°C overnight with Krishan's stain as described above.

Quantitation of apoptosis by acridine orange staining. L929, HEK293, MDCK, and HeLa cells were seeded and infected with reovirus as described above. The percentage of apoptotic cells was determined at 48 h postinfection as previously described (16, 45). Cells were harvested, washed once with PBS, resuspended in 25 μl of cell culture medium, and stained with 1 μl of a dye solution containing 100 μg of acridine orange (Sigma) per ml and 100 μg of ethidium bromide (Sigma) per ml. Cells were examined by epifluorescence microscopy (Nikon Labophot-2; B-2A filter; excitation, 450 to 490 nm; barrier, 520 nm; dichroic mirror, 505 nm) and scored as apoptotic if their nuclei contained uniformly stained condensed or fragmented chromatin (16, 45).

Apoptosis inhibitors. L929 cells were seeded in 24-well plates at 3.7×10^4 cells per well in a volume of 0.5 ml per well. After 24 h of incubation, cells were incubated with the calpain inhibitor PD150606 (Parke-Davis Pharmaceutical Research, Ann Arbor, Mich.) (50 μM, L929 cell), the caspase 3 inhibitor DEVD-CHO (Clontech, Palo Alto, Calif.) (100 μM, HEK293), or anti-TRAIL antibody (Affinity Bioreagents, Golden, Colo.) (30 μM, HEK293) for 1 h. Cells were then infected with T3A at an MOI of 100 PFU per cell at 37°C for 1 h. Following infection, media containing the apoptosis inhibitor was added. Cells were harvested and analyzed for either apoptosis or cell cycle arrest at 48 h postinfection.

Inducible expression of σ1s. C127 stable transformants expressing T3D σ1s (BPX-6) from the mouse metallothionein promoter and vector control (BPV-12) were provided by Aaron Shatkin (21). BPX-6 and BPV-12 cells were seeded in 24-well plates at 3.0×10^4 cells per well in a volume of 0.5 ml per well. After 24 h of incubation, cells were incubated with 1 μM $CdCl_2$ to induce σ1s expression (22) and harvested at various times postinduction for cell cycle analysis.

RESULTS

Reovirus strains T1L and T3A differ in the capacity to inhibit cellular proliferation. We have previously shown that T1 and T3 reovirus strains differ in the capacity to inhibit cellular DNA synthesis as measured by [^{3}H]thymidine incorporation (40, 44). To determine whether reovirus-induced DNA synthesis inhibition is associated with inhibition of cellular proliferation, we infected L929 cells with either T1L or T3A at an MOI of 100 PFU per cell. At various intervals after infection, viable cells were counted (Fig. 1). Infection with T3A resulted in complete inhibition of cellular proliferation. A modest reduction in proliferation was observed for cells infected with T1L compared to mock-infected controls. Therefore, strain-specific differences in inhibition of cellular proliferation parallel those previously reported for DNA synthesis inhibition.

T3 reoviruses induce G_2/M arrest. To identify the phase in the cell cycle that T3 reoviruses inhibit cellular proliferation,

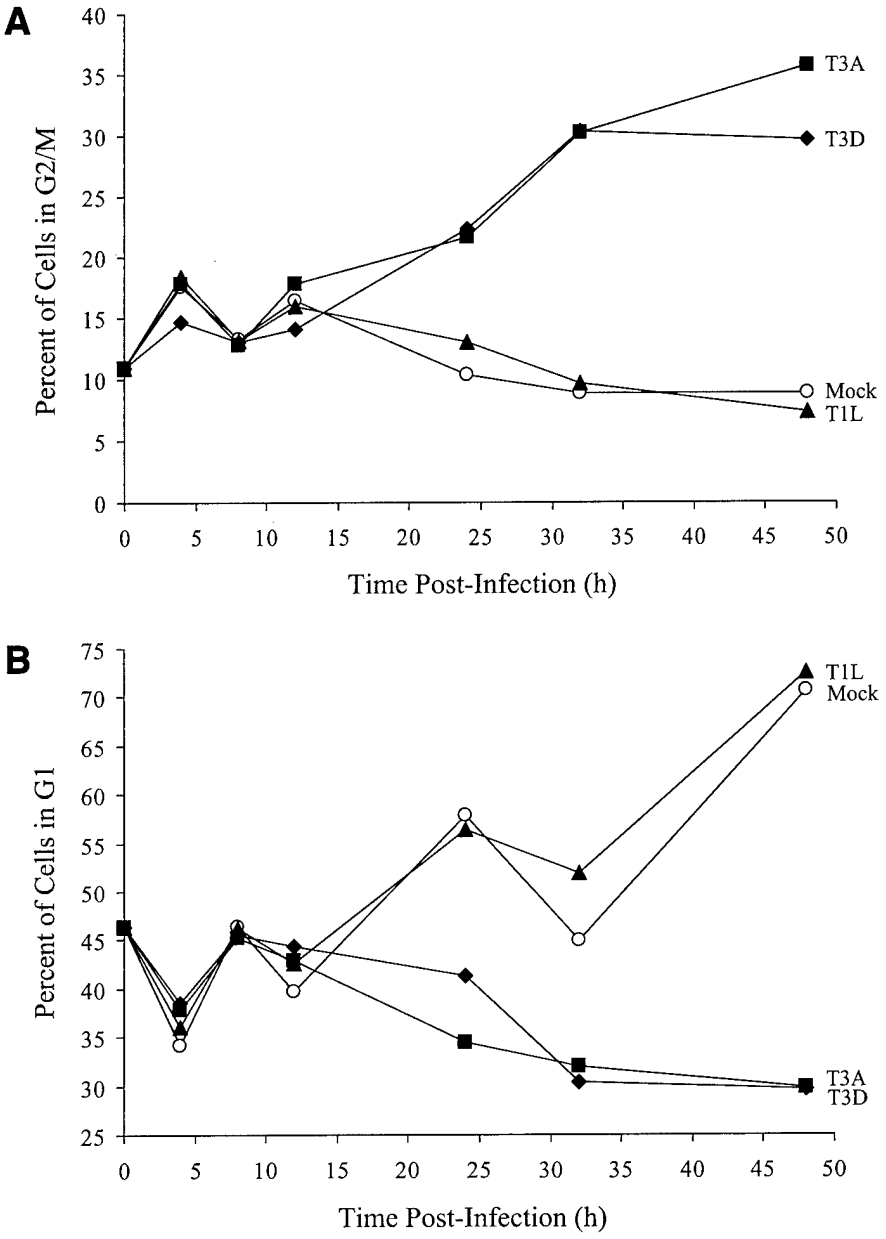

FIG. 2. T3 reovirus induces an increase in the percentage of cells in the G_2/M phase of the cell cycle. Asynchronous, subconfluent monolayers of L929 cells were either mock infected (circles) or infected with T1L (triangles), T3A (squares), or T3D (diamonds) at an MOI of 100 PFU per cell. Cells were harvested at the indicated times postinfection, stained with Krishan's stain, and analyzed for DNA content using flow cytometry. Results are presented as the percentage of cells in G_2/M phase (A) or G_1 phase (B) of the cell cycle. Results of a representative experiment of three independent experiments are shown. (C) L929 cells were synchronized with 1 μM methotrexate and 50 μM adenosine for 16 h. Cells were released using fresh media containing 2 mg of thymidine per ml and either mock infected or infected with T1L or T3A at an MOI of 100 PFU per cell. Cells were harvested at the indicated times postinfection, stained with Krishan's stain, and analyzed for DNA content using flow cytometry. Results are presented as the cell cycle distribution following either mock, T1L, or T3A infection at the indicated times postinfection.

we analyzed reovirus-infected cells using flow cytometry. L929 cells were infected with T1L, T3A, or T3D at an MOI of 100 PFU per cell and stained with Krishan's stain (33) containing propidium iodide to determine cellular DNA content at various intervals postinfection. The results were converted to the percentage of cells in G_2/M phase of the cell cycle using Modfit LT software (Fig. 2). Infection with either T3A or T3D resulted in a substantial increase in the percentage of cells in the G_2/M phase of the cell cycle compared to T1L-infected or mock-infected cells by 24 h postinfection (Fig. 2A). There also was a corresponding decrease in the percentage of cells in G_1 phase following infection with either T3A or T3D compared to T1L-infected or mock-infected cells (Fig. 2B). To confirm these results, L929 cells were synchronized with methotrexate prior to reovirus infection and assessed for cell cycle progression (Fig. 2C). Similar to findings with unsynchronized cells, T3A induced a significant increase in the proportion of cells in the G_2/M phase of the cell cycle compared to T1L or mock infection. The increase in the proportion of cells in G_2/M was first seen at 12 h postinfection and was maintained throughout the observation period (48 h). These findings indicate that the inhibition of proliferation induced by T3 reoviruses is caused by a block in the G_2/M phase of the cell cycle. Following T1L or mock infection, cells traverse the cell cycle, proliferate, and

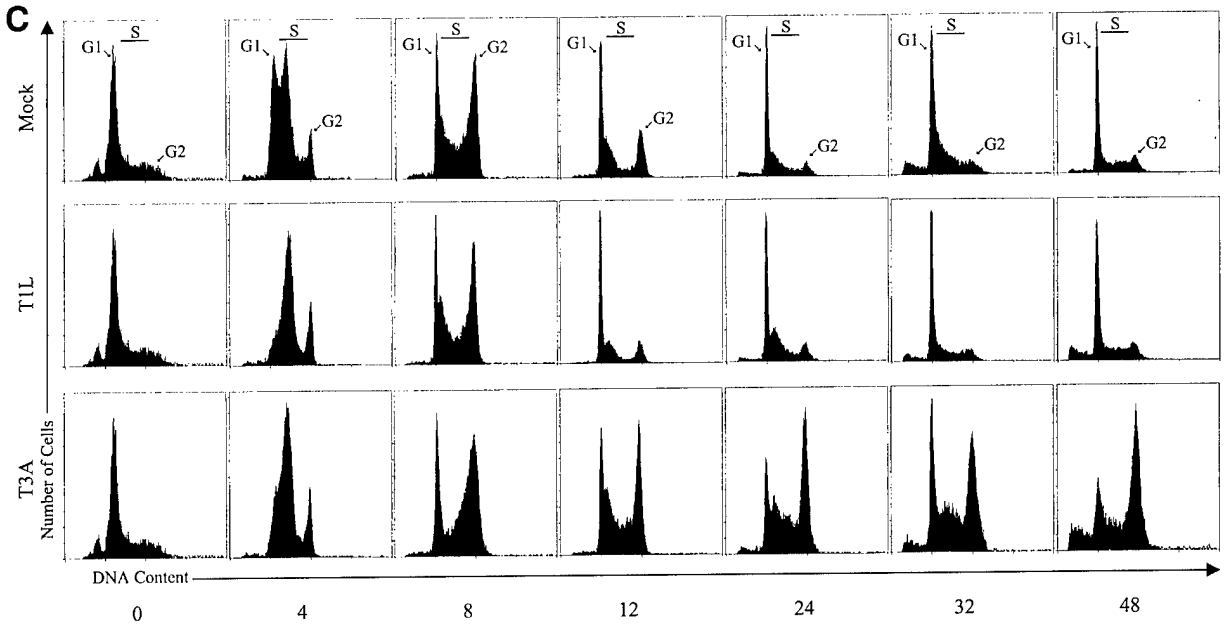

FIG. 2—*Continued.*

reenter the cell cycle. Conversely, T3-infected cells enter the cell cycle, stall in G_2/M phase, and do not proliferate.

T3 reovirus-induced G_2/M arrest is dose dependent. To investigate the relationship between MOI and the induction of G_2/M arrest, we infected L929 cells with T3A at MOIs of 1, 10, and 100 PFU per cell. Cells were harvested at 48 h postinfection, stained with Krishan's stain (33), and analyzed for DNA content by flow cytometry (Fig. 3). T3A infection induced a greater percentage of cells in G_2/M than mock infection at each MOI tested, and the effect was dose dependent.

G_2/M arrest occurs in a variety of cell lines following T3 reovirus infection. To determine whether the capacity of reovirus to block cell cycle progression is cell type dependent, L929, MDCK, C127, HEK293, and HeLa cells were either mock infected or infected with T1L or T3A at an MOI of 100 PFU per cell. Cells were harvested at 48 h postinfection, stained with Krishan's stain (33), and analyzed for DNA content by flow cytometry (Fig. 4). T3A infection induced a greater percentage of cells in G_2/M than either T1L or mock infection in all cell lines tested. However, the magnitude of the strain-specific difference was greatest in L929 (Fig. 4A), MDCK (Fig. 4B), and C127 (Fig. 4C) cells. Therefore, reovirus-induced G_2/M arrest is not cell type specific and likely requires non-cell-type-specific factors to mediate G_2/M arrest.

T3 reovirus G_2/M arrest phenotype is dominant. To determine whether G_2/M arrest resulting from T3 reovirus infection could be overcome by T1 reovirus infection, we coinfected L929 cells with equivalent MOIs of T1L and T3A and measured the percentage of cells in G_2/M by flow cytometry at 48 h postinfection. The percentage of cells in G_2/M after coinfection with T1L and T3A was identical to that of T3A alone and significantly greater than that of T1L alone (Fig. 5). These results indicate that the G_2/M arrest phenotype of T3 reovirus is dominant.

G_2/M arrest by T1L × T3D reassortant viruses. To identify viral genes associated with differences in the capacity of T1L and T3D to induce G_2/M arrest, we tested 12 T1L × T3D reassortant viruses for the capacity to induce G_2/M arrest in unsynchronized and synchronized L929 cells (Table 1). The results demonstrate a significant association between the capacity of reassortant viruses to induce G_2/M arrest in unsynchronized L929 cells and the S1 gene segment (Student t test, $P = 0.004$; Mann-Whitney, $P = 0.007$). No other viral genes were significantly associated with G_2/M arrest in this analysis (t test and Mann-Whitney, all $P > 0.05$). However, when L929 cells were synchronized prior to infection, the results demonstrate a significant association between the capacity of reassortant viruses to induce G_2/M arrest and the derivation of the S1 gene segment (Student t test, $P = 0.007$; Mann-Whitney, $P = 0.016$) and the M2 gene segment (Student t test, $P = 0.007$; Mann-Whitney, $P = 0.016$). We used parametric stepwise linear regression analysis to determine whether the S1 and M2

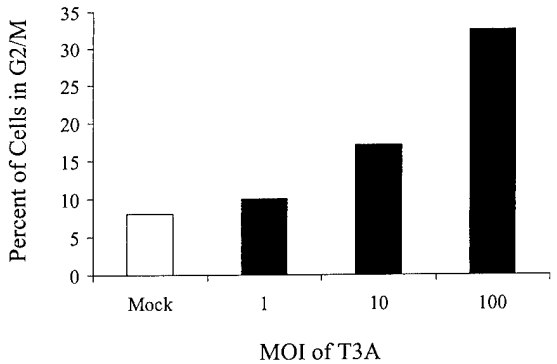

FIG. 3. G_2/M arrest induced by T3 reovirus is dose dependent. Asynchronous, subconfluent monolayers of L929 cells were either mock infected or infected with T3A at MOIs of 1, 10, and 100 PFU per cell. Cells were harvested at 48 h postinfection, stained with Krishan's stain, and analyzed for DNA content using flow cytometry. Results are presented as the percentage of cells in G_2/M phase.

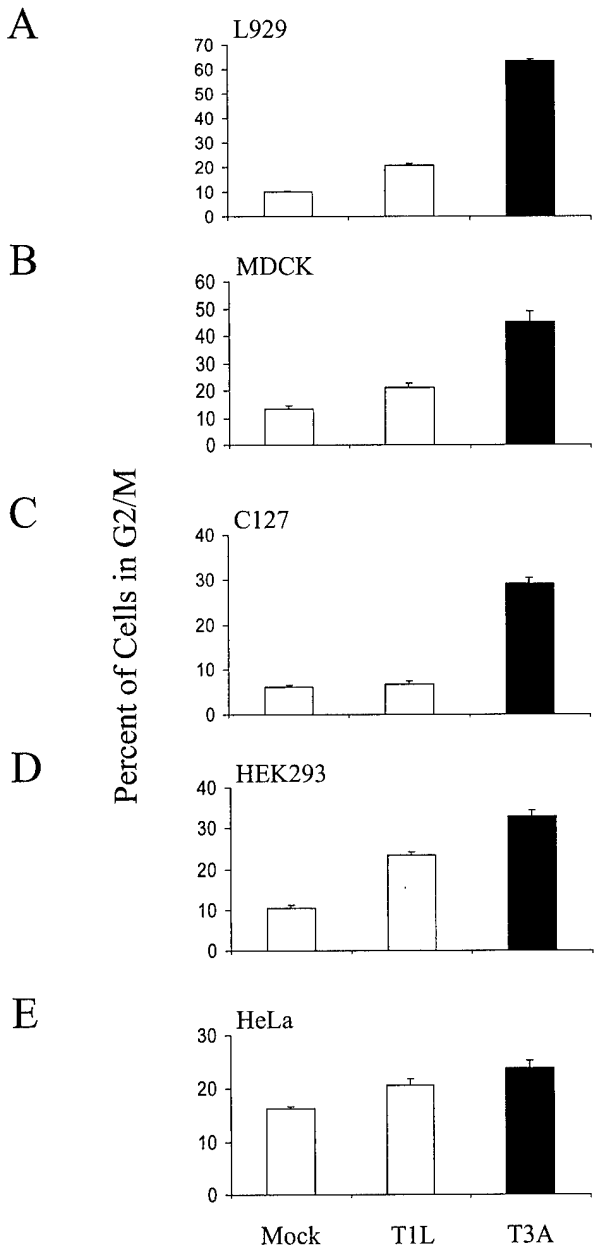

FIG. 4. T3 reovirus induces G_2/M arrest in murine, canine, and human cells. Asynchronous, subconfluent monolayers of L929 (A), MDCK (B), C127 (C), HEK293 (D), and HeLa (E) cells were either mock infected (white) or infected with T1L (gray) or T3A (black) at an MOI of 100 PFU per cell. Cells were harvested at 48 h postinfection, stained with Krishan's stain, and analyzed for DNA content using flow cytometry. Results are presented as the mean percentage of cells in G_2/M phase for three independent experiments. The error bars indicate the standard errors of the mean. A significantly greater percentage of T3A-infected cells were in G_2/M than mock-infected cells in all cell lines tested ($P < 0.01$ to 0.001). A significantly greater percentage of T3A-infected cells were in G_2/M than T1L-infected cells in all cell lines tested ($P < 0.01$ to 0.001) except HeLa. A significantly greater percentage of T1L-infected cells were in G_2/M than mock-infected cells in L929 and HEK293 cells ($P < 0.001$).

genes contributed independently to the capacity of T1L × T3D reassortant viruses to induce G_2/M arrest. We obtained R^2 values of 91.3 and 96.7% for the regression equation using all 10 reovirus genes for unsynchronized and synchronized L929 cells, respectively: 52.2% ($P = 0.004$) for S1 in unsynchronized L929 cells and 84.9% ($P < 0.001$) for S1 and M2 and 53.5% ($P = 0.007$) for the S1 gene alone in synchronized L929 cells. These results indicate that the S1 gene segment is the primary determinant of strain-specific differences in reovirus-induced G_2/M arrest.

G_2/M arrest induced by T3 reovirus. The S1 gene segment encodes two proteins, the viral attachment protein σ1 and the nonstructural protein σ1s (20, 30, 39). To determine whether σ1s is required for G_2/M arrest, we infected L929 cells with reovirus strain T3C84-MA, which does not express σ1s (37) (Fig. 6). The percentage of cells in G_2/M following infection with T3C84-MA was significantly less than the percentage of cells in G_2/M following infection with the σ1s-expressing parental virus, T3C84. T3C84-MA failed to induce G_2/M arrest, even at an MOI 10-fold greater than T3C84. T3C84-MA/σ1s+, a MEL-cell-adapted strain that does not contain the point mutation in S1 that results in an early stop codon in σ1s but contains the tryptophan-to-arginine substitution at position 202 in σ1, induced a level of G_2/M arrest that was significantly greater than T3C84-MA at an MOI of 100 in L929 cells ($P = 0.002$; percentage of cells in G_2/M following T3C84-MA/σ1s+ infection, 23.02 ± 1.1%). These findings indicate that functional σ1s is required for reovirus-induced G_2/M arrest.

Expression of T3 σ1s induces an increase in the percentage of cells in G_2/M phase. To determine whether σ1s alone is sufficient to induce the accumulation of cells in G_2/M phase, we analyzed the DNA content of C127 cells engineered to express the T3D σ1s protein. Expression of σ1s from the mouse metallothionein promoter was induced by 1 μM $CdCl_2$ (21) however, levels of σ1s were substantially less than levels found following natural virus infection (data not shown). The percentage of cells in G_2/M following induction was significantly greater in cells expressing σ1s than in vector control cells at 45 and 55 h postinduction ($P = 0.03$ and $P = 0.005$, respectively) (Fig. 7). These results provide additional evidence that σ1s expression is involved in the accumulation of cells in the G_2/M phase of the cell cycle.

Reovirus-induced apoptosis can be dissociated from reovirus-induced G_2/M arrest. Previous studies indicate that the capacity of reovirus to inhibit DNA synthesis correlates with the capacity to induce apoptosis (44). Like strain-specific differences in reovirus-induced G_2/M arrest, differences in the capacity of reovirus strains to inhibit DNA synthesis and induce apoptosis are determined by the S1 gene (40, 44). To determine whether apoptosis-associated disruption of cellular DNA is required for reovirus-induced inhibition of cellular proliferation, L929 cells or HEK293 cells were either mock infected or infected with T3A in the presence or absence of inhibitors of reovirus-induced apoptosis (7, 8, 11). Treatment of cells with the calpain inhibitor PD150606 (11), the caspase inhibitor DEVD-CHO (D. J. Kominsky, personal communication), or anti-TRAIL antibody (7) blocks reovirus-induced apoptosis, as does expression of an IκB mutant that blocks NF-κB activation (7, 8). G_2/M arrest was evaluated by flow cytometry at 48 h postinfection (Fig. 8). Treatment with the calpain inhibitor PD150606 (Fig. 8A), the caspase 3 inhibitor DEVD-CHO (Fig. 8B), or anti-TRAIL antibody (Fig. 8C) using conditions that inhibit reovirus-induced apoptosis, had no effect on T3A-induced G_2/M arrest, nor did inhibition of NF-κB by expression of a dominant-negative IκB (7, 8) (Fig. 8D). Therefore, inhibitors of reovirus-induced apoptosis do not inhibit reovirus-induced G_2/M arrest. These findings indicate that apoptosis induced DNA damage is not required for reovirus-induced G_2/M arrest.

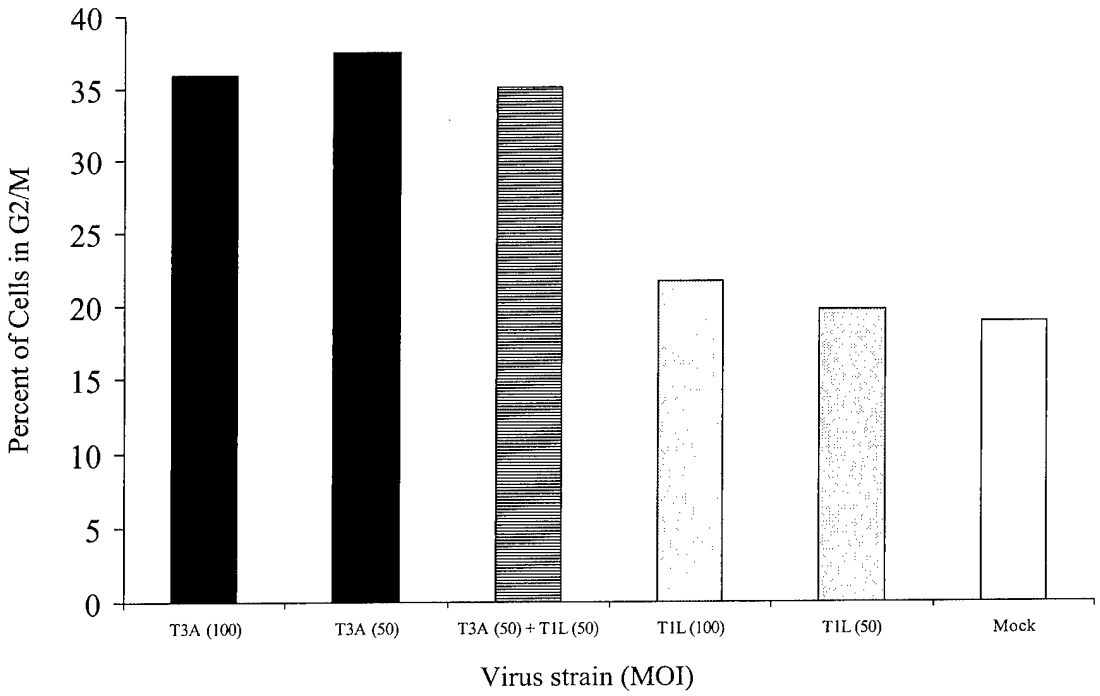

FIG. 5. T3A-induced G_2/M arrest phenotype is dominant. L929 cells were either mock infected (white), coinfected with equivalent MOIs of T1L and T3A (the MOI of each virus was 50 PFU per cell) (hatched), or infected with T1L (shaded) or T3A (solid) alone at MOIs of 50 or 100 PFU per cell. L929 cells were harvested at 48 h postinfection and analyzed using flow cytometry. The results are presented as the percentage of cells in the G_2/M phase of the cell cycle.

DISCUSSION

T3 reovirus strains inhibit host cell proliferation, as measured by cellular DNA synthesis inhibition, to a substantially greater extent than T1 reovirus strains (40, 44). It had been suggested, based on extrapolation of results obtained using [^{3}H]thymidine incorporation, that T3 reoviruses induce cell cycle arrest at the G_1-to-S transition. We now show, using flow cytometry to directly analyze cell cycle progression in reovirus-infected cells, that reovirus-induced inhibition of cellular pro-

TABLE 1. Capacities of T1L × T3D reassortant viruses to induce G_2/M arrest

Virus strain	Genome segment[a]										% Cells in G_2/M[b]	
	L1	L2	L3	M1	M2	M3	S1	S2	S3	S4	Unsynchronized	Synchronized
EB138	3D	1L	1L	3D	3D	1L	3D	3D	1L	1L	ND	24.56
EB28	3D	3D	1L	3D	3D	3D	3D	1L	3D	3D	38.13	28.59
KC150	3D	1L	1L	1L	3D	1L	3D	3D	1L	3D	33.91	36.47
EB97	3D	3D	1L	3D	3D	3D	3D	3D	3D	1L	30.30	28.35
G2	1L	3D	1L	1L	1L	1L	3D	1L	1L	1L	29.09	13.92
H41	3D	3D	1L	1L	1L	3D	1L	1L	3D	1L	26.56	ND
T3D	3D	3D	3D	3D	3D	3D	3D	3D	3D	3D	25.71	38.51
H15	1L	3D	3D	1L	3D	3D	3D	3D	3D	1L	24.95	31.63
EB127	3D	3D	1L	1L	3D	1L	1L	3D	3D	1L	23.54	ND
H9	3D	3D	1L	3D	1L	1L	3D	3D	3D	3D	23.11	17.17
EB85	1L	1L	1L	1L	1L	3D	1L	3D	1L	1L	21.88	ND
T1L	1L	1L	1L	1L	1L	1L	1L	1L	1L	1L	19.23	5.56
EB145	3D	3D	3D	3D	3D	1L	1L	3D	3D	3D	15.72	14.72
EB121	3D	3D	1L	3D	1L	3D	1L	3D	3D	3D	14.98	9.45
EB1	1L	3D	1L	1L	3D	1L	1L	1L	3D	1L	11.89	16.19
Significance (P)[c]												
Unsynchronized L cells												
t test	0.30	0.84	0.60	0.85	0.46	0.36	**0.004**	0.78	0.58	0.66		
MW	0.30	1	0.77	0.95	0.41	0.38	**0.007**	0.80	0.73	0.85		
Synchronized L cells												
t test	0.25	1	0.27	0.73	**0.007**	0.16	**0.007**	0.18	0.67	0.53		
MW	0.28	1	0.28	0.76	**0.016**	0.2	**0.016**	0.21	0.57	0.48		

[a] The parental origin of each genome segment in the reassortants strains: 1L, genome segment derived from T1L; 3D, genome segment derived from T3D.
[b] Unsynchronized or synchronized L cells were infected with viral strains at an MOI of 100 PFU per cell and analyzed by flow cytometry at 48 h postinfection. ND, not determined.
[c] As determined by two-sample parametric Student t test (t test) and Mann-Whitney nonparametric analysis (MW). Values in boldface are statistically significant.

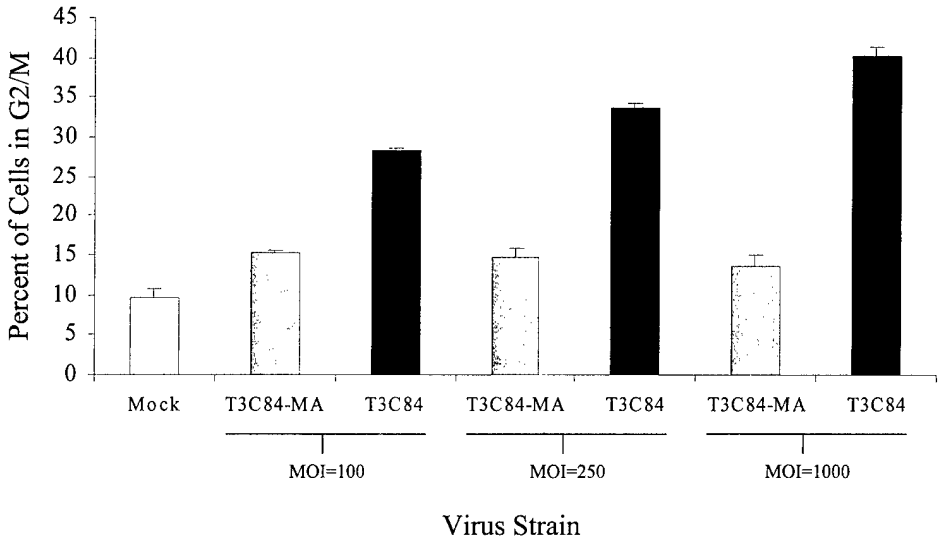

FIG. 6. Reovirus-induced G_2/M arrest requires σ1s. L929 cells were either mock infected (white) or infected with wild-type T3C84 (black) or σ1s-null mutant T3C84-MA (gray) at MOIs of 100, 250, or 1,000 PFU per cell. Cells were harvested 48 h postinfection, stained with Krishan's stain, and analyzed using flow cytometry. The results are presented as the mean percentage of cells in G_2/M phase of the cell cycle for six independent experiments at an MOI of 100 and three independent experiments at MOIs of 250 and 1,000. The error bars indicate the standard errors of the mean. A significantly greater percentage of T3C84-infected cells were in G_2/M than T3C84-MA-infected cells at each MOI tested ($P < 0.001$).

liferation results from G_2/M arrest. This effect is not cell type specific and is dominant in strains that block cell cycle progression.

Differences in the capacity of reovirus strains to inhibit cellular proliferation are determined by the viral S1 gene (40, 44). Our results indicate that the same is true for G_2/M arrest. The reovirus S1 gene is bicistronic, encoding the structural protein σ1 and the nonstructural protein σ1s using overlapping, alternative reading frames (20, 30, 39). As a result of this coding strategy, there is no sequence similarity between the σ1 and σ1s proteins (12). To determine which of the two S1-encoded proteins are required for G_2/M arrest, we examined the capacity of the σ1s null mutant T3C84-MA to induce G_2/M arrest. T3C84-MA and its σ1s expressing parent, T3C84, produce equivalent yields of viral progeny in L929 cells, and both viruses are equally effective in inducing apoptosis (37). However,

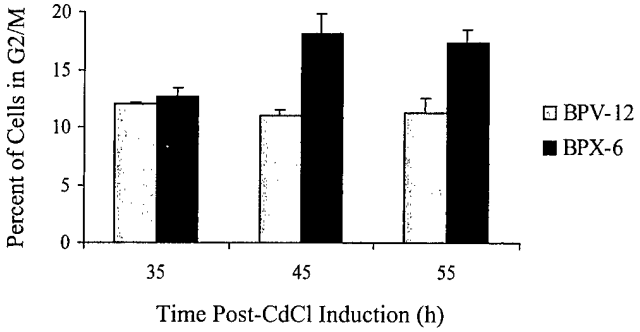

FIG. 7. σ1s expression induces an increase in the percentage of cells in G_2/M phase. C127 cells stably transfected with σ1s (BPX-6) or vector control (BPV-12) under the control of the mouse metallothioncin promoter were induced with $CdCl_2$, harvested at the indicated times postinduction, and analyzed for DNA content by flow cytometry. The results are presented as the mean percentage of cells in the G_2/M phase of the cell cycle for three to six independent experiments. The error bars indicate the standard errors of the mean. The percentage of cells in G_2/M was significantly greater in the σ1s-expressing cells than in the vector-control cells at 45 h ($P = 0.03$, $n = 4$) and 55 h ($P = 0.005$, $n = 6$) postinduction.

T3C84-MA fails to induce G_2/M arrest. This finding suggests that σ1s is required for blockade of cell cycle progression following T3 reovirus infection. It is also possible that differences in the capacity of T3C84 and T3C84-MA to induce cell cycle arrest are influenced by other sequence differences. The mutation in the S1 gene that introduces a termination codon in the σ1s open reading frame also results in a lysine-to-isoleucine substitution at residue 26 in the deduced amino acid sequence of σ1. The T3C84-MA S1 gene also contains an additional mutation that results in a tryptophan-to-arginine substitution at residue 202 in σ1, which determines the capacity of this strain to bind sialic acid. To exclude the possibility that sialic acid binding influences cell cycle arrest, we isolated and characterized an additional T3C84-MA variant, T3C84-MA/σ1s+, that binds to sialic acid and expresses σ1s. In contrast to T3C84-MA, which binds sialic acid but does not express σ1s, T3C84-MA/σ1s+ induces G_2/M arrest. Therefore, it is unlikely that the capacity to bind sialic acid influences the efficiency of cell cycle arrest induced by T3 reoviruses.

To corroborate findings made using viruses that vary in σ1s expression, we also tested the capacity of cells engineered to express σ1s under the control of an inducible promoter to undergo cell cycle arrest. Following induction of σ1s expression, we observed an increase in the percentage of cells in the G_2/M phase of the cell cycle, which suggests that σ1s is capable of mediating cell cycle blockade at the G_2/M checkpoint. This observation suggests that the reovirus σ1s protein is similar to the human immunodeficiency virus (HIV) Vpr protein (2, 28, 31, 35) or the human papillomavirus (HPV) E2 protein (23), which similarly block cell cycle progression at the G_2/M boundary. Thus, our findings indicate that reovirus-induced G_2/M arrest requires σ1s and provide the first evidence of a functional role for this nonstructural protein.

We have previously shown that the capacity of reovirus to induce apoptosis correlates with the capacity to inhibit cellular proliferation and that both properties are determined by the viral S1 gene (44). Our results clearly show that G_2/M arrest can occur in cells treated with potent inhibitors of reovirus-

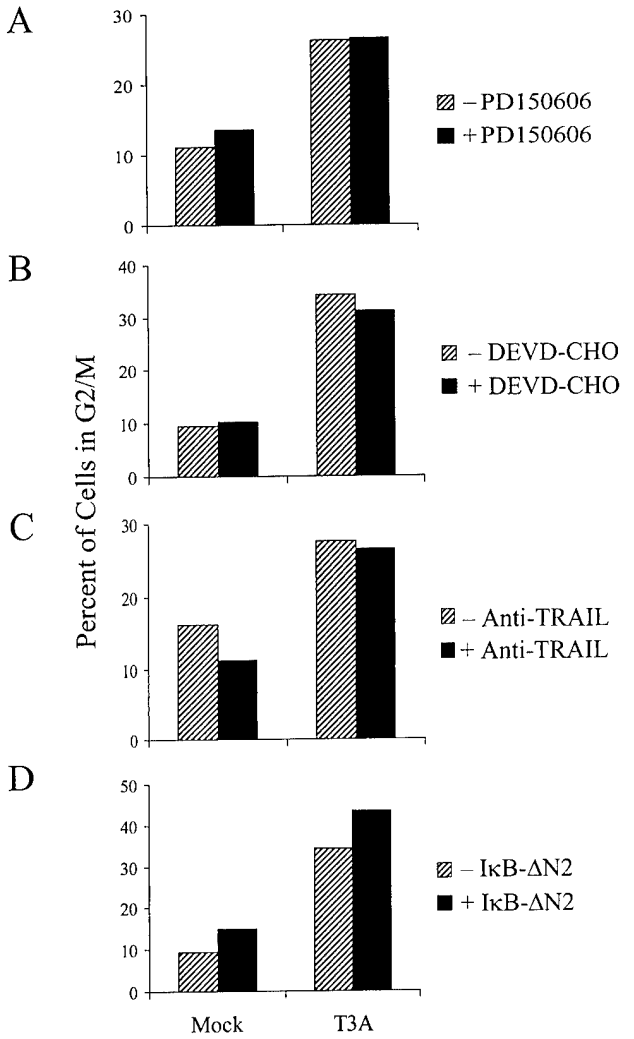

FIG. 8. Inhibitors of reovirus-induced apoptosis do not inhibit reovirus-induced G_2/M arrest. (A) Effect of calpain inhibitor PD150606 on T3A-induced G_2/M arrest. L929 cells were treated with either 25 μM calpain inhibitor PD150606 or an ethanol control and then either mock infected or infected with T3A at an MOI of 100 PFU per cell. (B) Effect of caspase 3 inhibitor DEVD-CHO on T3A-induced G_2/M arrest. HEK293 cells were treated with either 100 μM caspase 3 inhibitor DEVD-CHO or a dimethyl sulfoxide control and then either mock infected or infected with T3A at an MOI of 100 PFU per cell. (C) Effect of anti-TRAIL antibodies on T3A-induced G_2/M arrest. HEK293 cells were treated with either 30 μg of an anti-TRAIL antibody per ml or mock treated as a control and then either mock infected or infected with T3A at an MOI of 100 PFU per cell. (D) Effect of NF-κB inhibition on T3A-induced G_2/M arrest. HEK293 cells expressing a dominant-negative form of IκB (IκB-ΔN2) to inhibit NF-κB activation or untransfected HEK293 cells were either mock infected or infected with T3A at an MOI of 100 PFU per cell. In all cases, G_2/M arrest was assessed 48 h postinfection.

induced apoptosis. These findings indicate that the induction of G_2/M arrest and apoptosis by reovirus are functionally independent at some stage following infection. Moreover, although strain-specific differences in reovirus-induced G_2/M arrest and apoptosis induction segregate with the viral S1 gene, each property is determined by a different S1 gene product. Strain-specific differences in reovirus-induced G_2/M arrest are determined by σ1s, whereas differences in reovirus-induced apoptosis are determined by σ1 (36, 45). The induction of G_2/M arrest by HIV Vpr is apparently required for Vpr-induced apoptosis (42), whereas reovirus-induced apoptosis can occur in the absence of G_2/M arrest (37). These findings suggest that viruses may utilize different mechanisms to induce G_2/M arrest and apoptosis.

The G_2/M transition is regulated by the kinase cdc2/cdk1 (13–15, 32, 34). Expression of HIV Vpr (28, 35) or HPV E2 protein (23) results in inhibition or delayed activation of cdc2 kinase activity resulting in an accumulation of cells in the G_2/M phase of the cell cycle. In contrast, the baculovirus *Autographa californica* nuclear polyhydrosis virus (AcNPV) (3) and herpes simplex virus (HSV) (1, 29) induce G_2/M arrest by a mechanism that is cdc2 independent, since cells infected with either of these viruses maintain high levels of cdc2 kinase activity. HIV, HPV, AcNPV, and HSV require a nuclear phase to replicate, whereas reovirus replicates in the cytoplasm. T3 σ1s has been detected in the nucleus as well as in the cytoplasm following reovirus infection (5, 37), and it is possible that this nuclear localization is required for reovirus-induced G_2/M arrest. Future studies will be aimed at identifying which cell cycle regulatory proteins are involved in reovirus-induced cell cycle perturbation, the role of cellular localization of σ1s in this process, and the significance of cell cycle arrest in reovirus-induced cytopathology and pathogenesis.

ACKNOWLEDGMENTS

This work was supported by Public Health Service grant 1RO1AG14071 from the National Institute of Aging, Merit and REAP grants from the Department of Veterans Affairs, and a U.S. Army Medical Research and Material Command grant (USAMRMC 98293015) (K.L.T.). This work also was supported by Public Health Service grant AI38296 from the National Institute of Allergy and Infectious Diseases and the Elizabeth B. Lamb Center for Pediatric Research (T.S.D.).

The University of Colorado Cancer Center provided core flow cytometry facilities.

REFERENCES

1. **Advani, S. J., R. Brandimarti, R. R. Weichselbaum, and B. Roizman.** 2000. The disappearance of cyclins A and B and the increase in activity of the G(2)/M-phase cellular kinase cdc2 in herpes simplex virus 1-infected cells require expression of the alpha22/U(S)1.5 and U(L)13 viral genes. J. Virol. **74**:8–15.
2. **Bartz, S. R., M. E. Rogel, and M. Emerman.** 1996. Human immunodeficiency virus type 1 cell cycle control: Vpr is cytostatic and mediates G_2 accumulation by a mechanism which differs from DNA damage checkpoint control. J. Virol. **70**:2324–2331.
3. **Braunagel, S. C., R. Parr, M. Belyavskyi, and M. D. Summers.** 1998. *Autographa californica* nucleopolyhedrovirus infection results in Sf9 cell cycle arrest at G2/M phase. Virology **244**:195–211.
4. **Brown, E. G., M. L. Nibert, and B. N. Fields.** 1983. The L2 gene of reovirus serotype 3 controls the capacity to interfere, accumulate deletions and establish persistent infection, p. 275–287. *In* R. W. Compans and D. H. L. Bishop (ed.), Double-stranded RNA viruses. Elsevier, New York, N.Y.
5. **Ceruzzi, M., and A. J. Shatkin.** 1986. Expression of reovirus p14 in bacteria and identification in the cytoplasm of infected mouse L cells. Virology **153**:35–45.
6. **Chappell, J. D., V. L. Gunn, J. D. Wetzel, G. S. Baer, and T. S. Dermody.** 1997. Mutations in type 3 reovirus that determine binding to sialic acid are contained in the fibrous tail domain of viral attachment protein sigma1. J. Virol. **71**:1834–1841.
7. **Clarke, P., S. M. Meintzer, G. Spencer, C. Widmann, T. P. Garrington, G. L. Johnson, and K. L. Tyler.** 2000. Reovirus-induced apoptosis is mediated by TRAIL. J. Virol. **74**:8135–8139.
8. **Connolly, J. L., S. E. Rodgers, P. Clarke, D. W. Ballard, L. D. Kerr, K. L. Tyler, and T. S. Dermody.** 2000. Reovirus-induced apoptosis requires activation of transcription factor NF-κB. J. Virol. **74**:2981–2989.
9. **Coombs, K. M., B. N. Fields, and S. C. Harrison.** 1990. Crystallization of the reovirus type 3 Dearing core. Crystal packing is determined by the lambda 2 protein. J. Mol. Biol. **215**:1–5.
10. **Cox, D. C., and J. E. Shaw.** 1974. Inhibition of the initiation of cellular DNA synthesis after reovirus infection. J. Virol. **13**:760–761.
11. **Debiasi, R. L., M. K. Squier, B. Pike, M. Wynes, T. S. Dermody, J. J. Cohen, and K. L. Tyler.** 1999. Reovirus-induced apoptosis is preceded by increased cellular calpain activity and is blocked by calpain inhibitors. J. Virol. **73**:695–701.

12. **Dermody, T. S., M. L. Nibert, R. Bassel-Duby, and B. N. Fields.** 1990. Sequence diversity in S1 genes and S1 translation products of 11 serotype 3 reovirus strains. J. Virol. **64:**4842–4850.
13. **Draetta, G., and D. Beach.** 1988. Activation of cdc2 protein kinase during mitosis in human cells: cell cycle-dependent phosphorylation and subunit rearrangement. Cell **54:**17–26.
14. **Draetta, G., and J. Eckstein.** 1997. Cdc25 protein phosphatases in cell proliferation. Biochim. Biophys. Acta **1332:**M53–M63.
15. **Draetta, G., H. Piwnica-Worms, D. Morrison, B. Druker, T. Roberts, and D. Beach.** 1988. Human cdc2 protein kinase is a major cell-cycle regulated tyrosine kinase substrate. Nature **336:**738–744.
16. **Duke, R. C., and J. J. Cohen.** 1992. Morphological and biochemical assays of apoptosis, p. 3.17.1–3.17.16. *In* J. E. Coligan (ed.), Current protocols in immunology. Wiley, New York, N.Y.
17. **Duncan, M. R., S. M. Stanish, and D. C. Cox.** 1978. Differential sensitivity of normal and transformed human cells to reovirus infection. J. Virol. **28:**444–449.
18. **Ensminger, W. D., and I. Tamm.** 1969. Cellular DNA and protein synthesis in reovirus-infected L cells. Virology **39:**357–360.
19. **Ensminger, W. D., and I. Tamm.** 1969. The step in cellular DNA synthesis blocked by reovirus infection. Virology **39:**935–938.
20. **Ernst, H., and A. J. Shatkin.** 1985. Reovirus hemagglutinin mRNA codes for two polypeptides in overlapping reading frames. Proc. Natl. Acad. Sci. USA **82:**48–52.
21. **Fajardo, E., and A. J. Shatkin.** 1990. Expression of the two reovirus S1 gene products in transfected mammalian cells. Virology **178:**223–231.
22. **Fajardo, J. E., and A. J. Shatkin.** 1990. Translation of bicistronic viral mRNA in transfected cells: regulation at the level of elongation. Proc. Natl. Acad. Sci. USA **87:**328–332.
23. **Fournier, N., K. Raj, P. Saudan, S. Utzig, R. Sahli, V. Simanis, and P. Beard.** 1999. Expression of human papillomavirus 16 E2 protein in *Schizosaccharomyces pombe* delays the initiation of mitosis. Oncogene **18:**4015–4021.
24. **Gaulton, G. N., and M. I. Greene.** 1989. Inhibition of cellular DNA synthesis by reovirus occurs through a receptor-linked signaling pathway that is mimicked by antiidiotypic, antireceptor antibody. J. Exp. Med. **169:**197–211.
25. **Gomatos, P., and I. Tamm.** 1963. Macromolecular synthesis in reovirus-infected L cells. Biochim. Biophys. Acta **72:**651–653.
26. **Hand, R., W. D. Ensminger, and I. Tamm.** 1971. Cellular DNA replication in infections with cytocidal RNA viruses. Virology **44:**527–536.
27. **Hand, R., and I. Tamm.** 1974. Initiation of DNA replication in mammalian cells and its inhibition by reovirus infection. J. Mol. Biol. **82:**175–183.
28. **He, J., S. Choe, R. Walker, P. Di Marzio, D. O. Morgan, and N. R. Landau.** 1995. Human immunodeficiency virus type 1 viral protein R (Vpr) arrests cells in the G_2 phase of the cell cycle by inhibiting p34cdc2 activity. J. Virol. **69:**6705–6711.
29. **Hobbs, W. E., and N. A. DeLuca.** 1999. Perturbation of cell cycle progression and cellular gene expression as a function of herpes simplex virus ICP0. J. Virol. **73:**8245–8255.
30. **Jacobs, B. L., and C. E. Samuel.** 1985. Biosynthesis of reovirus-specified polypeptides: the reovirus s1 mRNA encodes two primary translation products. Virology **143:**63–74.
31. **Jowett, J. B., V. Planelles, B. Poon, N. P. Shah, M. L. Chen, and I. S. Chen.** 1995. The human immunodeficiency virus type 1 vpr gene arrests infected T cells in the G_2 + M phase of the cell cycle. J. Virol. **69:**6304–6313.
32. **King, R. W., P. K. Jackson, and M. W. Kirschner.** 1994. Mitosis in transition. Cell **79:**563–571.
33. **Krishan, A.** 1975. Rapid flow cytofluorometric analysis of mammalian cell cycle by propidium iodide staining. J. Cell Biol. **66:**188–193.
34. **Morla, A. O., G. Draetta, D. Beach, and J. Y. Wang.** 1989. Reversible tyrosine phosphorylation of cdc2: dephosphorylation accompanies activation during entry into mitosis. Cell **58:**193–203.
35. **Re, F., D. Braaten, E. K. Franke, and J. Luban.** 1995. Human immunodeficiency virus type 1 Vpr arrests the cell cycle in G_2 by inhibiting the activation of p34cdc2-cyclin B. J. Virol. **69:**6859–6864.
36. **Rodgers, S. E., E. S. Barton, S. M. Oberhaus, B. Pike, C. A. Gibson, K. L. Tyler, and T. S. Dermody.** 1997. Reovirus-induced apoptosis of MDCK cells is not linked to viral yield and is blocked by Bcl-2. J. Virol. **71:**2540–2546.
37. **Rodgers, S. E., J. L. Connolly, J. D. Chappell, and T. S. Dermody.** 1998. Reovirus growth in cell culture does not require the full complement of viral proteins: identification of a σ1s-null mutant. J. Virol. **72:**8597–8604.
38. **Roner, M. R., and D. C. Cox.** 1985. Cellular integrity is required for inhibition of initiation of cellular DNA synthesis by reovirus type 3. J. Virol. **53:**350–359.
39. **Sarkar, G., J. Pelletier, R. Bassel-Duby, A. Jayasuriya, B. N. Fields, and N. Sonenberg.** 1985. Identification of a new polypeptide coded by reovirus gene S1. J. Virol. **54:**720–725.
40. **Sharpe, A. H., and B. N. Fields.** 1981. Reovirus inhibition of cellular DNA synthesis: role of the S1 gene. J. Virol. **38:**389–392.
41. **Shaw, J. E., and D. C. Cox.** 1973. Early inhibition of cellular DNA synthesis by high multiplicities of infectious and UV-inactivated reovirus. J. Virol. **12:**704–710.
42. **Stewart, S. A., B. Poon, J. B. Jowett, and I. S. Chen.** 1997. Human immunodeficiency virus type 1 Vpr induces apoptosis following cell cycle arrest. J. Virol. **71:**5579–5592.
43. **Tyler, K. L., R. T. Bronson, K. B. Byers, and B. Fields.** 1985. Molecular basis of viral neurotropism: experimental reovirus infection. Neurology **35:**88–92.
44. **Tyler, K. L., M. K. Squier, A. L. Brown, B. Pike, D. Willis, S. M. Oberhaus, T. S. Dermody, and J. J. Cohen.** 1996. Linkage between reovirus-induced apoptosis and inhibition of cellular DNA synthesis: role of the S1 and M2 genes. J. Virol. **70:**7984–7991.
45. **Tyler, K. L., M. K. Squier, S. E. Rodgers, B. E. Schneider, S. M. Oberhaus, T. A. Grdina, J. J. Cohen, and T. S. Dermody.** 1995. Differences in the capacity of reovirus strains to induce apoptosis are determined by the viral attachment protein sigma 1. J. Virol. **69:**6972–6979.

JOURNAL OF VIROLOGY, Jan. 2001, p. 351–361
0022-538X/01/$04.00+0 DOI: 10.1128/JVI.75.1.351–361.2001

Vol. 75, No. 1

Calpain Inhibition Protects against Virus-Induced Apoptotic Myocardial Injury

ROBERTA L. DEBIASI,[1,2,3] CHARLES L. EDELSTEIN,[4] BARBARA SHERRY,[5] AND KENNETH L. TYLER[2,3,4,6]*

Departments of Pediatric Infectious Diseases,[1] Neurology,[2] Medicine,[4] and Microbiology and Immunology,[6] University of Colorado Health Sciences Center, and Denver Veterans Affairs Medical Center,[3] Denver, Colorado 80262, and Department of Microbiology, College of Veterinary Medicine, North Carolina State University, Raleigh, North Carolina 27606[5]

Received 23 May 2000/Accepted 14 September 2000

Viral myocarditis is an important cause of human morbidity and mortality for which reliable and effective therapy is lacking. Using reovirus strain 8B infection of neonatal mice, a well-characterized experimental model of direct virus-induced myocarditis, we now demonstrate that myocardial injury results from apoptosis. Proteases play a critical role as effectors of apoptosis. The activity of the cysteine protease calpain increases in reovirus-infected myocardiocytes and can be inhibited by the dipeptide alpha-ketoamide calpain inhibitor Z-Leu-aminobutyric acid-CONH(CH_2)3-morpholine (CX295). Treatment of reovirus-infected neonatal mice with CX295 protects them against reovirus myocarditis as documented by (i) a dramatic reduction in histopathologic evidence of myocardial injury, (ii) complete inhibition of apoptotic myocardial cell death as identified by terminal deoxynucleotidyltransferase-mediated dUTP-biotin nick end labeling, (iii) a reduction in serum creatine phosphokinase, and (iv) improved weight gain. These findings are the first evidence for the importance of a calpain-associated pathway of apoptotic cell death in viral disease. Inhibition of apoptotic signaling pathways may be an effective strategy for the treatment of viral disease in general and viral myocarditis in particular.

The mechanisms by which viruses produce cytopathic effects in their host cells are not well understood. Such knowledge is essential to an understanding of viral pathogenesis and development of novel antiviral therapies. Apoptosis is a mechanism of active cell death distinct from necrosis, characterized by DNA fragmentation, cell shrinkage, and membrane blebbing without rupture (26). Apoptosis plays a critical role in many physiologic (28, 74), as well as infectious and noninfectious, pathologic conditions (72). Viruses may either promote or inhibit apoptosis as a strategy to maximize pathogenicity in their hosts (40, 54, 67). Several viruses, including adenovirus, poxviruses, herpesviruses, and human papillomavirus, proliferate and evade host immune responses by interfering with programmed cell death (1, 19, 31, 68). Many other viruses, such as human immunodeficiency virus, human T-cell leukemia virus, influenza virus, measles virus, rubella virus, poliovirus, human herpesvirus 6, Sindbis virus, and reoviruses, cause cytopathic effect by induction of apoptosis in their target cells (11, 14, 21–23, 34, 40, 42, 50, 70).

We have used reovirus-induced apoptosis as an experimental model system to study the viral and cellular mechanisms involved in apoptotic cell death (39). Reoviruses are nonenveloped viruses that contain a genome of segmented, double-stranded RNA. Infection of cultured fibroblasts and epithelial cells with reoviruses induces apoptosis. Reoviral strains differ in the efficiencies with which they induce this cellular response, and these differences are determined by the viral S1 gene (44, 69). Apoptosis also occurs following reovirus infection in vivo and colocalizes with areas of pathologic injury (38, 39). This finding suggests that apoptosis is an important mechanism of tissue damage in reoviral infection.

Reovirus strain 8B is a reassortant reovirus that efficiently produces myocarditis in infected neonatal mice (55, 58). Damage has been shown to be a direct effect of viral infection of myocardiocytes (60). This damage differs from that of several other models of viral myocarditis (such as coxsackievirus and murine cytomegalovirus) in which secondary inflammatory responses, or lymphocyte recognition of viral or self-antigens on myocardial cells, may be the predominant cause of cardiac damage (12, 17, 20, 30, 46). SCID mice infected with reovirus 8B develop myocarditis, and passive transfer of reovirus-specific immune cells is protective, rather than harmful, to 8B-infected mice (58, 60). This finding indicates that immune mechanisms contribute to amelioration rather than induction of reovirus-induced viral injury (60). However, the mechanism by which direct myocardial injury occurs is not well characterized. Since tissue damage occurs by apoptosis in other in vivo models of reoviral infection (38), and apoptosis has been suggested in some models of viral myocarditis (6, 25), we wished to determine if reoviral myocarditis occurs as a result of apoptotic cell injury and, if so, whether manipulation of known signaling pathways preceding apoptosis is protective.

Protease cascades appear to play critical roles as effectors of apoptosis, as with the cysteine proteases caspases and calpain (10, 32, 41, 62, 79). Caspases are the most extensively investigated members of this class of protease and have been implicated in a wide variety of apoptotic models. However, the role of calpain in apoptosis has been recognized recently. Calpain is a calcium-dependent neutral cysteine protease that is ubiqui-

* Corresponding author. Mailing address: Department of Neurology (B-182), University of Colorado Health Sciences Center, 4200 E. 9th Ave., Denver, CO 80262. Phone: (303) 393-2874. Fax: (303) 393-4686. E-mail: Ken.Tyler@UCHSC.edu.

tous in the cytosols of many cell types (35, 63). Calpains have recently been implicated in several models of apoptosis, including dexamethasone-induced thymocyte apoptosis (65), neuronal cell apoptosis (36), neutrophil apoptosis (64), ischemia-induced rat liver apoptosis (27, 61), myonuclear apoptosis in limb-girdle dystrophy (3), and chemical hypoxia-induced apoptosis of rat myocytes (8). We have recently shown that reovirus-induced apoptosis in vitro is preceded by increased cellular calpain activity and is inhibited by two classes of calpain inhibitors (13).

We now show that reovirus 8B-induced myocarditis occurs by apoptosis. Calpain activity increases in cardiomyocytes following infection with reovirus 8B, and calpain inhibition reduces myocardial injury and morbidity in infected mice. This is evidence that interference with apoptotic signaling pathways may prove of benefit as a therapeutic strategy in the treatment of viral infection in general and viral myocarditis in particular.

MATERIALS AND METHODS

Virus. Reovirus 8B is an efficiently myocarditic reovirus that has been previously characterized (58). 8B stocks were subjected to plaque assay three times and passaged twice in mouse L cells prior to use.

Mice. Swiss-Webster (Taconic) mouse litters were housed in individual filter-topped cages in an American Association for Laboratory Animal Care-accredited animal facility. All animal procedures were performed under protocols approved by the appropriate institutional committees.

Mouse inoculations. Two-day-old Swiss-Webster (Taconic) mice were intramuscularly inoculated with 1,000 PFU of 8B reovirus in the left hind limb (20-μl volume). Mock-infected mice received gel saline vehicle inoculation (equal volume) (137 mM NaCl, 0.2 mM $CaCl_2$, 0.8 mM $MgCl_2$, 19 mM H_3BO_3, 0.1 mM $Na_2B_4O_7$, 0.3% gelatin).

Histologic analysis. At 7 days postinfection, mice were sacrificed and hearts were immediately immersed in 10% buffered formalin solution. After being mounted as transverse sections, hearts were embedded in paraffin and sectioned to 6 μm in thickness. For quantification of degree of myocardial injury, hematoxylin- and eosin-stained midcardiac sections (at least six per heart) were examined at a ×125 magnification by light microscopy and scored blindly. Scoring was performed using a previously validated system (58), with scores ranging from 0 to 4 (0, no lesions; 1, one or a few small lesions; 2, many small or a few large lesions; 3, multiple small and large lesions; and 4, massive lesions). Twenty-three to 24 mice were scored from each group.

DNA fragmentation. The presence of internucleosomal DNA cleavage in myocardial tissue was investigated by phenol-chloroform extraction of DNAs from 8B-infected and mock-infected hearts and precipitation in 95% ethyl alcohol. The DNA was then end labeled with 5 μCi of [^{32}P]dGTP using 10 U of terminal transferase (M187; Promega Corporation), resolved by electrophoresis on a 2% agarose gel, fixed in 5% acetic acid–5% methanol, dried, and scanned on a Instant Imager (Packard Instrument Company).

TUNEL. Evaluation of fragmented DNA was performed by terminal deoxynucleotidyltransferase (TdT)-mediated dUTP-biotin nick end labeling (TUNEL), as previously described (38). Paraffin-embedded cardiac midsections were prepared by removing paraffin with xylene and then rehydrating them in 100, 95, and then 70% ethanol solutions. After digestion in proteinase K solution (Boehringer Mannheim) for 30 min at 37°C, slides were pretreated in 0.3% H_2O_2 in phosphate-buffered saline for 15 min at room temperature and then washed. The TdT labeling reaction was carried out under coverslips in a humidified chamber for 1 h at 37°C with TdT and digoxigenin 11-dUTP. (Boehringer Mannheim). The reaction was stopped with SSC (1× SSC is 0.15 M NaCl plus 0.015 M sodium citrate) buffer. After being blocked in 2% bovine serum albumin for 10 min, sections were probed with Vectastain ABC (avidin DH and biotinylated enzyme; Vector Laboratories) for 1 h at room temperature, and then visualized with a diaminobenzadine peroxidase substrate kit (Vector Laboratories). Negative and positive controls were used with all reactions.

Viral-antigen stain. Cardiac midsections were prepared as noted above. Following the hydrogen peroxide incubation, slides were blocked in 2% normal goat serum for 30 min at room temperature. Sections were then incubated in rabbit polyclonal anti-reovirus type 3 Dearing antiserum as the primary antibody (gift of Terence Dermody, Vanderbilt University) at a dilution of 1:1,000 for 1 h at 37°C. Biotinylated goat anti-rabbit antibody was used as the secondary antiserum (1:200 dilution in 2% normal goat serum) for 30 min at 37°C. Sections were probed and visualized as noted above.

Calpain activity in myocytes. The determination of the presence of calpain-specific spectrin (fodrin) breakdown products (150- and 145-kDa doublet) by immunoblotting was used as an assay of calpain activity (36). Mouse primary cardiac myocyte cultures were prepared as previously described (5). Cells were plated at 1.6×10^6 cells/well in 24-well plates and incubated for 48 h. Cells were then infected with reovirus strain 8B (multiplicity of infection [MOI], 20, in Dulbecco modified Eagle medium [DMEM]) or mock infected (DMEM) and then incubated at 37°C. Mock-infected cells were harvested at 48 h. 8B-infected cells were harvested at 24, 48, and 72 h postinfection. Cell lysates were prepared by sonication in lysis buffer (15 mM Tris [pH 7.4], 10 mM EDTA, 0.1% NP-40, 20% glycerol, 50 mM β-mercaptoethanol, 50 μg of pepstatin per ml, 100 μg of leupeptin per ml, 1 mM phenylmethylsulfonyl fluoride), and the cytoplasmic fractions were run on a 7.5% polyacrylamide gel. Protein loading for these gels (25 μg/well) was normalized by protein concentration analysis of cell lysates. Following transfer (15 V overnight), the nitrocellulose membrane was blocked in 5% nonfat dried milk–Tris normal saline for 2 h, probed with anti-fodrin mouse monoclonal antibody (ICN) at a dilution of 1:1,000 for 1.5 h, and then washed. Membranes were then incubated in anti-mouse immunoglobulin G horseradish peroxidase-linked whole antibody (Amersham) at a dilution of 1:1,000, as the secondary antibody. After the membranes were washed, ECL Plus (Amersham) was used for detection.

In additional experiments, primary cardiac myocytes were infected with 8B reovirus (using the method described above) with and without pretreatment in CX295 (100 μM). Cell lysates were prepared and analyzed for calpain activity by immunoblotting as described above.

Specificity of the calpain inhibitor CX295. *Z*-Leu-aminobutyric acid-$CONH(CH_2)$3-morpholine (CX295) is a dipeptide alpha-ketoamide compound which inhibits calpain at the active site (kindly provided by Gary Rogers at Cortex Pharmaceuticals, Inc.). To determine the efficacy of CX295 as a calpain inhibitor, 10 μg of purified μ-calpain (porcine RBC; Calbiochem) was added to the preferred fluorogenic calpain substrate sucrose-Leu-Tyr-amino-methyl-coumarin (SLY-AMC) in the presence and absence of CX295 (100 μM), as well as in the presence of the pan-caspase inhibitor *Z*-D-DCB (100 μM). The calpain assay was performed as previously described (16). Proteolytic hydrolysis of the substrate by purified calpain liberates the highly fluorescent AMC moiety. Fluorescence at a 380-nm excitation and 460-nm emission was quantified with a Hitachi F2000 spectrophotometer. An AMC standard curve was determined for each experiment. Calpain activity was expressed in picomoles of AMC released per minute of incubation time per microgram of purified calpain.

To determine the specificity of CX295 as a calpain inhibitor, 10 ng of purified caspase 3 (Upstate) was added to the preferred fluorogenic caspase-3 substrate DEVD-AMC in the presence and absence of the pan-caspase inhibitor *Z*-D-DCB (100 μM), as well as CX295 (100 μM). In addition, 57 ng of purified caspase-1 (provided by Nancy Thornberry, Merck) was added to the preferred fluorogenic caspase-1 substrate YVAD-AMC in the presence and absence of *Z*-D-DCB, as well as CX295. The caspase activity assay was performed as previously described (16). Caspase activity was expressed as picomoles of AMC released per minute of incubation time per nanogram of purified caspase. Experiments were all performed in triplicate.

Calpain inhibition in vivo. For calpain inhibition experiments, animals received daily intraperitoneal injections of either active CX295 (70 mg/kg of body weight in a 50-μl volume) or its inactive saline diluent. The first dose was given 30 min prior to infection with 8B virus. A total of six doses were given, at 24-h intervals. Mice were sacrificed at 7 days postinfection.

Viral titer determination. Injected hind limbs and whole hearts were placed in 1 ml of gel saline and immediately frozen at −70°C. After three freeze (−70°C)-thaw (37°C) cycles, the tissues were sonicated approximately 15 to 30 s by using a microtip probe (Heat Systems model XL2020) until a homogenous solution was obtained. The virus suspensions were serially diluted in 10-fold steps in gel saline and placed in duplicate on L-cell monolayers for plaque assay, as previously described (13). Virus titers were expressed as $\log_{10}$ PFU per milliliter.

Serum CPK. Following decapitation of mice, whole blood was collected from individual mice into plasma separator tubes with lithium heparin to prevent coagulation (Microtainer; Becton Dickinson). Samples were collected from 8B-infected mice treated with CX295 (n = 20), 8B-infected mice treated with the inactive diluent (n = 20), and uninfected age-matched controls (n = 9). Serum creatine phosphokinase (CPK) measurements were performed by the University of Colorado Health Sciences Center Clinical Laboratory and were expressed as units per liter.

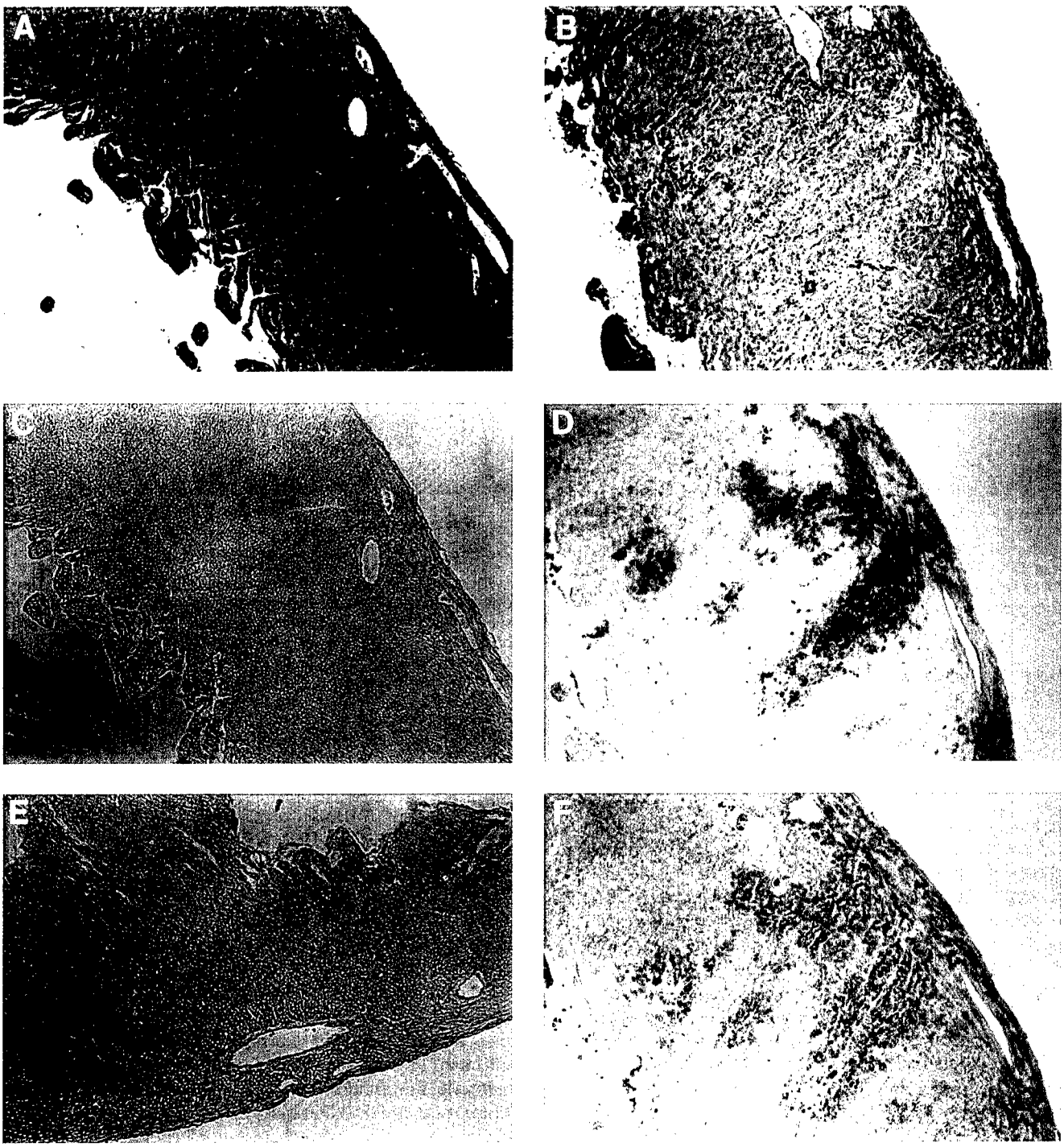

FIG. 1. Consecutive cardiac midsections from mock-infected (A, C, and E) and reovirus 8B-infected (B, D, and F) neonatal mice 7 days after left hind limb inoculation with 1,000 PFU of strain 8B reovirus or mock inoculation. Hematoxylin- and eosin-stained tissue reveals marked disruption of myocardial architecture in the 8B-infected heart (B) compared to that in the mock-infected heart (A). Despite the degree of injury, there is minimal inflammatory cell infiltrate. The degree of cellularity seen in both mock-infected and infected hearts is normal for neonatal mice. In situ detection of DNA nick ends by TUNEL revealed positively staining nuclei in the same region of an injured 8B-infected heart (D), which are absent in a mock-infected animal (C). Immunohistochemistry with anti-type 3 Dearing reovirus antibody reveals the presence of viral antigen in the areas of myocardial injury in the 8B-infected mouse (F), absent in the mock-infected animal (E). Original magnification, ×25.

Growth. Mice were infected with 10 PFU of 8B reovirus. Infected drug-treated (n = 15) and infected control (n = 15) mice were weighed daily on days 0 to 14 postinfection. Additional experiments using a higher dose of virus (1,000 PFU) were also completed, with daily weighing on days 0 to 7 postinfection. In these experiments, weights were also compared to those of normal age-matched uninfected mice.

Statistics. The results of all experiments are reported as means ± standard errors of the means. Means were compared using parametric two-tailed t tests

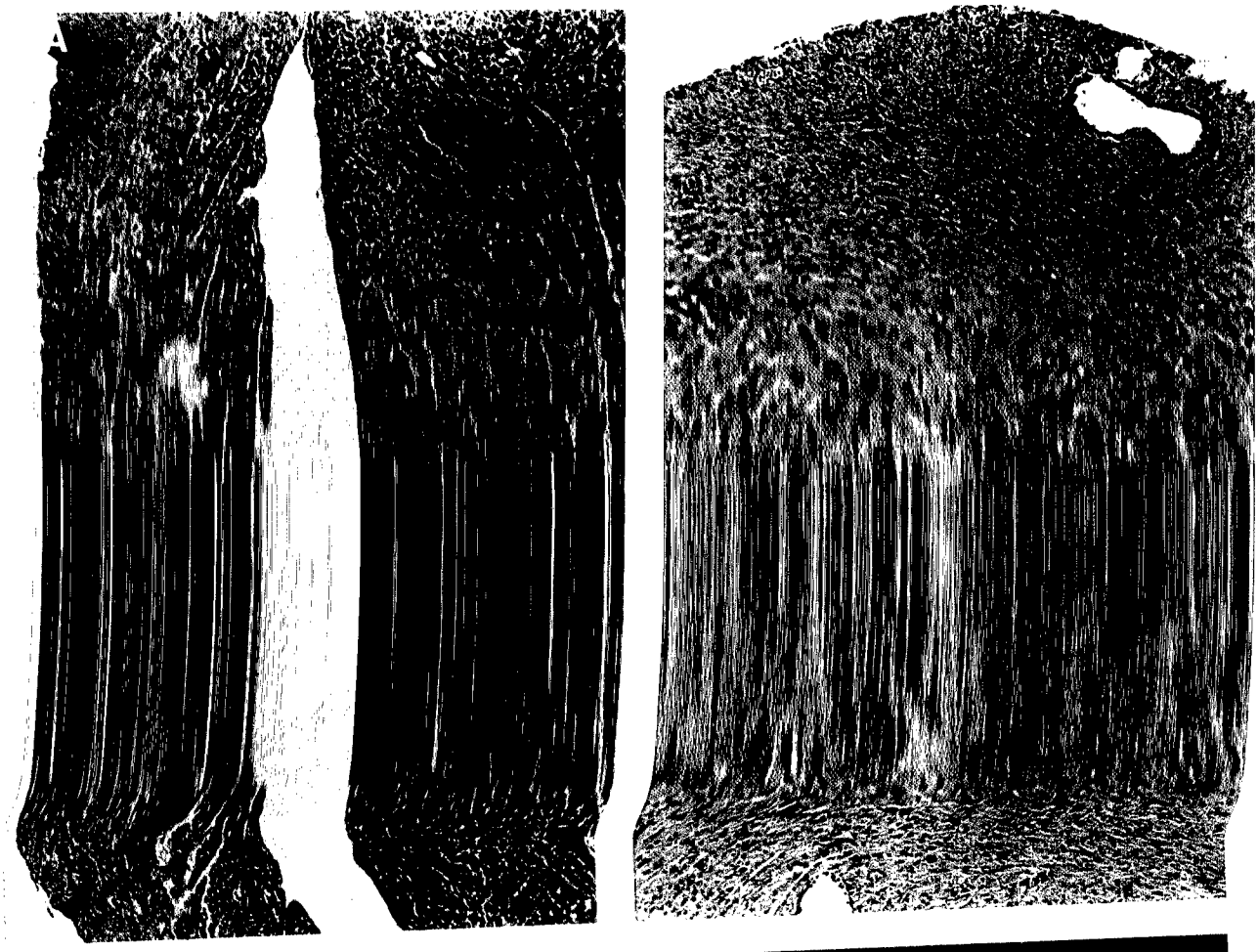
A
B
C
D
E
F

munoblotting in reovirus-infected myocytes, in the presence and absence of CX295. Calpain activity (measured by densitometric analysis of the 150- and 145-kDa calpain-specific fodrin breakdown product) increased by 2.4-fold in 8B-infected cardiomyocytes compared to that in mock-infected cardiomyocytes. Calpain activity was significantly reduced in CX295-treated, 8B-infected cells compared to that in infected, untreated cells ($P = 0.04$) (Fig. 4D and E).

These experiments confirm that CX295 is both an effective and a specific calpain inhibitor.

(iv) Calpain inhibitor CX295 inhibits 8B-induced myocardial injury. Two-day-old Swiss-Webster mice were infected with 1,000 PFU of 8B virus and received six daily intraperitoneal injections of either active CX295 (70 mg/kg) or its inactive saline diluent as a control (see Materials and Methods). Mice were sacrificed on day 7 postinfection, and myocardial sections were prepared.

Transverse cardiac sections from 8B-infected mice treated with CX295 or its inactive diluent (control) were stained with hematoxylin and eosin and viewed by light microscopy (Fig. 5A to F). Cardiac tissue from control mice (Fig. 5A) showed extensive focal areas of myocardial damage, which were absent in the CX295-treated animals, despite identical viral infection (Fig. 5B). Marked disruption of the normal myocardial architecture was evident in hearts of control mice (Fig. 5C), compared to that of drug-treated animals (Fig. 5D). Nuclei with apoptotic morphology were easily seen within these areas in the control mice (Fig. 5E), including in cells with condensed and pyknotic nuclei, as well as apoptotic bodies. These characteristics were absent in the drug-treated animals (Fig. 5F). Staining by TUNEL of comparable sections from drug-treated and diluent-treated (control) infected mice was examined. Nuclei that stained positive by TUNEL were virtually absent in the drug-treated mice (Fig. 5H), unlike with control infected animals (Fig. 5G).

For quantification of the degree of myocardial injury, hematoxylin- and eosin-stained midcardiac sections (at least six sections per heart) were scored using a previously validated scoring system (58). Twenty infected, CX295-treated animals and 23 control (infected, diluent-treated) mice were evaluated. There was a highly significant reduction in the myocardial injury scores of animals treated with CX295. The mean score for control animals was 3.0 ± 0.1 (range, 2 to 4), compared to 0.6 ± 0.1 (range 0 to 1.5) for CX295-treated animals ($P < 0.0001$) (Fig. 6).

CPK is an intracellular enzyme present in cardiac and skeletal muscle that is released upon tissue injury. It can be measured in the serum and used as a quantitative marker of skeletal and cardiac muscle damage (2). Blood was collected from infected mice treated with CX295 and inactive diluent-treated

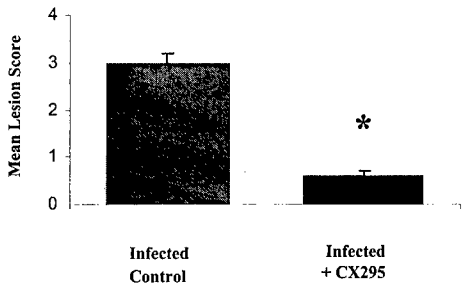

Heart Lesion Scoring
0 = no lesions
1 = one or a few small
2 = many small or a few large
3 = multiple small and large
4 = massive

FIG. 6. Reduction in myocardial injury score. Myocardial injury of 8B-infected animals was quantified by blindly scoring hematoxylin- and eosin-stained midcardiac sections of drug-treated and control (inactive-diluent-treated) animals upon light microscopy. At least six sections per heart were scored from 20 to 23 animals in each group. A highly significant reduction in myocardial injury score was noted for drug-treated animals. The mean lesion score was 3.0 ± 0.1 (range 2 to 4) for controls, compared to 0.6 ± 0.1 (range 0 to 1.5) for CX295-treated animals. *, $P < 0.0001$. See Materials and Methods for explanations of mean lesion scores.

controls at 7 days postinfection, as well as uninfected age-matched mice. Serum CPK levels were significantly elevated in 8B-inoculated mice compared to those in uninfected mice, indicative of 8B-induced muscle injury. There was a statistically significant reduction in serum CPK level toward a normal level in CX295-treated mice compared to the level in control mice (Fig. 7). Uninfected age-matched mice had a mean CPK level of 4,521 ± 431 U/liter. 8B-infected mice had a mean CPK level of 5,658 ± 359 U/liter, representing an increase of 1,137 U/liter above normal. Treatment of infected animals with CX295 reduced the mean CPK value to 4,634 ± 350 U/liter, not significantly elevated compared to normal levels but significantly reduced compared to levels in infected, nontreated animals ($P < 0.05$).

To determine if reductions in myocardial injury were also associated with reduction in viral titer at primary (hind limb) and secondary (heart) sites of replication, the titers of virus in tissues were determined by plaque assay of tissue homogenates. There was a 0.5-$\log_{10}$-PFU/ml reduction in viral titers in the hind limbs of CX295-treated animals compared to those for controls (7.2 ± 0.1 to 6.7 ± 0.2 $\log_{10}$ PFU/ml; $P = 0.003$). Hearts of CX295-treated animals had a 0.7-$\log_{10}$-PFU/ml reduction in viral titer (6.1 ± 0.2 to 5.4 ± 0.2 $\log_{10}$ PFU/ml; $P < 0.01$) (Fig. 8). Although these decrements were statistically

FIG. 5. Cardiac midsections from reovirus 8B-infected neonatal mice treated with the calpain inhibitor CX295 (B, D, F, and H) compared to those from inactive diluent control mice (A, C, E, and G) 7 days following intramuscular inoculation with 1,000 PFU of reovirus 8B. Hematoxylin- and eosin-stained sections at an original magnification of ×25 reveal extensive focal areas of myocardial injury (arrows) in the control animal (A), which is absent in the CX295-treated animal (B), despite identical viral infections. Views at an original magnification of ×50 demonstrate minimal inflammatory cell infiltrate in the affected area (C), but myocardial architecture is dramatically disrupted, compared to that of a CX295-treated mouse (D). At an original magnification of ×100, nuclei with apoptotic morphology are easily seen in the control animal (E), as are cells with condensed and pyknotic nuclei (long arrow) as well as apoptotic bodies (shorter arrows). These characteristics are absent in the drug-treated mouse (F). TUNEL analysis of the control animal reveals extensive areas of positively staining cells in the same regions of injury (G) but no TUNEL-positive areas in the drug-treated mouse (H).

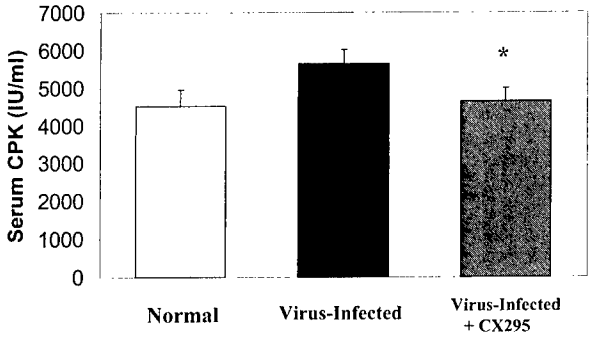

FIG. 7. Reduction in serum CPK. CPK was measured as a marker of myocardial damage in 8B-infected animals treated with CX295, and levels were compared to those for control (inactive-diluent-treated) infected animals, as well as age-matched uninfected controls. There was a significant reduction in serum CPK toward normal levels in CX295-treated infected mice compared to levels in infected control animals ($P < 0.05$).

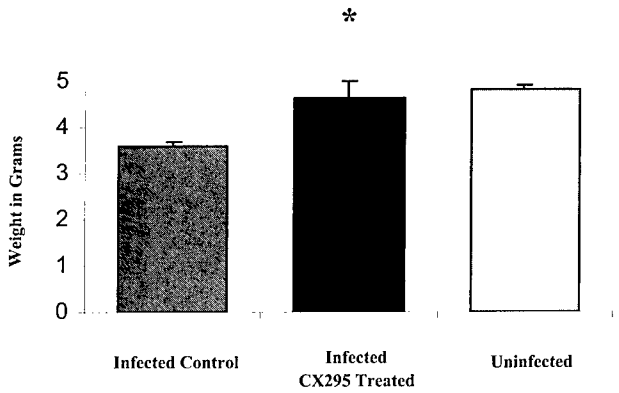

FIG. 9. Growth of infected mice. Growth, as measured by weight gain, was assessed in 8B-infected mice treated with CX295 and inactive diluent (control). Improved growth was noted for infected, CX295-treated animals at 7 days postinfection compared to the growth of infected controls (*, $P = 0.008$). Weights of infected, treated animals were not significantly different from those of uninfected, age-matched controls.

significant, they were modest in degree, and substantial viral replication occurred in both the drug-treated and the control animals (1,000- to 10,000-fold).

We wished to determine whether the reduction in myocardial damage caused by CX295 treatment reduced morbidity in mice. We therefore measured growth (weight gain) in infected, drug-treated mice and compared to that in infected, untreated controls. CX295-treated mice had improved growth compared to that of control mice (4.6 ± 0.4 versus 3.6 ± 0.1 g at 7 days postinfection; $P = 0.008$), and growth was not significantly different from that of uninfected age-matched animals (4.6 ± 0.4 versus 4.8 ± 0.1 g; $P = 0.6$, not significant) (Fig. 9).

DISCUSSION

Viral myocarditis remains a serious disease without reliable or effective treatment. The events following viral attachment and replication in myocardial tissue that lead to myocarditis are not clearly understood. A variety of mechanisms from various models have been suggested, including direct viral injury and persistence (9, 24), autoimmune phenomena (17, 45, 51), cytokine fluxes (18, 33, 52, 59), inflammation (29, 53), and apoptosis (12, 77, 78). A clearer understanding of pathogenic mechanisms is crucial for the development of effective therapeutic strategies, since currently employed antiviral agents have not made a significant impact on outcomes from this clinical syndrome. Reoviral myocarditis is an ideal model with which to study these events, since myocardial injury is a direct effect of virus infection and does not involve immune-mediated effects.

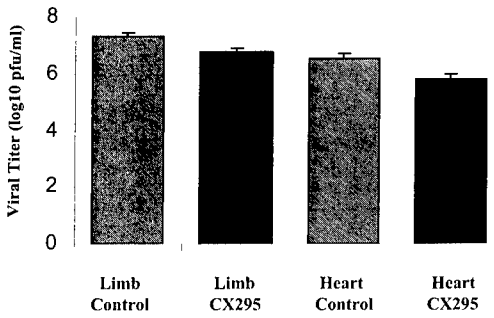

FIG. 8. Tissue-specific viral titers. Titers were measured by plaque assay at 7 days postinfection from homogenates of limbs (site of primary replication) and hearts (site of secondary replication) of 8B-infected mice. A slight reduction in peak viral titers was seen in the CX295-treated group. Both CX295-treated and control animals showed a >3-$\log_{10}$-unit increase in virus over the input inoculum (10^3 PFU/mouse).

Reovirus 8B induces myocarditis by apoptosis. Reovirus 8B induces myocarditis in mice by direct viral injury to myocytes, and we now show that this occurs by induction of apoptosis. This conclusion is supported by the presence of distinctive morphologic criteria upon microscopic examination of infected heart tissues; TUNEL-positive nuclei were found exclusively in regions of viral infection and myocardial injury. The presence of apoptosis was confirmed by the presence of the characteristic intranucleosomal cleavage pattern of extracted DNA. It has been shown previously that multiple viral genes (M1, L1 and L2, and S1) encoding core and attachment proteins are determinants of reovirus-induced acute myocarditis (56). Interactions between these proteins determine myocarditic potential. Several of these genes have been associated with reovirus RNA synthesis and reovirus induction of and sensitivity to beta interferon in cardiac myocyte cultures, which are determinants of reovirus myocarditic potential. In addition, the S1 gene, which codes for the viral attachment protein σ1, is the primary determinant of apoptotic potential among strains of reovirus (69). It is likely, therefore, that the extent of reovirus-induced myocardial injury is determined by a combination of host responses, encompassing both the interferon and the apoptosis pathways. Indeed, just as inhibition of the interferon pathway was sufficient to enhance reovirus-induced myocarditis (59), we show here that inhibition of the apoptotic pathway is sufficient to abrogate reovirus-induced myocarditis. Thus, apoptosis is an integral component of reovirus-induced myocardial injury.

Calpain activity is increased in reovirus-infected myocardiocytes, and calpain inhibition is protective against reovirus-induced myocarditis. Calpain is a calcium-activated cysteine protease that has proven importance with regard to the initiation of apoptosis in the reoviral model, as well as several other unrelated models of apoptosis (see the introduction). We first demonstrated that calpain activity is increased in cardiac myocytes in vitro following 8B infection, in a time course paralleling induction of apoptosis. We then demonstrated that calpain inhibition resulted in a reduction of calpain activity in infected cells and dramatic reductions in reovirus-induced injury, as well as apoptosis. Clinically significant reduction in myocardial injury was documented by reduced serum CPK levels and improved growth in treated mice.

It is likely that CX295 acted primarily by interfering with crucial signal transduction cascades involving calpain, required for induction of apoptotic cell death. Additionally, it is possible that CX295 provided some portion of its effect by inhibiting viral growth at either the primary (hind limb) or secondary (heart) site of replication, since viral titers were slightly lower in drug-treated animals than in controls. Slight reductions in viral titer do not seem a likely explanation for the majority of drug effect, since in prior experiments involving reovirus-induced myocarditis, yields of virus at early and late times postinfection did not correlate with the degree of myocardial injury (57). In addition, efficiently myocarditic and poorly myocarditic reovirus strains replicate to similar titers in the heart; thus, differences in myocarditic potential do not simply reflect viral growth in the heart (56).

One must be cautious in attributing a role for calpain in disease pathogenesis based solely on data derived from calpain inhibition. Currently available calpain inhibitors suitable for in vivo use have weak, but measurable, inhibitory activities against other cysteine proteases. However, the inhibitor employed in our experiments, CX295, is 500- to 900-fold more active against calpains than cathepsins (the K_i for calpain is 0.027 − 0.042 μM, versus a K_i for cathepsin B of 24 μM) and failed to inhibit caspase activity in vitro, as described in this paper. We believe that inhibition of calpain, rather than of other cysteine proteases, is the essential element of CX295's protective effect against 8B-induced myocardial apoptosis and injury.

It is not clear what constitutes the upstream and downstream components of a signaling cascade within which calpain might fit, either during reovirus infection or in other systems where calpain is involved. The mechanisms by which reovirus triggers increased cellular calpain activity are not known but may include initiation of calcium fluxes following viral attachment, as demonstrated with rotavirus, a closely related virus (15); upregulation of growth factors which facilitate calpain activation (37, 66); or upregulation of endogenous calpain activator proteins which have been characterized for several cell types (49). Calpain may play a physiologic role in the regulation of a variety of cellular transcription factors and cell cycle-regulating factors implicated in apoptosis, including Jun, Fos, p53, cyclin D, and NF-κB (3, 7, 73). We have recently shown that activation of NF-κB is required for reovirus-induced apoptosis (J. L. Connolly, S. E. Rodgers, B. Pike, P. Clarke, K. L. Tyler, and T. S. Dermody, Abstr. 17th Ann. Meet. Am. Soc. Virology, abstr. 17-2, 1998), suggesting the possibility that calpain inhibition acts to modulate NF-κB-induced signal transduction. Calpains may also modulate cell death by cleaving Bax, a proapoptotic protein located in the cytosol (75). In addition, the caspase and calpain proteolytic cascades may interact. Caspases may play a role in the regulation of calpain by cleavage of calpastatin, the endogenous inhibitor of calpain (43, 71, 76). Reflexively, calpain may be involved in the proteolytic activation of some caspases (47).

Potential therapeutic efficacy of calpain inhibitors. In conclusion, our data suggest that reovirus-induced myocarditis occurs by direct viral induction of apoptotic cell death and that injury can be markedly reduced with the use of a calpain inhibitor. To our knowledge, this is the first successful demonstration of the use of calpain inhibition in vivo to ameliorate myocarditis in particular and virus-induced disease in general. However, future experiments are needed to determine whether calpain inhibition remains effective when it is administered after the onset of viral infection. Our results demonstrate the utility of apoptosis inhibition as a strategy for protection against viral infection.

ACKNOWLEDGMENTS

We thank Gary Rogers of Cortex Pharmaceutical for providing the calpain inhibitor CX295 and its inactive diluent. The University of Colorado Cancer Center provided core tissue culture and medium facilities.

This work was supported by Public Health Service grant 1RO1AG14071 from the National Institute of Aging, Merit and REAP grants from the Department of Veterans Affairs, a U.S. Army Medical Research and Material Command grant (USAMRMC 98293015) (K.L.T.), a Young Investigator Award from the National Kidney Foundation (C.L.E.), Public Health Service grant 1RO1HL57161, and North Carolina State University College of Veterinary Medicine grant 204743 (B.S.).

REFERENCES

1. **Aubert, M., and J. A. Blaho.** 1999. The herpes simplex virus type 1 regulatory protein ICP27 is required for the prevention of apoptosis in human cells. J. Virol. **73**:2803–2813.
2. **Bachmeir, K., J. Mair, F. Offner, C. Pummerer, and N. Neu.** 1995. Serum cardiac troponin T and creatine kinase-MB elevations in murine autoimmune myocarditis. Circulation **92**:1927–1932.
3. **Baghdiguian, S., M. Martin, I. Richard, F. Pons, C. Astier, N. Bourg, R. T. Hay, R. Chemaly, G. Haleby, J. Loiselet, L. V. Anderson, A. Lopez de Muvigin, M. Fardeu, P. Mangeat, J. S. Beckmann, and G. Lefranc.** 1999. Calpain 3 deficiency is associated with myonuclear apoptosis and profound perturbation of the IκBα/NF-KB pathway in limb-girdle muscular dystrophy type 2A. Nat. Med. **5**:503–511.
4. **Bartus, R. T., K. L. Baker, A. D. Heiser, S. D. Sawyer, R. L. Dean, P. J. Elliott, and J. A. Straub.** 1994. Postischemic administration of AK275, a calpain inhibitor, provides substantial protection against focal ischemic brain damage. J. Cerebr. Blood Flow Metab. **14**:537–544.
5. **Baty, C. J., and B. Sherry.** 1993. Cytopathogenic effect in cardiac myocytes but not in cardiac fibroblasts is correlated with reovirus-induced myocarditis. J. Virol. **67**:6295–6298.
6. **Bowles, N. E., and J. A. Towbin.** 1998. Molecular aspects of myocarditis. Curr. Opin. Cardiol. **13**:179–184.
7. **Chen, F., Y. Lu, D. C. Kuhn, M. Maki, X. Shi, and L. M. Demers.** 1997. Calpain contributes to silica-induced IKB-degradation and nuclear factor κB activation. Arch. Biochem. Biophys. **34**:383–388.
8. **Chen, S. J., M. E. Bradley, and T. C. Lee.** 1998. Chemical hypoxia triggers apoptosis of cultured neonatal rat cardiac myocytes: modulation by calcium-regulated proteases and protein kinases. Mol. Cell. Biochem. **178**:141–149.
9. **Chow, L. H., K. W. Beisel, and B. M. McManus.** 1992. Enteroviral infection of mice with severe combined immunodeficiency. Evidence for direct viral pathogenesis of myocardial injury. Lab. Investig. **66**:24–31.
10. **Cohen, G. M.** 1997. Caspases: the executioners of apoptosis. Biochem. J. **326**:1–16.
11. **Colamussi, M. L., M. R. White, E. Crouch, and K. L. Hartshorn.** 1999. Influenza A virus accelerates neutrophil apoptosis and markedly potentiates apoptotic effects of bacteria. Blood **93**:2395–2403.

12. **Colston, J. T., B. Chandrasakar, and G. L. Freeman.** 1998. Expression of apoptosis-related proteins in experimental coxsackie myocarditis. Cardovasc. Res. **38**:158–168.
13. **DeBiasi, R. L., M. K. T. Squier, B. Pike, M. Wynes, T. S. Dermody, and K. L. Tyler.** 1999. Reovirus-induced apoptosis is preceded by increased cellular calpain activity and is blocked by calpain inhibitors. J. Virol. **73**:695–701.
14. **Dockrell, D. H., A. D. Badley, J. S. Villacian, C. J. Heppelman, A. Algeciras, S. Ziesvnar, H. Yagita, D. H. Lynch, P. C. Roche, P. J. Leibson, and C. V. Paya.** 1998. The expression of Fas ligand by macrophages and its upregulation by human immunodeficiency virus infection. J. Clin. Investig. **101**:2394–2405.
15. **Dong, Y., C. Q. Zeng, J. M. Ball, M. K. Estes, and A. P. Morris.** 1997. The rotavirus enterotoxin NSP4 mobilizes calcium in human intestinal cells by stimulating phospholipase C-mediated inositol 1,4,5-triphosphate production. Proc. Natl. Acad. Sci. USA **94**:3960–3965.
16. **Edelstein, C. L., H. Ling, P. E. Gengaro, R. A. Nemenoff, B. A. Bahr, and R. W. Schrier.** 1997. Effect of glycine on prelethal and postlethal increases in calpain activity in rat renal proximal tubules. Kidney Int. **52**:1271–1278.
17. **Fairweather, D., C. M. Lawson, A. J. Chapman, C. M. Brown, T. W. Booth, J. M. Papadimitriou, and G. R. Snellam.** 1998. Wild isolates of murine cytomegalovirus induce myocarditis and antibodies that cross-react with virus and cardiac myosin. Immunology **94**:263–270.
18. **Freeman, G. L., J. T. Colston, M. Zabalgoitia, and B. Chandrasekar.** 1998. Contractile depression and expression of proinflammatory cytokines and iNOS in viral myocarditis. Am. J. Physiol. **274**:H249–H258.
19. **Galvan, V., R. Brandimarti, and B. Roizman.** 1999. Herpes simplex virus 1 blocks caspase-3-independent and caspase-dependent pathways to cell death. J. Virol. **73**:3219–3226.
20. **Gauntt, C. J.** 1997. Roles of the humoral response in coxsackievirus B-induced disease. Curr. Top. Microbiol. Immunol. **223**:259–282.
21. **Girard, S., T. Couderc, J. D. Destombes, J. Thiesson, F. Delpeyroux, and B. Blondel.** 1999. Poliovirus induces apoptosis in the mouse central nervous system. J. Virol. **73**:6066–6072.
22. **Ichimi, R., T. Jin-o, and M. Ito.** 1999. Induction of apoptosis in cord blood lymphocytes by HHV-6. J. Med. Virol. **58**:63–68.
23. **Jaworski, A., and S. M. Crowe.** 1999. Does HIV cause depletion of CD4+ T cells in vivo by the induction of apoptosis? Immunol. Cell Biol. **77**:90–98.
24. **Kanda, T., H. Koike, M. Arai, J. E. Wilson, C. M. Carthy, D. Yang, B. M. McManus, R. Nagai, and I. Kobayashi.** 1999. Increased severity of viral myocarditis in mice lacking lymphocyte maturation. Int. J. Cardiol. **68**:13–22.
25. **Kawai, C.** 1999. From myocarditis to cardiomyopathy: mechanisms of inflammation and cell death: learning from the past for the future. Circulation **99**:1091–1100.
26. **Kerr, J. F. R., A. H. Wylie, and A. R. Currie.** 1972. Apoptosis: a basic biological phenomenon with wide-ranging implications in tissue kinetics. Br. J. Cancer **26**:239–257.
27. **Kohli, V., J. F. Madden, R. C. Bentley, and P. A. Clavien.** 1999. Calpain mediates ischemic injury of the liver through modulation of apoptosis and necrosis. Gastroenterology **116**:168–178.
28. **Krammer, P. H., I. Behrmann, P. Daniel, J. Dhein, and K. M. Debatin.** 1994. Regulation of apoptosis in the immune system. Curr. Opin. Immunol. **6**:276–289.
29. **Lee, J. K., S. H. Zaidi, P. Liu, F. Dawood, A. Y. Cheah, W. H. Wen, Y. Saiki, and M. Rabinovitch.** 1998. A serine elastase inhibitor reduces inflammation and fibrosis and preserves cardiac function after experimentally-induced murine myocarditis. Nat. Med. **4**:1383–1391.
30. **Liu, P., T. Martino, M. A. Opavsky, and J. Penninger.** 1996. Viral myocarditis: balance between viral infection and immune response. Can. J. Cardiol. **12**:935–943.
31. **Marshall, W. L., C. Yim, E. Gustafson, T. Graf, D. R. Sage, K. Hanify, L. Williams, J. Fingeroth, and R. W. Finberg.** 1999. Epstein-Barr virus encodes a novel homolog of the bcl-2 oncogene that inhibits apoptosis and associates with Bax and Bak. J. Virol. **73**:5181–5185.
32. **Martin, S. J., and D. R. Green.** 1995. Protease activation during apoptosis: death by a thousand cuts? Cell **82**:349–352.
33. **Matsumori, A.** 1996. Cytokines in myocarditis and cardiomyopathies. Curr. Opin. Cardiol. **11**:302–309.
34. **Megyeri, K., K. Berencsi, T. D. Halazonetis, G. C. Prendergast, G. Gri, S. A. Plotkin, G. Rovera, and E. Gonczol.** 1999. Involvement of a p53-dependent pathway in rubella virus-induced apoptosis. Virology **259**:74–84.
35. **Murachi, T.** 1983. Calpain and calpastatin. Trends Biochem. Sci. **8**:167–169.
36. **Nath, R., K. J. Raser, D. Stafford, I. Hajimohammadreza, A. Posner, H. Allen, R. V. Talanian, P. Yuen, R. B. Gilbertsen, and K. K. Wang.** 1996. Non-erythroid α-spectrin breakdown by calpain and interleukin 1 B-converting-enzyme-like protease(s) in apoptotic cells: contributory roles of both protease families in neuronal apoptosis. Biochem. J. **319**:686–690.
37. **Neuberger, T., A. K. Chakrabarti, T. Russell, G. H. DeVreis, E. L. Hogan, and N. L. Banik.** 1997. Immunolocalization of cytoplamic and myelin mCalpain in transfected Schwann cells. I. Effect of treatment with growth factors. J. Neurosci. Res. **47**:521–530.
38. **Oberhaus, S. M., R. L. Smith, G. H. Clayton, T. S. Dermody, and K. L. Tyler.** 1997. Reovirus infection and tissue injury in the mouse central nervous system are associated with apoptosis. J. Virol. **71**:2100–2106.
39. **Oberhaus, S. M., T. S. Dermody, and K. L. Tyler.** 1998. Apoptosis and the cytopathic effects of reovirus. Curr. Top. Microbiol. Immunol. **233**:23–49.
40. **O'Brien, V.** 1998. Viruses and apoptosis. J. Gen. Virol. **79**:1833–1834.
41. **Patel, T., G. J. Gores, and S. H. Kaufmann.** 1996. The role of proteases during apoptosis. FASEB J. **10**:587–597.
42. **Pignata, C., M. Fiore, S. deFilippo, M. Cavalcanti, L. Gaetaniello, and I. Scotese.** 1998. Apoptosis as a mechanism of peripheral blood mononuclear cell death after measles and varicella-zoster virus infections in children. Pediatr. Res. **43**:77–83.
43. **Porn-Ares, M. I., A. Samali, and S. Orenius.** 1998. Cleavage of the calpain inhibitor, calpastatin, during apoptosis. Cell Death Differ. **5**:1028–1033.
44. **Rodgers, S. E., E. S. Barton, S. M. Oberhaus, B. Pike, C. A. Gibson, K. L. Tyler, and T. S. Dermody.** 1997. Reovirus-induced apoptosis of MDCK cells is not linked to viral yield and is blocked by Bcl-2. J. Virol. **71**:2540–2546.
45. **Rose, N. R., A. Herskowitz, and D. A. Neumann.** 1993. Autoimmunity in myocarditis: models and mechanisms. Clin. Immunol. Immunopathol. **68**: 95–99.
46. **Rose, N. R., and S. L. Hill.** 1996. The pathogenesis of postinfectious myocarditis. Clin. Immunol. Immunopathol. **80**:S92–S99.
47. **Ruiz-Vela, A., G. Gonzalez de Buitrago, and A.-C. Martinez.** 1999. Implication of calpain in caspase activation during B cell clonal deletion. EMBO J. **18**:4988–4998.
48. **Saatman, K. E., H. Murai, R. T. Bartus, D. H. Smith, N. J. Hayward, B. R. Perri, and T. K. McIntosh.** 1996. Calpain inhibitor AK295 attenuates motor and cognitive deficits following experimental brain injury in the rat. Proc. Natl. Acad. Sci. USA **93**:3428–3433.
49. **Salamino, F., R. DeTullio, P. Mengotti, P. L. Viotti, E. Melloni, and S. Pontremoli.** 1993. Site-directed activation of calpain is promoted by a membrane-associated natural activator protein. Biochem. J. **290**:191–197.
50. **Schultz-Cherry, S., and V. S. Hinshaw.** 1996. Influenza virus neuraminidase activates latent transforming growth factor beta. J. Virol. **70**:8624–8629.
51. **Schwimmbeck, P. L., S. A. Huber, and H. P. Schultheiss.** 1997. Roles of T cells in coxsackie-B induced disease. Curr. Top. Microbiol. Immunol. **223**: 283–303.
52. **Seko, Y., N. Takahashi, H. Yagita, K. Okumura, and Y. Yazaki.** 1997. Expression of cytokine mRNA's in murine hearts with acute myocarditis caused by coxsackievirus b3. J. Pathol. **183**:105–108.
53. **Seko, Y., N. Takahashi, M. Azuma, H. Yagita, K. Okumura, and Y. Yazaki.** 1998. Expression of costimulatory molecule CD40 in murine heart with acute myocarditis and reduction of inflammation by treatment with anti-CD40L/B7–1 monoclonal antibodies. Circ. Res. **83**:463–469.
54. **Shen, Y., and T. E. Shenk.** 1995. Viruses and apoptosis. Curr. Opin. Genet. Dev. **5**:105–111.
55. **Sherry, B.** 1998. Pathogenesis of reovirus myocarditis, p. 51–66. *In* K. L. Tyler and M. B. A. Oldstone (ed.), Reoviruses II: cytopathogenicity and pathogenesis. Springer-Verlag, Berlin, Germany.
56. **Sherry, B., and M. A. Blum.** 1994. Multiple viral core proteins are determinants of reovirus-induced acute myocarditis. J. Virol. **63**:8461–8465.
57. **Sherry, B., C. J. Baty, and M. A. Blum.** 1996. Reovirus-induced acute myocarditis in mice correlates with viral RNA synthesis rather than generation of infectious virus in cardiac myocytes. J. Virol. **70**:6709–6715.
58. **Sherry, B., F. J. Schoen, E. Wenske, and B. N. Fields.** 1989. Derivation and characterization of an efficiently myocarditic reovirus variant. J. Virol. **63**: 4840–4849.
59. **Sherry, B., J. Torres, and M. A. Blum.** 1998. Reovirus induction of and sensitivity to beta interferon in cardiac myocyte cultures correlate with induction of myocarditis and are determined by viral core proteins. J. Virol. **72**:1314–1323.
60. **Sherry, B., X.-Y. Li, K. L. Tyler, J. M. Cullen, and H. W. Virgin.** 1993. Lymphocytes protect against and are not required for reovirus-induced myocarditis. J. Virol. **67**:6119–6124.
61. **Sindram, D., V. Kohli, J. F. Madden, and P. A. Clavien.** 1999. Calpain inhibition prevents sinusoidal endothelial cell apoptosis in the cold ischemic rat liver. Transplantation **68**:136–140.
62. **Solary, E., B. Eymin, N. Droin, and M. Haugg.** 1998. Proteases, proteolysis, and apoptosis. Cell Biol. Toxicol. **14**:11–32.
63. **Sorimachi, H., S. Ishiura, and K. Suzuki.** 1997. Structure and physiological function of calpains. Biochem. J. **328**:721–732.
64. **Squier, M. K., A. J. Sehnert, K. S. Sellins, A. M. Malkinson, E. Takanoand, and J. J. Cohen.** 1999. Calpain and calpastatin regulate neutrophil apoptosis. J. Cell. Physiol. **178**:311–319.
65. **Squier, M. K. T., and J. J. Cohen.** 1997. Calpain, an upstream regulator of thymocyte apoptosis. J. Immunol. **158**:3690–3697.
66. **Strong, J. E., D. Tang, and P. W. K. Lee.** 1993. Evidence that the epidermal growth factor receptor on host cells confers reovirus infection efficiency. Virology **197**:405–411.
67. **Teodoro, J. G., and P. E. Branton.** 1997. Regulation of apoptosis by viral gene products. J. Virol. **71**:1739–1746.
68. **Thomas, M., and L. Banks.** 1999. Human papillomavirus (HPV) E6 interactions with Bak are conserved amongst E6 proteins from high and low risk HPV types. J. Gen. Virol. **80**:1513–1517.

69. **Tyler, K. L., M. K. T. Squier, S. E. Rodgers, B. E. Schneider, S. M. Oberhaus, T. A. Grdina, J. J. Cohen, and T. S. Dermody.** 1995. Differences in the capacity of reovirus strains to induce apoptosis are determined by viral attachment protein σ1. J. Virol. **69:**6972–6979.
70. **Valentin, H., O. Azocar, B. Horvat, R. Willeims, R. Garrone, A. Evlasher, M. L. Toribio, and C. Rabourdin-Combe.** 1999. Measles virus infection induces terminal differentiation of human thymic epithelial cells. J. Virol. **73:**2212–2221.
71. **Wang, K. K., R. Postmantur, R. Nadimpalli, R. Nath, P. Mohan, R. A. Nixon, R. V. Talanian, M. Keegan, L. Herzog, and H. Allen.** 1998. Caspase-mediated fragmentation of calpain inhibitor protein calpastatin during apoptosis. Arch. Biochem. Biophys. **356:**187–196.
72. **Wang, K. K. W., and P. Yuen.** 1994. Calpain inhibition: an overview of its therapeutic potential. Trends Pharmacol. Sci. **15:**412–419.
73. **Watt, F., and P. L. Molloy.** 1993. Specific cleavage of transcription factors by the thiol protease, m-calpain. Nucleic Acids Res. **21:**5092–5100.
74. **Weller, M., J. B. Schulz, U. Wullner, P. A. Loschmann, T. Klockgether, and J. Dichgans.** 1997. Developmental and genetic regulation of programmed neuronal death. J. Neural Transm. **50:**115–123.
75. **Wood, D. E., A. Thomas, L. A. Devi, Y. Berman, R. C. Beavis, J. C. Reed, and E. W. Newcomb.** 1998. Bax cleavage is mediated by calpain during drug-induced apoptosis. Oncogene **17:**1069–1078.
76. **Wood, D. E., and E. W. Newcomb.** 1999. Caspase-dependent activation of calpain during drug-induced apoptosis. J. Biol. Chem. **274:**8309–8315.
77. **Yang, D., J. Yu, Z. Luo, C. M. Carthy, J. E. Wilson, Z. Liu, and B. M. McManus.** 1999. Viral myocarditis: identification of five differentially expressed genes in coxsackievirus B3-infected mouse heart. Circ. Res. **84:**704–712.
78. **Yeh, E. T.** 1997. Life and death in the cardiovascular system. Circulation **95:**782–786.
79. **Zhivotovsky, B., D. H. Burgess, D. M. Vanags, and S. Orrenius.** 1997. Involvement of cellular proteolytic machinery in apoptosis. Biochem. Biophys. Res. Commun. **230:**481–488.

JOURNAL OF VIROLOGY, Aug. 2001, p. 7429–7434 Vol. 75, No. 16
0022-538X/01/$04.00+0 DOI: 10.1128/JVI.75.16.7429–7434.2001

Reovirus-Induced σ1s-Dependent G_2/M Phase Cell Cycle Arrest Is Associated with Inhibition of $p34^{cdc2}$

GEORGE J. POGGIOLI,[1] TERENCE S. DERMODY,[2,3,4] AND KENNETH L. TYLER[1,5,6,7,8]*

Departments of Neurology,[5] Medicine,[6] Microbiology,[1] and Immunology,[7] University of Colorado Health Sciences Center, and Neurology Service, Denver Veterans Affairs Medical Center,[8] Denver, Colorado 80220, and Departments of Pediatrics[2] and Microbiology and Immunology[3] and Elizabeth B. Lamb Center for Pediatric Research,[4] Vanderbilt University School of Medicine, Nashville, Tennessee 37232

Received 28 February 2001/Accepted 23 May 2001

Serotype 3 reoviruses inhibit cellular proliferation by inducing a G_2/M phase cell cycle arrest. Reovirus-induced G_2/M phase arrest requires the viral S1 gene-encoded σ1s nonstructural protein. The G_2-to-M transition represents a cell cycle checkpoint that is regulated by the kinase $p34^{cdc2}$. We now report that infection with serotype 3 reovirus strain Abney, but not serotype 1 reovirus strain Lang, is associated with inhibition and hyperphosphorylation of $p34^{cdc2}$. The σ1s protein is necessary and sufficient for inhibitory phosphorylation of $p34^{cdc2}$, since a viral mutant lacking σ1s fails to hyperphosphorylate $p34^{cdc2}$ and inducible expression of σ1s is sufficient for $p34^{cdc2}$ hyperphosphorylation. These studies establish a mechanism by which reovirus can perturb cell cycle regulation.

Mammalian reoviruses are nonenveloped, double-stranded RNA viruses having a broad host range in nature (68). Mechanisms underlying reovirus-induced cytopathicity are not completely understood. Although reovirus replication is thought to be entirely cytoplasmic (reviewed in reference 47), reovirus infection is associated with dramatic alterations of nuclear function that likely contribute to cell death. Reovirus induces apoptosis (57, 70) and inhibits cellular proliferation (55, 69).

Reovirus inhibits cellular proliferation by inducing a G_2/M phase cell cycle arrest. Serotype 3 prototype strains type 3 Abney (T3A) and type 3 Dearing (T3D) induce G_2/M cell cycle arrest to a greater extent than the prototype serotype 1 strain Lang (T1L) (55). Strain-specific differences in the capacity of reovirus to induce G_2/M cell cycle arrest are determined by the viral S1 gene (55, 69). The S1 gene is bicistronic, encoding the viral attachment protein σ1 and the nonstructural protein σ1s in overlapping but out-of-sequence reading frames (15, 30, 62). The σ1s protein is necessary and sufficient for reovirus-induced G_2/M cell cycle arrest since a σ1s-deficient reovirus mutant fails to induce G_2/M cell cycle arrest and ectopic expression of σ1s results in accumulation of cells in the G_2/M phase of the cell cycle (55).

The transition from G_2 to M is under the control of the cyclin-dependent kinase $p34^{cdc2}$/cdk1 (cdc2) (29, 31, 49, 50). Activation of cdc2 requires its association with cyclin B (13, 22, 35, 42, 44, 46). Cyclin B expression varies with the phase of the cell cycle, with levels peaking during G_2 and early M phase (27, 28, 40, 54). Regulated expression of cyclin B ensures that the cdc2-cyclin B heterodimeric complex forms at the appropriate time during cell cycle progression (54).

The cdc2-cyclin B complex is maintained in an inactive state as a result of hyperphosphorylation of cdc2 (5, 12, 14, 54, 63). Cdc2 migrates in acrylamide gels as three distinct bands corresponding to the level of inhibitory phosphorylation. Cdc2-PP is phosphorylated on both Thr14 and Tyr15, and cdc2-P is phosphorylated on Thr14 or Tyr15 (48). The protein kinases wee1 and myt1 are capable of phosphorylating cdc2 (4, 18, 45, 51, 52, 60). Entry into mitosis requires removal of the inhibitory phosphorylation on cdc2 by the dual-specificity phosphatase cdc25C (23, 34, 37, 43, 59, 65). Dephosphorylation results in cdc2 kinase activation, which initiates events necessary for mitosis (reviewed in reference 29).

Having shown that reovirus-induced inhibition of cellular proliferation (69) results from G_2/M phase cell cycle arrest (55), we conducted experiments to determine how reovirus infection perturbs G_2-to-M checkpoint regulatory mechanisms. We found that the capacity of cdc2 kinase to phosphorylate a cdc2-specific histone H1 peptide substrate is dramatically inhibited in cell lysates following infection with serotype 3 reovirus. Reovirus-induced inhibition of cdc2 kinase activity is associated with an increase in hyperphosphorylated forms of cdc2. Expression of σ1s results in hyperphosphorylation of cdc2, and a σ1s-deficient mutant reovirus fails to inactivate cdc2. These results indicate that serotype 3 reovirus-induced G_2/M phase cell cycle arrest is associated with cdc2 kinase inhibition and provide biochemical evidence linking the σ1s protein to this process.

MATERIALS AND METHODS

Cells and viruses. Spinner-adapted mouse L929 cells (ATCC CCL1) were grown in Joklik's modified Eagles's minimal essential medium, which was supplemented to contain 5% heat-inactivated fetal bovine serum (Gibco BRL, Gaithersburg, Md.) and 2 mM L-glutamine (Gibco). Human embryonic kidney (HEK293) cells (ATCC CRL1573), Madin-Darby canine kidney (MDCK) cells (ATCC CCL34), C127 cells (ATCC CRL1616), and HeLa cells (ATCC CCL2) were grown in Dulbecco's modified Eagle's medium, which was supplemented to contain 10% heat-inactivated fetal bovine serum (HEK293, MDCK, and C127) or 10% non-heat-inactivated fetal bovine serum (HeLa), 2 mM L-glutamine, 1 mM sodium pyruvate (Gibco), 100 U of penicillin per ml, and 100 μg of streptomycin per ml (Gibco).

Reovirus strains T1L and T3A are laboratory stocks. The reovirus field isolate

* Corresponding author. Mailing address: Department of Neurology (B-182), University of Colorado Health Sciences Center, 4200 E. 9th Ave., Denver, CO 80262. Phone: (303) 393-2874. Fax: (303) 393-4686. E-mail: Ken.Tyler@UCHSC.edu.

strain type 3 clone 84 was isolated from a human host (11). T3C84-MA was isolated as previously described (9). Type 3 clone 84 and T3C84-MA are abbreviated herein as T3/σ1s+ and T3/σ1s−, respectively. Viral strains were plaque purified and passaged two to three times in L929 cells to generate working stocks as previously described (67).

Reovirus infection. Cells were seeded in six-well plates (Costar, Cambridge, Mass.) at 5×10^5 cells per well in a volume of 2 ml of the appropriate medium. After 24 h of incubation, when cells were 50 to 60% confluent, the medium was removed, and cells were infected with reovirus at a multiplicity of infection (MOI) of either 100 PFU per cell (T1L and T3A) or 1,000 PFU per cell (T3/σ1s+ and T3/σ1s−) in a volume of 200 μl at 37°C for 1 h. After viral infection, 2 ml of fresh medium was added to each well. At various times postinfection, cells were harvested and washed with 1 ml of phosphate-buffered saline.

Inducible expression of σ1s. C127 stable transformants expressing T3D σ1s (BPX6-2) from the mouse metallothionein promoter and vector control cells (BPV1-2) were gifts of Aaron Shatkin (16). BPX6 (σ1s-expressing) and BPV1 (vector control) cells were seeded in six-well plates at 5×10^5 cells per well in a volume of 2 ml per well. After 24 h of incubation, cells were incubated with 1 μM $CdCl_2$ to induce σ1s expression (17) and harvested at various times postinduction for cdc2 kinase migration analysis.

Gel electrophoresis and immunoblot analysis. Cell pellets were lysed in 2× Laemmli buffer (36) (approximately 10^6 cells per 50 μl) containing 4% sodium dodecyl sulfate, 20% glycerol, 10% β-mercaptoethanol, 0.004% bromphenol blue, and 0.125 M Tris-HCl (pH 6.8) (Sigma, St. Louis, Mo.). Lysates were sonicated for 5 to 10 s on ice, boiled for 10 min, and electrophoresed in 10 or 15% polyacrylamide gels as described previously (3, 36) (Hoefer Pharmacia Biotech, San Francisco, Calif.) at constant voltage (60 V through the stacking gel and 150 V through the resolving gel).

Following electrophoresis, gels and Hybond-C nitrocellulose membranes (Amersham, Piscataway, N.J.) were separately equilibrated to Towbin's transfer buffer (0.025 M Tris base, 0.15 M glycine, 20% methanol [pH 8.0]) for 5 min (66). Proteins were electroblotted onto nitrocellulose membranes for 30 to 45 min at 100 V in a Hoefer Scientific blotting tank at 4°C. Membranes were rinsed in Tris-buffered saline (TBS; 20 mM Tris base, 137 mM NaCl [pH 7.6]), incubated with fresh 5 to 10% nonfat dry milk (NFDM) in TBS at 22°C for 2 h, and rinsed with TBS.

Immunoblots were normalized for actin content as determined by the density of actin staining detected using an antiactin antibody (CP01; Calbiochem, San Diego, Calif.) (1:5,000 dilution in TBS containing 5% NFDM at 22°C for 1 h) and probed for either cyclin B1 (554177, PharMingen; San Diego, Calif.) at a 1:375 dilution in TBS at 22°C for 16 h, cdc2 (SC-54; Santa Cruz Biotechnology, Santa Cruz, Calif.) at a 1:500 dilution in TBS at 22°C for 3 to 4 h, or cdc25C (67211A; PharMingen) at a 1:300 dilution in TBS at 22°C for 3 h. Bound antibodies were probed with an anti-mouse immunoglobulin conjugated to horseradish peroxidase (NA931; Amersham) at a 1:2,000 dilution in TBS containing 2% NFDM at 22°C for 2 to 3 h. Antibody binding was visualized using enhanced chemiluminescence (Amersham), and densitometric analysis was performed using a FluorS MultiImager system and Quantity One software (Bio-Rad, Hercules, Calif.).

The fold increases in cyclin B1 levels following reovirus infection were calculated by dividing the densitometric value for cyclin B1 following infection by the densitometric value for cyclin B1 following mock infection for each time point. The fraction of cdc2-PP was calculated by dividing the densitometric value for cdc2-PP by the densitometric value for the total amount of cdc2 kinase. The fold increase in cdc2-PP following reovirus infection was calculated by dividing the fraction of cdc2-PP following virus infection by the fraction of cdc2-PP following mock infection for each time point. Nocodazole treatment (5 μg per ml for 20 h) resulted in the fastest-migrating, nonphosphorylated/active form of cdc2 (data not shown). The three phosphorylation states for cdc2 and cdc25C were confirmed by treating L929 cell lysates with 0, 2, 5, or 10 U of potato acid phosphatase (Roche Molecular Biochemicals, Indianapolis, Ind.) for 1.5 h and 15 min, respectively, in 50 mM PIPES [piperazine-*N*,*N*′-bis(2-ethanesulfonic acid)] containing 1 mM dithiothreitol at 30°C prior to cdc2 or cdc25C detection (data not shown).

Cdc2 protein kinase assay. Cdc2 kinase activity was determined by using the SignaTECT cdc2 protein kinase assay system (Promega, Madison, Wis.). Cells were lysed by sonication in cdc2 extraction buffer containing 50 mM Tris-HCl (pH 7.4), 250 mM NaCl, 1 mM EDTA, 50 mM NaF, 1 mM dithiothreitol, 0.1% Triton X-100, 10 μM leupeptin, and 100 μg of aprotinin per ml and normalized for actin content. Aliquots of cell lysate corresponding to equivalent amounts of actin content were incubated with 50 μM [γ-^{32}P]ATP and 25 μM histone H1 biotinylated peptide substrate. The radiolabeled phosphate substrate was recovered on a streptavidin matrix and analyzed by scintillation counting. Nocodazole treatment (5 μg per ml for 20 h) was used as a positive control.

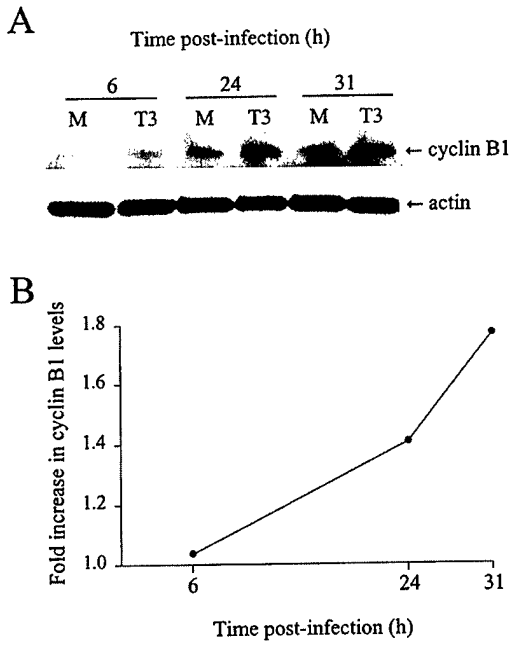

FIG. 1. T3A infection induces increased cyclin B1 levels. L929 cells were either mock infected (M) or infected with T3A (T3) at an MOI of 100 PFU per cell. Cell lysates were collected, normalized for actin content, and probed for cyclin B1 (A). At each time point postinfection, the band intensity for cyclin B1 following T3A infection was compared to that following mock infection and represented as the fold increase in cyclin B1 level (B).

RESULTS

Cyclin B1 levels are increased following infection with reovirus T3A. Cyclin B1 levels oscillate with the cell cycle, peaking during G_2 and early M phase (27, 28, 40, 54). To determine whether reovirus infection alters levels of cyclin B1, we analyzed cyclin B1 levels in L929 cells following T3A infection (Fig. 1). At various intervals after infection, L929 cell lysates were collected, normalized for actin content, and probed for cyclin B1 protein (Fig. 1A). T3A infection resulted in increased cyclin B1 levels at 24 h postinfection (1.4-fold increase over mock-infected cells), and these levels were further increased at 31 h postinfection (1.75-fold increase over mock-infected cells) (Fig. 1B). These results indicate that reovirus-induced G_2/M phase cell cycle arrest does not result from loss of cyclin B1.

T3A reovirus infection inhibits cdc2 kinase activity. Cdc2 kinase activity plays an important regulatory role at the G_2-to-M checkpoint (29, 31, 49, 50). We therefore analyzed cdc2 kinase activity following T3 reovirus infection. L929 cells were infected with T3A, and cdc2 kinase activity in cell lysates was assessed at 48 h postinfection. Lysates were normalized for actin content to allow kinase activity in lysates from infected and mock-infected cells to be directly compared. T3A infection resulted in a 4.8-fold reduction in cdc2 kinase activity in comparison to mock-infected cells, $P = 0.028$ (Fig. 2). Thus, reovirus-induced G_2/M phase cell cycle arrest is associated with inhibition of the major G_2-to-M transition control kinase, cdc2.

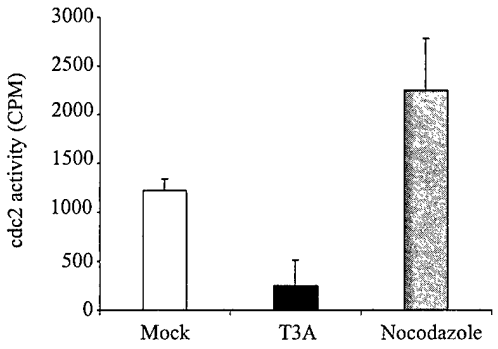

FIG. 2. Cdc2 kinase activity is inhibited following T3A infection. L929 cells were mock infected, infected with T3A at an MOI of 100 PFU per cell, or treated with nocodazole. Cell lysates were collected at 48 h postinfection, normalized for actin content, and assayed for cdc2 kinase activity. Results are presented as the mean product formed in counts per minute minus a no-cell lysate control for three independent experiments. The error bars indicate the standard errors of the mean.

T3A induces inhibitory phosphorylation of cdc2 kinase. Reduced cdc2 kinase activity may result from either protein degradation or kinase inactivation by inhibitory hyperphosphorylation (5, 12, 14, 54, 63). We therefore analyzed the amounts of phosphorylated cdc2 by immunoblot assay at 6, 24, and 48 h postinfection (Fig. 3). In comparison to mock-infected control cells, T3A infection was associated with an increase in the slower-migrating, hyperphosphorylated form of cdc2 (cdc2-PP) at both 24 (1.5-fold) and 48 (2.5-fold) h postinfection (Fig. 3A). The increase in cdc2-PP following T3A reovirus infection was significantly greater than the increase in cdc2-PP following T1L infection at 24 and 48 h postinfection, $P = 0.006$ and $P = 0.003$, respectively (Fig. 3B). These results indicate that T3 reovirus infection is associated with hyperphosphorylation of cdc2. Furthermore, infection with T1 reovirus, which induces substantially less G_2/M cell cycle arrest than T3 reovirus (55), likewise induces less inhibitory phosphorylation of cdc2 (Fig. 3C).

Cdc2 is phosphorylated in cell lines that undergo G_2/M phase cell cycle arrest in response to reovirus infection. Given that the capacity of reovirus to induce G_2/M phase cell cycle arrest is not cell type specific (55), we considered whether hyperphosphorylation of cdc2 occurred following reovirus infection of other cell types. MDCK, C127, HEK293, and HeLa cells were either infected with T3A or mock infected as a control, and cdc2 phosphorylation status in cell lysates was determined at 48 h postinfection. Increases in the fraction of cdc2-PP following T3A infection was observed in all cell lines tested except HeLa cells (Fig. 4). Therefore, reovirus-induced hyperphosphorylation of cdc2, like G_2/M cell cycle arrest, is not limited to cell type.

The σ1s protein is necessary and sufficient to inhibit cdc2 kinase. We have previously shown that σ1s expression is required for G_2/M phase cell cycle arrest in response to serotype 3 reovirus infection (55). To determine whether σ1s is required for reovirus-induced cdc2 kinase inhibition, we compared levels of hyperphosphorylated cdc2 in L929 cells following infection with reovirus strains T3/σ1s+ and T3/σ1s−, which vary in the capacity to express σ1s (58). The accumulation of phosphorylated cdc2 following infection with T3/σ1s- was significantly less than the accumulation of phosphorylated cdc2 following infection with its σ1s-expressing parent virus, T3/σ1s+ (Fig. 5A). Therefore, functional σ1s is required for serotype 3 reovirus-induced hyperphosphorylation of cdc2.

We also have shown that ectopic expression of σ1s results in G_2/M phase cell cycle arrest (55). To determine whether σ1s expression alone is sufficient to induce cdc2 kinase inhibition, we analyzed the phosphorylation status of cdc2 in C127 cells engineered to express the T3D σ1s protein under the control of the mouse metallothionein promoter (16). The fraction of cdc2-PP following induction of σ1s by 1 μM $CdCl_2$ was 1.6- and 2.0-fold greater in cells expressing σ1s than in vector control cells at 45 and 55 h postinduction, respectively (Fig. 5B). These results indicate that σ1s is necessary and sufficient to induce inhibition of cdc2 kinase.

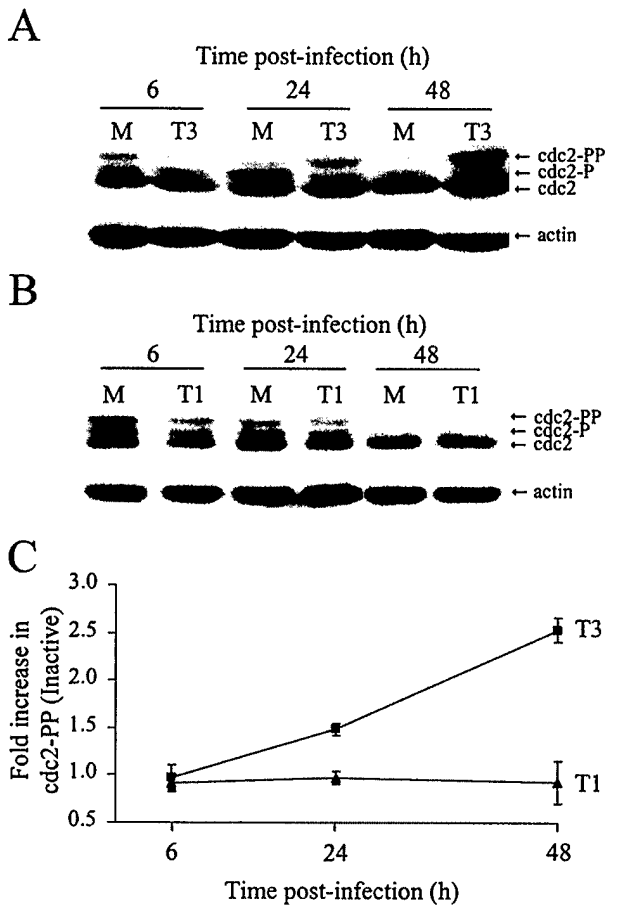

FIG. 3. Cdc2 kinase inhibition following T3A infection results from hyperphosphorylation. L929 cells were either mock infected (M) or infected with T3A (T3) (A) or T1L (T1) (B) at an MOI of 100 PFU per cell. Cell lysates were collected at the indicated times postinfection, normalized for actin content, and probed for cdc2 kinase. Phosphorylated forms of cdc2 are shown. Cdc2-P indicates either Thr14 or Tyr15 phosphorylation, and cdc2-PP indicates Thr14 and Tyr15 phosphorylation. (C) The fraction of cdc2-PP was determined for each condition, and at each time point postinfection, the fraction of cdc2-PP following T1L (triangles) or T3A (squares) infection was compared to that following mock infection and represented as the fold increase in cdc2-PP. Results are presented as the mean fold increase in cdc2-PP for four (T3A) or two (T1L) independent experiments. The error bars indicate the standard errors of the mean.

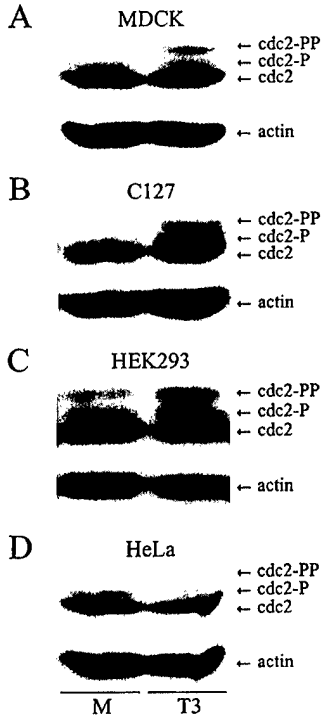

FIG. 4. T3A infection inhibits cdc2 kinase in a variety of cell lines. MDCK (A), C127 (B), HEK293 (C), and HeLa (D) cells were either mock infected (M) or infected with T3A (T3) at an MOI of 100 PFU per cell. Cell lysates were collected at 48 h postinfection, normalized for actin content, and probed for cdc2 kinase. Phosphorylated forms of cdc2 are shown. Cdc2-P indicates either Thr14 or Tyr15 phosphorylation, and cdc2-PP indicates Thr14 and Tyr15 phosphorylation.

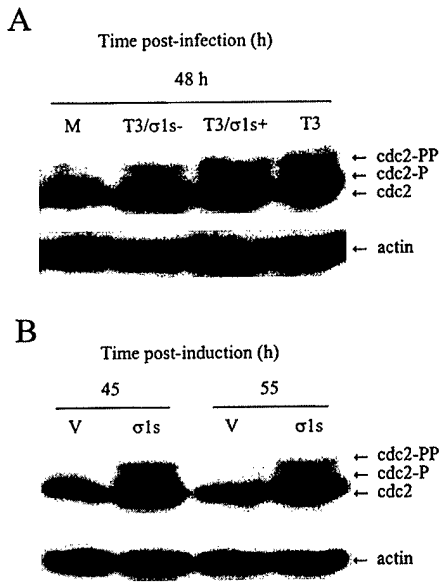

FIG. 5. The σ1s protein is necessary and sufficient to inhibit cdc2. (A) L929 cells were mock infected (M), infected with T3A (T3) at an MOI of 100 PFU per cell, or infected with T3C84 (T3/σ1s+) or σ1s-null mutant T3C84-MA (T3/σ1s−) at an MOI of 1,000 PFU per cell. Cell lysates were collected at 48 h postinfection, normalized for actin content, and probed for cdc2 kinase. Phosphorylated forms of cdc2 are shown. cdc2-P indicates either Thr14 or Tyr15 phosphorylation, and cdc2-PP indicates Thr14 and Tyr15 phosphorylation. (B) C127 cells stably transfected with T3D-σ1s under the control of the mouse metallothionein promoter (σ1s) or vector control cells (V) were induced with $CdCl_2$, harvested at the indicated times postinfection, normalized for actin content, and probed for cdc2 kinase. Phosphorylated forms of cdc2 are shown.

Cdc25C is inhibited following serotype 3 reovirus infection. To determine whether increased inhibitory phosphorylation of cdc2 following reovirus infection resulted from inactivation of the cdc2-specific phosphatase cdc25C, we analyzed the different phosphorylation states of cdc25C in polyacrylamide gels since cdc25C activity is regulated by phosphorylation. At 6, 24, 31, and 48 h postinfection, L929 cell lysates were run on polyacrylamide gels, transferred to nitrocellulose, and probed for cdc25C phosphatase (Fig. 6). T3A infection resulted in a decrease in the slower-migrating/hyperphosphorylated or active form of cdc25C (hyperphosphorylated cdc25C) at 24, 31, and 48 h postinfection compared to mock-infected controls. There was a corresponding increase in the inactive Ser216-phosphorylated and nonphosphorylated forms of cdc25C compared to mock-infected controls. These results suggest that one pathway by which reovirus inhibits cdc2 is to prevent cdc2 dephosphorylation by inhibiting the cdc2-dependent phosphatase cdc25C.

DISCUSSION

Serotype 3 reovirus strains induce G_2/M phase cell cycle arrest in a variety of target cells in vitro (55). The progression from G_2 to M is regulated by the association of cyclin B1 with the cdc2 kinase (13, 22, 35, 42, 44, 46). We hypothesized that either decreased levels of cyclin B1 or decreased activity of cdc2 kinase might mediate reovirus-induced cell cycle arrest at the G_2-to-M checkpoint. Our findings demonstrate that reovirus infection does not result in decreased cyclin B1 levels. Instead, we found a striking reduction in cdc2 kinase activity and a concomitant increase in cdc2 hyperphosphorylation.

Cdc2-cyclin B activity is inhibited by phosphorylation of cdc2 (12, 54, 63). Following serotype 3 reovirus infection, there is a significant reduction in cdc2 kinase activity and an increase in inhibitory phosphorylation of cdc2. Inhibition of cdc2 kinase by

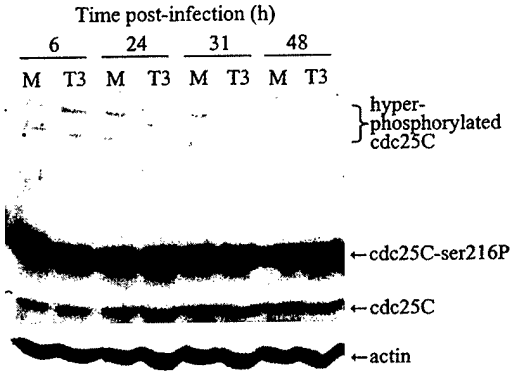

FIG. 6. Cdc25C is inhibited following reovirus infection. L929 cells were either mock infected (M) or infected with T3A (T3) at an MOI of 100 PFU per cell. Cell lysates were collected at the indicated times postinfection, normalized for actin content, and probed for cdc25C. Phosphorylated forms of cdc25C are shown. Reovirus infection results in reduction of the hyperphosphorylated/active form of cdc25C. Results are representative of three independent experiments.

reovirus is not cell type specific and occurs in all cell lines that were found to undergo significant amounts of G_2/M phase cell cycle arrest following serotype 3 reovirus infection except in HeLa cells, which show the least amount of reovirus-induced G_2/M arrest.

We have previously shown that σ1s expression is required for reovirus-induced G_2/M phase cell cycle arrest (55). We now show that σ1s expression is also required for inhibition of cdc2 kinase activity. Furthermore, σ1s expression alone, which induces an increase in the percentage of cells in the G_2/M phase of the cell cycle (55), is capable of inhibiting cdc2. These results provide strong evidence that the viral S1 gene product σ1s induces G_2/M phase cell cycle arrest at the G_2-to-M checkpoint by activating a pathway leading to hyperphosphorylation of cdc2 kinase; however, alternative mechanisms may contribute to reovirus-induced G_2/M phase cell cycle arrest. These results are consistent with observations that σ1s is present in the nucleus of serotype 3-infected cells (8, 58), where it could interact with proteins responsible for G_2-to-M transition.

Several viruses are influenced by or alter cdc2 kinase activity. For example, the herpes simplex virus U_L13 and $\alpha22/U_S1.5$ (ICP22) gene products (1), *Autographa californica* nucleopolyhedrovirus ODV-EC27 (6, 7), and human papillomavirus E6 and E7 (64) can all increase cdc2 activity. In cases where viruses increase cdc2 kinase activity, it is possible that this activity is required to phosphorylate viral proteins. For example, varicella-zoster virus glycoprotein gI (72), Epstein-Barr virus EBNA-LP (33), hepatitis E virus ORF3 (73), and herpes simplex virus ICP0 (2) are phosphorylated by cdc2. Conversely, human immunodeficiency virus (HIV) Vpr (25, 56) and human papillomavirus E2 (19) inhibit or delay the activation of cdc2. These observations suggest that viruses have evolved mechanisms to alter cdc2 function. At least in the case of HIV Vpr, cdc2 inhibition and subsequent G_2/M cell cycle arrest result in increased viral replication (24, 71). The role of reovirus-induced G_2/M arrest in viral replication remains unknown. However, it is clear that reovirus-induced G_2/M cell cycle arrest does not require apoptotic DNA damage (55).

The mechanism by which reovirus inhibits cdc2 kinase activity remains to be established. Cdc2 kinase activity is negatively regulated by the kinase wee1 and positively regulated by the phosphatase cdc25C (reviewed in reference 29). Following reovirus infection, cdc25C is inhibited by dephosphorylation. It is suggested that HIV Vpr can inhibit cdc2 activity (25, 56) via activation of wee1 and inactivation of cdc25C (26, 41). Vpr may inactivate cdc25C through physical interaction with protein phosphatase 2A (26), which inhibits cdc25C activity by dephosphorylation (10, 32, 38). Cdc25C activity is also inhibited following phosphorylation by the kinases chk1 and chk2 (20, 21, 39, 53, 61). Based on these observations, it is possible that the reovirus σ1s protein mediates inactivation of cdc2 kinase by increasing the levels of wee1 and/or chk1 or by increasing the translocation of protein phosphatase 2A to the nucleus. Wee1 directly phosphorylates and inactivates cdc2, whereas chk1 inactivates cdc25C so that cdc25C is no longer available to dephosphorylate and activate cdc2. Recent supportive investigation revealed that reovirus infection is associated with increased expression of wee1 and chk1 (G. J. Poggioli and R. L. DeBiasi, unpublished observation). Our ongoing work is directed at defining the biochemical mechanisms underlying σ1s-mediated inactivation of cdc2 kinase and establishing the pathological significance of this process.

ACKNOWLEDGMENTS

This work was supported by Public Health Service award AG14071 from the National Institute of Aging, Merit and REAP grants from the Department of Veterans Affairs, and a U.S. Army Medical Research Acquisition Activity Grant (DAMD17-98-1-8614) (K.L.T.). This work also was supported by Public Health Service award AI38296 from the National Institute of Allergy and Infectious Diseases and the Elizabeth B. Lamb Center for Pediatric Research (T.S.D.).

REFERENCES

1. **Advani, S. J., R. Brandimarti, R. R. Weichselbaum, and B. Roizman.** 2000. The disappearance of cyclins A and B and the increase in activity of the G_2/M-phase cellular kinase cdc2 in herpes simplex virus 1-infected cells require expression of the $\alpha22/U_S1.5$ and U_L13 viral genes. J. Virol. **74:**8–15.
2. **Advani, S. J., R. R. Weichselbaum, and B. Roizman.** 2000. The role of cdc2 in the expression of herpes simplex virus genes. Proc. Natl. Acad. Sci. USA **97:**10996–11001.
3. **Ames, G. F.** 1974. Resolution of bacterial proteins by polyacrylamide gel electrophoresis on slabs. Membrane, soluble, and periplasmic fractions. J. Biol. Chem. **249:**634–644.
4. **Atherton-Fessler, S., F. Liu, B. Gabrielli, M. S. Lee, C. Y. Peng, and H. Piwnica-Worms.** 1994. Cell cycle regulation of the $p34^{cdc2}$ inhibitory kinases. Mol. Biol. Cell **5:**989–1001.
5. **Atherton-Fessler, S., L. L. Parker, R. L. Geahlen, and H. Piwnica-Worms.** 1993. Mechanisms of $p34^{cdc2}$ regulation. Mol. Cell. Biol. **13:**1675–1685.
6. **Belyavskyi, M., S. C. Braunagel, and M. D. Summers.** 1998. The structural protein ODV-EC27 of *Autographa californica* nucleopolyhedrovirus is a multifunctional viral cyclin. Proc. Natl. Acad. Sci. USA **95:**11205–11210.
7. **Braunagel, S. C., R. Parr, M. Belyavskyi, and M. D. Summers.** 1998. *Autographa californica* nucleopolyhedrovirus infection results in Sf9 cell cycle arrest at G_2/M phase. Virology **244:**195–211.
8. **Ceruzzi, M., and A. J. Shatkin.** 1986. Expression of reovirus p14 in bacteria and identification in the cytoplasm of infected mouse L cells. Virology **153:**35–45.
9. **Chappell, J. D., V. L. Gunn, J. D. Wetzel, G. S. Baer, and T. S. Dermody.** 1997. Mutations in type 3 reovirus that determine binding to sialic acid are contained in the fibrous tail domain of viral attachment protein σ1. J. Virol. **71:**1834–1841.
10. **Clarke, P. R., I. Hoffmann, G. Draetta, and E. Karsenti.** 1993. Dephosphorylation of cdc25-C by a type-2A protein phosphatase: specific regulation during the cell cycle in *Xenopus* egg extracts. Mol. Biol. Cell **4:**397–411.
11. **Dermody, T. S., M. L. Nibert, R. Bassel-Duby, and B. N. Fields.** 1990. Sequence diversity in S1 genes and S1 translation products of 11 serotype 3 reovirus strains. J. Virol. **64:**4842–4850.
12. **Draetta, G., and D. Beach.** 1988. Activation of cdc2 protein kinase during mitosis in human cells: cell cycle-dependent phosphorylation and subunit rearrangement. Cell **54:**17–26.
13. **Draetta, G., F. Luca, J. Westendorf, L. Brizuela, J. Ruderman, and D. Beach.** 1989. Cdc2 protein kinase is complexed with both cyclin A and B: evidence for proteolytic inactivation of MPF. Cell **56:**829–838.
14. **Endicott, J. A., P. Nurse, and L. N. Johnson.** 1994. Mutational analysis supports a structural model for the cell cycle protein kinase p34. Protein Eng. **7:**243–253.
15. **Ernst, H., and A. J. Shatkin.** 1985. Reovirus hemagglutinin mRNA codes for two polypeptides in overlapping reading frames. Proc. Natl. Acad. Sci. USA **82:**48–52.
16. **Fajardo, E., and A. J. Shatkin.** 1990. Expression of the two reovirus S1 gene products in transfected mammalian cells. Virology **178:**223–231.
17. **Fajardo, J. E., and A. J. Shatkin.** 1990. Translation of bicistronic viral mRNA in transfected cells: regulation at the level of elongation. Proc. Natl. Acad. Sci. USA **87:**328–332.
18. **Featherstone, C., and P. Russell.** 1991. Fission yeast $p107^{wee1}$ mitotic inhibitor is a tyrosine/serine kinase. Nature **349:**808–811.
19. **Fournier, N., K. Raj, P. Saudan, S. Utzig, R. Sabli, V. Simanis, and P. Beard.** 1999. Expression of human papillomavirus 16 E2 protein in *Schizosaccharomyces pombe* delays the initiation of mitosis. Oncogene **18:**4015–4021.
20. **Furnari, B., A. Blasina, M. N. Boddy, C. H. McGowan, and P. Russell.** 1999. Cdc25 inhibited in vivo and in vitro by checkpoint kinases Cds1 and Chk1. Mol. Biol. Cell **10:**833–845.
21. **Furnari, B., N. Rhind, and P. Russell.** 1997. Cdc25 mitotic inducer targeted by chk1 DNA damage checkpoint kinase. Science **277:**1495–1497.
22. **Gautier, J., J. Minshull, M. Lohka, M. Glotzer, T. Hunt, and J. L. Maller.** 1990. Cyclin is a component of maturation-promoting factor from *Xenopus*. Cell **60:**487–494.
23. **Gautier, J., M. J. Solomon, R. N. Booher, J. F. Bazan, and M. W. Kirschner.** 1991. cdc25 is a specific tyrosine phosphatase that directly activates $p34^{cdc2}$. Cell **67:**197–211.

24. **Goh, W. C., M. E. Rogel, C. M. Kinsey, S. F. Michael, P. N. Fultz, M. A. Nowak, B. H. Hahn, and M. Emerman.** 1998. HIV-1 vpr increases viral expression by manipulation of the cell cycle: a mechanism for selection of vpr in vivo. Nat. Med. **4**:65–71.
25. **He, J., S. Choe, R. Walker, P. Di Marzio, D. O. Morgan, and N. R. Landau.** 1995. Human immunodeficiency virus type 1 viral protein R (Vpr) arrests cells in the G_2 phase of the cell cycle by inhibiting $p34^{cdc2}$ activity. J. Virol. **69**:6705–6711.
26. **Hrimech, M., X. J. Yao, P. E. Branton, and E. A. Cohen.** 2000. Human immunodeficiency virus type 1 vpr-mediated G_2 cell cycle arrest: Vpr interferes with cell cycle signaling cascades by interacting with the B subunit of serine/threonine protein phosphatase 2A. EMBO J. **19**:3956–3967.
27. **Hwang, A., W. G. McKenna, and R. J. Muschel.** 1998. Cell cycle-dependent usage of transcriptional start sites. A novel mechanism for regulation of cyclin B1. J. Biol. Chem. **273**:31505–31509.
28. **Jackman, M., M. Firth, and J. Pines.** 1995. Human cyclins B1 and B2 are localized to strikingly different structures: B1 to microtubules, B2 primarily to the Golgi apparatus. EMBO J. **14**:1646–1654.
29. **Jackman, M. R., and J. N. Pines.** 1997. Cyclins and the G_2/M transition. Cancer Surv. **29**:47–73.
30. **Jacobs, B. L., and C. E. Samuel.** 1985. Biosynthesis of reovirus-specified polypeptides: the reovirus S1 mRNA encodes two primary translation products. Virology **143**:63–74.
31. **King, R. W., P. K. Jackson, and M. W. Kirschner.** 1994. Mitosis in transition. Cell **79**:563–571.
32. **Kinoshita, N., H. Ohkura, and M. Yanagida.** 1990. Distinct, essential roles of type 1 and 2A protein phosphatases in the control of the fission yeast cell division cycle. Cell **63**:405–415.
33. **Kitay, M. K., and D. T. Rowe.** 1996. Cell cycle stage-specific phosphorylation of the Epstein-Barr virus immortalization protein EBNA-LP. J. Virol. **70**: 7885–7893.
34. **Kumagai, A., and W. G. Dunphy.** 1991. The cdc25 protein controls tyrosine dephosphorylation of the cdc2 protein in a cell-free system. Cell **64**:903–914.
35. **Labbe, J. C., J. P. Capony, D. Caput, J. C. Cavadore, J. Derancourt, M. Kaghad, J. M. Lelias, A. Picard, and M. Doree.** 1989. MPF from starfish oocytes at first meiotic metaphase is a heterodimer containing one molecule of cdc2 and one molecule of cyclin B. EMBO J. **8**:3053–3058.
36. **Laemmli, U. K.** 1970. Cleavage of structural proteins during the assembly of the head of bacteriophage T4. Nature **227**:680–685.
37. **Lee, M. S., S. Ogg, M. Xu, L. L. Parker, D. J. Donoghue, J. L. Maller, and H. Piwnica-Worms.** 1992. cdc25+ encodes a protein phosphatase that dephosphorylates $p34^{cdc2}$. Mol. Biol. Cell **3**:73–84.
38. **Lee, T. H., M. J. Solomon, M. C. Mumby, and M. W. Kirschner.** 1991. INH, a negative regulator of MPF, is a form of protein phosphatase 2A. Cell **64**:415–423.
39. **Lopez-Girona, A., B. Furnari, O. Mondesert, and P. Russell.** 1999. Nuclear localization of Cdc25 is regulated by DNA damage and a 14-3-3 protein. Nature **397**:172–175.
40. **Maity, A., W. G. McKenna, and R. J. Muschel.** 1995. Evidence for post-transcriptional regulation of cyclin B1 mRNA in the cell cycle and following irradiation in HeLa cells. EMBO J. **14**:603–609.
41. **Masuda, M., Y. Nagai, N. Oshima, K. Tanaka, H. Murakami, H. Igarashi, and H. Okayama.** 2000. Genetic studies with the fission yeast *Schizosaccharomyces pombe* suggest involvement of wee1, ppa2, and rad24 in induction of cell cycle arrest by human immunodeficiency virus type 1 Vpr. J. Virol. **74**:2636–2646.
42. **Meijer, L., D. Arion, R. Golsteyn, J. Pines, L. Brizuela, T. Hunt, and D. Beach.** 1989. Cyclin is a component of the sea urchin egg M-phase specific histone H1 kinase. EMBO J. **8**:2275–2282.
43. **Millar, J. B., C. H. McGowan, G. Lenaers, R. Jones, and P. Russell.** 1991. $p80^{cdc25}$ mitotic inducer is the tyrosine phosphatase that activates $p34^{cdc2}$ kinase in fission yeast. EMBO J. **10**:4301–4309.
44. **Minshull, J., R. Golsteyn, C. S. Hill, and T. Hunt.** 1990. The A- and B-type cyclin associated cdc2 kinases in *Xenopus* turn on and off at different times in the cell cycle. EMBO J. **9**:2865–2875.
45. **Mueller, P. R., T. R. Coleman, A. Kumagai, and W. G. Dunphy.** 1995. Myt1: a membrane-associated inhibitory kinase that phosphorylates cdc2 on both threonine-14 and tyrosine-15. Science **270**:86–90.
46. **Murray, A. W., and M. W. Kirschner.** 1989. Cyclin synthesis drives the early embryonic cell cycle. Nature **339**:275–280.
47. **Nibert, M. L., L. A. Schiff, and B. N. Fields.** 1996. Reoviruses and their replication, p. 1557–1596. *In* B. N. Fields, D. M. Knipe, and P. M. Howley (ed.), Fields virology. Lippincott-Raven Press, New York, N.Y.
48. **Norbury, C., J. Blow, and P. Nurse.** 1991. Regulatory phosphorylation of the $p34^{cdc2}$ protein kinase in vertebrates. EMBO J. **10**:3321–3329.
49. **Nurse, P.** 1990. Universal control mechanism regulating onset of M-phase. Nature **344**:503–508.
50. **Ohi, R., and K. L. Gould.** 1999. Regulating the onset of mitosis. Curr. Opin. Cell Biol. **11**:267–273.
51. **Parker, L. L., S. Atherton-Fessler, M. S. Lee, S. Ogg, J. L. Falk, K. I. Swenson, and H. Piwnica-Worms.** 1991. Cyclin promotes the tyrosine phosphorylation of $p34^{cdc2}$ in a wee1+ dependent manner. EMBO J. **10**:1255–1263.
52. **Parker, L. L., S. Atherton-Fessler, and H. Piwnica-Worms.** 1992. $p107^{wee1}$ is a dual-specificity kinase that phosphorylates $p34^{cdc2}$ on tyrosine 15. Proc. Natl. Acad. Sci. USA **89**:2917–2921.
53. **Peng, C. Y., P. R. Graves, R. S. Thoma, Z. Wu, A. S. Shaw, and H. Piwnica-Worms.** 1997. Mitotic and G_2 checkpoint control: regulation of 14-3-3 protein binding by phosphorylation of Cdc25C on serine-216. Science **277**:1501–1505.
54. **Pines, J., and T. Hunter.** 1989. Isolation of a human cyclin cDNA: evidence for cyclin mRNA and protein regulation in the cell cycle and for interaction with $p34^{cdc2}$. Cell **58**:833–846.
55. **Poggioli, G. J., C. Keefer, J. L. Connolly, T. S. Dermody, and K. L. Tyler.** 2000. Reovirus-induced G_2/M cell cycle arrest requires σ1s and occurs in the absence of apoptosis. J. Virol. **74**:9562–9570.
56. **Re, F., D. Braaten, E. K. Franke, and J. Luban.** 1995. Human immunodeficiency virus type 1 Vpr arrests the cell cycle in G_2 by inhibiting the activation of $p34^{cdc2}$ cyclin B. J. Virol. **69**:6859–6864.
57. **Rodgers, S. E., E. S. Barton, S. M. Oberhaus, B. Pike, C. A. Gibson, K. L. Tyler, and T. S. Dermody.** 1997. Reovirus-induced apoptosis of MDCK cells is not linked to viral yield and is blocked by Bcl-2. J. Virol. **71**:2540–2546.
58. **Rodgers, S. E., J. L. Connolly, J. D. Chappell, and T. S. Dermody.** 1998. Reovirus growth in cell culture does not require the full complement of viral proteins: identification of a σ1s-null mutant. J. Virol. **72**:8597–8604.
59. **Russell, P., and P. Nurse.** 1986. cdc25+ functions as an inducer in the mitotic control of fission yeast. Cell **45**:145–153.
60. **Russell, P., and P. Nurse.** 1987. Negative regulation of mitosis by wee1+, a gene encoding a protein kinase homolog. Cell **49**:559–567.
61. **Sanchez, Y., C. Wong, R. S. Thoma, R. Richman, Z. Wu, H. Piwnica-Worms, and S. J. Elledge.** 1997. Conservation of the Chk1 checkpoint pathway in mammals: linkage of DNA damage to Cdk regulation through Cdc25. Science **277**:1497–1501.
62. **Sarkar, G., J. Pelletier, R. Bassel-Duby, A. Jayasuriya, B. N. Fields, and N. Sonenberg.** 1985. Identification of a new polypeptide coded by reovirus gene S1. J. Virol. **54**:720–725.
63. **Solomon, M. J., M. Glotzer, T. H. Lee, M. Philippe, and M. W. Kirschner.** 1990. Cyclin activation of $p34^{cdc2}$. Cell **63**:1013–1024.
64. **Steinmann, K. E., X. F. Pei, H. Stoppler, R. Schlegel, and R. Schlegel.** 1994. Elevated expression and activity of mitotic regulatory proteins in human papillomavirus-immortalized keratinocytes. Oncogene **9**:387–394.
65. **Strausfeld, U., J. C. Labbe, D. Fesquet, J. C. Cavadore, A. Picard, K. Sadhu, P. Russell, and M. Doree.** 1991. Dephosphorylation and activation of a $p34^{cdc2}$/cyclin B complex in vitro by human CDC25 protein. Nature **351**:242–245.
66. **Towbin, H., T. Staehelin, and J. Gordon.** 1979. Electrophoretic transfer of proteins from polyacrylamide gels to nitrocellulose sheets: procedure and some applications. Proc. Natl. Acad. Sci. USA **76**:4350–4354.
67. **Tyler, K. L., R. T. Bronson, K. B. Byers, and B. Fields.** 1985. Molecular basis of viral neurotropism: experimental reovirus infection. Neurology **35**:88–92.
68. **Tyler, K. L., and B. N. Fields.** 1996. Reoviruses, p. 1597–1623. *In* B. N. Fields, D. M. Knipe, and P. M. Howley (ed.), Fields virology. Lippincott-Raven Press, New York, N.Y.
69. **Tyler, K. L., M. K. Squier, A. L. Brown, B. Pike, D. Willis, S. M. Oberhaus, T. S. Dermody, and J. J. Cohen.** 1996. Linkage between reovirus-induced apoptosis and inhibition of cellular DNA synthesis: role of the S1 and M2 genes. J. Virol. **70**:7984–7991.
70. **Tyler, K. L., M. K. Squier, S. E. Rodgers, B. E. Schneider, S. M. Oberhaus, T. A. Grdina, J. J. Cohen, and T. S. Dermody.** 1995. Differences in the capacity of reovirus strains to induce apoptosis are determined by the viral attachment protein σ1. J. Virol. **69**:6972–6979.
71. **Yao, X. J., A. J. Mouland, R. A. Subbramanian, J. Forget, N. Rougeau, D. Bergeron, and E. A. Cohen.** 1998. Vpr stimulates viral expression and induces cell killing in human immunodeficiency virus type 1-infected dividing Jurkat T cells. J. Virol. **72**:4686–4693.
72. **Ye, M., K. M. Duus, J. Peng, D. H. Price, and C. Grose.** 1999. Varicella-zoster virus Fc receptor component gI is phosphorylated on its endodomain by a cyclin-dependent kinase. J. Virol. **73**:1320–1330.
73. **Zafrullah, M., M. H. Ozdener, S. K. Panda, and S. Jameel.** 1997. The ORF3 protein of hepatitis E virus is a phosphoprotein that associates with the cytoskeleton. J. Virol. **71**:9045–9053.

Brain Pathology 11: 452-464(2001)

SYMPOSIUM: Herpesvirus Infections of the Nervous System

Polymerase Chain Reaction as a Diagnostic Adjunct in Herpesvirus Infections of the Nervous System

B. K. Kleinschmidt-DeMasters, M.D.[1,2], Roberta L. DeBiasi, M.D.[2,3], Kenneth L. Tyler, M.D.[2,4,5]

Departments of [1]Pathology, [2]Neurology, [3]Pediatrics, [4]Microbiology, and [5]Immunology and Medicine, University of Colorado Health Sciences Center and The Denver Veterans Administration Hospital, Denver, Colorado, USA

Polymerase chain reaction (PCR) is a powerful technique that allows detection of minute quantities of DNA or RNA in cerebrospinal fluid (CSF), vesicle and endoneurial fluids, blood, fresh-frozen, and even formalin-fixed tissues. Various infectious agents can be detected with high specificity and sensitivity, including bacteria, parasites, rickettsia and viruses. PCR analysis of CSF has revolutionized the diagnosis of nervous system viral infections, particularly those caused by human herpesviruses (HHV), and has now replaced brain biopsy as the gold standard for diagnosis of herpes simplex virus (HSV) encephalitis. PCR analysis of both CSF and nervous system tissues has also broadened our understanding of the spectrum of disease caused by HSV-1 and -2, cytomegalovirus (CMV), Epstein-Barr virus (EBV), varicella zoster virus (VZV), and HHV-6. Nonetheless, positive tissue PCR results must be interpreted cautiously, especially in cases that lack corroborating clinical and neuropathologic evidence of infection. Moreover, positive PCR results from tissues do not distinguish latent from productive (lytic) viral infections. In several neurological diseases, negative PCR results have provided strong evidence against a role for herpesviruses as the causative agents. This review focuses on the use of PCR tests to diagnose HSV and VZV infections of the nervous system.

Introduction

Polymerase chain reaction (PCR) can be applied to the diagnosis of any disease in which nucleic acids (*e.g.* DNA, RNA) or their expression as messenger RNA (mRNA) play a role. PCR is useful to study congenital diseases, malignancies, autoimmune disorders, and infections (23); PCR aids in diagnosis, therapy, disease classification, epidemiology, and basic research. In infectious disorders, PCR is ideally suited for identifying fastidious organisms that may be difficult, or impossible, to culture (24). The technique can be performed rapidly and inexpensively, and test results are typically available faster than with standard culture or serological methods. Nucleic acids of bacteria, mycobacteria, rickettsia, parasites, treponemes, and viruses can be identified by PCR analysis of any body secretion, fluid, or tissue. The widespread availability of an in-house test in most hospitals, or ready access to a reference laboratory, has led to the incorporation of PCR testing on CSF and body fluids into medical practice in the United States and other developed countries. Unfortunately, the rapid proliferation of testing has led to substantial variation among laboratories in terms of quality control, techniques and procedures.

Despite the wide application of PCR to CSF and other body fluids, such as vesicle or endoneurial fluids, PCR analysis of central (CNS) and peripheral (PNS) nervous system tissues remains primarily a research tool and is not available at all institutions. PCR on tissues and CSF, sometimes in conjunction with immunohistochemistry or *in situ* hybridization techniques, have furthered our understanding of the role of herpesvirus in cases of encephalitis, meningitis, meningoencephalitis, myelitis, ventriculoencephalitis, polymyeloradiculitis, and brainstem infections. PCR of cerebral arteries has established a direct role for VZV in cases of waxing and waning vasculitis (36), and PCR of temporal arteries has negated a role for VZV in giant cell arteritis (66).

Interpretation of positive PCR amplification of herpesvirus genome in brain tissues from patients with neurological disorders of uncertain etiology can be problematic. Since amplification of viral nucleic acid does

Corresponding author:
B.K. Kleinschmidt-DeMasters, Department of Pathology B216, University of Colorado Health Sciences Center, 4200 East Ninth Avenue, Denver, CO 80262; Tel.: (303) 315-7298; Fax (303) 315-6721; E-mail: BK.DeMasters@UCHSC.edu

not distinguish between genomic fragments, latent infection, low-grade persistent infection, or active (lytic) infection. The interpretation of a positive result may depend on the precise gene or genes being amplified, and whether the methods used are designed to detect genomic DNA, RNA, or mRNA. Herpesviruses are generally classified as either neurotropic (HSV, VZV) or lymphotropic (EBV, HHV-6, HHV-7, HHV-8) based on their tissue location during latency; defined as "the persistence of the virus in a host in the absence of clinically apparent infection," with the capacity to reactivate (31). Considerable information is available about the physical state, viral nucleic acids and proteins during latency of neurotropic herpesviruses (see companion article by Cohrs *et al.*) Numerous studies have also documented latency of herpesviruses in cells other than those of the nervous system, including peripheral blood mononuclear cells (78), B-lymphocytes, and T-lymphocytes.

In the CNS, nucleic acid hybridization first detected HSV viral genome in human brains in 1979 (73) and again in 1981 (32). PCR on human brain revealed HSV DNA in brainstem, olfactory bulbs and limbic areas (7). Since HSV has never been isolated from normal human brain tissue, the presence of the viral genome does not definitively signal latent viral infection or the capacity for reactivation, and instead might represent random viral sequences or fragments of virus. Although the viral transcripts associated with latency (LATS) have been identified in a mouse model of HSV infection (27), their presence has not been definitively demonstrated in human brain tissue (see accompanying article by Cohrs *et al.*). Several laboratories have also reported detection of viral genomic material of HHV-6, HHV-7, and HHV-8 in normal autopsy human brain (15, 21). It remains to be proven whether these viruses establish latency within brain. In contrast, VZV DNA has not been detected in normal human brain in most studies, and its presence on tissue PCR usually indicates productive infection of CNS.

This review summarizes the principles of PCR testing and the role of CSF PCR in the diagnosis and therapeutic management of herpesvirus infections of the nervous system, particularly HSV and VZV. Problems inherent in interpretation of positive tissue PCR for viruses that may become latent in the nervous system are also discussed.

Principles of PCR testing

PCR techniques allow the *in vitro* synthesis of millions of copies of a specific gene segment, and in turn,

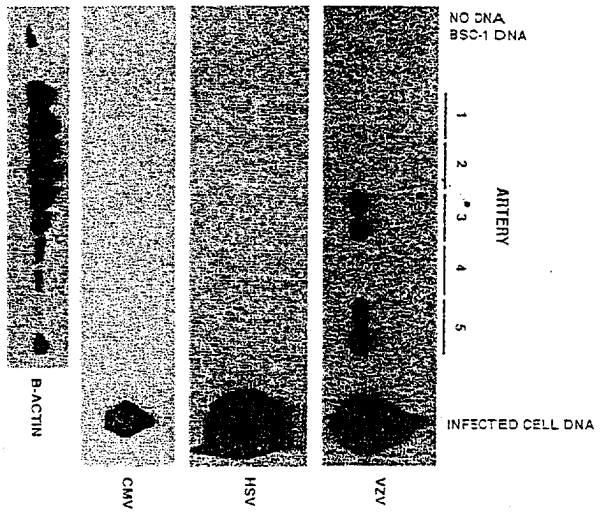

Figure 1. *PCR gel.* PCR detection of VZV DNA in cerebral artery sections from a patient with waxing/waning vasculitis (see ref 36). Total DNA was extracted from: BSC-1 cells; sections of multiple cerebral arteries; VZV- or HSV-1-infected BSC-1 cells; and CMV-infected human WI38 cells. Template DNA was omitted from one of the reaction tubes (no DNA). One ng of DNA from uninfected and virus-infected cells, and 10 μl of duplicate samples of DNA from sections of right middle cerebral artery (1), anterior cerebral artery (2), basilar artery (3), right vertebral artery (4), and right posterior cerebral artery (5) were PCR-amplified, using primers specific for VZV gene 29, HSV-1 gene UL30, genes corresponding to the CMV major immediate early genes, or human β-actin. Figure reproduced with permission, American Academy of Neurology.

the rapid detection of even a few copies of the target nucleic acid (see refs. 23 and 24 for reviews). DNA is often the target nucleic acid, although RNA can also be detected by reverse transcription (RT-PCR).

PCR uses the heat-stable DNA-synthesizing enzyme, DNA polymerase, to extend synthetic DNA fragments onto oligonucleotide primers designed to bind to target DNA segments. Oligonucleotide primers have sequences complementary to each strand of DNA to be amplified and are (usually) 20 to (rarely) 40 bases in length. Primer design is crucial for efficient and accurate PCR analysis. In the past, primer sequences were generated manually. Currently, software programs that facilitate optimal primer design are available *(http://www.genome.wi.mit.edu/cgi-bin/primer/primer3.cgi)* to address issues such as guanine-cytosine content, melting points that match for both primer sequences, and the reduction of unwanted primer-primer formation.

The first step in PCR is the denaturation of the double-stranded target DNA by heating the sample to 95°C. During heating, the DNA polymerase remains intact.

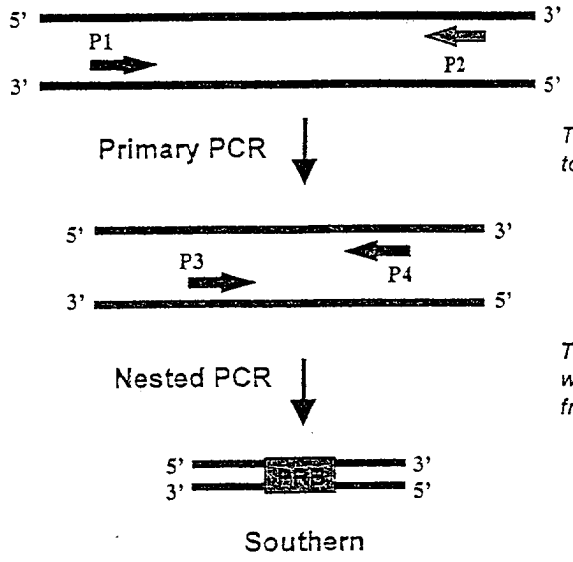

The first round of PRC is done with primers P1 and P2, to yield a DNA fragment from P1 to P2

The second round of PCR is done with primers P3 and P4 which are internal to P1 and P2 to yield a DNA fragment from P3 and P4

The nested PCR product is analyzed by Southern blot hybridization using a probe internal to the nested PCR product

Figure 2. *Schematic of Nested PCR.*

Oligonucleotide primers are supplied in considerable excess to ensure that more primers rather than the original (*de novo*) complementary strand of DNA are available for binding. As the sample containing the denatured DNA, primers, and DNA polymerase is cooled to 55-70°C, the primers anneal (bind) to their respective complementary template strands. The nucleotide building blocks adenine, guanine, thymidine, and cytosine are also supplied in molar excess. Using these nucleotides, the DNA polymerase (usually *Taq*) "reads" the target DNA strand in a 5′ to 3′ direction and forms a new, complementary DNA sequence downstream from the primer. This results in two complete double-stranded DNA pairs concluding the first cycle of PCR testing. Multiple cycles (30-40) of denaturing, annealing of new primers and strand elongation amplify DNA into 10^6-10^9 copies over 2-3 hours.

The resulting PCR product is visualized and identified based on its migration in an electrophoretic agarose gel containing ethidium bromide. The generation of a PCR product (amplicon) of the appropriate size, as predicted from the target gene and primer set used is the first indication of a positive reaction. However, Southern blotting is usually performed to ensure that the products generated are specific. The amplified fragment is transferred from the gel and analyzed using a radioactively or fluorescently labeled probe that is complementary to the expected target gene (Figure 1). Failure of the probe to bind to the amplicon indicates a false-positive PCR product due to mispriming or other technical issues, whereas confirmation of the specificity of amplified PCR products by Southern blot ensures that the product is derived from the target gene. Direct sequencing of the amplified product is also used for PCR product confirmation; however, this approach is limited primarily to the research setting since it is too labor-intensive for routine use.

Nested PCR is a modification that increases the specificity and especially the sensitivity of PCR. Nested PCR involves a second round of PCR in which an additional set of new primers internal to the original primers is utilized (Figure 2). A fragment smaller than the original target fragment becomes the second target. While nested PCR can increase the sensitivity of PCR, it also increases the likelihood of false-positive reactions. Results from studies using nested PCR may vary considerably from those that utilize non-nested PCR.

Quantitative PCR (using Taqman) is increasingly being applied to CSF, and occasionally to tissues. The technique involves the use of internal oligonucleotides — labeled at one end with a fluorescent dye and at the other end with a quencher dye — along with the PCR primers during amplification. Fluorescence emitted during PCR is measured and directly correlated to the number of copies of the target.

The ability of PCR to generate and amplify a high number of DNA strand copies from the original sample, which may contain as few as 1 to 10 copies of the target DNA, is both its greatest virtue and greatest limitation. The exquisite sensitivity of the test can easily lead to false-positive results from amplification of minute amounts of contaminating DNA. This problem is well-recognized by experienced laboratories, and rigorous controls are run simultaneously with the clinical samples, using all reagents except the unknown specimen to insure that the reagents do not harbor contaminants. Dedicated work areas and separate reagents used exclusively for PCR testing, frequent glove changes, and testing in laminar flow hoods alleviate false-positives. False-negative test results due to deterioration of the original sample specimen, incorrect heating of the sample, or use of incorrect proportions of the various mixture reagents are more easily rectified.

PCR works very well on biopsy or autopsy tissues frozen soon after removal from the body; DNA can be amplified by PCR even when tissues are stored for several years at -80°C. Although one of the greatest assets of PCR is that it can also be used on archival, formalin-fixed, paraffin-embedded tissue samples, yields of extracted DNA are usually less from fixed than from fresh tissues. Extraction of target DNA involves removal of the wax with several rounds of xylene immersion and centrifugation, and the procedure itself may slightly diminish the DNA yield from fixed tissues. The DNA yield from fixed tissues may also be reduced due to cross-linking after prolonged fixation (several years), or in association with use of osmic acid or other fixatives. Both fresh-frozen and fixed tissues must be digested with proteinase K prior to performing the PCR techniques described above. The protocol for extraction of DNA is described in the commercial kit literature (DNeasy Tissue Kit Handbook, Qiagen, 28159 Avenue Stanford, Valencia, CA, 91355, USA).

PCR of CSF

One of the most successful applications of CSF PCR is in the diagnosis of viral nervous system infections (8, 67, 88). PCR is preferable to serological testing, which usually requires 2-4 weeks after acute infection to reveal an antibody response. In contrast, CSF PCR yields positive results during acute infections, when the amount of replicating virus is maximal. Unlike traditional culture methods that may show negative results after the patient receives even small doses of antimicrobial drugs, CSF PCR retains its sensitivity after short courses of antiviral therapy (24). This allows the rapid start of empiric therapy when the patient initially presents with suspected meningitis or encephalitis, without potentially compromising the definitive diagnostic test. CSF PCR is also ideal for patients in whom brain biopsy is contraindicated clinically, such as patients with advanced acquired immunodeficiency syndrome (AIDS) (22).

Positive CSF PCR testing indicates the presence of viral DNA and is a marker of recent or ongoing active viral infection. Despite the high prevalence of seropositivity to HSV in the population and the fact that the virus becomes latent in multiple ganglia of most humans, HSV DNA is not detected in CSF of HSV-seropositive individuals without neurological disease or with other types of inflammatory non-HSV CNS infections (82). In general, a positive CSF PCR for viral DNA indicates a CNS infection by that particular pathogen, especially in an immunocompetent individual (82). A possible exception might arise from a breakdown of the blood-brain barrier (e.g., in severe bacterial meningitis), or contamination of the CSF with blood, resulting in a positive CSF PCR in the absence of viral infection (82). However, in one very recent study that addressed this problem, false-positive CSF PCR results for herpesviruses were not seen in any of 10 control patients with bacterial meningitis, despite high CSF white cell counts (75).

Replicating virus and viral DNA do not persist indefinitely, so that the CSF PCR test becomes negative over time, especially in immunocompetent patients. While most CSF testing in the clinical setting of suspected meningitis or meningoencephalomyelitis is performed within 1-2 days following onset of neurological symptoms, positive test results at least 2 and up to 4 weeks after onset of clinical disease have been recorded (88). False-negative tests can occur if PCR inhibitors are present in the CSF, such as hemoglobin products resulting from breakdown of red blood cells. However, modest xanthochromia does not negatively impact CSF PCR testing, nor does high CSF protein level or white blood cell count (24).

CSF PCR testing is optimally performed on fresh samples. However, DNA is more stable than RNA, and usually refrigeration for a few hours or even days does

not appear to significantly reduce the yield of the test although this has not been rigorously studied (24). In order to avoid cell lysis that liberates viral DNA into the supernatant and effectively dilutes the sample, CSF and body fluids for PCR should not be frozen prior to shipping. Optimally, samples are shipped overnight at room temperature, centrifuged, and the pellet examined for virus-specific DNA. The exquisite sensitivity of the technique implies the need for only small volumes of CSF for analysis (*i.e.* 30 μl) although laboratories generally request at least 0.5 ml.

Occasional immunocompetent or immunocompromised patients reveal more than one herpesvirus on CSF PCR, and EBV has been the most frequent agent associated with a dual positive result (75). In a large series of 662 patients, mostly immunocompetent, detection of HHV-6 and EBV by CSF PCR did not correlate clinically in several individuals with the presence of a CNS infection known to be caused by that virus (75). In contrast, detection of HSV-1, HSV-2, CMV, and VZV DNA correlated strongly with specific clinical syndromes of encephalitis/myelitis and meningitis (75). Similarly, in a large study of HIV-infected individuals, conducted to assess the diagnostic reliability of CSF PCR by comparison with biopsy or autopsy diagnoses, the most frequent false-positive herpesvirus detected was HHV-6 (19). In this study, seven of the 219 patients with corresponding tissue samples lacked histological evidence of a CNS disease that could be attributed to their HHV-6 DNA detected by CSF PCR (19). Additional large studies are necessary to determine the extent of false-positive PCR results for herpesviruses, especially HHV-6 and EBV.

Occasional false-negative and false-positive CSF PCR results for CMV have been seen in AIDS patients. In AIDS patients, CSF PCR detected HSV-1 or HSV-2 in all six cases (100%) of histologically confirmed HSV encephalitis, compared to 37 of 45 cases (82%) with CMV infections of CNS (19). An earlier study had suggested that a CSF PCR positive for CMV DNA correlated strongly with systemic CMV infections but not with CMV brain infections in AIDS patients at autopsy (1). Recent studies employing quantitative CSF PCR for CMV have indicated that AIDS patients with autopsy-confirmed CMV encephalitis harbor significantly higher levels of viral genome than do those with symptoms unrelated to CMV (91). These studies suggest the usefulness of quantitation in clarifying the clinical relevance of a positive CSF PCR result for CMV in AIDS patients (6). Despite these difficulties, CSF PCR for CMV has been used to monitor the efficacy of antimicrobial therapies and clearance of CMV viral burden in AIDS patients (16). Overall, CSF PCR testing has been crucial in diagnosing herpesviruses nervous system infections in AIDS patients and a positive CSF PCR result for herpesvirus in the majority of patients corresponds to CNS infection by that pathogen, just as it does in immunocompetent patients. CSF PCR has the potential to identify infections in AIDS patients who may not mount a classical serological response to viral infection or demonstrate protracted clinical manifestations (37).

CSF PCR testing has played a critical role in establishing the frequency and distribution of herpesvirus infections in immunocompetent populations. In the study by Studahl *et al.*, 87% of patients with herpesvirus DNA detected in CSF were immunocompetent, with HSV-1 identified in 18 patients, EBV in 16, HSV-2 in 9, CMV in 7, HHV-6 in 6, and VZV in 6 of 69 positive patients (75).

The sensitivity and specificity of CSF PCR exceeds 95% for HSV encephalitis (55, 88). For HSV-1, the existing standards to which CSF PCR results are compared, such as brain biopsy, are actually *less* sensitive than PCR (55). Hence, CSF PCR has dramatically reduced the need for brain biopsy as a diagnostic test. CSF PCR has also led to the identification of mild or atypical forms of HSV encephalitis that were formerly attributed to other viruses, often in the absence of brain biopsy (26, 30), and that may account for 17% of total cases of HSV encephalitis (30). CSF PCR has established the diagnosis and role of HSV-1 in brainstem encephalitis (84), myelitis (75), multifocal or diffuse encephalitis without temporal lobe involvement in children (71), and neonatal encephalitis (75). HSV encephalitis in children may relapse after therapy, and CSF PCR has been used to identify the subset of children in which HSV viral DNA reappears (43, 49). Quantitative CSF PCR may also provide valuable information in cases of pediatric HSV encephalitis in monitoring response to antiviral drugs (4)

CSF PCR has helped clinicians to recognize that HSV-2 can cause aseptic meningitis even in the absence of genital herpetic lesions (72), and has established HSV-2 as the most common cause of benign recurrent lymphocytic meningitis, including many cases previously diagnosed as Mollaret's meningitis (79). Even when CSF viral cultures are negative, CSF PCR is positive in patients with recurrent episodes of meningitis following an initial episode of herpes simplex meningitis (79). CSF PCR has illustrated that immunocompetent adults may manifest HSV-2-induced meningoencephalitis as well as meningitis (75). CSF PCR has identified

rare cases of HSV-2 brainstem encephalitis and recurrent thoracic myelitis (65).

CSF PCR testing has been found to be nearly 100% specific and sensitive as a tumor marker for EBV-related CNS lymphoma (18, 19, 22, 87), and has changed the way in which clinicians diagnose CNS lymphoma in immunocompromised individuals. In one study of AIDS patients with CNS mass lesions, a positive EBV CSF PCR correctly identified all 17 CNS lymphoma cases and was positive in only 1 of 68 AIDS patients with non-CNS lymphoma mass lesions (18). CSF PCR for EBV is also positive during the acute phase of the illness in children with infectious mononucleosis and neurological complications such as transverse myelitis, meningoencephalitis, and aseptic meningitis (88).

A sensitivity of 82% and specificity of 99% of CSF PCR for detecting CMV CNS infections has been reported in AIDS patients (16). A sensitivity of 60% for GSF PCR is cited for congenital CMV infections, and positive results may correlate with poorer neurologic outcome in affected infants (81). CMV viral load has also been monitored in peripheral blood leukocytes as a method to predict which immunosuppressed patients might develop a systemic (and CNS) infection (9, 29).

CSF PCR testing has corroborated the role of HHV-6 in febrile seizures, meningitis, encephalitis, and encephalopathy in immunocompetent and immunocompromised individuals (48, 92). HHV-6 genome has been demonstrated in CSF from up to 57% of children younger than one year of age who have febrile seizures ,and has also been seen in children with recurrent febrile convulsions (92). The role of HHV-7 in neurological disease is unclear, although detection of HHV-7 DNA in CSF and serum of children with exanthem subitum and encephalopathy has been reported (80, 85). Encephalitis in immunocompromised individuals associated with HHV-8 has been described (68), but this awaits additional confirmation. HHV-8 DNA has been detected in primary CNS lymphomas in some studies (20) but not others (5). In the study in which HHV-8 was detected, the virus was surmised to play an indirect role in the development of primary CNS lymphoma, and was thought to be present in the adjacent non-neoplastic lymphocytes but not the lymphoma cells (20).

CSF PCR for VZV has considerably broadened the understanding of the neurologic complications due to this virus (3, 8). VZV, along with EBV, displays the most protean manifestations of nervous system infection of any of the herpesviruses (35, 50, 51). Serological techniques and CSF PCR for VZV have been particularly helpful in identifying cases of VZV CNS infections without associated rash (*sine herpete*) (8, 11). Since the virus can rarely be cultured from CSF, diagnosis of meningitis or meningoencephalitis previously depended on the presence of a characteristic vesicular erythematous rash before, during, or after CNS infection, and VZV-mediated neurologic diseases were under-recognized. CSF PCR for VZV has shown that aseptic meningitis and brainstem encephalitis due to this virus can occur in immunocompetent hosts (75). In a study of 514 consecutive HIV-positive patients, CSF PCR for VZV became negative in patients whose clinical conditions improved following antiviral therapy and remained positive despite appropriate therapy in several patients who subsequently died (17). Hence, CSF PCR for VZV DNA may have utility in monitoring therapeutic response and in predicting outcomes. In the same study, several patients with positive CSF PCR for VZV DNA, but without clinically recognizable VZV meningoencephalitis, were considered to have subclinical reactivation of VZV, treated with antiviral agents and survived. In those cases, positive CSF PCR was considered to antedate clinical disease and allowed effective use of prophylactic therapy (17).

CSF PCR testing for VZV has established a role for the virus in cases of stroke (granulomatous arteritis), multifocal infarcts, myelitis, and neuritis. CSF PCR has served as the diagnostic test for large vessel encephalitis (also called granulomatous arteritis, herpes zoster ophthalmicus with contralateral hemiplegia, or simply stroke with VZV) (62), small vessel vasculopathy (leukoencephalitis) (3), myelitis (34), and zoster *sine herpete* (39). Some of these complications had been previously linked to VZV but received full confirmation from PCR testing.

PCR testing of body fluids other than CSF

PCR testing of skin vesicle fluid from patients with varicella (chickenpox) and zoster (shingles) has identified VZV in 97% of patients; in traditional viral culture methods, virus was isolated in only 23% of these same patients (25). PCR for VZV DNA was positive for vesicles up to 14 days after the onset of the rash, even from crusted cutaneous lesions, compared to culture specimens that were positive only when taken within 5 days of rash onset (25).

PCR analysis of peripheral blood mononuclear cells and CSF has furthered our understanding of the pathogenic mechanism in postherpetic neuralgia, the most common complication of VZV reactivation from latency in the elderly. Postherpetic neuralgia is characterized by pain that persists for more than the 4-6 weeks asso-

ciated with zoster (shingles) (35). The cause of the persistent pain is unknown. Using PCR, VZV DNA was detected in blood mononuclear cells from 11 of 51 postherpetic neuralgia patients, but not in any of 19 zoster patients without the persistent pain syndrome or in any of 11 elderly control individuals without zoster (58). While it is not possible to examine dorsal root ganglia — the site of VZV latency (56) — during the life of these patients, it seems likely that the PCR results reflect the greater level of VZV present in these ganglia during pain episodes than during periods of latency. Blood mononuclear cells may traffic through ganglia during periods of putative ganglionitis and acquire viral DNA. Thus, PCR analysis of blood mononuclear cells provides a window to indirectly assess levels of VZV replication in deep ganglionic tissues of patients with postherpetic neuralgia.

PCR on both CSF and fluid from auricular vesicles has confirmed that VZV causes Ramsey-Hunt syndrome, the second most common cause of 7th nerve facial paralysis after Bell palsy (64). Ramsey-Hunt syndrome can be difficult to recognize since the rash is hidden in the ear or mouth, and rash may be delayed, particularly in pediatric patients (41). PCR on endoneurial fluids and posterior auricular muscle samples collected during decompressive facial nerve surgery for Bell palsy identified HSV-1 DNA in 79% of patients and suggested that neither EBV or VZV is an important cause of idiopathic Bell palsy (63). A subsequent study using PCR identified a subset of patients with acute peripheral facial palsy that have zoster *sine herpete* (33). Acute facial palsy due to VZV constituted a significant percentage of the overall patient population (29%) in that study, and an even higher incidence of VZV reactivation (88%) was responsible for the palsy in the patients who were HSV-seronegative (33). Hence, PCR has verified a role for herpesviruses in both of the common causes of facial nerve paralysis and distinguishes which virus is causative in clinically confusing cases.

PCR testing on blood mononuclear cells has also impacted patient care for transplant recipients, AIDS patients, and other populations at-risk for CMV infections or EBV-related lymphoproliferative disorders. Monitoring of CMV viral loads by PCR in blood has led to prophylactic therapy with antiviral agents in AIDS and transplant patients to prevent systemic (and CNS) viral infections (29).

Confirmation of herpesvirus etiology in nervous system infections by tissue PCR

PCR testing on fresh, frozen, or archival fixed and paraffin-embedded tissues has allowed assessment of viral presence, even from small or imperfectly preserved specimens. Tissue PCR of cerebral arteries has established a direct role for VZV in cases of large vessel (62) and small vessel vasculopathy. In a patient with waxing and waning VZV vasculitis, detection of VZV DNA by PCR led to the discovery that VZV antigen was also present, indicating a productive infection in blood vessels as the cause of disease (36). Brain tissues may be positive for VZV DNA by PCR even when virus is no longer detectable by other methods, such as light microscopy for viral inclusions, immunohistochemistry, or *in situ* hybridization (52).

VZV latency in human sensory ganglia was originally demonstrated with Southern blotting by Gilden *et al.* (38) and was later confirmed by PCR (59). More recently, PCR techniques have been used on dorsal root ganglionic tissues to address the important question of whether neurons, satellite cells, or both harbor latent virus. PCR combined with *in situ* hybridization on sorted neuronal and non-neuronal cells fractions showed that latent VZV resides primarily, if not exclusively, in neurons at a level of two to five viral copies per latently infected neuron (54).

Our laboratory has used PCR to address the role of subclinical reactivation of VZV. Understanding the extent of viral burden in transplant recipients may help in monitoring their response to the doses of prophylactic antiviral agents currently being utilized. Quantitative PCR applied to autopsy trigeminal ganglia to assess VZV DNA burden in transplant recipients at risk for reactivation demonstrated an average of 119 copies of VZV DNA/μg of total ganglionic DNA, compared to an average of 71 copies in controls (B.K. Kleinschmidt-DeMasters, R. Mahalingam, unpublished data). These results suggest an increased viral burden in transplant recipients despite "optimal" antiviral prophylactic therapies. Future studies are needed to determine the clinical and statistical significance of the increased viral load in a larger number of transplant recipients, as well as the extent of host inflammatory response and viral antigen production, if any.

Exclusion of herpesvirus etiology in nervous system disease by tissue PCR

Given the protean manifestations of herpesvirus-mediated infections of the central and peripheral nervous system, efforts have been made to detect these viruses by PCR on tissues from several disease entities characterized by arteritis and/or inflammation. PCR

testing of various tissue specimens has suggested that VZV is not the cause of giant cell arteritis (66) and has shown no role for VZV, CMV, EBV, or HSV in childhood multifocal encephalomalacia (89). PCR also suggests that HSV is not the cause of Meniere's disease (90). A survey of a variety of normal and disease peripheral nerve conditions, including inflammatory peripheral neuropathies, revealed no HSV DNA by PCR in peripheral nerves (76), thus excluding a role for this herpesvirus in several disorders with a plausible viral etiology.

Questionable herpesvirus etiology in nervous system disease despite positive tissue PCR

Positive PCR on tissues from patients without definite clinicopathologic evidence of infection is difficult to interpret. For example, the HSV genome is present in brain tissues from both controls and patients with a variety of neurologic diseases (7), so that assignment of a role for this herpesvirus in a disease condition is especially problematic. Positive PCR results on tissues have been most challenging to interpret in patients who might not manifest classic clinical features of infection, but who exhibit tissue inflammation, such as putative chronic herpes simplex encephalitis in children (47), Rasmussen encephalitis (46, 86), and multiple sclerosis (MS) (69). Also problematic are positive PCR results in tissues from certain other non-inflammatory seizure disorders (28, 70), Alzheimer's disease (44, 45, 60), and brain tumors (14, 21).

Jay *et al.* identified HSV DNA in surgical resection tissues of pediatric patients with remote, antecedent clinical histories of HSV-1 encephalitis, subsequent intractable seizure disorders, and chronic encephalitis (47). That study described 3 pediatric patients whose brains revealed microglial nodules, lymphocytic infiltrates, and gliosis, but negative immunohistochemistry and electron microscopy for virus (47), suggesting that the HSV genome was present but that infectious virus was not being produced or produced only at extremely low levels. It remains unclear whether the chronic inflammation was a result of persistent low-grade viral replication or an immune response to prior infection. HSV DNA detection might reflect either the presence of latent virus no longer responsible for the encephalitis or the presence of herpesviruses that "simply accumulate in CNS with the passage of time," a possible explanation for some positive tissue PCR results offered by Vinters *et al.* (86). Clinicopathologic features in encephalitic cases such as these do not help clarify the interpretation of positive PCR results.

Identification of viral genomes in patients with Rasmussen encephalitis has been similarly problematic. Jay *et al.* detected CMV and HSV genomic sequences in 10 patients with intractable seizures and chronic encephalitis, and several controls (46). In another study, PCR revealed small amounts of CMV and EBV DNA in 6 patients with Rasmussen encephalitis (86). Comparison of the PCR signal strength for the CMV and EBV DNA found in the Rasmussen encephalitis cases to that in controls (AIDS patients with documented CMV encephalitis or EBV-driven CNS lymphomas, respectively) revealed considerably lower amounts of viral nucleic acid in Rasmussen encephalitis patients than those in patients with diseases known to be caused by these viruses (86). The authors suggested that EBV and CMV did not directly cause Rasmussen encephalitis, but could not rule out an indirect role for these herpesviruses. The issue of viral etiology versus autoimmunity in Rasmussen encephalitis has recently been reviewed (40). Greenlee and Rose note that virus has never been cultured from brain tissues of Rasmussen encephalitis patients and conclude that "at the present time, there is no convincing evidence for a viral etiology" for the disease (40).

PCR has also identified HSV DNA in brain samples from other non-inflammatory types of epilepsy patients (70), but methodology and selection of controls in that study have been questioned (83). An additional report of HSV, CMV, and HHV-6 DNA in brain tissues from young seizure patients (28) awaits corroboration. A higher than expected prevalence of HSV genomic material in brain tissue from patients with Alzheimer's disease has been reported by some investigators (44, 45), but could not be confirmed by others (60).

Unlike the situation for HSV DNA, PCR studies have not demonstrated VZV DNA in autopsy brain tissues. Liedtke *et al.* detected VZV in only 1% of olfactory bulbs (56). VZV DNA was not detected by PCR of temporal lobe cortex from any of 8 schizophrenic patients, 8 non-schizophrenic suicide victims, or 8 normal control subjects (2). In a study using frozen brain tissue from 31 schizophrenic and 23 control subjects, no CMV, EBV, HSV-1, VZV, or HHV-6 was detected (77). No VZV DNA was found in brain from either Alzheimer's disease patients or normal age-matched controls (57). Only one group has reported detection of VZV DNA, as well as many other herpesviruses (HSV, EBV, CMV, HHV-6), in a significant percentage of both multiple sclerosis and control brains (69). Others have not reproduced these results.

The presence of low copy numbers of CMV and EBV in immunosuppressed patients and in patients with Rasmussen encephalitis suggests that quantitation of viral load in tissues or CSF may further assist in identifying disorders directly caused by productive infection by these viruses. Finally, the very recent identification by tissue PCR of HHV-6, HHV-7, and HHV-8 genomic sequences in normal and neoplastic brain awaits further studies to establish whether these lymphotropic viruses are latent in cells of the CNS.

Acknowledgements

The authors thank Ravi Mahalingam and Mary Wellish for helpful comments regarding technical aspects of the PCR methodology; Ravi Mahalingam and Tiffany White for assistance with Figure 2; Marina Hoffman for editorial review, and Virginia McCullough and Nancy Hart for typing.

Supported in part by grants from the Department of Veteran's Affairs (KLT, RBD), U.S. Army DAMD17-98-1-8614 (KLT, BKD), and NIH AI38296 (KLT).

References

1. Achim CL, Nagra RM, Wang R, Nelson JA, Wiley CA (1994) Detection of cytomegalovirus in cerebrospinal fluid autopsy specimens form AIDS patients. *J Infect Dis* 169: 623-627
2. Alexander RC, Cabirac G, Lowenkopf T, Casanova M, Kleinman J, Wyatt RJ, Kirch DG (1992) Search for evidence of herpes simplex virus, type 1, or varicella-zoster virus infection in postmortem brain tissue from schizophrenic patients. *Acta Psychiatr Scand* 86: 418-420
3. Amlie-Lefond C, Kleinschmidt-DeMasters BK, Mahalingam R, Davis LE, Gilden DH (1995) The vasculopathy of varicella-zoster virus encephalitis. *Ann Neurol* 37: 784-790
4. Ando Y, Kimura H, Miwata H, Kudo T, Shibata M, Morishima T (1993) Quantitative analysis of herpes simplex virus DNA in cerebrospinal fluid of children with herpes simplex encephalitis. *J Med Virol* 41: 170-173
5. Antinori A, Larocca LM, Fassone L, Cattani P, Capello D, Cingolani A, Saglio G, Fadda G, Gaidano G, Ortona L (1999) HHV-8/KSHV is not associated with AIDS-related primary central nervous system lymphoma. *Brain Pathol* 9: 199-208
6. Arribas JR, Clifford DB, Fichtenbaum CJ, Commins DL, Powderly WG, Storch GA (1995) Level of cytomegalovirus (CMV) DNA in cerebrospinal fluid of subjects with AIDS and CMV infections of the central nervous system. *J Infect Dis* 172: 527-531
7. Baringer JR, Pisani P (1994) Herpes simplex virus genomes in human nervous system tissue analyzed by polymerase chain reaction. *Ann Neurol* 36: 823-829
8. Bergström T (1996) Polymerase chain reaction for diagnosis of varicella zoster virus central nervous system infections without skin manifestations. *Scan J Dis Suppl* 100: 41-45
9. Bitsch A, Kirchner H, Dupke R, Bein G (1993) Cytomegalovirus transcripts in peripheral blood leukocytes of actively infected transplant patients detected by reverse transcription-polymerase chain reaction. *J Infect Dis* 167: 740-743
10. Blumberg BM, Mock DJ, Powers JM, Ito M, Assouline JG, Baker JV, Chen B, Goodman AD (2000) The HHV6 paradox: ubiquitous commensal or insidious pathogen? A two-step in situ PCR approach. *J Clin Virol* 16: 159-78
11. Burke DG, Kalayjian RC, Vann VR, Madreperla SA, Shick HE, Leonard DGB (1997) Polymerase chain reaction detection and clinical significance of varicella-zoster virus in cerebrospinal fluid from human immunodeficiency virus-infected patients. *J Infect Dis* 176: 1080-1084
12. Cantin EM, Lange W, Openshaw H. (1991) Application of polymerase chain reaction assays to studies of herpes simplex virus latency. *Intervirology* 32: 93-100
13. Challoner PB, Smith KT, Parker JD, MacLeod DL, Coulter SN, Rose TM, Schultz ER, Bennett JL, Garber RL, Chang M, Schad PA, Stewart PM, Nowinski RC, Brown JP, Burmer GC (1995) Plaque-associated expression of human herpesvirus 6 in multiple sclerosis. *Proc Natl Acad Sci USA* 92: 7440-7444
14. Chan PK, Ng HK, Cheung AF (1999) Detection of human herpesviruses 6 and 7 genomic sequences in brain tumours. *J Clin Path* 52: 620-623
15. Chan PK, Ng HK, Hui M, Ip M,Cheung JL, Cheng AF (1999) Presence of human herpesviruses 6, 7, and 8 DNA sequences in normal brain tissue. *J Med Virol* 59: 491-495
16. Cinque P, Baldanti F, Vago L, Terreni MR, Lillo F, Furione M, Castagna A, Monforte AD, Lazzarin A, Linde A (1995) Ganciclovir therapy for cytomegalovirus (CMV) infection of the central nervous system in AIDS patients: monitoring by CMV DNA detection in cerebrospinal fluid. *J Infect Dis* 171: 1603-1606
17. Cinque P, Bossolasco S, Vago L, Fornara C, Lipari S, Racca S, Lazzarin A, Linde A (1997) Varicella-zoster virus (VZV) DNA in cerebrospinal fluid of patients infected with human immunodeficiency virus: VZV disease of the central nervous system or subclinical reactivation of VZV infection? *Clin Infect Dis* 25: 634-639
18. Cinque P, Brytting M, Vago L, Castagna A, Parravicini C, Zanchetta N, D'Arminio Monforte A, Wahren B, Lazzarin A, Linde A (1993) Epstein-Barr virus DNA in cerebrospinal fluid from patients with AIDS-related primary lymphoma of the central nervous system. *Lancet* 342: 398-401
19. Cinque P, Vago L, Dahl H, Brytting M, Terreni MR, Fornara C, Racca S, Castagna A, Monforte AD, Wahren B, Lazzarin A, Linde A (1996) Polymerase chain reaction on cerebrospinal fluid for diagnosis of virus-associated opportunistic diseases of the central nervous system in HIV-infected patients. *AIDS* 10: 951-958
20. Corboy JR, Garl PJ, Kleinschmidt-DeMasters BK (1998) Human herpesvirus 8 DNA in CNS lymphomas from patients with and without AIDS. *Neurology* 50: 335-340
21. Cuomo L, Trivedi P, Cardillo MR, Gagliardi FM, Vecchione A, Caruso R, Calogero A, Frati L, Faggioni A, Ragona G (2001) Human herpesvirus 6 infection in neoplastic and normal brain tissue. *J Med Virol* 63: 45-51

The presence of low copy numbers of CMV and EBV in immunosuppressed patients and in patients with Rasmussen encephalitis suggests that quantitation of viral load in tissues or CSF may further assist in identifying disorders directly caused by productive infection by these viruses. Finally, the very recent identification by tissue PCR of HHV-6, HHV-7, and HHV-8 genomic sequences in normal and neoplastic brain awaits further studies to establish whether these lymphotropic viruses are latent in cells of the CNS.

Acknowledgements

The authors thank Ravi Mahalingam and Mary Wellish for helpful comments regarding technical aspects of the PCR methodology; Ravi Mahalingam and Tiffany White for assistance with Figure 2; Marina Hoffman for editorial review, and Virginia McCullough and Nancy Hart for typing.

Supported in part by grants from the Department of Veteran's Affairs (KLT, RBD), U.S. Army DAMD17-98-1-8614 (KLT, BKD), and NIH AI38296 (KLT).

References

1. Achim CL, Nagra RM, Wang R, Nelson JA, Wiley CA (1994) Detection of cytomegalovirus in cerebrospinal fluid autopsy specimens form AIDS patients. *J Infect Dis* 169: 623-627
2. Alexander RC, Cabirac G, Lowenkopf T, Casanova M, Kleinman J, Wyatt RJ, Kirch DG (1992) Search for evidence of herpes simplex virus, type 1, or varicella-zoster virus infection in postmortem brain tissue from schizophrenic patients. *Acta Psychiatr Scand* 86: 418-420
3. Amlie-Lefond C, Kleinschmidt-DeMasters BK, Mahalingam R, Davis LE, Gilden DH (1995) The vasculopathy of varicella-zoster virus encephalitis. *Ann Neurol* 37: 784-790
4. Ando Y, Kimura H, Miwata H, Kudo T, Shibata M, Morishima T (1993) Quantitative analysis of herpes simplex virus DNA in cerebrospinal fluid of children with herpes simplex encephalitis. *J Med Virol* 41: 170-173
5. Antinori A, Larocca LM, Fassone L, Cattani P, Capello D, Cingolani A, Saglio G, Fadda G, Gaidano G, Ortona L (1999) HHV-8/KSHV is not associated with AIDS-related primary central nervous system lymphoma. *Brain Pathol* 9: 199-208
6. Arribas JR, Clifford DB, Fichtenbaum CJ, Commins DL, Powderly WG, Storch GA (1995) Level of cytomegalovirus (CMV) DNA in cerebrospinal fluid of subjects with AIDS and CMV infections of the central nervous system. *J Infect Dis* 172: 527-531
7. Baringer JR, Pisani P (1994) Herpes simplex virus genomes in human nervous system tissue analyzed by polymerase chain reaction. *Ann Neurol* 36: 823-829
8. Bergström T (1996) Polymerase chain reaction for diagnosis of varicella zoster virus central nervous system infections without skin manifestations. *Scan J Dis Suppl* 100: 41-45
9. Bitsch A, Kirchner H, Dupke R, Bein G (1993) Cytomegalovirus transcripts in peripheral blood leukocytes of actively infected transplant patients detected by reverse transcription-polymerase chain reaction. *J Infect Dis* 167: 740-743
10. Blumberg BM, Mock DJ, Powers JM, Ito M, Assouline JG, Baker JV, Chen B, Goodman AD (2000) The HHV6 paradox: ubiquitous commensal or insidious pathogen? A two-step in situ PCR approach. *J Clin Virol* 16: 159-78
11. Burke DG, Kalayjian RC, Vann VR, Madreperla SA, Shick HE, Leonard DGB (1997) Polymerase chain reaction detection and clinical significance of varicella-zoster virus in cerebrospinal fluid from human immunodeficiency virus-infected patients. *J Infect Dis* 176: 1080-1084
12. Cantin EM, Lange W, Openshaw H. (1991) Application of polymerase chain reaction assays to studies of herpes simplex virus latency. *Intervirology* 32: 93-100
13. Challoner PB, Smith KT, Parker JD, MacLeod DL, Coulter SN, Rose TM, Schultz ER, Bennett JL, Garber RL, Chang M, Schad PA, Stewart PM, Nowinski RC, Brown JP, Burmer GC (1995) Plaque-associated expression of human herpesvirus 6 in multiple sclerosis. *Proc Natl Acad Sci USA* 92: 7440-7444
14. Chan PK, Ng HK, Cheung AF (1999) Detection of human herpesviruses 6 and 7 genomic sequences in brain tumours. *J Clin Path* 52: 620-623
15. Chan PK, Ng HK, Hui M, Ip M,Cheung JL, Cheng AF (1999) Presence of human herpesviruses 6, 7, and 8 DNA sequences in normal brain tissue. *J Med Virol* 59: 491-495
16. Cinque P, Baldanti F, Vago L, Terreni MR, Lillo F, Furione M, Castagna A, Monforte AD, Lazzarin A, Linde A (1995) Ganciclovir therapy for cytomegalovirus (CMV) infection of the central nervous system in AIDS patients: monitoring by CMV DNA detection in cerebrospinal fluid. *J Infect Dis* 171: 1603-1606
17. Cinque P, Bossolasco S, Vago L, Fornara C, Lipari S, Racca S, Lazzarin A, Linde A (1997) Varicella-zoster virus (VZV) DNA in cerebrospinal fluid of patients infected with human immunodeficiency virus: VZV disease of the central nervous system or subclinical reactivation of VZV infection? *Clin Infect Dis* 25: 634-639
18. Cinque P, Brytting M, Vago L, Castagna A, Parravicini C, Zanchetta N, D'Arminio Monforte A, Wahren B, Lazzarin A, Linde A (1993) Epstein-Barr virus DNA in cerebrospinal fluid from patients with AIDS-related primary lymphoma of the central nervous system. *Lancet* 342: 398-401
19. Cinque P, Vago L, Dahl H, Brytting M, Terreni MR, Fornara C, Racca S, Castagna A, Monforte AD, Wahren B, Lazzarin A, Linde A (1996) Polymerase chain reaction on cerebrospinal fluid for diagnosis of virus-associated opportunistic diseases of the central nervous system in HIV-infected patients. *AIDS* 10: 951-958
20. Corboy JR, Garl PJ, Kleinschmidt-DeMasters BK (1998) Human herpesvirus 8 DNA in CNS lymphomas from patients with and without AIDS. *Neurology* 50: 335-340
21. Cuomo L, Trivedi P, Cardillo MR, Gagliardi FM, Vecchione A, Caruso R, Calogero A, Frati L, Faggioni A, Ragona G (2001) Human herpesvirus 6 infection in neoplastic and normal brain tissue. *J Med Virol* 63: 45-51

22. d'Arminio Monforte A, Cinque P, Vago L, Rocca A, Castagna A, Gervasoni C, Terreni MR, Novati R, Gori A, Lazzarin A, Moroni M (1997) A comparison of brain biopsy and CSF-PCR in the diagnosis of CNS lesions in AIDS patients. *J Neurol* 244: 35-39

23. Darnell RB (1993) The polymerase chain reaction: Application to nervous system disease. *Ann Neurol* 34: 513-523

24. DeBiasi RL, Tyler KL (1999) Polymerase chain reaction in the diagnosis and management of central nervous system infections. *Arch Neurol* 56: 1215-1219

25. Dlugosch D, Eis-Hübinger AM, Kleim J-P, Kaiser R, Bierhoff E, Schneweis KR (1991) Diagnosis of acute and latent varicella-zoster virus infections using the polymerase chain reaction. *J Med Virol* 35: 136-141

26. Domingues RB, Tsanaclis AMC, Pannuti CS, Mayo MS, Lakeman FD (1997) Evaluation of the range of clinical presentations of herpes simplex encephalitis by using polymerase chain reaction assay of cerebrospinal fluid samples. *Clin Infect Dis* 25: 86-91

27. Drummond CW, Eglin RP, Esiri MM (1994) Herpes simplex virus encephalitis in a mouse model: PCR evidence for CNS latency following acute infection. *J Neurol Sci* 127: 159-163

28. Eeg-Olofsson O, Bergstrom T, Osterland CK, Andermann F, Oliver A (1995) Epilepsy etiology with special emphasis on immune dysfunction and neurovirology. *Brain Dev* 17: 58-60

29. Ehrnst A (1996) The clinical relevance of different laboratory tests in CMV diagnosis. *Scand J Infect Dis Suppl* 100: 64-71

30. Fodor PA, Levin MJ, Weinberg A, Sandberg E, Sylman J, Tyler KL (1998) Atypical herpes simplex virus encephalitis diagnosed by PCR amplification of viral DNA from CSF. *Neurology* 51: 554-559

31. Fraser NW, Block TM, Spivack JG (1992) The latency-associated transcripts of herpes simplex virus: RNA in search of function. *Virology* 191: 1-8.

32. Fraser NW, Lawrence WC, Wroblewska Z, Gilden DH, Koprowski H (1981) Herpes simplex type 1 DNA in human brain tissue. *Proc Natl Acad Sci USA* 78: 6461-6465

33. Furuta Y, Ohtani F, Kawabata H, Fukuda S, Bergstrom T (2000) High prevalence of varicella-zoster virus reactivation in herpes simplex virus-seronegative patients with acute peripheral facial palsy. *Clin Infect Dis* 30: 529-533

34. Gilden DH, Beinlich BR, Rubinstein EM, Stommel E, Swenson R, Rubinstein D, Mahalingam R (1994) Varicella-zoster virus myelitis: An expanding spectrum. *Neurology* 44: 1818-1823

35. Gilden DH, Kleinschmidt-DeMasters BK, LaGuardia JJ, Mahalingam R, Cohrs RJ (2000) Neurologic complications of varicella zoster virus reactivation. *N Engl J Med* 342: 635-646

36. Gilden DH, Kleinschmidt-DeMasters BK, Wellish M, Hedley-Whyte ET, Rentier B, Mahalingam R (1996) Varicella zoster virus, a cause of waxing and waning vasculitis: The New England Journal of Medicine case 5-1995 revisited. *Neurology* 47: 1441-1446

37. Gilden DH, Murray RS, Wellish M, Kleinschmidt-DeMasters BK, Vafai A (1988) Chronic progressive varicella-zoster virus encephalitis in an AIDS patient. *Neurology* 38: 1150-1153

38. Gilden DH, Vafai A, Shtram Y, Becker Y, Devlin M, Wellish M (1983) Varicella-zoster virus DNA in human sensory ganglia. *Nature* 306: 478-480

39. Gilden DH, Wright RR, Schneck SA, Gwaltney JM, Mahalingam R (1994) Zoster sine herpete, a clinical variant. *Ann Neurol* 35: 530-533

40. Greenlee JE, Rose JW (2000) Controversies in neurological infectious diseases. *Semin Neurol* 20: 375-386

41. Hato N, Kisaki H, Honda N, Gyo K, Murakami S, Yanagihara N (2000) Ramsay Hunt syndrome in children. *Ann Neurol* 48: 254-256

42. Ito M, Baker JV, Mock DJ, Goodman AD, Blumberg BM, Shrier DA, Powers JM (2000) Human herpesvirus 6-meningoencephalitis in an HIV patient with progressive multifocal leukoencephalopathy. *Acta Neuropathol* 100: 337-41

43. Ito Y, Kimura H, Yabuta Y, Ando Y, Murakami T, Shiomi M, Morishima T (2000) Exacerbation of herpes simplex encephalitis after successful treatment with acyclovir. *Clin Inf Dis* 30: 185-187

44. Itzhaki RF, Lin WR, Shang D, Wilcock GK, Faragher B, Jamisson GA (1997) Herpes simplex virus type 1 in brain and risk of Alzheimer's disease. *Lancet* 349: 241-244.

45. Jamieson GA, Maitland NJ, Wilcock GK, Craske J, Itzhaki RF (1991) Latent herpes simplex virus type I in normal and Alzheimer's disease brains. *J Med Virol* 33: 224-227

46. Jay V, Becker LE, Otsubo H, Cortez M, Hwang P, Hoffman HJ, Zielenska M (1995) Chronic encephalitis and epilepsy (Rasmussen's encephalitis): detection of cytomegalovirus and herpes simplex virus 1 by the polymerase chain reaction and *in situ* hybridization. *Neurology* 45: 108-117

47. Jay V, Hwang P, Hoffman HJ, Becker LE, Zielenska M (1998) Intractable seizure disorder associated with chronic herpes infection. HSV1 detection in tissue by the polymerase chain reaction. *Child Nerv Syst* 14: 15-20

48. Kimberlin DW, Whitley RJ (1998) Human herpesvirus-6: neurologic implications of a newly-described viral pathogen. *J Neurovirol* 4: 474-485

49. Kimura H, Aso K, Kuzushima K, Hanada N, Shibata M, Morishima T (1992) Relapse of herpes simplex encephalitis in children. *Pediatrics* 89: 891-894

50. Kleinschmidt-DeMasters BK, Amlie-Lefond C, Gilden DH (1996) The patterns of varicella zoster virus encephalitis. *Hum Pathol* 27: 927-938

51. Kleinschmidt-DeMasters BK, Gilden DH (2001) Varicella zoster virus infections of the nervous system—clinical and pathological correlates. *Arch Path Lab Med* 125: 770-780

52. Kleinschmidt-DeMasters BK, Mahalingam R, Shimek C, Marcoux HL, Wellish M, Tyler KL, Gilden DH (1998) Profound cerebrospinal fluid pleocytosis and Froin's syndrome secondary to widespread necrotizing vasculitis in an HIV-positive patient with varicella zoster virus encephalomyelitis. *J Neurol Sci* 159: 213-218

53. Kuhn JE, Wendland T, Eggers HJ, Lorentzen E, Wieland U, Eing B, Kiessling M, Gass P (1995) Quantitation of human cytomegalovirus genomes in the brain of AIDS patients. *J Med Virol* 47: 70-82

54. LaGuardia JJ, Cohrs RJ, Gilden DH (1999) Prevalence of varicella-zoster virus DNA in dissociated human trigeminal ganglion neurons and nonneuronal cells. *J Virol* 73: 8571-8577

55. Lakeman FD, Whitley RJ, the National Institute of Allergy and Infectious Diseases Collaborative Antiviral Study Group (1995) Diagnosis of herpes simplex encephalitis: Application of polymerase chain reaction to cerebrospinal fluid from brain-biopsied patients and correlation with disease. *J Infect Dis* 171: 857-863

56. Liedtke W, Opalka B, Zimmermann CW, Lignitz E (1993) Age distribution of latent herpes simplex virus 1 and varicella-zoster virus genome in human nervous tissue. *J Neurol Sci* 116: 6-11

57. Lin WR, Casas I, Wilcock GK, Itzhaki RF (1997) Neurotropic viruses and Alzheimer's disease: a search for varicella zoster virus DNA by the polymerase chain reaction. *J Neurol Neurosurg Psychiatry* 62: 586-589

58. Mahalingam R, Wellish M, Brucklier J, Gilden DH (1995) Persistence of varicella-zoster virus DNA in elderly patients with postherpetic neuralgia. *J Neurovirol* 1: 130-133

59. Mahalingam R, Wellish M, Wolf W, Dueland AN, Cohrs R, Vafai A, Gilden D (1990) Latent varicella-zoster viral DNA in human trigeminal and thoracic ganglia. *N Engl J Med* 323: 627-631

60. Marques AR, Straus SE (2001) Lack of association between HSV-1 DNA in the brain, Alzheimer's disease and apolipoprotein E4. *J Neurovirol* 7: 82-83.

61. Martin C, Enbom M, Söderström M, Fredrikson S, Dahl H, Lycke J, Bergström T, Linde A (1997) Absence of seven human herpesviruses, including HHV-6, by polymerase chain reaction in CSF and blood from patients with multiple sclerosis and optic neuritis. *Acta Neurol Scand* 95: 280-283

62. Melanson M, Chalk C, Georgevich L, Fett K, Lapierre Y, Duong H, Richardson J, Marineau C, Rouleau GA (1996) Varicella-zoster virus DNA in CSF and arteries in delayed contralateral hemiplegia: Evidence for viral invasion of cerebral arteries. *Neurology* 47: 569-570

63. Murakami S, Mizobuchi M, Nakashiro Y, Doi T, Hato N, Yanagihara N (1996) Bell palsy and herpes simplex virus: Identification of viral DNA in endoneurial fluid and muscle. *Ann Intern Med* 124: 27-30

64. Murakami S, Nakashiro Y, Mizobuchi M, Hato N, Honda N, Gyo K (1998) Varicella-zoster virus distribution in Ramsay Hunt syndrome revealed by polymerase chain reaction. *Acta Oto-Laryngol* 118: 145-149

65. Nakajima H, Furutama D, Kimura F, Shinoda K, Nakagawa T, Shimizu A, Ohsawa N (1995) Herpes simplex virus type 2 infections presenting as brainstem encephalitis and recurrent myelitis. *Intern Med* 34: 839-842

66. Nordborg C, Nordborg E, Petursdottir V, LaGuardia J, Mahalingam R, Wellish M, Gilden DH (1998) Search for varicella zoster virus in giant cell arteritis. *Ann Neurol* 44: 413-414

67. Read SJ, Kurtz JB (1999) Laboratory diagnosis of common viral infections of the central system by using a single multiplex PCR screening assay. *J Clin Micro* 37: 1352-1355

68. Said JW, Tasaka T, de Vos S, Koeffler HP (1997) Kaposi's sarcoma-associated herpesvirus/human herpesvirus type 8 encephalitis in HIV-positive and-negative individuals. *AIDS* 11: 1119-1122

69. Sanders VJ, Felisan S, Waddell A, Tourtellotte WW (1996) Detection of herpesviridae in postmortem multiple sclerosis brain tissue and controls by polymerase chain reaction. *J Neurovirol* 2: 249-258

70. Sanders VJ, Felisan SL, Waddell AE, Conrad AJ, Schmid P, Swartz BE, Kaufman M, Walsh GO, DeSalles AA, Tourtellotte WW (1997) Presence of herpes simplex DNA in surgical tissue from human epileptic seizure foci detected by polymerase chain reaction: preliminary study. *Arch Neurol* 54: 954-960

71. Schlesinger Y, Buller RS, Brunstrom JE, Moran CJ, Storch GA (1995) Expanded spectrum of herpes simplex encephalitis in childhood. *J Ped* 126: 234-241

72. Schlesinger Y, Tebas P, Gaudreault-Keener M, Buller RS, Storch GA (1995) Herpes simplex virus type 2 meningitis in the absence of genital lesions: improved recognition with use of the polymerase chain reaction. *Clin Infect Dis* 20: 842-848

73. Sequiera LW, Jennings LC, Carrasco LH, Lord MA, Curry A, Sutton RN (1979) Detection of herpes-simplex viral genome in brain tissue. *Lancet* 2: 609-612

74. Stahl H-D, Hubner B, Seidl B, Liebert UG, van der Heijden IM, Wilbrink B, Kraan MC, Emmrich F, Tak PP (2000) Detection of multiple viral DNA species in synovial tissue and fluid of patients with early arthritis. *Ann Rheum Dis* 59: 342-346

75. Studahl M, Hagberg L, Rekabdar E, Bergstrom T (2000) Herpesvirus DNA detection in cerebral spinal fluid: differences in clinical presentation between alpha-, beta-, and gamma-herpesviruses. *Scand J Inf Dis* 32: 237-248

76. Sze C-I, Mahalingam R, Wellish M, Levy AS, Wu E, Pfister SJ, Gilden DH, Kleinschmidt-DeMasters BK (1999) Attempts to identify herpes simplex virus DNA in normal and diseased human peripheral nerve. *Neurology* 52: 1293-1295

77. Taller AM, Asher DM, Pomeroy KL, Eldadah, BA, Godec, MS, Falkai PG, Bogert B, Kleinman JE, Stevens JR, Torrey, EF (1996) Search for viral nucleic acid sequences in brain tissues of patients with schizophrenia using nested polymerase chain reaction. *Arch Gen Psych* 53: 32-40

78. Taylor-Wiedeman J, Sissons JGP, Borysiewicz LK, Sinclair JH (1991) Monocytes are a major site of persistence of human cytomegalovirus in peripheral blood mononuclear cells. *J Gen Virol* 72: 2059-2064

79. Tedder DG, Ashley R, Tyler KL, Levin MJ (1994) Herpes simplex virus infection as a cause of benign recurrent lymphocytic meningitis. *Ann Intern Med* 121: 334-338

80. Torigoe S, Koide W, Yamada M, Miyashiro E, Tanaka-Taya K, Yamanishi K (1996) Human herpesvirus 7 infection associated with central nervous system manifestations. *J Ped* 129: 301-305

81. Troendle-Atkins J, Demmler GJ, Williamson WD, McDonald JM, Istas AS, Buffone GJ (1994) Polymerase chain reaction to detect cytomegalovirus DNA in the cerebrospinal fluid of neonates with congenital infection. *J Infect Dis* 169: 1334-1337

82. Tyler KL (1994) Polymerase chain reaction and the diagnosis of viral central nervous system disease. *Ann Neurol* 36: 809-811

83. Tyler KL (1998) Serious methodological failures concerning presence of HSV DNA in surgical tissue from human epileptic seizure foci detected by PCR. *Arch Neurol* 55: 1031-1032

84. Tyler KL, Tedder DG, Yamamoto LJ, Klapper JA, Ashley R, Lichtenstein KA, Levin MJ (1995) Recurrent brainstem encephalitis associated with herpes simplex virus type 1 DNA in cerebrospinal fluid. *Neurology* 45: 2246-2250

85. Van den Berg JS, van Zeijl JH, Rotteveel JJ, Melchers WJ, Gabreels FJ, Galama JM (1999) Neuroinvasion by human herpesvirus type 7 in a case of exanthem subitum with severe neurologic manifestations. *Neurology* 52: 1077-1079

86. Vinters HV, Wang R, Wiley CA (1993) Herpesviruses in chronic encephalitis associated with intractable childhood epilepsy. *Hum Pathol* 24: 871-879

87. Weber T (1999) Cerebrospinal fluid analysis for the diagnosis of human immunodeficiency virus-related neurologic diseases. *Semin Neurol* 19: 223-233

88. Weber T, Frye S, Bodemer M, Otto M, Luke W (1996) Clinical implications of nucleic acid amplification methods for the diagnosis of viral infections of the nervous system. *J Neurovirol* 2: 175-190

89. Weidenheim KM, Bodhireddy SR, Nuovo GJ, Nelson SJ, Dickson DW (1995) Multicystic encephalopathy: Review of eight cases with etiologic considerations. *J Neuropathol Exp Neurol* 54: 268-275

90. Welling DB, Miles BA, Western L, Prior TW (1997) Detection of viral DNA in vestibular ganglia tissue from patients with Meniere's disease. *Am J Otol* 18: 734-737

91. Wildemann B, Haas J, Lynen N, Stingele K, Storch-Hagenlocher B (1998) Diagnosis of cytomegalovirus encephalitis in patients with AIDS by quantitation of cytomegalovirus genomes in cells of cerebrospinal fluid. *Neurology* 50: 693-697

92. Yoshikawa T, Asano Y (2000) Central nervous system complications in human herpesvirus-6 infection. *Brain Develop* 22: 307-314

Oncogene (2001) 00, 00–00

www.nature.com/onc

ORIGINAL PAPERS

Caspase 8-dependent sensitization of cancer cells to TRAIL-induced apoptosis following reovirus infection

Penny Clarke[1], Suzanne M Meintzer[1], Aaron C Spalding[2], Gary L Johnson[2] and Kenneth L Tyler[*,1,3,4]

[1]*Department of Neurology, University of Colorado Health Sciences, Denver, Colorado, CO 80262, USA;* [2]*Department of Pharmacology, University of Colorado Health Sciences, Denver, Colorado, CO 80262, USA;* [3]*Department of Medicine, Microbiology and Immunology, University of Colorado Health Sciences, Denver, Colorado, CO 80262, USA;* [4]*Denver Veteran's Affairs Medical Center, Denver, Colorado, CO 80220, USA*

TRAIL (TNF-related apoptosis-inducing ligand) induces apoptosis in susceptible cells by binding to death receptors 4 (DR4) and 5 (DR5). TRAIL preferentially induces apoptosis in transformed cells and the identification of mechanisms by which TRAIL-induced apoptosis can be enhanced may lead to novel cancer chemotherapeutic strategies. Here we show that reovirus infection induces apoptosis in cancer cell lines derived from human breast, lung and cervical cancers. Reovirus-induced apoptosis is mediated by TRAIL and is associated with the release of TRAIL from infected cells. Reovirus infection synergistically and specifically sensitizes cancer cell lines to killing by exogenous TRAIL. This sensitization both enhances the susceptibility of previously resistant cell lines to TRAIL-induced apoptosis and reduces the amount of TRAIL needed to kill already sensitive lines. Sensitization is not associated with a detectable change in the expression of TRAIL receptors in reovirus-infected cells. Sensitization is associated with an increase in the activity of the death receptor-associated initiator caspase, caspase 8, and is inhibited by the peptide IETD-fmk, suggesting that reovirus sensitizes cancer cells to TRAIL-induced apoptosis in a caspase 8 dependent manner. Reovirus-induced sensitization of cells to TRAIL is also associated with increased cleavage of PARP, a substrate of the effector caspases 3 and 7. *Oncogene* (2001) 00, 000–000.

Keywords: apoptosis; TRAIL; reovirus; caspase 8; chemotherapy

Introduction

TNF-related apoptosis-inducing ligand (TRAIL, also called Apo2L) belongs to a family of structurally related molecules, which also includes TNF, Fas ligand (FasL), and APO3 ligand. These ligands are expressed as type II membrane proteins that are cleaved into soluble, active forms and which bind to members of the TNF receptor super-family. Ligand-mediated receptor activation triggers a cascade of events that begins with death receptor (DR) oligomerization and the close association of their cytoplasmic death domains (DDs). This is followed by DD-associated interaction with adapter molecules and cellular proteases critical to DR-induced apoptosis, including the initiator caspase, caspase 8 and its associated effector caspases, caspase 3 and 7 (reviewed in Ashkenasi and Dixit, 1998). In addition to activating caspase 8, TRAIL-induced apoptosis is also associated with the cleavage of Bid and the loss of mitochondrial potential (Belka *et al.*, 2001). TRAIL induces apoptosis by binding to the TNF super-family members DR4 (also called TRAIL-R1) and DR5 (also called Apo2, TRAIL-R2, TRACK2 or KILLER). TRAIL can also bind to the receptors DcR-1 (for Decoy Receptor 1) and DcR-2 that do not transmit apoptotic signals and can prevent the induction of apoptosis in TRAIL-treated cells.

Many cancer chemotherapeutic drugs in clinical use induce apoptosis in sensitive cells suggesting that death-receptor ligands might prove useful as cancer therapeutic agents. Unfortunately, the apoptosis-inducing ligands FasL and TNF are also toxic to non-transformed cells (Nagata, 1997). TRAIL induces apoptosis in a variety of transformed cells (Wiley *et al.*, 1995; Pitti *et al.*, 1996), including cells derived from lung, breast, colon, kidney, brain and skin cancers (Ashkenazi *et al.*, 1999) and is effective at reducing mammary adenocarcinoma growth in mice (Walczak *et al.*, 1999). Although normal cultured hepatocytes do show some sensitivity to TRAIL-induced killing (Jo *et al.*, 2000), this toxicity can be overcome by simultaneous exposure to the caspase inhibitor, Z-LEHD-FMK (Ozoren *et al.*, 2000).

TRAIL kills cancer cells derived from a variety of human cancers of diverse type. However, cancer cells of all types appear to differ in their sensitivity to TRAIL-induced apoptosis (Keane *et al.*, 1999; Zhang *et al.*, 1999). Understanding the basis of TRAIL sensitivity is thus crucial in designing TRAIL-based cancer therapeutic strategies. TRAIL induced apopto-

*Correspondence: KL Tyler, Department of Neurology (B 182), University of Colorado Health Sciences Center, 4200 East 9th Avenue, Denver, Colorado 80262, USA; E-mail: Ken.Tyler@uchsc.edu
Received 2 June 2001; revised 16 July 2001; accepted 16 July 2001

sis is dependent, in part, on the surface expression of its receptors (Zhang *et al.*, 1999) and agents which increase the cell surface expression of DR4 and DR5 enhance TRAIL-induced killing in some epithelial-derived tumor cells (Gibson *et al.*, 2000). Alteration in receptor expression, however, does not fully explain TRAIL sensitivity (Keane *et al.*, 1999; Zhang *et al.*, 1999; Cuello *et al.*, 2001).

Reovirus infection induces apoptosis in cultured cells *in vitro* (Tyler *et al.*, 1985, 1995, 1996). Apoptosis occurs through a p53-independent mechanism that involves cellular proteases including caspases and calpains (DeBiasi *et al.*, 1999). Reovirus-induced apoptosis in HEK293 cells is mediated by TRAIL and is inhibited by anti-TRAIL antibodies or by soluble forms of DR4 and DR5 (Clarke *et al.*, 2000). Reovirus infection results in the release of TRAIL from infected HEK293 cells and reovirus sensitizes these cells to TRAIL-induced killing (Clarke *et al.*, 2000). In neonatal mice, reovirus also induces apoptosis in infected tissues *in vivo* (Oberhaus *et al.*, 1997, 1998; DeBiasi *et al.*, 2001). However, reovirus infection is not associated with significant disease in adult mice or in humans. Reovirus infection may therefore provide a useful model system for investigations of TRAIL-induced apoptosis in cancer cells and a better understanding of how reovirus infection sensitizes cancer cells to TRAIL-induced cell death may suggest novel mechanisms for increasing the efficacy of TRAIL as a cancer therapeutic agent.

Reovirus has previously been shown to induce killing of human glioblastoma cells *in vitro* as well as inducing regression of transplanted tumors in mice, although the mechanism for reovirus-induced 'oncolysis' has not been fully identified (Coffey *et al.*, 1998; Strong *et al.*, 1998). We now show that reovirus kills cancer cells by apoptosis and that this apoptosis is both mediated by TRAIL and is associated with the release of TRAIL from infected cells. We further show that reovirus specifically sensitizes cancer cell lines to TRAIL-induced apoptosis and that this sensitization requires the activation of caspase 8 and is associated with increased activity of effector caspases.

Results

Reovirus and TRAIL induce similar amounts of apoptosis in human cancer cells

It has been reported that reovirus can infect and kill cancer cells (Coffey *et al.*, 1998; Strong *et al.*, 1998). Our previous work in tissue culture has shown that reovirus-induced killing of many types of non-cancerous cells (Tyler *et al.*, 1985, 1995, 1996) and of cells derived from a human cervical carcinoma (HeLa cells) is due to apoptosis. We therefore wished to determine whether reovirus induced killing of other cancer cell lines was due to apoptosis. Cell lines derived from two different human lung (A157 and H549) and breast cancers (MDA231 and ZR75-1) were infected with reovirus (multiplicity of infection, MOI 100) and were harvested and assayed for apoptosis at 48 h post infection. We first assayed apoptosis by determination of the percentage of cells with apoptotic nuclear morphology (Figure 1a). The specificity of this assay for the detection of apoptotic nuclear morphology in reovirus-infected cells has been previously established by our laboratory using DNA laddering techniques and electron microscopy (Tyler *et al.*, 1995). HeLa cells, which have previously been shown to be susceptible to both reovirus-infection and reovirus-induced apoptosis (Connolly *et al.*, 2000), were used as positive controls. Reovirus induced significant ($P<0.05$) apoptosis in all of the cancer cell lines tested, but with different degrees of efficiency. HeLa, A549 and MDA231 cells were the

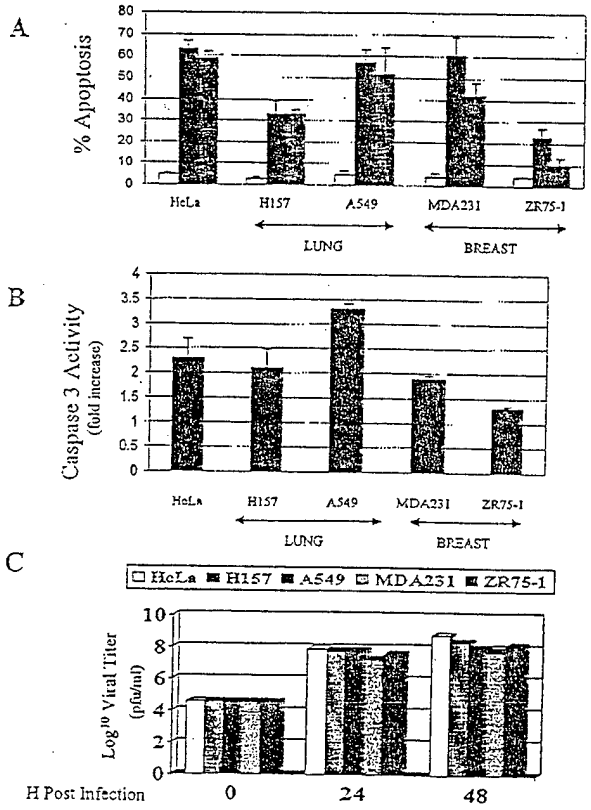

Figure 1 Reovirus induces apoptosis in human tumor cell lines. (a) Cell lines derived from human cervical (HeLa), lung (H157 and A549) and breast (MDA MB231 and ZR75-1) cancers were infected with reovirus (MOI 100) and were harvested and assayed for apoptosis at 48 h post infection. In a parallel experiment cells were treated with TRAIL (200 ng/ml). The graph shows the mean per cent apoptosis in reovirus (black bars), mock-infected (clear bars) and TRAIL-treated (shaded bars) cancer cells from at least three separate experiments. Error bars represent standard errors of the mean. (b) Caspase 3 activation in reovirus (MOI 100) compared to mock-infected cancer cell lines, at 24 h post infection, as determined by fluorogenic substrate assay. The graph shows the mean fold-increase in fluorescence from at least three separate experiments. Error bars represent standard errors of the mean. (c) One step growth curves of reovirus in human cancer cell lines used. Cells were infected with reovirus and were harvested and assayed for growth at 24 and 48 h post infection. The graph shows Log_{10} virus yield over time

most susceptible to reovirus-induced apoptosis whereas H157 and ZR75-1 cells showed the least susceptibility. These differences were not caused by differences in viral growth since one-step growth curves indicated that reovirus grows efficiently and equivalently in all the cell lines (Figure 1c).

The sensitivity of cells to reovirus-induced apoptosis was compared to their sensitivity to TRAIL-induced apoptosis. Cells were treated with 200 ng/ml TRAIL and assayed for apoptosis after 24 h. All but one (ZR75-1) of the cell lines tested demonstrated significant sensitivity ($P<0.05$) to TRAIL induced apoptosis (Figure 1a). A significant correlation was shown between the sensitivity of these cancer lines to reovirus-induced and TRAIL-induced apoptosis (Pearson linear correlation test: correlation coefficient (R) = 0.9154, coefficient of determination (R sq.) = 0.8380, *P* value (2-tailed) 0.0291).

To confirm that reovirus-induced killing of cancer cells was due to apoptosis we investigated the activity of the apoptosis-specific effector caspase, caspase 3, in reovirus-infected cells. Reovirus infection induced a twofold or more activation of caspase 3 in all of the cell lines tested except for ZR75-1 cells. The smaller increase in caspase 3-activation (1.3-fold), seen in ZR75-1 cells corresponds to the low level of apoptosis induced in these cells following reovirus infection (Figure 1b).

Reovirus induced apoptosis is mediated by TRAIL

Reovirus induced apoptosis of HEK293 and L929 cells requires the binding of TRAIL to the apoptosis-inducing cell surface receptors DR4 and DR5 (Clarke *et al*., 2000). Soluble TRAIL receptors (Fc:DR4 and Fc:DR5), but not soluble TNF receptor (Fc:TNFR), specifically inhibit TRAIL-induced apoptosis by binding TRAIL and preventing its interaction with functional cell surface DR4 and DR5 (Clarke *et al*., 2000). We wished to determine whether reovirus-induced apoptosis of cancer cell lines was also mediated by TRAIL. Human lung, breast and cervical cancer cell lines were infected with reovirus (MOI 50), in the presence or absence of soluble TRAIL receptor (Fc:DR5) or a soluble control receptor (Fc:TNFR), and assayed for apoptosis 48 h following infection with reovirus. Reovirus-induced apoptosis in all of the cancer cell lines, except ZR75-1, was significantly inhibited ($P<0.05$), by treatment with Fc:DR5, but not by Fc:TNFR, indicating that apoptosis in these cells is mediated by TRAIL (Figure 2a). In the case of ZR75-1 cells, the low basal level of reovirus-induced apoptosis may have precluded the determination of a significant level of inhibition.

To further demonstrate the involvement of TRAIL in reovirus-induced apoptosis we next showed that reovirus-induced apoptosis could be inhibited in a cell line that stably over-expresses the anti-apoptotic TRAIL receptor, DcR-1. MDA-231 cells were transfected with a vector expressing DcR-1 and enhanced cell surface expression of DcR-1 was determined by flow cytometry (data not shown). These cells were then infected with reovirus (MOI 100) and assayed for apoptosis after 48 h (Figure 2b). Over-expression of DcR-1 significantly ($P<0.01$) inhibited reovirus-induced apoptosis in MDA-231 cells, when compared to MDA-231 control cells transfected with empty vector, again indicating that TRAIL plays a key role in reovirus-induced apoptosis.

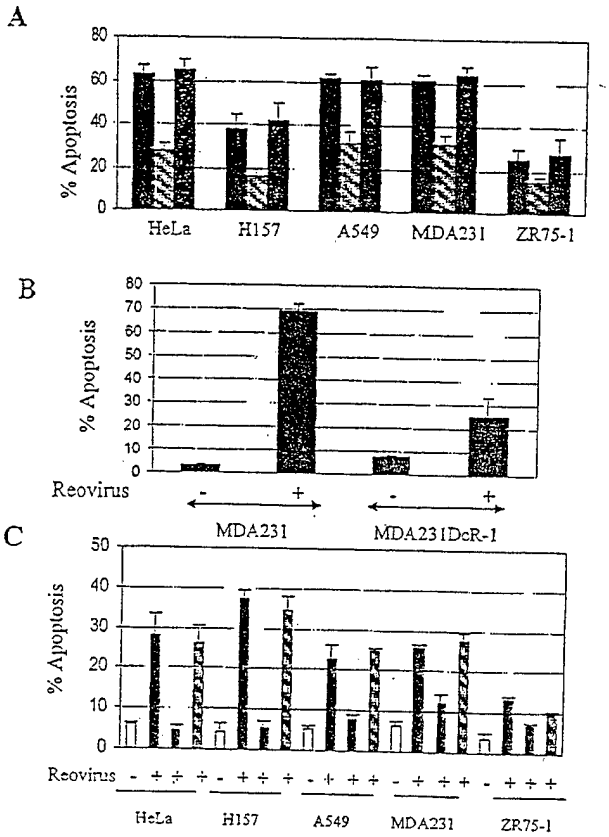

Figure 2 Reovirus induced apoptosis of cancer cells is inhibited by soluble TRAIL receptor (Fc:DR5) or the over-expression of DcR-1 and is associated with the release of TRAIL from infected cells. (a) Human cancer cell lines were infected with reovirus (MOI 50), in the absence (black bars) or presence of soluble TRAIL receptor (Fc:DR5, shaded bars) or a soluble control receptor (Fc:TNFR, grey bars) and were assayed for apoptosis 48 h following infection with reovirus. (b) MDA231 cells over-expressing DcR-1 (MDA231DcR-1) and MDA231 cells expressing vector control were infected with reovirus. Forty-eight hours following infection cells were harvested and assayed for the presence of apoptotic nuclear morphology. (c) Twenty-four hours following infection of cells with reovirus (MOI 100) the supernatant was collected and transferred onto a TRAIL-sensitive indicator cell line (HeLa). After a further 24 h the indicator cells were assayed for apoptosis. Empty bars represent supernatants from mock infected cells, black bars represent supernatants from reovirus infected cells, grey bars represent supernatants from reovirus infected cells that were treated with Fc:DR5 to determine that the apoptosis seen in the indicator cell line was TRAIL-specific and shaded bars represent supernatants from reovirus infected cells that were treated with anti-reovirus antibody to ensure that apoptosis in the indicator cell line was not due to any reovirus present in the transferred supernatant. The graphs (a, b and c) show per cent apoptosis from three separate experiments. Error bars represent standard errors of the mean

TRAIL is released from reovirus infected cancer cells

TRAIL is normally expressed as a type II membrane protein that is cleaved into a soluble form. We have previously shown that TRAIL is released from reovirus-infected HEK293 cells (Clarke *et al*., 2000). We next investigated whether TRAIL was released from reovirus-infected cancer cells into the supernatant. Twenty-four hours following infection of cancer cells with reovirus the supernatant was collected and transferred onto a TRAIL-sensitive indicator cell line (HeLa). After a further 24-h the indicator cells were assayed for apoptosis. Significant apoptosis ($P<0.05$) was induced in the indicator cell line following treatment with supernatant collected from reovirus-infected, but not from mock-infected Hela, H157, A549 and MDA231 cells (Figure 2c). This apoptosis was blocked by soluble DR5 (Fc:DR5) indicating that the apoptosis seen in the indicator cells following supernatant transfer from reovirus-infected cancer cells was specific to TRAIL. Supernatant from reovirus-infected ZR75-1 cells did not induce significant apoptosis in the indicator cell line. A neutralizing polyclonal anti-reovirus antisera, that we have previously shown inhibits virus attachment, neutralizes infectivity and blocks apoptosis induced by infectious virus (Tyler *et al*., 1996), did not block apoptosis induced in the indicator cells by supernatant transfer from reovirus-infected cancer cells. This antibody did inhibit viral growth and virus-induced apoptosis in reovirus-infected cancer cells (data not shown) indicating that the apoptotic effects of infected cancer cell supernatants are not due to the presence of infectious virus.

Reovirus synergistically augments TRAIL-mediated apoptosis in infected cancer cells

Reovirus infection sensitizes HEK293 cells to TRAIL-induced apoptosis. We next wished to determine whether reovirus infection also sensitized cancer cells to TRAIL-induced apoptosis, and if so, whether this sensitization was specific for TRAIL-induced apoptosis or whether it also occurred with other death-receptor associated ligands. ZR75-1 and H157 cells, which were the cancer cell lines that showed the least susceptibility to TRAIL (200 ng/ml)-induced apoptosis (Figure 1a), were infected with reovirus (MOI 10). After 24 h infected cells were treated with a low dose of TRAIL (20 ng/ml) and apoptosis assays were performed after a further 24 h. In H157 and ZR75-1 cells neither low doses of TRAIL (20 ng/ml) or reovirus (MOI 10) alone induce significant apoptosis compared to untreated cells (Figure 3a). However, when cells were infected with reovirus and were then treated with TRAIL the number of apoptotic cells was significantly increased ($P<0.05$) when compared to uninfected cells, or to cells treated with either TRAIL or reovirus alone. The increase in apoptosis induced by a combination of reovirus-infection and TRAIL treatment was synergistic rather than additive, compared to that seen with either agent alone, and the amount of apoptosis seen with TRAIL and reovirus together was significantly different from the sum of reo- and TRAIL-induced apoptosis when each was administered separately. To confirm that cell death resulting from a combination of reovirus-infection and TRAIL treatment was due to apoptosis we also showed that a combination of reovirus and TRAIL, but not the same doses of reovirus or TRAIL alone, produced oligosomal DNA fragmentation, also known as 'DNA laddering' (Figure 3b).

Reovirus infection also significantly ($P<0.05$) augmented apoptosis induced in ZR75-1 and H157 cells by an activating Fas antibody (0.025 g/ml) compared to cells treated with either the antibody or reovirus alone (Figure 3c). This augmentation was additive rather

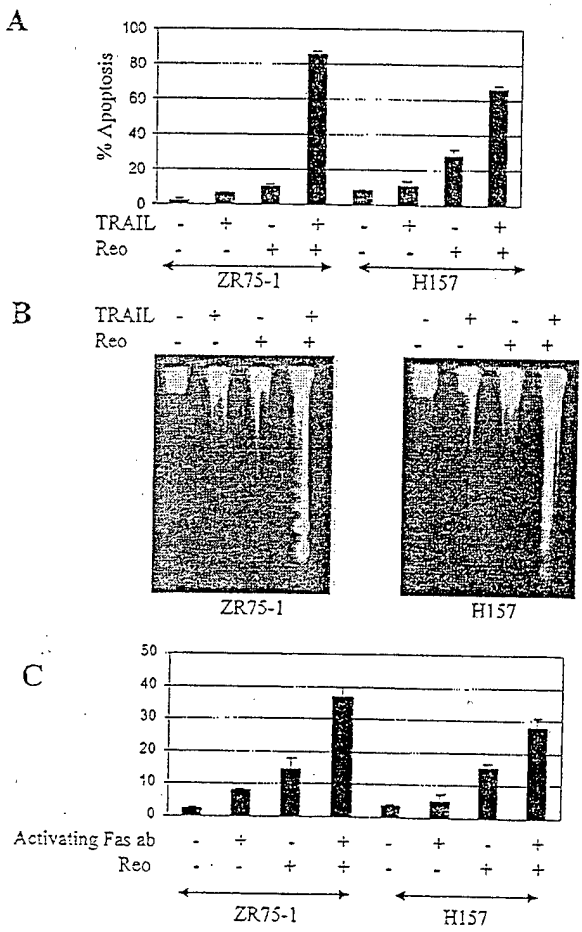

Figure 3 Reovirus infection synergistically sensitizes cancer cells to TRAIL-induced apoptosis but not to an activating Fas antibody. (a) H157 and ZR75-1 cells were either mock-infected or infected with reovirus (MOI 10). After 24 h cells were treated with TRAIL (20 ng/ml), an activating Fas antibody (0.025 μg/ml), or were left untreated. The graphs (a and c) show the mean per cent of apoptotic nuclei in cells from three separate experiments (error bars represent standard errors of the mean) in reovirus-infected TRAIL/Fas antibody treated cells. The gels (b) show the presence of fragmented DNA in the reovirus-infected, TRAIL-treated cells

than synergistic and the amount of apoptosis seen with a combination of antibody and reovirus was not significantly different from the sum of reo- and antibody-induced apoptosis when each was administered separately. This indicates that the synergistic sensitization of reovirus-infected cells to TRAIL is a specific event.

Reovirus does not augment doxorubicin-induced apoptosis

Doxorubicin is a cancer therapeutic agent that augments TRAIL induced apoptosis. Doxorubicin induces apoptosis in treated cells, as demonstrated by caspase 3 activation (Keane *et al*, 1999) but this apoptosis does not occur through cellular death receptors. We wondered whether reovirus infection might enhance doxorubicin-induced, as well as TRAIL-induced, apoptosis. ZR75-1 cells, which are sensitized to TRAIL-induced apoptosis following reovirus infection, were treated with different concentrations of doxorubicin 24 h following reovirus or mock-infection and were assayed for the presence of apoptotic nuclear morphology after a further 24 h. Figure 4a shows that doxorubicin concentrations of below 0.5 M did not induce apoptosis in either infected or uninfected ZR75-1 cells, concentrations of 1–2 M induced around 60–80% apoptosis in either infected or uninfected cells and doxorubicin concentrations of 3 M killed 100% of treated cells. There was no significant difference in doxorubicin-induced apoptosis in reovirus-infected, compared to uninfected cells, at any of the doxorubicin concentrations tested. We selected concentrations of 0.25 and 0.5 M doxorubicin to further investigate the effect of reovirus-infection on doxorubicin-induced apoptosis. We also investigated the effect of TRAIL (20 ng/ml) on doxorubicin-induced apoptosis. Cells were infected with reovirus (MOI 10), or were mock-infected. Twenty-four hours later cells were treated with doxorubicin (0.25 and 0.5 M) and/or TRAIL (20 ng/ml) and were assayed for apoptosis after a further 24 h. Figure 4b shows that reovirus-infection does not significantly augment 0.25 M doxorubicin-induced apoptosis in ZR75-1 cells, compared to cells treated with 0.25 M doxorubicin alone (similar results were obtained with 0.5 M doxorubicin, results not shown). As shown above ZR75-1 cells were sensitized to TRAIL-induced apoptosis following reovirus infection. Doxorubicin also augmented TRAIL-induced apoptosis in ZR75-1 cells. Similar results were obtained in H157 cells (data not shown). These results suggest that reovirus infection does not sensitize cells to doxorubicin-induced apoptosis and supports our finding that the sensitization of reovirus-infected cells to TRAIL is a specific event.

Reovirus infection does not alter the expression of TRAIL receptors in cancer cell lines

Having shown that reovirus specifically augments TRAIL-induced apoptosis we wished to determine the mechanism by which this occurs. The sensitivity of cells

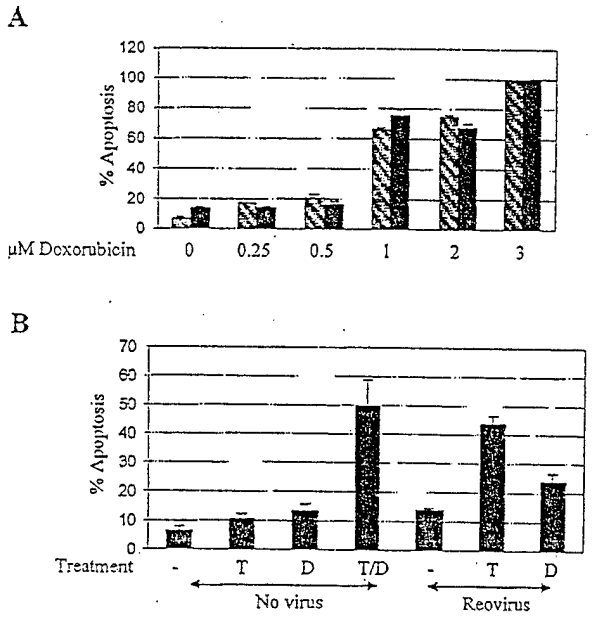

Figure 4 Reovirus infection does not sensitize cells to doxorubicin-induced apoptosis. (a) ZR75-1 cells were infected with reovirus (MOI 10, black bars) or were mock-infected (shaded bars). After 24 h cells were treated with increasing concentrations of doxorubicin and were assayed for apoptosis after a further 24 h. (b) ZR75-1 cells were infected with reovirus (MOI 10) or were mock-infected. After 24 h cells were treated with TRAIL (T), doxorubicin (D) or a combination of TRAIL and doxorubicin (T/D). The graphs show the mean numbers of cells with apoptotic nuclear morphology from three separate experiments. Error bars represent standard errors of the mean

to TRAIL-induced apoptosis is dependent, in part on the expression of the apoptosis-inducing receptors DR4 and DR5. We therefore assayed TRAIL receptor expression in reovirus-infected cancer cells to determine whether reovirus sensitizes cells to TRAIL-induced apoptosis by altering TRAIL receptor expression in infected cells. Gene expression was analysed in mock- and reovirus-infected lung and cervical cancer cells by semi-quantitative RTPCR, 12 and 24 h post infection (Figure 5a) and by FACS analysis of cell surface receptor expression in breast cancer cells, 24 h post infection (Figure 5b). DR5 mRNA was expressed in all the cell lines tested and did not alter following infection with reovirus. DR5 cell surface expression was also unaltered following infection with reovirus and FACS analysis of DR5 staining in mock-infected and reovirus-infected cells produced identical traces (Figure 5b). The expression of DR4 mRNA is dependent on cell type. HeLa and H157 cells express DR4 mRNA whereas A549 cells express very little DR4 mRNA. However, there is no change in the expression of either DR4 mRNA (Figure 5a), or of cell surface DR4 (Figure 5b), in cells following reovirus infection. The expression of neither DcR-1 nor DcR-2 mRNA was altered by reovirus infection (data not shown).

Taken together these results indicate that reovirus infection does not alter TRAIL-receptor expression and that changes in receptor expression do not

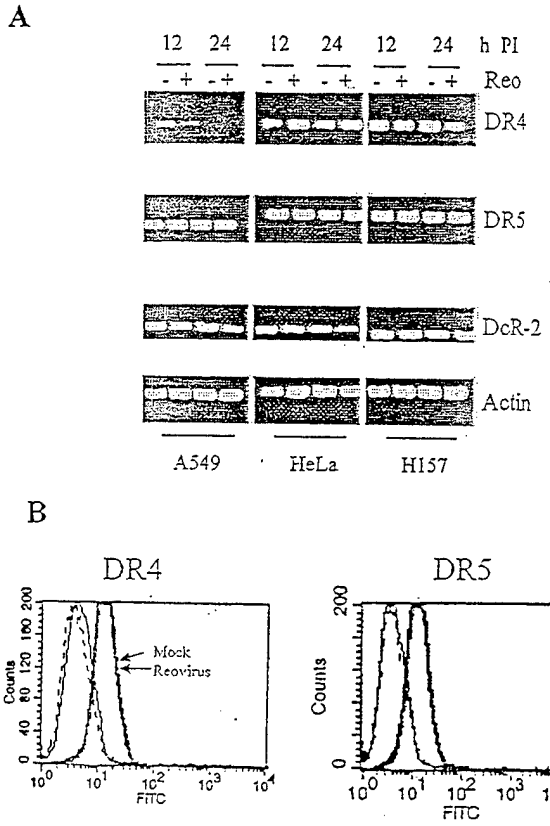

Figure 5 Expression of TRAIL receptors following reovirus infection in cancer cell lines. (a) Expression of TRAIL receptor mRNA does not change in reovirus infected cells. Lung (A549 and H157) and cervical (HeLa) cancer cells were infected with reovirus (MOI 100). After 12 and 24 h cells were harvested and semi-quantitative RTPCR was performed using primers specific for DR4, DR5, DcR-2 and actin. (b) Flow cytometric analysis of TRAIL receptor expression in breast cancer cells following infection with reovirus. MDA231 cells were infected with reovirus (MOI 100). Twenty-four hours post infection cells were harvested, stained and analysed for surface expression of TRAIL receptors DR4 and DR5. The unlabeled traces correspond to mock and reovirus-infected cells stained with an anti FITC antibody

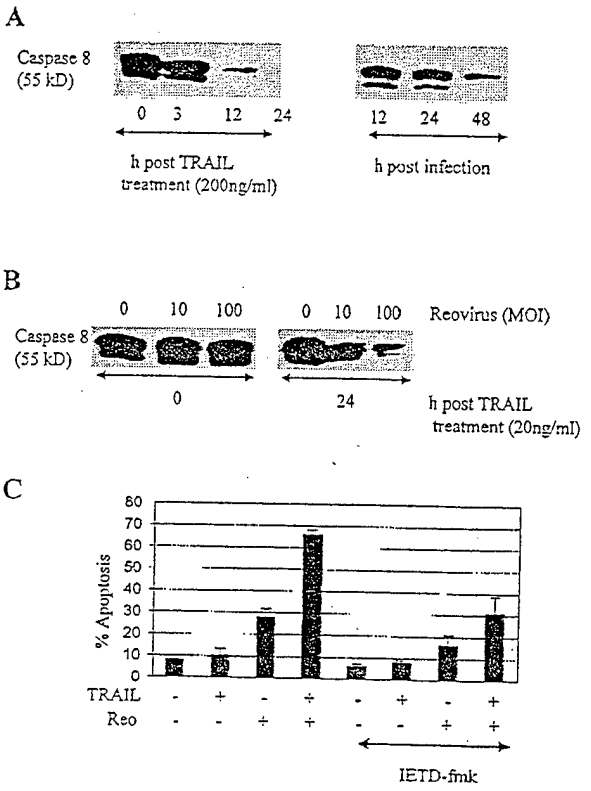

Figure 6 Reovirus infection increases the activation of caspase 8 in TRAIL treated cells and reovirus-induced sensitization of cells to TRAIL is blocked by an inhibitor of caspase 8 activity. (a) High doses of TRAIL (200 ng/ml) alone and reovirus (MOI 100) alone both induce the cleavage of procaspase 8 in H157 cells. (b) H157 cells were infected with reovirus (MOI 0, 10, 100). Twelve hours following infection cells were treated with low dose TRAIL (20 ng/ml) and were harvested at various times post treatment. For the detection of caspase 8 activation extracts were run on tricine gels and were probed with antibody directed against pro-caspase 8. All samples were standardized for protein concentration using actin (not shown). (c) ZR75-1 cells were either mock-infected or infected with reovirus (MOI 10). After 24 h cells were treated with TRAIL (20 ng/ml), or were left untreated, in the presence or absence of IETD-fmk (50 μM). The graph shows the mean per cent of apoptotic nuclei in cells from three separate experiments. Error bars represent standard errors of the mean

contribute to the capacity of reovirus infection to sensitize cancer cells to TRAIL-induced killing.

Reovirus-induced sensitization to TRAIL is associated with an increase in the activity of caspase 8

Since both TRAIL (Muhlenbeck *et al.*, 1998) and reovirus-induced (Kominsky *et al.*, submitted) apoptosis are associated with the activation of caspase 8 we wished to determine whether caspase 8 was involved in reovirus-induced sensitization of cells to TRAIL. As expected high doses of TRAIL alone (200 ng/ml) and of reovirus alone (MOI 100) activated caspase 8 in H157 cells, as determined by the cleavage of pro-caspase 8 (Figure 6a). We next looked to see if the activity of caspase 8 was increased in reovirus-infected, TRAIL-treated cells compared to cells treated with TRAIL alone. We tested the ability of increasing doses of reovirus (MOI 0, 10, 100) to augment TRAIL-induced caspase 8 activation in cells treated with low levels of TRAIL (20 ng/ml), that are insufficient to activate caspase 8 by themselves. H157 cells were infected with reovirus and 12 h following infection were treated with TRAIL (20 ng/ml). Cells were harvested 0 and 24 h later and extracts were run on tricine gels and were probed with antibody directed against pro-caspase 8 (Figure 6b). Pro-caspase 8 was not cleaved in the presence of low doses (20 ng/ml) of TRAIL alone but was cleaved in the presence of TRAIL (20 ng/ml) and reovirus, in a MOI-dependent manner (Figure 6b). These results indicate that reovirus augments caspase 8 activation in TRAIL treated cells.

Having shown that reovirus-induced sensitization to TRAIL is associated with an increase in the activation of caspase 8 we next wanted to see if reovirus-induced sensitization of cells was blocked using IETD-fmk, a

peptide capable of inhibiting caspase 8 activity. The presence of IETD-fmk (50 M) significantly ($P<0.05$) reduced the ability of reovirus to sensitize cells to TRAIL in both H157 (data not shown) and ZR75-1 cells (Figure 6c), providing further evidence that reovirus-induced sensitization of cells to TRAIL involves a caspase 8-dependent pathway.

Reovirus-induced sensitization to TRAIL is associated with an increase in the activity of effector caspases

Having shown that reovirus-induced sensitization to TRAIL is associated with an increase in the activation of caspase 8 we next looked to see whether there was an increase in the activation of downstream, effector, caspases in reovirus-infected, TRAIL-treated cells compared to cells treated with TRAIL alone. The effector caspases that have been shown to operate downstream of caspase 8 are caspases 3 and 7. We thus examined the cleavage of the caspase 3 and 7 substrate PARP, as a monitor of activation of effector caspases. Cells were infected with reovirus (MOI 0, 10, 100) and were treated with TRAIL (20 ng/ml) 12 h following infection. After a further 3 h cells were harvested and probed with an antibody directed against PARP. Figure 7 shows the disappearance of PARP (corresponding to its cleavage) in the cell lysates, following treatment with TRAIL. This was enhanced when the cells were first infected with reovirus, indicating that reovirus infection increases the amount of effector caspase activation in TRAIL-treated cells.

Discussion

Our results demonstrate that reovirus induces apoptosis in a variety of cell lines derived from human cancers. Apoptosis was determined by the presence of apoptotic nuclear morphology and the increase in the activity of caspase 3 in reovirus-infected cells. Although the 2–3-fold increase in the activity of caspase 3 that we obtained following reovirus infection is fairly modest it is typical of results obtained in other cell lines (Dr D Kominski, personal communication). It is unclear to us why reovirus produces such a low level of caspase 3 activity in infected cells. Possibly, a low level of activation over a long period of time is

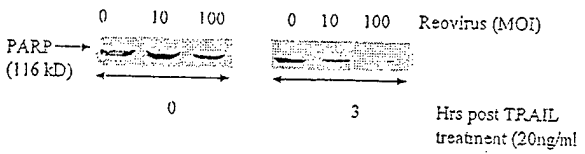

Figure 7 Reovirus infection increases the activation of caspase 3 in TRAIL treated cells. (a) H157 cells were infected with reovirus (MOI 0, 10, 100). Twelve hours following infection cells were treated with low dose TRAIL (20 ng/ml) and were harvested at various times post treatment. Extracts were probed with antibody directed against the caspase 3 substrate, PARP. Samples were standardized for protein concentration using actin (not shown)

sufficient for reovirus-induced apoptosis. Alternatively reovirus may induce increased levels of additional effector caspases, which contribute to apoptosis in reovirus-infected cells. Certainly, the cancer cell lines that we have used show a much higher caspase 3 activity (20 + fold) following TRAIL treatment (results not shown).

Similar to a recent report that showed that cells that were resistant to chemotherapy were also resistant to TRAIL (Cuello *et al*., 2001), there is a significant correlation between the sensitivity of the cancer cell lines to apoptosis induced by reovirus and TRAIL. Further, reovirus-induced apoptosis is blocked both by the presence of soluble TRAIL receptor Fc:DR5 and by the over-expression of DcR-1. These results indicate that reovirus-induced apoptosis in cancer cells is mediated by TRAIL. Similar to our results in HEK293 cells (Clarke *et al*., 2000) we now show that TRAIL is released from all but one of the cancer cell lines tested following infection with reovirus. (17)

Reovirus-induced oncolysis has been previously described (Coffey *et al*., 1998). Our current results indicate that oncolysis results from apoptosis and that TRAIL plays an essential role in this process. Other viruses may also utilize the TRAIL apoptotic pathway. For example, HIV infection increases the expression of TRAIL and sensitizes T-cells to TRAIL-mediated apoptosis (Jeremias *et al*., 1998). Modulation of TRAIL and TRAIL receptor expression also occurs following infection with human cytomegalovirus (Sedger *et al*., 1999) and Theiler's murine encephalomyelitis virus has been shown to induce apoptosis through a mechanism involving TRAIL (Jelachich and Lipton, 2001). Previous studies have suggested that other members of the TNFR death receptor superfamily may also be involved in virus-induced apoptosis. Alteration of the cell surface expression of Fas may be involved in virus-induced, or viral regulation of, apoptosis in cells infected with influenza virus (Takizawa *et al*., 1993, 1995), herpes simplex virus type 2 (Sieg *et al*., 1996), bovine herpesvirus 4 (BHV 4) (Wang *et al*., 1997), adenovirus (Tollefson *et al*., 1998) and human immunodeficiency virus type 1 (HIV 1) (Conaldi *et al*., 1998; Kaplan and Sieg, 1998). Similarly, apoptosis induced by Hepatitis B (Su and Schneider, 1997), HIV-1 (Herbein *et al*., 1999), BHV 4 (Wang *et al*., 1997) parvovirus H-1 (Rayet *et al*., 1998) and Theiler's murine encephalomyelitis virus (Jelachich and Lipton, 2001), may involve the TNFR signaling pathway. (12) (14) (16) (18) (21) (5) (18)

In addition to its capacity to kill cancer cells by apoptosis, we show that reovirus infection also sensitizes cancer cells to TRAIL induced apoptosis in a synergistic manner. H157 and ZR75-1 cells, which are relatively resistant to TRAIL-induced killing, became much more susceptible following infection with reovirus. Reovirus-induced sensitization of cells is specific for TRAIL and reovirus does not synergistically sensitize cells to Fas-mediated apoptosis (another death receptor apoptotic pathway) or to apoptosis

induced by doxorubicin (a non-death receptor apoptotic agent).

We next investigated the mechanism by which reovirus sensitizes cells to TRAIL. The level of TRAIL receptor expression at the cell surface does not change following infection with reovirus indicating that up-regulation of TRAIL receptor is not the mechanism by which reovirus sensitizes cells to TRAIL. The activation of caspase 8 however, is increased in cells following a combination of reovirus-infection and TRAIL-treatment, compared to uninfected cells or to cells treated with TRAIL or reovirus alone. Caspase 8, an initiator caspase, activates the effector caspases 3 and 7 and we show that there is increased cleavage of the effector caspase substrate, PARP, in reovirus-infected, TRAIL-treated cells, compared to cells treated with TRAIL alone. The role of caspase 8 in reovirus-induced sensitization of cells to TRAIL is supported by our demonstration that the peptide IETD-fmk, which inhibits caspase 8 activity and blocks both TRAIL-induced (Yu *et al.*, 2000) and reovirus-induced (Clarke *et al.*, 2000) apoptosis, blocks reovirus-induced sensitization to TRAIL. The expression of DN-FADD, which blocks the activation of caspase 8, also blocks reovirus-induced sensitization to TRAIL in HEK293 cells (results not shown).

The involvement of caspase 8 in reovirus-induced sensitization of cells to TRAIL suggests that reovirus sensitizes cells to TRAIL-induced apoptosis by augmenting the TRAIL pathway of apoptosis rather than by activating a second apoptotic pathway. This suggests that the mechanism by which reovirus sensitizes cells to TRAIL-induced apoptosis differs from the recently identified mitochondrial-dependent pathway by which sodium nitroprusside (Lee *et al.*, 2001) and ionizing radiation (Belka *et al.*, 2001) enhance TRAIL-induced apoptosis. The release of TRAIL from reovirus-infected cells may contribute to the increased activation of caspase 8 in reovirus-infected, TRAIL treated cells. However, ZR75-1 cells, which do not release TRAIL following reovirus infection, are sensitized to TRAIL-induced apoptosis following infection with reovirus. This implies that TRAIL release cannot be the only mechanism for the increased levels of caspase 8 activation in reovirus-infected, TRAIL-treated cells.

The cleavage of procaspase 8 to its active counterpart is required for TRAIL-induced apoptosis. The caspase 8 homologue, FLICE inhibitory protein (cFLIP), promotes cell survival by blocking this reaction and its has been shown that inducers of the transcription factor NF-κB can upregulate cFLIP (Kreuz *et al.*, 2001). Although reovirus induces the activation of NF-κB (Connolly *et al.*, 2000) similar levels of expression of the cellular inhibitor of caspase 8 activation (FLIP) were observed in reovirus-infected, TRAIL-treated cells compared to that in cells treated with TRAIL alone (results not shown) indicating that the increased activation of caspase 8 is not due to a reduction in FLIP-mediated inhibition of caspase 8.

These results show that reovirus-induced oncolysis of cancer cells occurs through TRAIL-mediated apoptosis and suggest that reovirus-infection is a useful model for investigations of TRAIL-induced apoptosis in cancer cells. Similar to the effects of genotoxins (Gibson *et al.*, 2000), reovirus sensitizes cells to TRAIL induced apoptosis. Our results show that reovirus-induced sensitization of cells to TRAIL is inhibited by IETD-fmk and is associated with the activation of caspase 8. Further studies of this phenomenon may suggest new strategies to enhance the killing of cancer cells by TRAIL.

Materials and methods

Cells and virus

HEK293 cells (ATCC CRL1573) were grown in Dulbecco's modified Eagle's medium (DMEM) supplemented with 100 U/ml each of penicillin and streptomycin and containing 10% fetal bovine serum. HeLa cells (ATCC CCL2) were grown in Eagle's minimal essential medium (MEM) supplemented with 2.4 mM L-glutamine, non-essential amino acids, 60 U/ml each of penicillin and streptomycin and containing 10% fetal bovine serum (Gibco BRL, Gaithersburg, MD, USA). HeLa cells were used as indicator cells in the supernatant transfer experiments. The lung cancer cell lines (A549 and H157) and breast cancer cell lines (MDA-MB231 and ZR75-1) were obtained from the University of Colorado Cancer Center. Reovirus (Type 3 Abney, T3A) is a laboratory stock, which has been plaque purified and passaged (twice) in L929 (ATCC CCL1) cells to generate working stocks (Tyler *et al.*, 1996). Virus growth was determined by plaque assay as previously described (Tyler *et al.*, 1985).

Apoptosis assays and reagents

Determination of Apoptotic Nuclear morphology: 48 h after infection with reovirus cells were harvested and stained with acridine orange, for determination of nuclear morphology and ethidium bromide, to distinguish cell viability, at a final concentration of 1 μg/ml each (Duke and Cohen, 1992). Following staining, cells were examined by epifluorescence microscopy (Nikon Labophot-2: B-2A filter, excitation, 450–490 nm; barrier, 520 nm; dichroic mirror, 505 nm). The percentage of cells containing condensed nuclei and/or marginated chromatin in a population of 100 cells was recorded. The specificity of this assay for detecting apoptotic cells has been previously established in reovirus-infected cells using DNA laddering techniques and electron microscopy (Tyler *et al.*, 1995). DNA laddering: Cells (5×10^6) were removed from culture flasks and resuspended in 2 ml digestion buffer (0.1 M NaCl, 10 mM Tris pH 8, 25 mM EDTA, 0.5% SDS and 0.3 mg/ml proteinase K). Following overnight incubation at 50°C the suspension was extracted with phenol/chloroform and then chloroform. DNA was then treated with RNase (20 μg/ml) for 1 h at 37°C, followed by further extraction with phenol/chloroform and then chloroform. DNA was then purified by overnight ethanol precipitation (1/2 volumes 7.5 M NH_4-acetate and three volumes cold 100% ethanol) at −20°C. The precipitate was spun down at 9000 r.p.m. for 30 min, washed in ethanol (85%), dried and resuspended in 200 μl TE. DNA was then

run on a 1.5% agarose gel, stained with ethidium bromide and visualized using a Fluor-S MultiImager and Quantity One software (BioRad, Hercules, CA, USA). For the sensitization experiments cells were infected with reovirus at a multiplicity of infection (MOI) of 10. After 24 h cells were treated with 20 ng/ml TRAIL (Upstate Biotechnology, Lake Placid, NY, USA), 0.025 μg/ml of an activating Fas antibody (Upstate Biotechnology) or 0.25–0.5 M doxorubicin (Sigma, St. Louis, MO, USA) and apoptosis assays were performed after a further 24 h. Soluble death receptors Fc:DR5 and Fc:TNFR were obtained from Alexis Corporation (Pittsburgh, PA, USA). The cell permeable caspase inhibitor IETD-fmk was obtained from Clontech (Palo Alto, CA, USA). Anti-reovirus antibody is a neutralizing polyclonal anti-reovirus antisera, that neutralizes infectivity and blocks apoptosis induced by infectious virus (Tyler *et al.*, 1995).

Caspase 3 activation assays

Caspase 3 activation assays were performed using a kit obtained from Clontech. Experiments were performed using 1×10^6 cells/time point. Cells were centrifuged at 200 *g* for 10 min, supernatants were removed and cell pellets were frozen at −70°C until all time points were collected. Assays were performed in 96 well plates and analysed using a fluoresent plate reader (CytoFluor 4000, PerSeptive Biosystems, Farmington, MA, USA). Cleavage of DEVD-AFC, a synthetic caspase-3 substrate, was used to measure caspase 3 activation in reovirus-infected cells. Cleavage after the second Asp residue produces free AFC that can be detected using a fluorescent plate reader. The amount of fluorescence detected is directly proportional to the amount of caspase 3 activity.

Western blot analysis

Following infection with reovirus, cells were pelleted by centrifugation, washed twice with ice-cold phosphate-buffered saline and lysed by sonication in 200 μl of a buffer containing 15 mM Tris, pH 7.5, 2 mM EDTA, 10 mM EGTA, 20% glycerol, 0.1% NP-40, 50 mM mercaptoethanol, 100 μg/ml leupeptin, 2 μg/ml aprotinin, 40 μM Z-D-DCB, and 1 mM PMSF. The lysates were then cleared by centrifugation at 16 000 *g* for 5 min, normalized for protein amount, mixed 1 : 1 with SDS sample buffer (100 mM Tris, pH 6.8, 2% SDS, 300 mM mercaptoethanol, 30% glycerol, and 5% pyronine Y), boiled for 5 min and stored at −70°C. Proteins were electrophoresed by SDS–PAGE (10% gels) and probed with anti-caspase 8 (B9-2, Pharmingen, San Diego, CA, USA) and anti-PARP (9542, Cell Signaling Technologies, CA, USA) antibodies. All lysates were standardized for protein concentration with antibodies directed against actin (CP01, Oncogene, Cambridge, MA, USA).

RTPCR

Cells were seeded (5×10^6) and were infected with reovirus (MOI 100). At 24 h post infection cells were washed in PBS and were harvested directly into RNA lysis buffer. Total cellular RNA was prepared using RNeasy minicolumns (Qiagen, Valencia, CA, USA). Two μg of RNA was used as template for first strand synthesis using a pre-amplification system (Life Technologies, Grand Island, NY, USA). Semi-quantitative RTPCR amplification reactions specific to DR4, DR5, DcR-1 and DcR-2 were performed (Griffith *et al.*, 1999). Actin primers were used as controls.

Flow cytometry

Cells were removed from tissue culture flasks by repeat pipetting or gentle tapping and were suspended in PBS (10^5 cells/ml). Cells were pelleted by centrifugation (2000 r.p.m. for 2 min, then maximum pulse for 10 s) and were then resuspended in 500 μl wash buffer 1 (PBS containing 2% fetal calf serum and 0.02% sodium azide). Cells were pelleted as above and resuspended in 500 μl staining solution (PBS containing 5% fetal calf serum and 0.02% sodium azide) for 5 min at room temperature. Cells were then pelleted as before and resuspended in 50 μl staining solution, alone for negative control and with primary antibody (2 μl/ml) for experimental samples. Cells were then incubated at 4°C in the dark for 30 min before being washed twice in wash buffer 1 (centrifuging as described above). After a final centrifugation step cells were resuspended in staining solution and secondary antibody conjugated to fluorophore (anti-mouse IgG1-FITC) and were incubated at 4°C in the dark for 30 min. Cells were then pelleted (as above) twice and resuspended first in wash buffer 1 and then in wash buffer 2 (PBS containing 0.02% sodium azide). Cells were then centrifuged (as above), fixed in 500 μl 1% paraformaldehyde and analysed by flow cytometry.

For these experiments monoclonal antibodies against human DR4 (huTR1-M271) and DR5 (huTRAILR2-M413) were used (Immunex Corporation, Seattle, WA, USA).

Acknowledgments

This work was supported by Public Health Service grant 1RO1AG14071 and GM30324 from the National Institute of Health, Merit and REAP grants from the Department of Veterans Affairs, a US Army Medical Research and Material Command grant (DAMD17-98-1-8614) (KL Tyler). The University of Colorado Cancer Center provided core tissue culture and media facilities.

References

Ashkenazi A and Dixit VM. (1998). *Science*, 281, 1305–1308.

Ashkenazi A *et al.* (1999). *J. Clin. Invest.*, 10, 155–162.

Belka C *et al.* (2000). *Oncogene*, 20, 2190–2196.

Clarke P *et al.* (2000). *J. Virol.*, 74, 8135–8139.

Coffey MC, Strong JE, Forsyth PA and Lee PWK. (1998). *Science*, 282, 1332–1334.

Conaldi PG *et al.* (1998). *J. Clin. Invest.*, 102, 2041–2049.

Connolly JL *et al.* (2000). *J. Virol.*, 74, 2981–2989.

Cuello M, Ettenberg SA, Nau MM and Lipkowitz S. (2001). *Gynecol. Oncol.*, 81, 380–390.

DeBiasi RL, Edelstein CL, Sherry B and Tyler KL. (2001). *J. Virol.*, 75, 351–361.

DeBiasi RL *et al.* (1999). *J. Virol.*, 73, 695–701.

Duke RC and Cohen JJ. (1992). *Current protocols in immunology*, Coligan, J.E. (ed), Wiley: NY, pp. 3.17.1–3.17.16.

Gibson SB, Oyer R, Spalding AC, Anderson SM and Johnson GL. (2000). *Mol. Cell Biol.*, 20, 205–212.

Griffith TS *et al.* (1999). *J. Exp. Med.*, 189, 1343–1353.

Herbein G *et al.* (1999). *Nature*, 395, 189–194.

Jelachich ML and Lipton HL. (2001). *J. Virol.*, 75, 5930–5938.
Jeremias I, Herr I, Boehler T and Debatin K-M. (1998). *Eur. J. Immunol.*, 28, 143–152.
(6) Jo M *et al.* (2000). *Nat. Med.*, 6, 564–567.
Kaplan D and Sieg S. (1998). *J. Virol.*, 72, 6279–6282.
Keane MM, Ettenburg SA, Nau MM, Russell EK and Lipkowitz S. (1999). *Cancer Res.*, 59, 734–741.
Kreuz S, Siegmund D, Scheurich P and Wajant H. (2001). *Mol. Cell Biol.*, 12, 3964–3973.
(8) Lee YJ *et al.* (2001). *Oncogene*, 20, 1476–1485.
(9) Muhlenbeck F. *et al.* (1998). *J. Biol. Chem.*, 273, 33091–33098.
Nagata S. (1997). *Cell*, 88, 355–365.
Oberhaus SM, Dermody TS and Tyler KL. (1998). *Retroviruses II: Cytopathicity and pathogenesis [Current Topics in Microbiology and Immunology]*. Tyler KL, Oldstone MBA (eds). Springer-Verlag, Berlin, vol. 233.
Oberhaus SM, Smith RL, Clayton GH, Dermody TS and Tyler KL. (1997). *J. Virol.*, 71, 2100–2106.
(10) Ozoren N *et al.* (2000). *Cancer Res.*, 60, 6259–6265.
(11) Pitti RM *et al.* (1996). *J. Biol. Chem.*, 27, 12687–12690.
Rayet B, Lopez-Guerro J-A, Rommelaere J and Dinsart C. (1998). *J. Virol.*, 72, 8893–8903.
Sedger LM *et al.* (1999). *J. Immunol.*, 163, 920–926. (12)
Sieg S *et al.* (1996). *J. Virol.*, 70, 8747–8751. (14)
Strong JE, Coffey MC, Tang D, Sabinin P and Lee PWK. (1998). *EMBO J.*, 17, 3351–3362.
Su F and Schneider RJ. (1997). *Proc. Natl. Acad. Sci. USA*, 94, 8744–8749.
Takizawa T, Fukuda R, Miyawaki T, Ohashi K and Nakanishi Y. (1995). *Virology*, 209, 288–296.
Takizawa T *et al.* (1993). *J. Gen. Virol.*, 74, 2347–2355. (15)
Tollefson AE *et al.* (1998). *Nature*, 392, 726–730.
Tyler KL, Bronson RT, Byers KB and Fields BN. (1985). *Neurol.*, 35, 88–92. (16)
Tyler KL *et al.* (1996). *J. Virol.*, 70, 7984–7991.
Tyler KL *et al.* (1995). *J. Virol.*, 69, 6972–6979.
Walczak H *et al.* (1999). *Nat. Med.*, 5, 157–163.
Wang GH *et al.* (1997). *J. Virol.*, 71, 8928–8932. (18)
Wiley SR *et al.* (1995). *Immunity*, 3, 673–682.
Yu R, Mandlekar S, Ruben S, Ni J and Kong A-NT. (2000). *Cancer Res.*, 60, 2384–2389. (19)
Zhang XD *et al.* (1999). *Cancer Res.*, 59, 2747–2753. (20)

Reoviruses and the host cell

Kenneth L. Tyler, Penny Clarke, Roberta L. DeBiasi, Douglas Kominsky and George J. Poggioli

Kenneth L. Tyler*
Depts of Neurology, Medicine, Microbiology & Immunology and Pediatrics,

Penny Clarke Dept of Neurology
Douglas Kominsky
Dept of Neurology,

Roberta L. DeBiasi
Dept of Pediatrics,

George J. Poggioli
Dept of Microbiology,
University of Colorado Health Sciences Center (Campus Box B-182),
~~Denver VA Medical Center, Denver, CO 80262, USA.~~ 4200 E. 9th Avenue. Denver, CO 80262
*e-mail: Ken.Tyler@UCHSC.edu

Reovirus infection of target cells can perturb cell cycle regulation and induce apoptosis. Differences in the capacity of reovirus strains to induce cell cycle arrest at G1 and G2/M have been mapped to the viral S1 genome segment, which also determines differences in the ability of reovirus strains to induce apoptosis and to activate specific mitogen-activated protein kinase (MAPK) cascades selectively. Reovirus-induced apoptosis involves members of the tumor necrosis factor (TNF) superfamily of death receptors and is associated with activation of both death receptor- and mitochondrial-associated caspases. Reovirus infection is also associated with activation of a variety of transcription factors, including nuclear factor (NF)-κB. Junctional adhesion molecule (JAM) has recently been identified as a novel reovirus receptor. Reovirus binding to JAM appears to be required for induction of apoptosis and activation of NF-κB, although the precise cellular pathways involved have not yet been identified.

Reovirus infection has long been a classical experimental system for studying the role played by individual viral genes and the proteins they encode during distinct stages of viral pathogenesis *in vivo* (reviewed in Ref. 1). Recent studies have dramatically enhanced our understanding of reovirus–host interactions at the cellular level and have shed light on how these viruses activate cellular signaling pathways, perturb cell cycle regulation and induce apoptotic cell death.

Virus–receptor interaction

The reovirus cell-attachment protein σ1 is an oligomer located at the icosahedral vertices in the outer capsid of the virion. σ1 has a globular head domain and a long fibrous tail. Most serotype three reoviruses (T3) contain a receptor-binding domain (RBD) within the fibrous tail of σ1 encompassing amino acids 198–205, which binds α-linked sialic acid (SA) residues[2,3]. A second RBD, common to both serotype 1 (T1) and T3 reoviruses, is located within the globular head of σ1; the head RBD plays a key role in determining the neurotropism of T3 reoviruses, both *in vitro* and *in vivo*[1]. Several T3 reovirus strains that fail to bind SA (T3SA–) have been identified (e.g. clones T3C43, T3C44 and T3C84) and these strains provide an opportunity to investigate cell attachment mediated by the σ1 head RBD in the absence of tail RBD-mediated binding to SA. Recent studies have provided compelling evidence that the σ1 head RBD binds to junctional adhesion molecule (JAM), and that JAM is a host cell receptor for reoviruses[4]. JAM was identified as a putative reovirus receptor by transfecting COS-7 cells, a reovirus-resistant cell line, with a cDNA library derived from reovirus-susceptible human neuronal precursor (NT2) cells. The transfected cells were selectively enriched for their ability to bind fluoresceinated T3SA– virions. Four clones were identified that each encoded human JAM (hJAM). The ability of JAM to function as a reovirus receptor was confirmed by showing that: (1) anti-hJAM monoclonal antibodies blocked binding of T3SA– virus to a variety of target cells including NT2, HeLa and Caco-2; and (2) murine erythroleukemia (MEL) cells, which are resistant to infection with T3SA–, and chick embryo fibroblasts (CEF), which are resistant to reovirus infection by both SA+ and SA– reovirus strains, both became permissive following transient transfection with either hJAM (MELs and CEFs) or murine JAM (CEFs). Surface plasmon resonance was used to show that a fusion protein comprising the extracellular domain of hJAM coupled to rabbit immunoglobulin Fc (Fc-hJAM) bound to purified T3 σ1 protein and to the proteolytically derived head domain of σ1. A monoclonal antibody specific for a conformational epitope within the σ1 head domain blocked binding of T3 virions to Fc-hJAM, an effect that was not seen with a competitive inhibitor of reovirus binding to SA (α-sialyllactose, SLL). This suggests that reovirus binding to JAM occurs via the virion head RBD and does not require SAs. Reovirus–JAM binding is of high affinity, with a calculated K_d of 6×10^{-8} M.

Junctional adhesion molecule

JAM is a member of the immunoglobulin superfamily that contains two extracellular immunoglobulin-like domains and a short cytoplasmic tail[5,6]. It is a type 1 transmembrane protein that is located predominantly at the subapical region of inter-epithelial cell tight junctions. Although the evidence is compelling that JAM is a reovirus receptor, some aspects of its biology suggest

reported to induce cell cycle arrest in both the G1 (see Ref. 12) and G2/M phase[30,31]. Differences in the capacity of reovirus strains to induce cell cycle arrest are determined by the viral S1 genome segment (see Ref. 24), which is bicistronic. Cell cycle arrest in G1 has been associated with the S1-encoded σ1 protein[12], whereas G2/M arrest requires the S1-encoded non-structural protein, σ1s (Ref. 30). T3 virions lacking σ1s fail to induce G2/M arrest and induced expression of σ1s causes an accumulation of cells in G2/M (Ref. 30). Reovirus-induced arrest in G2/M is associated with hyper-phosphorylation and inhibition of the key G2-to-M transition kinase, $p34^{cdc2}$ (Ref. 31). $p34^{cdc2}$ hyper-phosphorylation can be induced by σ1s expression, and fails to occur in cells infected with a T3 σ1s-deficient virus. Reovirus-induced G1 arrest in R1.1 thymoma cells is associated with Ras inhibition and can be reversed by constitutive expression of *v*-Ha-*ras* (Ref. 12).

Reovirus and the host

Reovirus-induced perturbations of cell signaling pathways including those involved in apoptosis regulation, cell cycle perturbation and MAPK cascades were all initially identified *in vitro*, and their potential significance to pathogenesis *in vivo* is only beginning to be understood. Following intracerebral inoculation of neonatal mice, T3D induces a lethal encephalitis. Within the central nervous system (CNS), there is an excellent correlation between the areas of viral infection as identified by antigen staining, the presence of apoptotic neurons identified by terminal deoxynucleotidyl transferase-mediated dUTP nick end labeling (TUNEL), the morphological characteristics of apoptosis and neuropathological injury[32]. A similar correlation has been seen in the heart following intramuscular inoculation of neonatal mice with the myocarditic reovirus 8B strain (Ref. 22). DNA isolated from either infected brains or hearts shows the inter-nucleosomal fragmentation pattern characteristic of apoptosis ('laddering'). In the CNS, double-labeling of cells for the presence of viral antigen and for apoptosis by TUNEL indicates that both infected cells and non-infected (bystander) cells in proximity to infected cells can undergo apoptosis[32]. In cultured fibroblasts and myocardiocytes, and in the heart, reovirus infection is associated with activation of calpain, a calcium-dependent cysteine protease[21,22]. Inhibition of calpain activation *in vitro* inhibits reovirus-induced apoptosis[21]. Administration of calpain inhibitors *in vivo* prevents myocardial apoptosis and dramatically inhibits reovirus-induced myocardial injury[22]. These studies strongly suggest that apoptosis is an important feature of reovirus infection *in vivo*, and a major contributory factor to virus-induced tissue injury.

Unlike apoptosis, the significance of reovirus-induced perturbations in cell cycle regulation and MAPK signaling in pathogenesis remains largely unknown. It has not yet been established whether reovirus infection alters cellular proliferation or cell cycle regulation following infection *in vivo*. The importance of reovirus-induced perturbations in Ras signaling or in JNK and ERK MAPK cascades for pathogenesis *in vivo* also remains to be established. One glimpse into this area comes from studies of the capacity of reovirus to kill homo- or xenografted tumor cells[26,33]. Intratumoral injection of virus has been shown to cause regression of U87 glioblastoma and transformed fibroblast-derived tumors established in mice[33]. It has been suggested that the susceptibility of transformed cells to reovirus infection both *in vitro* and in homo- and xenografts *in vivo* reflects the presence of an activated Ras signaling pathway[26,33]. However, it remains unknown whether the basal state or reovirus-induced changes in MAPK signaling pathways also influence the susceptibility of non-transformed cells to reovirus infection during natural infection in the host.

Conclusion

Reoviruses have long served as a model system for studying viral pathogenesis *in vivo*. Recent studies have dramatically advanced our understanding of reovirus–host interactions at the cellular level, and have provided new insights into viral host cell receptors, the mechanisms of virus-induced cell death, and the effects of viral infection on cellular signaling pathways and cell cycle regulation. A better understanding of the inter-relationships of these various events and their consequences for viral pathogenesis, are the key goals for future research.

Acknowledgements

Research support has been provided by the Dept of Veterans Affairs (MERIT and REAP Awards), the US Army (Medical Research Grant DAMD17-98-1-8614), and the National Institute on Aging (1R01 AG14071).

References

1 Tyler, K.L. (2001) Mammalian reoviruses. In *Fields Virology* (4th edn) (Knipe, D.M. et al., eds), pp. XXX–XXX, Lippincott–William & Wilkins 1729-1745

2 Chappell, J.D. *et al.* (1997) Mutations in type 3 reovirus that determine binding to sialic acid are contained in the fibrous tail domain of viral attachment protein σ1. *J. Virol.* 71, 1834–1841

3 Chappell, J.D. *et al.* (2000) Identification of carbohydrate-binding domains in the attachment proteins of type 1 and type 3 reoviruses. *J. Virol.* 74, 8472–8479

4 Barton, E.S. *et al.* (2001) Junctional adhesion molecule is a receptor for reovirus. *Cell* 104, 441–451

5 Liu, Y. *et al.* (2000) Human junction adhesion molecule regulates tight junction resealing in epithelia. *J. Cell Sci.* 113, 1–11

6 Martin-Padura, I. *et al.* (1998) Junctional adhesion molecule, a novel member of the immunoglobulin superfamily that distributes at intercellular junctions and mediates monocyte transmigration. *J. Cell Biol.* 142, 117–127

7 Cunningham, S.A. *et al.* (2000) A novel protein with homology to the junctional adhesion molecule. *J. Biol. Chem.* 275, 34750–34756

8 Aurrand-Lions, M. *et al.* (2001) JAM-2, a novel immunoglobulin superfamily molecule, expressed by endothelial and lymphatic cells. *J. Biol. Chem.* 276, 2733–2741

9 Ebnet, K. *et al.* (2000) Junctional adhesion molecule interacts with the PDZ-domain-containing proteins AF-6 and ZO-1. *J. Biol. Chem.* 275, 27979–27988

10 Boettner, B. *et al.* (2000) The junctional multidomain protein AF-6 is a binding partner of the Rap1A GTPase and associated with the actin cytoskeletal regulator profilin. *Proc. Natl. Acad. Sci. U. S. A.* 97, 9064–9069

11 Roux, E. *et al.* (1998) A cell cycle regulating receptor is localized on cell surface and in nuclei of mitotically and meiotically dividing cells. *DNA Cell Biol.* 17, 239–247

12 Saragovi, H.U. *et al.* (1999) A G_1 cell cycle arrest induced by ligands of the reovirus type 3 receptor is secondary to

that it might not be the exclusive target of reovirus head RBDs, and other candidate receptors have previously been identified. It is important to recognize that both SA and JAM can serve independently as reovirus receptors, and it is likely that additional virus–receptor interactions also occur. The predominant localization of JAM to subapical regions of tight junctions would seem to limit its accessibility for virus binding. Studies establishing JAM as a reovirus receptor were performed in cultured cells under conditions in which tight junctions could not form. It remains to be seen whether JAM is in fact accessible for viral attachment in target tissues *in vivo*. Although JAM is highly conserved among mammalian species and is expressed on many cell types that are susceptible to reovirus infection, it is unclear whether the tissue- and cell type-specific distribution of JAM correspond with the known cell and tissue tropisms of reovirus. However, the recent identification of proteins with homology to JAM (e.g. JAM-2)[7,8], which vary in their cell and tissue localization, raises the intriguing possibility that these could also be functional reovirus receptors.

Several recent studies suggest that JAM is associated with a complex of tight junction proteins that can interact with membrane-associated guanylate kinase homologues including the Ras- and Rap1A-interacting proteins AF-6 and ZO-1 (Refs 9,10). These membrane-associated guanylate kinases can in turn activate mitogen-activated protein kinase (MAPK) kinase (MEK) signaling cascades. Thus, although JAM is not conventionally considered a signal transduction protein, it will be intriguing to see what role, if any, it plays in mediating reovirus-induced changes in cellular signal transduction pathways. Nonetheless, reovirus interaction with JAM is unlikely to provide a complete explanation for reovirus-induced activation of cellular transcription factors, MAPK cascades and perturbation in cell cycle regulation. For example reovirus binding to a heterodimeric p65/p95 cell surface receptor found on certain proliferating cells including R1.1 thymoma cells and activated T cells has been associated with reovirus-induced G1 cell cycle arrest and inhibition of Ras-related signaling pathways[11,12].

Reovirus-induced activation of nuclear transcription factors

One of the earliest events following T3 infection is activation of the nuclear factor (NF)-κB family of transcription factors, and this activation appears to be required for the subsequent initiation of reovirus-induced apoptosis[13]. Using electrophoretic mobility-shift assays (EMSA), NF-κB complexes that include p50 and p65 (RelA) can be detected in the nucleus of infected HeLa cells within 4 hrs of infection and reovirus-induced expression of an NF-κB-dependent luciferase reporter gene can be detected within 12 hrs. Inhibition of NF-κB activation by stable expression of a super-repressor form of inhibitor of κB (IκB) or by inhibition of the proteosomal degradation of IκB, or by using immortalized mouse embryo fibroblasts (MEFs) lacking the p50 or p65 (RelA) components of the NF-κB complex, inhibits reovirus-induced apoptosis[13].

The upstream events leading to reovirus-induced NF-κB activation are just beginning to be elucidated. Monoclonal antibodies to hJAM inhibit NF-κB activation and the subsequent apoptosis in HeLa cells despite the fact that these cells remain susceptible to SA-mediated reovirus binding and infection[1]. However, removal of surface SA by neuraminidase treatment blocks both NF-κB activation and apoptosis[14], suggesting that engagement of both JAM and SA might be required for their optimal induction. It remains to be established whether these events are the result of activation of a signal transduction cascade initiated through JAM and/or SA binding, or whether these interactions are merely required to initiate appropriate early steps in reovirus cell entry and replication. However, as replication-incompetent UV-inactivated virus can induce both NF-κB activation[13] and apoptosis[15], this suggests that JAM and/or SA binding is likely to play a greater role than simply facilitating viral entry into target cells.

JAM has not been linked to canonical NF-κB activation pathways. Under normal circumstances, inactive NF-κB is retained in the cytoplasm complexed to its repressor, IκB. Phosphorylation of IκB by the IκB kinase complex (IKK) leads to the ubiquitination and proteosomal degradation of IκB. IKK is itself activated by proteins that function as IKK kinases, including MEK kinase 1 (MEKK1), NF-κB-inducing kinase (NIK), and the interferon (IFN)-induced double-stranded RNA-activated protein kinase (PKR)[16,17]. Cells expressing dominant-negative (DN) forms of NIK fail to activate NF-κB in response to reovirus infection. Embryonal stromal (ES) cells derived from mice with targeted disruptions in the gene encoding MEKK1 show normal levels of reovirus-induced NF-κB activation[18], suggesting that NIK rather than MEKK1 might be the significant IKK kinase activated following reovirus infection. Perhaps surprisingly, given the facility with which reovirus infection induces IFN (see Refs 19,20), PKR does not appear to play a role in reovirus-induced apoptosis or NF-κB activation. Cells transiently expressing DN-PKR, and MEFs lacking PKR have normal levels of reovirus-induced NF-κB activation and apoptosis [P. Clarke *et al.* (2000) MEKK1 and NIK contribute to the activation of NF-κB in reovirus-infected cells via IKK. Abstracts of the 19th Annual Meeting American Society for Virology, Fort Collins, CO, USA, Abstract [illegible])]. It is important to recognize that there are alternative pathways for NF-κB activation other than kinase-activated degradation of IκB. For example, calpain-mediated proteolysis of IκB can also lead to NF-κB activation. Calpains are activated in response to reovirus infection in a variety of target cells including fibroblasts and myocardiocytes *in vitro*, and in reovirus-infected tissue such as the heart *in vivo*[21,22].

W20-9

Reovirus activation of MAPK cascades

In addition to the activation of NF-κB, reovirus infection leads to the selective activation of MAPK cascades. Activation of MAPK cascades usually begins with a small G protein and then proceeds through sequential kinase cascades leading from MAP kinase kinase kinase kinases

(MAP4Ks) to MAP3Ks, MAP2Ks and MAPKs. MAPKs in turn phosphorylate and activate transcription factors. T3 reovirus infection is associated with activation of c-Jun amino-terminal kinase (JNK) and its substrate, the transcription factor c-Jun. JNK activation can be detected within 8–10 hrs of infection and persists for at least 24 hrs[18,23]. The capacity to activate JNK is reovirus strain-specific, with the prototype T3 strains Abney (T3A) and Dearing (T3D) being significantly more potent inducers than T1L. This difference is determined by the same viral genes (*S1* and *M2*) that determine strain-specific differences in apoptosis induction[15,24] and correlates with apoptosis-induction[23]. Reovirus infection of ES cells lacking the MAP3K MEKK1 results in a marked reduction in JNK activation[18], indicating that activation of MEKK1 plays a crucial role in this process.

Ras signaling

Reovirus infection of R1.1 thymoma cells decreases Raf-1 phosphorylation and extracellular signal response kinase (ERK) activity[12]. Raf-1 is part of a MAPK cascade that begins with conversion of Ras-GDP to Ras-GTP and leads sequentially to phosphorylation and activation of Raf-1, MEK 1/2 and ERK. Paradoxically, cells overexpressing constitutively active Ras signaling pathway molecules including Sos and Ras, which have increased levels of ERK 1/2 activity, show enhanced efficiency of reovirus infection[25]. It has been suggested that increases in Ras signaling might play a role, through as-yet-undefined mechanisms, in preventing reovirus-induced PKR activation and thereby augmenting viral protein synthesis[25,26].

Cellular pathways involved in reovirus-induced apoptosis

Reovirus-induced apoptosis involves JAM and/or SA binding, and the activation of transcription factors including NF-κB and possibly c-Jun. This suggests that new gene expression is an essential component of reovirus-induced cell death. Identification of the specific genes involved is likely to provide important insights into the mechanism of reovirus-induced apoptosis, and studies are currently under way to identify virus-associated changes in gene transcription using high-density oligonucleotide microarrays (GeneChip; Affymetrix, CA, USA). Preliminary studies suggest that reovirus infection leads to altered expression of a limited subset of host genes that can be functionally categorized as encoding proteins involved in IFN responses, apoptotic signaling, DNA damage and repair processes, and cell cycle regulation [R.L. Debiasi *et al.* (2000) Analysis of gene expression following reovirus T3 Abney infection using high density oligonucleotide microarrays. Abstracts of the 7th International Symposium on Double-Stranded RNA Viruses, Palm Beach, Aruba, FL, USA, Abstract W6–W8]. W6-5

Cell surface death receptors

Ribonuclease protection assays suggest that members of the tumor necrosis factor (TNF) superfamily of cell-surface death receptors, specifically death receptors 4 (DR4) and 5 (DR5) and their ligand (TNF-related apoptosis-inducing ligand, TRAIL), are involved in reovirus-induced apoptosis. Antibodies against TRAIL, or soluble forms of DR4 and DR5 inhibit reovirus-induced apoptosis[27,28]. A similar effect is seen in cells stably overexpressing DcR2 (Ref. 28), a decoy receptor that binds TRAIL but fails to activate apoptotic signaling pathways. Reovirus-induced apoptosis results in activation of the death-receptor-associated initiator caspase, caspase 8 [Ref. 28; D. Kominsky *et al.* (2000) Reovirus-induced apoptosis involves both death receptor and mitochondrial-mediated pathways of cell death. Abstracts of the 7th International Symposium on Double-Stranded RNA Viruses, Palm Beach, Aruba, FL, USA, Abstracts P6–P4] and subsequently activation of the downstream effector caspases, caspases 3 and 7 [Ref 28: D. Kominsky *et al.* (2000) Reovirus-induced apoptosis involves both death receptor and mitochondrial-mediated pathways of cell death. Abstracts of the 7th International Symposium on Double-Stranded RNA Viruses, Palm Beach, Aruba, FL, USA, Abstracts P6–P4]. Reovirus infection also induces activation of the mitochondrial apoptotic pathway with release of cytochrome *c* and activation of the mitochondrion-associated initiator caspase, caspase 9. Both caspase 8 and caspase 9 are capable of activating the effector caspase, caspase 3. The death receptor and mitochondrial apoptotic pathways are linked by Bid, a Bcl-2 family protein. Reovirus infection results in caspase-8-dependent cleavage of Bid, which can then translocate to the mitochondrion and trigger release of cytochrome *c* [D. Kominsky *et al.* (2000) Reovirus-induced apoptosis involves both death receptor and mitochondrial-mediated pathways of cell death. Abstracts of the 7th International Symposium on Double-Stranded RNA Viruses, Palm Beach, Aruba, FL, USA, Abstracts P6–P4]. Reovirus-induced apoptosis is significantly inhibited by cell-permeable tetrapeptide inhibitors of caspase 8 and by stable overexpression of DN Fas-associated death domain (FADD)[27]. Bid cleavage and cytochrome *c* release are also both inhibited in reovirus-infected cells stably expressing DN-FADD [D. Kominsky *et al.* (2000) Reovirus-induced apoptosis involves both death receptor and mitochondrial-mediated pathways of cell death. Abstracts of the 7th International Symposium on Double-Stranded RNA Viruses, Palm Beach, Aruba, FL, USA, Abstracts P6–P4], suggesting that activation of the mitochondrial apoptosis pathway is initiated by death-receptor activation and uses Bid-mediated crosstalk. The mitochondrial pathway provides a crucial amplification step in reovirus apoptosis, as inhibition of mitochondrial release of cytochrome *c* by stable overexpression of Bcl-2 inhibits reovirus-induced apoptosis[29] [D. Kominsky *et al.* (2000) Reovirus-induced apoptosis involves both death receptor and mitochondrial-mediated pathways of cell death. Abstracts of the 7th International Symposium on Double-Stranded RNA Viruses, Palm Beach, Aruba, FL, USA, Abstracts P6–P4]. P6-4 P6-4 P6-4 P6-4 P6-4

Reovirus-induced perturbation of cell cycle regulation

Reovirus infection is associated with inhibition of DNA synthesis and inhibition of cellular proliferation (see Ref. 24). Depending on the cells investigated and the experimental methods employed, reovirus has been

reported to induce cell cycle arrest in both the G1 (see Ref. 12) and G2/M phase[30,31]. Differences in the capacity of reovirus strains to induce cell cycle arrest are determined by the viral S1 genome segment (see Ref. 24), which is bicistronic. Cell cycle arrest in G1 has been associated with the S1-encoded σ1 protein[12], whereas G2/M arrest requires the S1-encoded non-structural protein, σ1s (Ref. 30). T3 virions lacking σ1s fail to induce G2/M arrest and induced expression of σ1s causes an accumulation of cells in G2/M (Ref. 30). Reovirus-induced arrest in G2/M is associated with hyper-phosphorylation and inhibition of the key G2-to-M transition kinase, $p34^{cdc2}$ (Ref. 31). $p34^{cdc2}$ hyper-phosphorylation can be induced by σ1s expression, and fails to occur in cells infected with a T3 σ1s-deficient virus. Reovirus-induced G1 arrest in R1.1 thymoma cells is associated with Ras inhibition and can be reversed by constitutive expression of *v*-Ha-*ras* (Ref. 12).

Reovirus and the host

Reovirus-induced perturbations of cell signaling pathways including those involved in apoptosis regulation, cell cycle perturbation and MAPK cascades were all initially identified *in vitro*, and their potential significance to pathogenesis *in vivo* is only beginning to be understood. Following intracerebral inoculation of neonatal mice, T3D induces a lethal encephalitis. Within the central nervous system (CNS), there is an excellent correlation between the areas of viral infection as identified by antigen staining, the presence of apoptotic neurons identified by terminal deoxynucleotidyl transferase-mediated dUTP nick end labeling (TUNEL), the morphological characteristics of apoptosis and neuropathological injury[32]. A similar correlation has been seen in the heart following intramuscular inoculation of neonatal mice with the myocarditic reovirus 8B strain (Ref. 22). DNA isolated from either infected brains or hearts shows the inter-nucleosomal fragmentation pattern characteristic of apoptosis ('laddering'). In the CNS, double-labeling of cells for the presence of viral antigen and for apoptosis by TUNEL indicates that both infected cells and non-infected (bystander) cells in proximity to infected cells can undergo apoptosis[32]. In cultured fibroblasts and myocardiocytes, and in the heart, reovirus infection is associated with activation of calpain, a calcium-dependent cysteine protease[21,22]. Inhibition of calpain activation *in vitro* inhibits reovirus-induced apoptosis[21]. Administration of calpain inhibitors *in vivo* prevents myocardial apoptosis and dramatically inhibits reovirus-induced myocardial injury[22]. These studies strongly suggest that apoptosis is an important feature of reovirus infection *in vivo*, and a major contributory factor to virus-induced tissue injury.

Unlike apoptosis, the significance of reovirus-induced perturbations in cell cycle regulation and MAPK signaling in pathogenesis remains largely unknown. It has not yet been established whether reovirus infection alters cellular proliferation or cell cycle regulation following infection *in vivo*. The importance of reovirus-induced perturbations in Ras signaling or in JNK and ERK MAPK cascades for pathogenesis *in vivo* also remains to be established. One glimpse into this area comes from studies of the capacity of reovirus to kill homo- or xenografted tumor cells[26,33]. Intratumoral injection of virus has been shown to cause regression of U87 glioblastoma and transformed fibroblast-derived tumors established in mice[33]. It has been suggested that the susceptibility of transformed cells to reovirus infection both *in vitro* and in homo- and xenografts *in vivo* reflects the presence of an activated Ras signaling pathway[26,33]. However, it remains unknown whether the basal state or reovirus-induced changes in MAPK signaling pathways also influence the susceptibility of non-transformed cells to reovirus infection during natural infection in the host.

Conclusion

Reoviruses have long served as a model system for studying viral pathogenesis *in vivo*. Recent studies have dramatically advanced our understanding of reovirus–host interactions at the cellular level, and have provided new insights into viral host cell receptors, the mechanisms of virus-induced cell death, and the effects of viral infection on cellular signaling pathways and cell cycle regulation. A better understanding of the inter-relationships of these various events and their consequences for viral pathogenesis, are the key goals for future research.

Acknowledgements

Research support has been provided by the Dept of Veterans Affairs (MERIT and REAP Awards), the US Army (Medical Research Grant DAMD17-98-1-8614), and the National Institute on Aging (1R01 AG14071).

References

1 Tyler, K.L. (2001) Mammalian reoviruses. In *Fields Virology* (4th edn) (Knipe, D.M. et al., eds), pp. ~~XXX–XXX~~, Lippincott–William & Wilkins 1729-1745

2 Chappell, J.D. *et al.* (1997) Mutations in type 3 reovirus that determine binding to sialic acid are contained in the fibrous tail domain of viral attachment protein σ1. *J. Virol.* 71, 1834–1841

3 Chappell, J.D. *et al.* (2000) Identification of carbohydrate-binding domains in the attachment proteins of type 1 and type 3 reoviruses. *J. Virol.* 74, 8472–8479

4 Barton, E.S. *et al.* (2001) Junctional adhesion molecule is a receptor for reovirus. *Cell* 104, 441–451

5 Liu, Y. *et al.* (2000) Human junction adhesion molecule regulates tight junction resealing in epithelia. *J. Cell Sci.* 113, 1–11

6 Martin-Padura, I. *et al.* (1998) Junctional adhesion molecule, a novel member of the immunoglobulin superfamily that distributes at intercellular junctions and mediates monocyte transmigration. *J. Cell Biol.* 142, 117–127

7 Cunningham, S.A. *et al.* (2000) A novel protein with homology to the junctional adhesion molecule. *J. Biol. Chem.* 275, 34750–34756

8 Aurrand-Lions, M. *et al.* (2001) JAM-2, a novel immunoglobulin superfamily molecule, expressed by endothelial and lymphatic cells. *J. Biol. Chem.* 276, 2733–2741

9 Ebnet, K. *et al.* (2000) Junctional adhesion molecule interacts with the PDZ-domain-containing proteins AF-6 and ZO-1. *J. Biol. Chem.* 275, 27979–27988

10 Boettner, B. *et al.* (2000) The junctional multidomain protein AF-6 is a binding partner of the Rap1A GTPase and associated with the actin cytoskeletal regulator profilin. *Proc. Natl. Acad. Sci. U. S. A.* 97, 9064–9069

11 Roux, E. *et al.* (1998) A cell cycle regulating receptor is localized on cell surface and in nuclei of mitotically and meiotically dividing cells. *DNA Cell Biol.* 17, 239–247

12 Saragovi, H.U. *et al.* (1999) A G_1 cell cycle arrest induced by ligands of the reovirus type 3 receptor is secondary to

inactivation of $p21^{cip1}$ and mitogen-activated protein kinase. *DNA Cell Biol.* 18, 763–770
13 Connolly, J.L. *et al.* (2000) Reovirus-induced apoptosis requires activation of transcription factor NF-κB. *J. Virol.* 74, 2981–2989
14 Connolly, J.L. *et al.* (2001) Reovirus binding to cell surface sialic acid potentiates virus-induced apoptosis. *J. Virol.* 75, 4029–4039
15 Tyler, K.L. *et al.* (1995) Differences in the capacity of reovirus strains to induce apoptosis are determined by the viral attachment protein sigma 1. *J. Virol.* 69, 6972–6979
16 Barkett, M. and Gilmore, T.D. (1999) Control of apoptosis by Rel/NF-κB transcription factors. *Oncogene* 18, 6910–6924
17 Hiscott, J. *et al.* (2001) Hostile takeovers: viral appropriation of the NF-κB pathway. *J. Clin. Invest.* 107, 143–151
18 Yujiri, T. *et al.* (2000) MEK kinase 1 gene disruption alters cell migration and c-Jun NH_2-terminal kinase regulation but does not cause a measurable defect in NF-κB activation. *Proc. Natl. Acad. Sci. U. S. A.* 97, 7272–7277
19 Sherry, B. *et al.* (1998) Reovirus induction of and sensitivity to beta interferon in cardiac myocyte cultures correlate with induction of myocarditis and are determined by viral core proteins. *J. Virol.* 72, 1314–1323
20 Samuel, C.E. *et al.* (1998) Reoviruses II. Cytopathicity and pathogenesis. *Curr. Topics Microbiol. Immunol.* 233, 125–146
21 Debiasi, R.L. *et al.* (1998) Reovirus-induced apoptosis is preceded by increased cellular calpain activity and is blocked by calpain inhibitors. *J. Virol.* 73, 695–701
22 Debiasi, R.L. *et al.* (2001) Calpain inhibition protects against virus-induced apoptotic myocardial injury. *J. Virol.* 75, 351–361
23 Clarke, P. *et al.* Reovirus–induced JNK activation is determined by the viral M2 and S1 gene segments and correlates with apoptosis. *J. Virol.* (in press)
24 Tyler, K.L. *et al.* (1996) Linkage between reovirus-induced apoptosis and inhibition of cellular DNA synthesis: role of the S1 and M2 genes. *J. Virol.* 70, 7984–7891
25 Strong, J.E. *et al.* (1998) The molecular basis of oncolysis: usurpation of the Ras signaling pathway by reovirus. *EMBO J.* 17, 3351–3362
26 Norman, K.L. and Lee, P.W.K. (2000) Reovirus as a novel oncolytic agent. *J. Clin. Invest.* 105, 1035–1038
27 Clarke, P. *et al.* (2000) Reovirus-induced apoptosis is mediated by TRAIL. *J. Virol.* 74, 8135–8139
28 Clarke, P. *et al.* Caspase-8 dependent sensitization of cancer cells to TRAIL–induced apoptosis following reovirus infection. *Oncogene* (in press)
29 Rodgers, S.E. *et al.* (1997) Reovirus-induced apoptosis of MDCK cells is not linked to viral yield and is inhibited by bcl-2. *J. Virol.* 71, 2540–2546
30 Poggioli, G.J. *et al.* (2000) Reovirus-induced G_2/M cell cycle arrest requires σ1s and occurs in the absence of apoptosis. *J. Virol.* 74, 9562–9570
31 Poggioli, G.J. *et al.* (2001) Reovirus-induced σ1s-dependent G_2/M cell cycle arrest is associated with inhibition of $p34^{cdc2}$. *J. Virol.* 75, 7429–7434
32 Oberhaus, S.M. *et al.* (1997) Reovirus infection and tissue injury in the mouse central nervous system are associated with apoptosis. *J. Virol.* 71, 2100–2106
33 Coffey, M.C. *et al.* (1998) Reovirus therapy of tumors with activated Ras pathway. *Science* 282, 1332–1334

Questions for future research

- What are the cellular pathways linking reovirus engagement of JAM and/or other host cell surface receptors and activation of MAPK pathways and transcription factors?
- What are the specific genes essential for reovirus-induced apoptosis and cell cycle dysregulation and which transcription factors control their expression?
- What is the role of apoptosis in reovirus-induced tissue injury in different organs *in vivo*, and what are the effects on viral pathogenesis of inhibiting apoptosis?
- What role do reovirus-induced alterations in cell cycle regulation play in viral replication *in vitro* and pathogenesis *in vivo*?
- What is the relationship between reovirus receptors identified *in vitro*, and the cell and tissue tropism of the virus *in vivo*? Do differences in patterns of receptor utilization or expression explain age-related and/or strain-specific differences in patterns of viral infection?

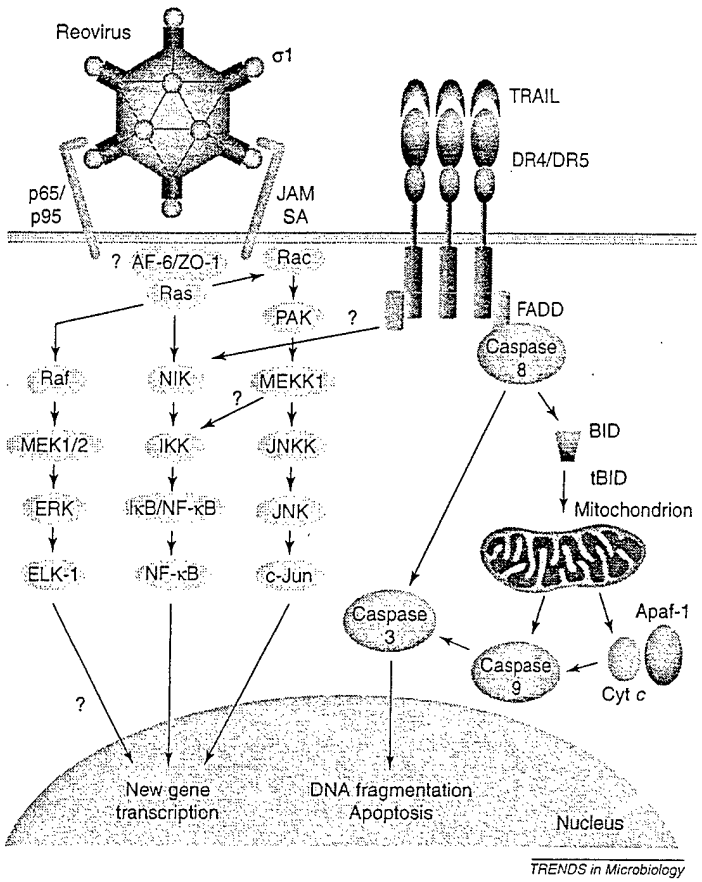

Fig. 1. Reovirus-induced changes in cellular signaling pathways. Reovirus infection is associated with changes in kinase pathways involved in the regulation of nuclear factor (NF)-κB, and mitogen-activated protein kinase (MAPK) cascades involving both c-Jun amino-terminal kinase (JNK) and extracellular signal response kinase (ERK). Infection results in new gene transcription and upregulation of apoptotic pathways including the tumor necrosis factor (TNF)-related apoptosis-inducing ligand (TRAIL)/death receptor 4 (DR4)/DR5 death receptor and mitochondrial pathways. Mitochondrial-mediated cell death involves the activation of the effector caspases, caspases 9 and 3. Reovirus receptors including junctional adhesion molecule (JAM), sialic acid (SA) and an uncharacterized heterodimeric 'p65/p95' receptor have all been implicated in reovirus-induced changes in cell signaling pathways. The mechanisms by which receptor engagement leads to changes in intracellular signaling and the exact receptor(s) involved in activating specific pathways remain to be defined. See text for details regarding individual pathways. Abbreviations: Cyt c, cytochrome c; FADD, Fas-associated death domain; IκB, inhibitor of κB; IKK, IκB kinase complex; JNKK, JNK kinase; MEK, MAPK kinase; NIK, NF-κB inducing kinase; PAK, p21-activated kinase.

Reovirus infection activates JNK and the JNK-dependent transcription factor c-Jun

PENNY CLARKE,[1] SUZANNE M. MEINTZER,[1] CHRISTIAN WIDMANN, [2,✣] GARY L. JOHNSON, [2] AND KENNETH L., TYLER [1,3,4,*]

Departments of Neurology[1], Pharmacology[2], Medicine, Microbiology and Immunology[3], University of Colorado Health Science Center, Denver, Colorado 80262, and Denver Veteran's Affairs Medical Center[4], Denver, Colorado 80220.

Running Title: Reovirus-induced JNK activation

* Corresponding author. Mailing address: Department of Neurology (127), Denver VA Medical Center, 1055 Clermont Street, Denver, CO 80220. Phone: (303) 393 2874. Fax: (303) 393 4686. E-mail: Ken.Tyler@uchsc.edu

✣ Current address is Institute de Biologie Cellulaire et de Morphologie, Lausanne, Switzerland.

ABSTRACT

Viral infection often perturbs host cell signaling pathways including those involving mitogen-activated protein kinases (MAPKs). We now show that reovirus infection results in the selective activation of c-Jun N-terminal kinase (JNK). Reovirus-induced JNK activation is associated with an increase in the phosphorylation of the JNK-dependent transcription factor c-Jun. Reovirus serotype 3 prototype strains Abney (T3A) and Dearing (T3D) induce significantly more JNK activation and c-Jun phosphorylation than the serotype 1 prototypic strain Lang (T1L). T3D and T3A also induce more apoptosis in infected cells than T1L and there was a significant correlation between the ability of these viruses to phosphorylate c-Jun and induce apoptosis. However, reovirus-induced apoptosis, but not reovirus-induced c-Jun phosphorylation, is inhibited by blocking TRAIL/receptor binding, suggesting that apoptosis and c-Jun phosphorylation involve parallel rather than identical pathways. Strain specific differences in JNK activation are determined by the reovirus S1 and M2 gene segments, which encode viral outer capsid proteins (σ1, μ1c) involved in receptor binding and host cell membrane penetration. These same gene segments also determine differences in the capacity of reovirus strains to induce apoptosis and again a significant correlation between the capacity of T1L x T3D reassortant reoviruses to both activate JNK and phosphorylate c-Jun and to induce apoptosis was shown. The extracellular signal-related kinase (ERK) is also activated in a strain-specific manner following reovirus infection. ERK activation. Unlike JNK activation, this could not be mapped to specific reovirus gene segments, suggesting that ERK and JNK activation are triggered by different events during virus-host cell interaction.

INTRODUCTION

Mitogen-activated protein kinases (MAPKs) play a critical role in the transduction of a wide variety of extracellular signals (22). MAPKs include the extracellular signal-related kinases (ERKs), which are activated by growth factors and many other mitogenic stimuli (11) and which are generally thought to have anti-apoptotic properties, and the c-Jun N-terminal kinases (JNKs, also called stress-activated protein kinases, SAPKs) (16, 39) and p38 MAPKs (23, 40, 53), which are activated by stress stimuli and which function to communicate growth inhibitory and apoptotic signals within cells. It is thought that the commitment to apoptosis and determination of cell fate may involve the balance between the activity of the JNK and p38 kinases and that of ERK (7). For example, the inhibition of ERK activity and the coordinate activation of JNK and p38 kinase correlate with the induction of apoptosis in nerve growth factor-deprived PC12 pheochromocytoma cells (61), Fas-treated Jurkatt cells (37, 60) and UV-irradiated mouse fibroblasts (3).

Infection with a wide variety of viruses can result in perturbation of host cell signaling pathways including MAPK cascades. Some viruses show a dependence on the ERK signaling cascades for replication and viral proteins that induce ERK activation have been identified (34, 36, 38, 57). Viral-induced MAPK activation, including JNK and p38 has also been described (19, 31, 32, 42, 44, 49, 54, 63), as has the activation of MAPK-associated transcription factors (33, 42, 54, 63). However, the purpose for their activation following infection remains largely unclear.

Reovirus is a double stranded RNA virus that induces apoptosis in cultured cells *in vitro* (46, 50, 58) and in target tissues *in vivo* including the central nervous system and

heart (14, 46, 47). Reovirus-induced apoptosis correlates with pathology *in vivo* and is a critical mechanism by which disease is triggered in the host (14, 47). Strain-specific differences in the capacity of reoviruses to induce apoptosis are determined by the viral S1 and M2 gene segments (58, 59). Reovirus-induced apoptosis requires viral binding to cell surface receptors, including junctional adhesion molecule (2), but not completion of the full viral replication cycle (50, 58). Reovirus induces apoptosis by a p53-independent mechanism that involves cellular proteases including calpains (15) and caspases (10), is dependent on reovirus-induced NF-κB activation (2, 12) and is inhibited by over-expression of Bcl-2 (50).

We have previously shown that reovirus-induced apoptosis is mediated by TNF related apoptosis-inducing ligand (TRAIL; 10), which is released from infected cells, and can be inhibited by antibodies against TRAIL or by treatment of infected cells with soluble forms of TRAIL receptors. TRAIL interacts with several members of the TNF receptor superfamily including the apoptosis-associated receptors DR4 (TRAIL-R1) and DR5 (TRAIL-R2/TRICK2/KILLER). These receptors contain an intracellular 80 amino acid "death domain" (DD; reviewed in 1) which is indispensable for apoptosis since it interacts with DDs found in cytoplasmic adaptor proteins such as TNF-R1-associated death domain protein (TRADD; 29) and Fas-associated protein with death domain (FADD; 5, 8). Adaptor proteins have additional domains that enable interaction with both the prodomains of apoptotic caspases (4, 17, 45) and with members of the TNF receptor-associated factor (TRAF) family (27, 28) molecules involved in the activation of NF- κB and JNK (52, 56). In addition to activating apoptotic caspases TRAIL-receptor activation

in reovirus-infected cells is thus also likely to result in the activation of NF-κB (35) and JNK (30).

The capacity of reovirus to induce apoptosis through a TRAIL-dependent pathway in infected cells suggests that proapoptotic MAPKs, including JNK, might be activated in reovirus-infected cells. Reovirus infection also disrupts cell cycle regulation by inducing a G2/M arrest (48) suggesting that ERK, which promotes cell-cycle progression, might also be inhibited following reovirus infection. This paper investigates the activation of MAPKs in reovirus-infected cells. We show that reovirus-infection causes the selective activation of both the JNK and ERK MAPK cascades. Strain specific differences in JNK, but not ERK, activation are determined by the viral S1 and M2 gene segments, suggesting that different mechanisms are involved in the activation of these kinases in reovirus-infected cells. The viral S1 and M2 gene segments also determine differences in the capacity of reoviruses to induce apoptosis and we now show that there is a significant correlation between the capacity of reassortant reoviruses to activate JNK and to induce apoptosis. Blocking TRAIL-receptor interaction does not prevent the early activation of c-Jun by reovirus, indicating that death-receptor independent signaling pathways are required for reovirus-induced JNK activation.

MATERIALS AND METHODS

Cells and Virus. Mouse L929 cells (ATCC CCL1) were grown in Jolik's modified Eagles medium (JMEM) supplemented to contain 5% fetal bovine serum and 2 mM L-glutamine (Gibco BRL). Reovirus strains Type 3 Abney (T3A), Type 3 Dearing (T3D) and Type 1 Lang (T1L) are laboratory stocks, which have been plaque purified

and passaged (twice) in L929 (ATCC CCL1) cells to generate working stocks (59). T1L x T3D reassortant viruses were grown from sticks originally isolated by Kevin Coombs, Max Nibert and Bernard Fields (6, 13). Virus infections were performed at a multiplicity of infection (MOI) of 100 in order to ensure that 100% of susceptible cells were infected and to maximize the synchrony of virus replication.

Western Blot Analysis and Antibodies. Following infection with reovirus, cells were pelleted by centrifugation, washed twice with ice-cold phosphate-buffered saline and lysed by sonication in 200 μl of a buffer containing 15 mM Tris, pH 7.5, 2 mM EDTA, 10 mM EGTA, 20% glycerol, 0.1% NP-40, 50 mM β-mercaptoethanol, 100 μg/ml leupeptin, 2 μg/ml aprotinin, 40 μM Z-D-DCB, and 1 mM PMSF. The lysates were then cleared by centrifugation at 16, 000 g for 5 min, normalized for protein amount, mixed 1:1 with SDS sample buffer (100 mM Tris, pH 6.8, 2% SDS, 300 mM β-mercaptoethanol, 30% glycerol, and 5% pyronine Y), boiled for 5 min and stored at –70°C. Proteins were electrophoresed by SDS-PAGE (10% gels) and probed with antibodies directed against phospho-ERK, phospo c-Jun and total c-Jun (New England Biolabs, Beverly, Ma). All lysates were standardized for protein concentration with antibodies directed against actin (Oncogene, Cambridge, Ma, #CP01). Autoradiographs were quantitated by densitometric analysis using a Fluor-S MultiImager (BioRad Laboratories, Hercules, Ca).

In vitro kinase assays. L929 cells were solubilized in TX-100 lysis buffer (70 mM β-glycerophosphate, 1 mM EGTA, 100 μM Na_3VO_4, 1 mM dithiothreitol, 2 mM $MgCl_2$, 0.5% Triton X-100, 20 μg/ml aprotinin). Cellular debris was removed by

centrifugation at 8000 x *g* for 5 min. Protein concentration was determined by a Bradford assay using bovine serum albumin as a standard. JNK activity was measured using a solid phase kinase assay in which glutathione s-transferase-c-Jun (GST-Jun) bound to glutathione-Sepharose 4B beads was used to affinity purify JNK from cell lysates as described (20, 25). Quantification of the phosphorylation of GST-Jun was performed with a Phosphoimager (Molecular Dynamics). ERK activation was measured by first incubating the lysate with 2 μg/ml of an anti-ERK2 antibody (Santa Cruz Biotechnology, Inc.) for 1 hr at 4°C with agitation followed by the addition of 15 μl of a slurry of protein A-sepharose beads (Sigma, catalog # P-3391) and a further 20 min incubation at 4°C. The beads were washed twice with 1 ml of lysis buffer and twice with 1 ml of lysis buffer without Triton X-100. 35 μl of the last wash was left in the tube and mixed with 20 μl of ERK reaction mix (50 mM β-glycerophosphate, 100 μM $Na_3 VO_4$, 20 mM $MgCl_2$, 200 μM ATP, 0.5 μCi/μl [γ^{32}P]ATP, 400μM epidermal growth factor receptor peptide 662-681, 100 μg/μl IP-20, 2 mM EGTA), incubated for 20 min at 20°C. The reaction was stopped with 10 μl of 25% trichloroacetic acid and spotted on P81 Whatman paper. The samples were washed 3 times for 5 min each in 75 mM phosphoric acid and once for 2 min in acetone. They were then air-dried and their radioactivity was measured in a β-counter. The activity of p38 was measured as described by Gerwins *et al.* (21).

Apoptosis Assays and Reagents. 48 hours after infection with reovirus cells were harvested and stained with acridine orange, for determination of nuclear morphology and ethidium bromide, to distinguish cell viability, at a final concentration of 1 μg/ml each (18). Following staining, cells were examined by epifluorescence microscopy (Nikon Labophot-2: B-2A filter, excitation, 450-490 nm; barrier, 520 nm; dichroic mirror, 505

nm). The percentage of cells containing condensed nuclei and/or marginated chromatin in a population of 100 cells was recorded. The specificity of this assay has been previously established in reovirus-infected cells using DNA laddering techniques and electron microscopy (10, 58). Soluble death receptors (Fc:DR5 and Fc:DR4) were obtained from Alexis Corporation (Pittsburgh, Pa.)

RESULTS

Reovirus activates JNK in infected cells. We first investigated whether JNK was activated in reovirus-infected cells. L929 cells were infected (MOI, 100) with two prototype strains of reovirus, T3D and T1L. At 0, 5, 10 and 24 hours post infection (PI) cells were harvested and the presence of JNK activity was detected by *in vitro* kinase assays (Fig. 1). In 3 independent experiments JNK activity was significantly increased ($p < 0.01$) at 24 h PI in T3D-infected cells, compared to mock-infected cells. However, JNK activity was not significantly increased ($p > 0.05$) at 24 h PI in T1L-infected cells, compared to mock-infected cells. An increase in JNK activity was apparent 10 h PI of T3D-infected cells. Although statistically significant, variability in JNK activity was greater in the T3D-infected cells at 24 h PI, than for other times and conditions, reflecting the increase in the mean value.

Levels of phosphorylated c-Jun are increased in reovirus-infected cells. The activation of JNK results in the phosphorylation and activation of the transcription factor c-Jun, which in turn regulates the transcription of a multitude of cellular genes. Having shown that JNK was activated in reovirus-infected cells we next wished to determine whether the JNK dependent transcription factor c-Jun was also activated following reovirus infection. Cells were infected with three different strains of reovirus, T1L, T3D

and T3 Abney (T3A), the second prototypic T3 strain. Cells were then harvested at various times PI and the activation state of c-Jun was determined by western blot analysis using an antibody directed against the phosphorylated, activated form of c-Jun. Levels of phosphorylated c-Jun were increased in cells infected with T1L, T3D and T3A strains of reovirus, compared to mock-infected cells (Fig. 2). Increased levels of activated c-Jun were present 12 hours PI, which closely parallels the activation of JNK (Fig. 1). There were serotype specific differences in the ability of reovirus to phosphorylate c-Jun with T3 strains (T3D and T3A), inducing higher levels of phosphorylated c-Jun at earlier times post infection, than T1L. For example, at 12 hours PI, levels of phosphorylated c-Jun in T1L-infected cells were increased 8-fold compared to those seen in mock-infected cells, whereas levels of phosphorylated c-Jun were increased 24-fold in T3D-infected cells and 33-fold in T3A-infected cells. Some increase in c-Jun phosphorylation was observed in mock-infected cells, which may be due to increasing cell confluence. We probed the same lysates with an antibody that detects total c-Jun (both phosphorylated and unphosphorylated forms, Fig. 2C). These blots show that there is also an increase in the levels of total c-Jun in both mock and reovirus-infected cells. Also visible on these blots are bands corresponding to the phosphorylated form of c-Jun (Fig. 2C). Once again serotype specific differences in the ability of reovirus to phosphorylate c-Jun were observed, with T3D and T3A inducing higher levels of phosphorylated c-Jun than T1L.

In support of the association between JNK activation and c-Jun phosphorylation, there was a high correlation between the ability of reovirus to induce JNK activation and to phosphorylate c-Jun ($R^2 = 0.97$).

Reovirus-induced JNK-activation is determined by the S1 and M2 gene segments. Having shown that T3D activates JNK to a greater extent than T1L, we next wished to identify whether specific viral genes determined these differences. L929 cells were infected with a panel of T1L x T3D reassortant reoviruses (MOI 100). 24 hours PI cells were harvested and JNK activity was determined by *in vitro* kinase assay. JNK activation following infection with different reassortant viruses, as well as with parental strains, and the derivation of the various genome segments of each virus is shown in Table 1. Results were analyzed using both parametric (*t*-test) and non-parametric (Mann-Whitney, M-W test) methods. The reovirus S1 (*t*-test, $P = 0.04$, M-W test, $P = 0.008$) and M2 (*t*-test, $P = 0.026$, M-W test, $P = 0.014$) gene segments were both significantly associated with strain-specific differences in virus-induced apoptosis. Using linear regression analysis we obtained R^2 values of 48.6% ($P = 0.017$) for the S1 gene segment and 42.5% ($P = 0.03$) for the M2 gene segment. These results indicate that both the S1 and M2 gene segments contribute to strain specific differences in the capacity of reovirus to activate JNK in infected cells. The nature of the reassortant pool tested, in which 8 of 9 viruses were concordant for the parental origin of their S1 and M2 segments, prevents us from more accurately defining the relative contribution of these two segments to JNK activation.

It is important to note that although statistical analysis identifies the S1 and M2 gene segments as important determining factors in the ability of reoviruses to induce JNK activation some viruses with differing genotypes (eg. KC150 and EB121) have closely related JNK activity levels. This suggests that non-genetic factors also contribute to reovirus-induced JNK activation.

Reovirus-induced c-Jun phosphorylation and reovirus-induced apoptosis are correlated. Reovirus prototypic strains T3D and T3A induce more apoptosis in infected cells than T1L (58, 59). Since our results indicate that Type 3 reoviruses also induce higher levels of phosphorylated c-Jun and JNK activity we compared the ability of the prototypic strains of reovirus to phosphorylate c-Jun, at 12 and 18 h PI (Fig. 2), with their ability to induce apoptosis (Fig. 3A and B). Apoptosis was measured at 48 h PI and the apoptosis experiments were set up in parallel to the c-Jun experiments in order to assure that the experimental conditions were as similar as possible. A significant association between the capacity of reoviruses to induce apoptosis and phosphorylate c-Jun was found (Pearson parametric correlation $R^2 = 0.964$, using c-Jun values obtained at 12 h PI, and $R^2 = 0.9330$, using c-Jun values obtained at 18 h PI). We also investigated whether there was a correlation between the capacity of T1L x T3D reassortants to phosphorylate c-Jun (Fig. 3C) or activate JNK (Fig. 3D) and to induce apoptosis. Significant associations between the capacity of reovirus reassortants to induce apoptosis and both activate JNK (Pearson parametric correlation $R^2 = 0.6077$, $P = 0.0028$) and phosphorylate c-Jun (Pearson parametric correlation $R^2 = 0.30$, $P = 0.0354$) were found. The larger pool of viruses used to generate the reassortant data enabled us to derive P values for these correlations.

Soluble TRAIL receptors block reovirus-induced apoptosis but not reovirus-induced c-Jun activation. TRAIL receptor ligation results in the activation of JNK (30). We have previously shown that reovirus-induced apoptosis requires TRAIL receptor ligation (10). We next investigated whether TRAIL receptor activation was required for

the activation of c-Jun in reovirus-infected cells. A combination of the soluble TRAIL receptors Fc:DR5 and Fc:DR4 were used to inhibit the binding of TRAIL to its functional cellular receptors. L929 cells were infected with T3D (MOI 50) in the presence, or absence, of Fc:DR5 and Fc:DR4 (final concentration 100 ng/ml each) and were harvested after 18 hours. Lysates were then analyzed by western blot analysis using an anti-phospho c-Jun antibody. In parallel, cells were infected with reovirus in the presence of a combination of Fc:DR5 and Fc:DR4 and were assayed for reovirus-induced apoptosis after 48 hours (Fig. 4). The presence of soluble TRAIL receptors did not inhibit c-Jun activation in T3D-infected cells (Fig. 4A and B). Infact, there seemed to be an increase in levels of phosphorylated c-Jun when cells were infected with reovirus in the presence of soluble TRAIL receptors compared to levels seen in untreated, infected cells. Conversely, the presence of soluble TRAIL receptors markedly reduced the ability of T3D to induce apoptosis (Fig. 4C) indicating that inhibition of TRAIL receptor ligation inhibits apoptosis but fails to reduce the activation of c-Jun in reovirus-infected cells. This suggests that pathways other than those initiated by TRAIL contribute to reovirus-induced JNK activation.

ERK, but not p38 MAPK, is activated following reovirus-infection. Having shown that JNK is activated in reovirus-infected cells we next wished to determine whether other MAPK pathways are also activated following reovirus-infection. The activities of p38 and ERK were thus investigated in reovirus-infected L929 cells (MOI 100) at 24 and 48 hours post-infection by *in vitro* kinase assays. T3D, but not T1L, infection resulted in the activation of ERK. ERK activation peaked at 24 hours post infection, with a 4-fold increase in levels of ERK activation compared to mock infected

cells (Fig. 5A). There was a slight decrease in p38 activity in following infection with both T1L and T3D strains of reovirus (Fig. 5B).

Since MAPKs can be activated rapidly in some systems we also looked at MAPK activation at very early times (under 2 hours) post reovirus infection. Using antibodies directed against the phosphorylated, active form of ERK we were able to show that ERK had an additional activation peak at around 20 mins PI (Fig. 5C). This activation peak was also strain specific with T3D and T3A inducing more activity than T1L. JNK and p38 were not activated within 2 hours of infection (results not shown). Taken together with our previously described data, these results indicate that reovirus preferentially and selectively activates the JNK and ERK MAPK pathways.

Although we were able to show strain specific differences in the activation of ERK in infected cells we have so far been unable to map this phenomenon to a specific reovirus gene segment (results not shown) suggesting that ERK and JNK activation involve different types of virus-host cell interactions. The activation of ERK is generally associated with anti-apoptotic effects. Conversely, the inhibition of ERK activity often correlates with the activation of JNK and p38 kinase and the resultant induction of apoptosis. We therefore wished to investigate whether reovirus-induced apoptosis would be enhanced by treatment with PD 98059, a chemical inhibitor of ERK activation. Cells were pre-treated with PD 98059 (10 μM) for 2 hrs prior to infection with reovirus and were maintained in media in the presence of inhibitor for 48 hrs following reovirus-infection. There was no change in reovirus-induced apoptosis in cells treated with PD 98059 (Fig. 6A) even though ERK activation following reovirus-infection was blocked (Fig. 6B). The activity of MAPK p38 is decreased in reovirus-infected cells and, as

expected, chemical inhibitors of p38 (PD 169316, SB 202190) did not affect reovirus-induced apoptosis (results not shown).

DISCUSSION

Our results indicate that reovirus infection selectively induces MAPK activation in infected cells. JNK is activated following reovirus infection in a strain specific manner, with the type 3 prototype reovirus strain (T3D) inducing more JNK activation than the type 1 prototype reovirus strain (T1L). Reovirus-induced JNK activation is associated with phosphorylation, and hence activation, of the JNK-dependent transcription factor c-Jun. The phosphorylation of c-Jun is also a strain-specific event, with the prototype 3 strains (T3D and T3A) inducing more JNK activation than T1L.

Strain-specific differences in JNK activation are determined by the S1 and M2 reovirus gene segments, which both encode reovirus capsid proteins. The reovirus S1 gene is bicistronic, encoding both the viral attachment protein σ1 and a non-virion-associated protein σ1s that is required for reovirus-induced G_2/M cell cycle arrest (48) but is not required for reovirus growth in cell culture or for the induction of apoptosis (51, 59). Reovirus-induced c-Jun activation is not blocked following infection by a σ1s-deficient virus strain (results not shown) indicating that σ1s is not required for c-Jun activation in reovirus-infected cells. The M2 segment encodes the main reovirus outer capsid protein μ1c, which plays a key role in membrane penetration and in the transmembrane transport of virions (24, 26, 41).

The S1 and M2 gene segments also determine the ability of reovirus to induce apoptosis (59) and there is a correlation between the ability of different prototype

reovirus strains, and T3D x T1L reassortant reoviruses, to induce apoptosis and to activate JNK and/or phosphorylate c-Jun. This suggests that JNK activation/c-Jun phosphorylation and apoptosis are either components of the same pathway that induces apoptosis following reovirus infection, or are components of distinct, parallel pathways induced by the same viral factors.

Reovirus-induced apoptosis is mediated by TRAIL-induced activation of death receptors and is associated with the release of TRAIL from infected cells (10). TRAIL receptor activation can also result in the activation of JNK (30), suggesting that this may be the mechanism by which reovirus induces JNK activation. However, reovirus-induced TRAIL release and TRAIL receptor activation do not occur until 24 - 48 hrs post-infection (10) suggesting that death receptor independent signaling pathways are responsible for the earlier (10 hrs PI) activation of JNK and c-Jun that occurs following reovirus-infection. The fact that reovirus-induced apoptosis can be inhibited by soluble TRAIL receptors, without affecting reovirus-induced c-Jun phosphorylation, indicates that pathways leading to apoptosis and JNK activity can be disassociated and also suggests that these pathways are distinct rather than identical. Both these observations are consistent with our previous studies showing that reovirus-induced JNK activity (62), but not apoptosis (results not shown) is inhibited in MEKK1 -/- embryonic stem cells. However, until we can find methods to completely block apoptosis or JNK activity we cannot rule out the possibility of a common pathway.

Reovirus-induced JNK activation is a specific event. For example, p38 MAPK is not activated following reovirus-infection. In addition, although ERK is activated in a serotype specific manner in infected cells, our inability to map this activation to a specific

reovirus gene segment indicates that ERK is activated by a different mechanism than JNK. The kinetics of ERK and JNK activation also differ, with ERK showing an early phase of activation that is not seen with JNK, again suggesting that ERK and JNK are activated by different mechanisms. The specificity of reovirus-induced JNK activation suggests that it is important for some aspect of the reovirus lifecycle. The role of virus-induced JNK activation is not yet known, however, reovirus growth is not inhibited in MEKK1 -/- cells (results not shown) despite a marked reduction in reovirus-induced JNK activation (62). This suggests that JNK activation is not essential for viral replication. Reovirus-induced JNK activation is associated with activation of the JNK-dependent transcription factor c-Jun. We have previously shown (12) that reovirus infection is also associated with activation of the transcription factor NF-κB, suggesting that virus-induced perturbation of gene expression plays a critical role in viral pathogenesis and cytopathicity. This is confirmed by our recent studies showing that reovirus infection is associated with alterations in the expression of a number of host cell genes involved in the regulation of cell cycle, apoptosis, and DNA repair (Dr R. DeBiasi, personal communication). In addition, one of the largest functional groups of genes whose expression is altered following reovirus infection are those associated with interferon activation, consistent with the known role of c-Jun in the optimal induction of $IFN_{\alpha 1}$ and IFN_{β} transcription (9) and onset of the anti-viral response (55).

ACKNOWLEDGEMENTS.

This work was supported by Public Health Service grant 1RO1AG14071 and GM30324 from the National Institute of Health, Merit and REAP grants from the Department of

Veterans Affairs and a U.S. Army Medical Research and Material Command grant (DAMD17-98-1-8614). The University of Colorado Cancer Center provided core tissue culture and media facilities.

References

1. **Ashkenazi, A. and V. M. Dixit.** 1998. Death receptors: signaling and modulation. Science **281:**1305-1308

2. **Barton, E. S., J. C. Forrest, J. L. Connolly, J. D. Chappell, Y. Liu, F. J. Schnell, A. Nusrat, C. A. Parkos and T. S. Dermody.** 2001. Junction Adhesion Molecule is a receptor for reovirus. Cell **104:**441-451.

3. **Berra, E., M. M. Municio, L. Sanz, S. Frutos, M. T. Diaz-Meco and J. Moscat.** 1997. Positioning atypical protein kinase C isoforms in the UV-induced apoptotic signaling cascade. Mol Cell Biol. **17:**4346-4354

4. **Boldin, M. P., T. M. Goncharov, Y. V. Goltsev, and D. Wallach**. 1996. Involvement of MACH, a novel MORT1/FADD-interacting protease, in Fas/APO-1- and TNF receptor-induced cell death. Cell **85:**803-815

5. **Boldin, M. P., E. E. Varfolomeev, Z. Pancer, I. L. Mett, J. H. Camonis, and D. Wallach.** 1995. A novel protein that interacts with the death domain of Fas/APO1 contains a sequence motif related to the death domain. J. Biol. Chem. **270:**7795-7798

6. **Brown, E. G., M. L. Nibert, and B. N. Fields.** 1983. The L2 gene of reovirus serotype 3 controls the capacity to interfere, accumulate deletions and establish persistent infection, p 275-287. In R. W. Compans and D. H. L. Bishop (ed.), Double-stranded RNA viruses. Elsevier, New York, N. Y.

7. **Canman, C. E. and M. B. Kastan.** 1996. Signal transduction. Three paths to stress relief. Nature **384:** 213-214

8. **Chinnaiyan, A. M., K. O'Rourke, M. Tewari, and V. M. Dixit.** 1995. FADD, a novel death domain containing protein, interacts with the death domain of Fas and initiates apoptosis. Cell **81:**505-512

9. **Chu, W-M., D. Ostertag, Z-W. Li, L. Chang, Y. Chen, Y. Hu, B. Williams, J. Perrault and M. Karin.** 1999. JNK2 and IKKβ are required for activating the inate response to viral infection. Immunity **11:**721-731

10. **Clarke, P., S. M. Meintzer, S. Gibson, C. Widmann, T. Garrington, G. L. Johnson, and K. L. Tyler.** 2000. Reovirus-induced apoptosis is mediated by TRAIL. J. Virol. **74:**8135-8139

11. **Cobb, M. H., T. G. Boulton, and D. J. Robbins.** 1991. Extracellular signal-related kinases: ERKs in progress. Cell Regul. **2:**965-978

12. **Connolly, J. L., S. E. Rodgers, P. Clarke, D. W. Ballard, L. D. Kerr, K. L. Tyler, and T. S. Dermody.** 2000. Reovirus-induced apoptosis requires activation of transcription factor NF-κB. J. Virol. **74:**2981-2989

13. **Coombs, K. M., B. N. Fields, and S. C. Harrison.** 1990. Crystallization of the reovirus type 3 Dearing core. Crystal packing is determined by the lambda 2 protein. J. Mol. Biol. **215:**1-5

14. **DeBiasi, R. L., C. L. Edelstein, B. Sherry, and K. L. Tyler.** 2001. Calpain inhibition protects against virus-induced apoptotic myocardial injury. J. Virol. **75:** 351-361

15. **DeBiasi, R. L., M. K. T. Squier, B. Pike, M. Wynes, T. S. Dermody, J. J. Cohen, and K. L. Tyler.** 1999. Reovirus-induced apoptosis is preceded by increased cellular calpain activity and is blocked by calpain inhibitors. J Virol. **73:**695-701

16. **Derijard, B., M. Hibi, I. H. Wu, T. Barrett, B. Su, T. Deng, M. Karin, and R. J. Davis.** 1994. JNK1: a protein kinase stimulated by UV light and Ha-Ras that binds and phosphorylates the c-Jun activation domain. Cell **76:**1025-1037

17. **Duan, H. and V. M. Dixit.** 1997. RAIDD is a new death adaptor molecule. Nature **385:**86-89

18. **Duke, R. C. and J. J. Cohen.** 1992. Morphological and biochemical assays of apoptosis, In: Coligan, J.E., *Current protocols in immunology*, Wiley, NY, 3.17.1-3.17.16.

19. **Eliopoulos, A. G. and L. S. Young.** 1988. Activation of c-Jun N-terminal kinase (JNK) by the Epstein-Barr virus-encoded latent membrane protein 1 (LMP-1). Oncogene **16:**1731-1742.

20. **Gardner, A. M., and G. L. Johnson.** 1996. Fibroblast growth factor 2 suppression of tumor nerosis factor alpha-mediated apoptosis requires Ras and the activation of mitogen-activated protein kinase. J. Biol. Chem. **271:**14560-14566

21. **Gerwins, P., J. L. Blank, and G. L. Johnson.** 1997. Cloning of a novel mitogen-activated protein kinase kinase kinase, MEKK4, that selectively regulates the c-Jun amino terminal kinase pathway. J. Biol. Chem. **272:**8288-8295.

22. **Graves, J. D., J. S. Campbell, and E. G. Krebs.** 1995. Protein serine/threonine kinases of the MAPK cascade. Ann. N.Y. Acad. Sci. **766:**320-343

23. **Han, J., J. D. Lee, L. Bibbs, and R. J. Ulevitch.** 1994. A MAP kinase targeted by endotoxin and hyperosmolarity in mammalian cells. Science **265:**808-811

24. **Hazelton, P. R. and Coombs, K. M.** 1995. The reovirus mutant tsA279 has temperature sensitive lesions in the M2 and L2 genes: the M2 gene is associated with decreased viral protein production and blockade in transmembrane transport. Virology **207:**46-58.

25. **Hibi, M., A. Lin, T. Smeal, A. Minden, and M. Karin.** 1993. Identification of an oncoprotein- and UV-responsive protein kinase that binds and potentiates the c-Jun activation domain. Genes Develop. **7:**2135-2148.

26. **Hooper, J. W. and Fields, B. N.** 1996. Role of the μ1 protein in reovirus stability and capacity to cause chromium release from host cells. J. Virol. **70:** 459-467

27. **Hsu, H., J. N. Huang, H. B. Shu, V. Baichwal, and D. V. Goeddel.** 1996b. TNF-dependent recruitment of the protein kinase RIP to the TNF receptor-1 signaling complex. Immunity, **4:**387-396

28. **Hsu, H., H. B. Shu, M. G. Pan, and D. V. Goeddel.** 1996a. TRADD-TRAF2 and TRADD-FADD interactions define two distinct TNF receptor 1 signal transduction pathways. Cell **84:**299-308

29. **Hsu, H., J. Xiong, and D. V. Goeddel.** 1995. The TNF receptor 1 –associated protein TRADD signals cell death and NF-kappa B activation. Cell **81:**495-504

30. **Hu, W. H., H. Johnson, and H. B. Shu.** 1999. Tumor necrosis factor-related apoptosis-inducing ligand receptors signals NF-kappaB and JNK activation and apoptosis through distinct pathways. J. Biol. Chem. **274:**30603-30610.

31. **Huttunen, P., T. Hyypia, P. Vihinen, L. Nissinen and J. Heino.** 1998. Echovirus 1 infection induces both the stress- and growth-activated mitogen-activated protein kinase pathways and regulates the transcription of cellular immediate-early genes. Virology **250:**85-93.

32. **Iordanov, M. S., J. M. Paranjape, A. Zhou, J. Wong, B. R. G. Williams, E. F. Meurs, R. H. Silverman and B. E. Magun.** 2000. Activation of p38 mitogen-activated protein kinase and c-Jun NH_2-terminal kinase by double stranded RNA and encephalomyocarditis virus: involvement of RNaseL, Protein kinase R and alternative pathways. Mol. Cell Biol. **20:**617-627

33. **Iwai, K., N. Mori, M. Oie, N. Yamamoto and M. Fujii.** 2001. Human T-cell leukemia virus type 1 Tax protein activates transcription through AP-1 site by inducing DNA binding activity in T cells. Virology **279:**38-46

34. **Jacque, J. M., A. Mann, H. Enslen, N. Sharuva, B. Brichacek, R. J. Davis, and M. Stevenson.** 1998. Modulation of HIV-1 infectivity by MAPK, a virion associated kinase. EMBO J. **17**:2607-2618

35. **Jeremias, I. and K. M. Debatin.** 1998. TRAIL induces apoptosis and activation of NFkappaB. Eur. Cytokine Netw. **9**:687-688

36. **Jung, J. U., and R. C. Desrosiers.** 1995. Association of viral oncoprotein, STP-C488, with cellular ras. Mol. Cell Biol. **15**:6506-6512

37. **Juo, P., C. J. Kuo, S. E. Reynold, R. F. Konz, J. Raingeaud, R. J. Davis, H. – P. Biemann, and J. Blenis.** 1997. Fas activation of the p38 mitogen activated protein kinase signaling pathway requires ICE/CED-3 family proteases. Mol. Cell Biol. **17**:24-35

38. **King, C. S., J. V. Cooper, B. Moss, and D. R. Twardzik.** 1986. Vaccinia virus growth factor stimulates tyrosine protein kinase activity of A431 cell epidermal growth factor receptors. Mol. Cell Biol. **6**:332-336.

39. **Kyriakis, J. M., P. Banerjee, E. Nikolakaki, T. Dai, E. A. Rubie, E. A., M. F. Ahmad, J. Avruch, J. and J. R. Woodgett.** 1994. The stress-activated protein kinase subfamily of c-Jun kinases. Nature London **369**:156-160

40. **Lee, J. C., J. T. Laydon, P. C. McDonnell, T. F. Gallagher, S. Kumar, D. Green, D., McNulty, M. J. Blumenthal, J. R. Heys, S. W. Landvatter, J. E. Strickler, M. M. McLaughlin, I. R. Siemens, S. M. Fisher, G. P. Livi, J. R. White, J. L. Adams, and P. R. Young.** A protein kinase involved in the

regulation of inflammatory cytokine biosynthesis. 1994 Nature London **372:**739-746

41. **Lucia-Jandris, P., Hooper, J. W. and Fields, B. W.** 1993. Reovirus M2 gene is associated with chromatin release from mouse L cells. J. Virol. **67:** 5339-5345.

42. **Ludwig, S., C. Ehrhardt, E. R. Neumeier, M. Kracht, U. R. Rapp and S. Pleschka.** 2001. Influenza virus-induced AP-1 dependent gene expression requires activation of the Jun-N-terminal kinase (JNK) signaling pathway. J. Biol. Chem. **276:**10990-10998.

43. **Martin, P., W. C. Vass, J. T. Schiller, D. R. Lowry, and T. J. Velu.** 1989. The bovine papilloma virus E5 transforming protein can stimulate the transforming activity of EGF and CSF-1 receptors. Cell **59:**21-32

44. **McLean, T. I. and S. L. Bachenheimer.** 1999. Activatiuon of cJun N-terminal kinase by herpes simplex virus type 1 enhances viral replication. J. Virol. **73:**8415-8426.

45. **Muzio, M., A. M. Chinnaiyan, F. C. Kischkel, K. O'Rourke, A. Shevchenko, J. Ni, C. Scaffidi, J. D. Bretz, M. Zhang, R. Gentz, M. Mann, P. H. Krammer, M. E. Peter, and V. M. Dixit.** 1996. FLICE, a novel FADD-homologous ICE/CED-3-like protease, is recruited to the CD95 (Fas/APO-1) death-inducing signaling complex. Cell **85:**817-827

46. **Oberhaus, S. M., T. S. Dermody, and K. L. Tyler.** 1998. Apoptosis and the cytopathic effects of reovirus, in: Tyler, K.L., Oldstone, M.B.A. Reoviruses II:

Cytopathicity and pathogenesis [Current Topics in Microbiology and Immunology, vol. 233], Springer-Verlag, Berlin, 1998).

47. **Oberhaus, S. M., R. L. Smith, G. H. Clayton, T. S. Dermody, and K. L. Tyler.** 1997. Reovirus infection and tissue injury in mouse central nervous system are associated with apoptosis. J. Virol. **71:**2100-2106

48. **Poggioli, G. J., C. Keefer, J. L. Connolly, T. S. Dermody and K. L. Tyler.** 2000. Reovirus-induced G2/M cell cycle arrest requires σ1s and occurs in the absence of apoptosis. J. Virol. **74:**9562-9570

49. **Popik, W. and P. M. Pitha.** 1998. Early activation of mitogen-activated protein kinase kinase, extracellular signal-regulated kinase, p38 mitogen-activated protein kinase, and c-Jun N-terminal kinase in response to binding of simian immunodeficiency virus to Jurkat TT cells expressing CCR5 receptor. Virology **252:**210-217.

50. **Rodgers, S. E., E. S. Barton, S. M. Oberhaus, B. Pike, C. A. Gibson, K. L. Tyler, and T. S. Dermody.** 1997. Reovirus-induced apoptosis of MDCK cells is not linked to viral yield and is blocked by Bcl-2. J. Virol. **71:**2540-2546

51. **Rodgers, S. E., J. L. Connolly, J. D. Chappell and T. S. Dermody.** 1998. Reovirus growth in cell culture does not require a full complement of viral proteins: identification of a σ1s-null mutant. J. Virol. **72:**8597-8604

52. **Rothe, M., V. Sarma, V. M. Dixit, and D. V. Goeddel**. 1995. TRAF2-mediated activation of NF-kappa B by TNF receptor 2 and CD40. Science **269:**1424-1427

53. **Rouse, J., P. Cohen, S. Trigon, M. Morange, A. Alonso Llamazares, D. Zamanillo, T. Hunt, and A. R. Nebreda.** 1994. A novel kinase cascade triggered by stress and heat shock that stimulates MAPKAP kinase-2 and phosphorylation of the small heat shock proteins. Cell **78:**1027-1037

54. **See, B. H. and Y. Shi.** 1998. Adenovirus E1B 19,000-molecular weight protein activates c-Jun N-terminal kinase and c-Jun-mediated transcription. Mol. Cell Biol. **18:**4012-4022.

55. **Sen, G. C. and P. Lengyel.** 1992. The interferon system. A birds eye view of its biochemistry. J. Biol. Chem. **267:**5017-5020.

56. **Song, H. Y., C. H. Regnier, C. J. Kirschning, D. V. Goeddel, and M. Rothe.** 1997. Tumor necrosis factor (TNF)-mediated kinase cascades: bifurcation of nuclear factor-kappa B and c-jun N-terminal kinase (JNK/SAPK) pathways at TNF receptor-associated factor. PNAS USA **94:**9792-9796

57. **Sontag, E., S. Fedorov, C. Kamibayashi, D. Robbins, M. Cobb, and M. Mumby.** 1993. The interaction of SV40 small tumor antigen with protein phosphatase 2A stimulates the MAP kinase pathway and induces cell proliferation. Cell **75:**887-897.

58. **Tyler, K. L., M. K. T. Squier, S. E. Rodgers, B. E. Schneider, S. M. Oberhaus, T. A. Grdina, J. J. Cohen, and T. S. Dermody.** 1995. Differences in the capacity of reovirus strains to induce apoptosis are determined by the viral attachment protein sigma 1. J.Virol. **69:**6972-6979.

59. **Tyler K. L., M. K. T. Squier, A. L. Brown, B. Pike, D. Willis, S. M. Oberhaus, T. S. Dermody, and J. J. Cohen.** 1996. Linkage between reovirus-induced apoptosis and inhibition of cellular DNA synthesis: role of the S1 and M2 genes. J. Virol. **70:**7984-7991

60. **Wilson, D. J., K. A. Fortner, D. H. Lynch, R. R. Mattingly, I. G. Macara, J. A. Posada, and R. C. Budd.** 1996. JNK, but not MAPK, activation is associated with Fas-mediated apoptosis in human T cells. Eur. J. Immunol. **26:**989-99

61. **Xia, Z., M. Dickens, J. Raingeaud, R. J., Davis, and M. E. Greenberg.** 1995. Opposing effects of ERK and JNK-p38 MAP kinases on apoptosis. Science **270:**1326-1331

62. **Yujuri, T., M. Ware, C. Widmann, R. Oyer, D. Russell, E. Chan, Y. Zaitsu, P. Clarke, K. L. Tyler, Y. Oka, G. R. Fanger, P. Henson, and G. L. Johnson.** 2000. Cell migration and c-jun NH2-terminal kinase but not NF-κB are regulated by MEK Kinase 1. PNAS **97:**7272-7277

63. **Zachos, G., B. Clements, and J. Conner.** 1999. Herpes simplex virus type 1 infection stimulates p38/c-Jun N-terminal mitogen-activated protein kinase pathways and activates transcription factor AP-1. J. Biol. Chem. **274:**5097-5103

Figure Legends

Fig. 1. Reovirus activates JNK infected cells. L929 cells were infected with 2 different serotypes reovirus, T1L and T3D (MOI 100) or were mock-infected. At various times PI lysates were prepared and JNK activity was determined by *in vitro* kinase assays. The graph shows the mean JNK activity, as measured by c-Jun phosphorylation (arbitary imager units), of three independent experiments. Error bars represent standard errors of the mean.

Fig. 2. c-Jun is activated following infection with reovirus. Cells were infected with different strains of reovirus (MOI 100) and were harvested at various times PI. Extracts were standardized for protein concentration, using an anti-actin antibody, and equal amounts of protein were separated by SDS-PAGE and probed with antibodies directed against phosphorylated (A) or total c-Jun (C). Bands corresponding to phosphorylated and unphosphorylated c-Jun are shown. The gels are representative of at least 2 independent experiments (B) Graphical representation of the western blot shown in A showing the fold increase in levels of phophorylayed c-Jun over time.

Fig. 3. There is a correlation between the capacities of different prototype strains of reovirus to phosphorylate c-Jun and induce apoptosis and between the capacities of T1L x T3D reassortant viruses to induce JNK activation or c-Jun phosphorylation and apoptosis. The ability of different strains of reovirus (T3A, T3D and T1L) and mock (M)-infection to induce increased levels of phosphorylated c-Jun, at 12 (A) and 18 (B) h PI (values taken from Fig. 2) and apoptosis are shown. Experiments to determine c-Jun

phosphorylation and apoptosis were set up in parallel. (C) The capacity of reovirus reassortants (MOI 100) to induce phosphorylated c-Jun and apoptosis were plotted. Each point represents a single reassortant virus. Lysates were harvested at 18 h PI, standardized for protein concentration and analyzed by western blot analysis using an antibody directed against phospho c-Jun. Apoptosis values were obtained in a parallel experiment and represent the mean value from 3 separate wells (24-well tissue culture plate) of the same experiment. (D) The capacity of reovirus reassortants (MOI 100) to induce JNK activity and apoptosis were plotted. Each point represents a single reassortant virus. JNK activity values were taken from Table 1. Apoptosis values were obtained in a parallel experiment and represent the mean value from 3 separate wells (24-well tissue culture plate) of the same experiment.

Fig. 4. Apoptosis but not c-Jun phosphorylation is inhibited in T3D-infected cells in the presence of the soluble TRAIL receptors, Fc:DR5 and Fc:DR4. In parallel experiments cells were infected with T3D (MOI 50) and were assayed for c-Jun activation at various times PI and for apoptosis after 48 hours. (A) Autoradiograph showing levels of phosphorylated c-Jun following infection with reovirus (T3D), in the presence or absence of Fc:DR5 and Fc:DR4 (final concentration 100 ng/ml each). Equal amounts of protein, as determined by actin concentration (not shown), were loaded. (B) Graphical analysis of results shown in A showing the fold increase in c-Jun phosphorylation, compared to mock-infected, untreated cells, at 12 (gray bars), 20 (black bars) and 30 (stippled bars) h PI. (C) Graph showing the percentage of cells with apoptotic nuclear morphology in reovirus (T3D) or mock infected cells in the presence or absence of soluble TRAIL

receptors (final concentration 100 ng/ml each). Error bars represent standard errors of the mean from 3 separate wells (24-well tissue culture plate) of the same experiment.

Fig. 5. Reovirus activates ERK but not p38 in infected cells. The activities of ERK (A) and p38 (B) were investigated in reovirus-infected L929 cells (MOI 100) at 24 (black bars) and 48 hours (stippled bars) PI by *in vitro* kinase assays. The graphs show fold activation compared to mock-infected cells. Error bars represent standard errors of the mean for 3 independent experiments. (C) ERK is activated at early times post reovirus infection. L929 cells were infected with reovirus (MOI 100) and harvested at various times PI. Proteins were separated by SDS-PAGE followed by western blot analysis using antibodies directed against phospho-ERK. Actin was used to standardize for protein loading (not shown).

Fig. 6. Inhibition of ERK activation does not affect reovirus-induced apoptosis. (A) Reovirus-induced apoptosis (MOI 100) was measured in the presence of a chemical inhibitor of ERK activation (PD 98059). L929 cells were pre-treated with inhibitor (10 μM) for 2 hrs prior to infection with reovirus and were maintained in media in the presence of inhibitor for 48 hrs following reovirus-infection. Cells were then harvested and assayed for apoptosis. The graph shows % apoptosis. Error bars represent standard errors of the mean. (B) Activation/phosphorylation of ERK following reovirus-infection (MOI 100, T3D) in the presence of PD 98059 (10 μM) as determined by western blot analysis using antibodies directed against phospho-ERK.

Table 1: Reovirus-induced JNK activation is determined by the S1 and M2 gene segments.

Virus strain	JNK Activity Imager Units	Reovirus gene segment									
		L1	L2	L3	M1	M2	M3	S1	S2	S3	S4
EB97	189000	T3D	T3D	T1L	T3D	T3D	T3D	T3D	T3D	T3D	T1L
T3D	108000	T3D	T3D	T3D	T3D	T3D	T3D	T3D	T3D	T3D	T3D
EB13	108000	T3D	T3D	T3D	T3D	T3D	T3D	T3D	T3D	T3D	T1L
H15	102000	T1L	T3D	T3D	T1L	T3D	T3D	T3D	T3D	T3D	T1L
KC150	84000	T3D	T1L	T1L	T1L	T3D	T1L	T3D	T3D	T1L	T3D
EB121	81000	T3D	T3D	T1L	T3D	T1L	T3D	T1L	T3D	T3D	T3D
EB1	78000	T1L	T3D	T1L	T1L	T3D	T1L	T1L	T1L	T3D	T1L
EB85	75000	T1L	T1L	T1L	T1L	T1L	T3D	T1L	T3D	T1L	T1L
EB31	63000	T1L	T1L	T1L	T3D	T1L	T1L	T1L	T3D	T3D	T1L
T1L	54000	T1L	T1L	T1L	T1L	T1L	T1L	T1L	T1L	T1L	T1L
H41	24000	T3D	T3D	T1L	T1L	T1L	T3D	T1L	T3D	T3D	T1L
Mock	20000										
t-test		0.33	0.18	0.19	0.15	**0.026**	0.20	**0.04**	0.24	0.19	0.83
M-W		0.17	0.16	0.08	0.12	**0.014**	0.22	**0.008**	0.29	0.24	0.41

Left Blank

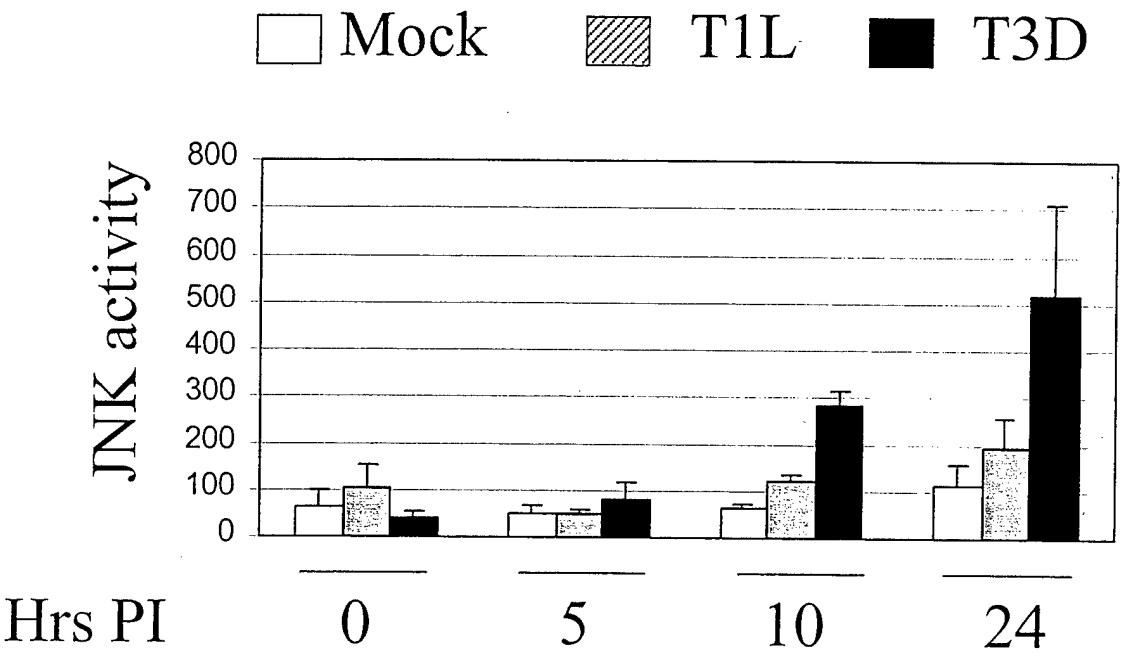
Mock
T1L
T3D
JNK activity
800
700
600
500
400
300
200
100
0
Hrs PI
0
5
10
24

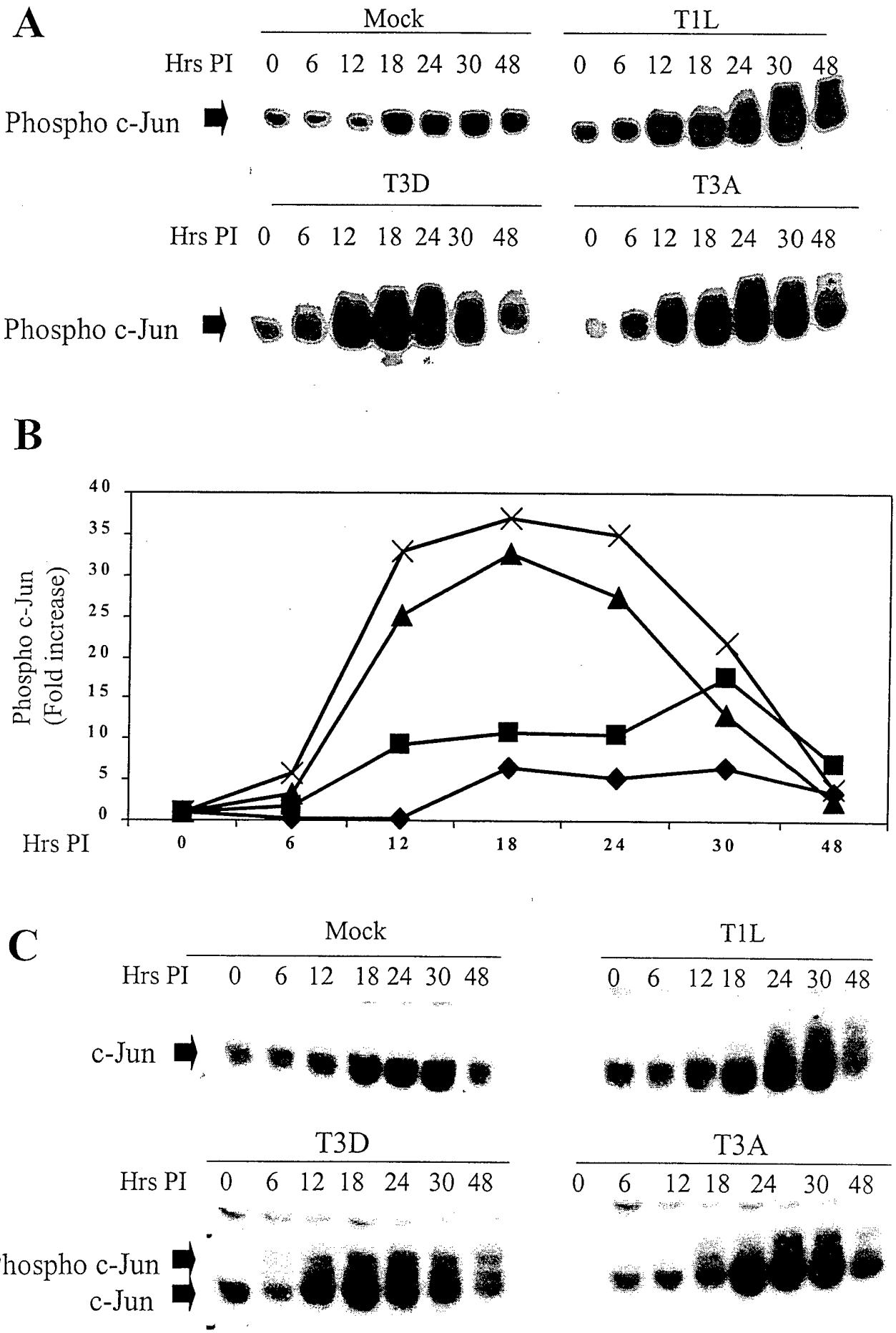
A
Mock
T1L
Hrs PI 0 6 12 18 24 30 48
0 6 12 18 24 30 48
Phospho c-Jun
T3D
T3A
Hrs PI 0 6 12 18 24 30 48
0 6 12 18 24 30 48
Phospho c-Jun
B
Phospho c-Jun (Fold increase)
40
35
30
25
20
15
10
5
0
Hrs PI
0
6
12
18
24
30
48
C
Mock
T1L
Hrs PI 0 6 12 18 24 30 48
0 6 12 18 24 30 48
c-Jun
T3D
T3A
Hrs PI 0 6 12 18 24 30 48
0 6 12 18 24 30 48
Phospho c-Jun
c-Jun

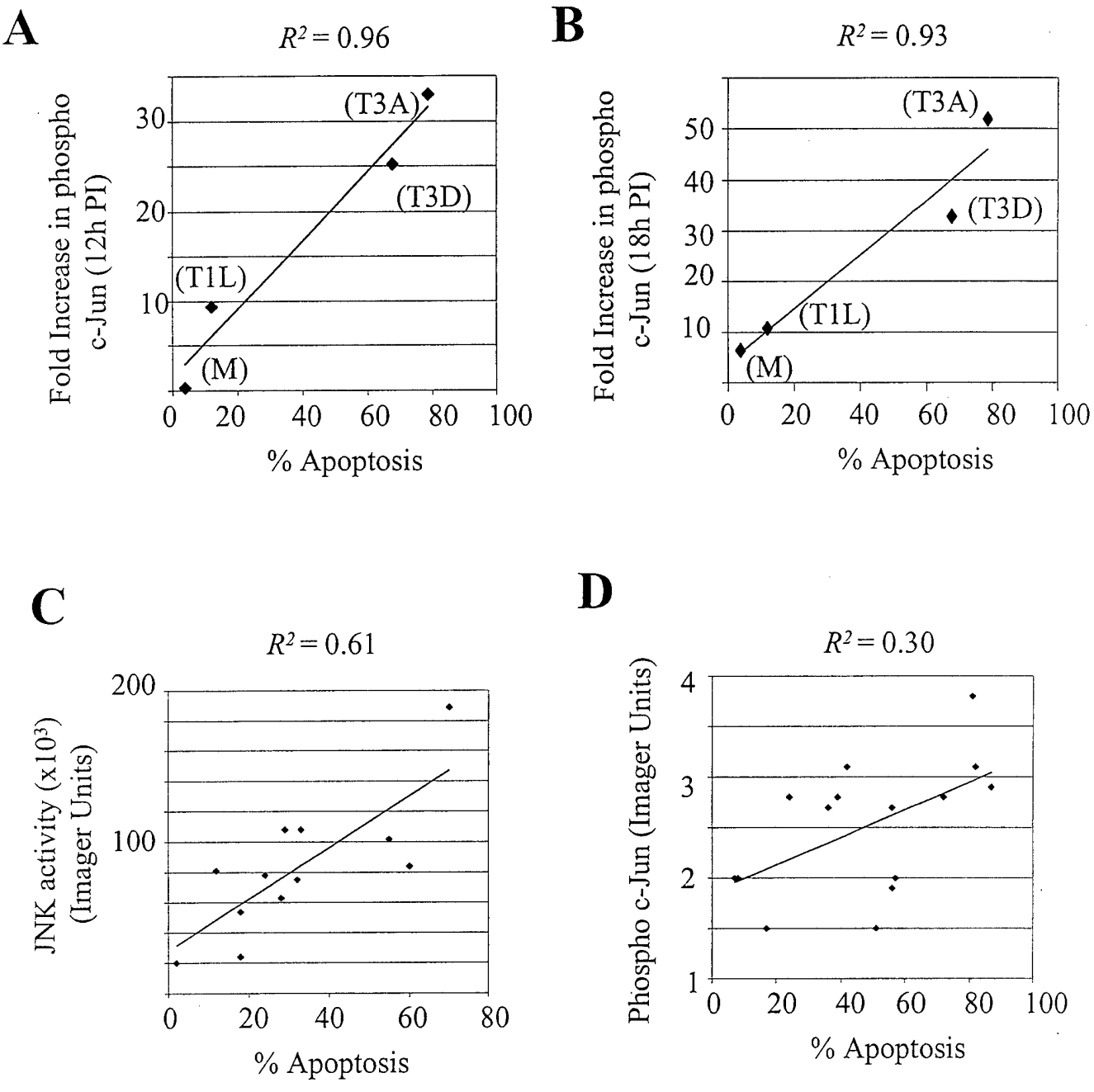
A
$R^2 = 0.96$
Fold Increase in phospho c-Jun (12h PI)
30
20
10
(T3A)
(T3D)
(T1L)
(M)
0
20
40
60
80
100
% Apoptosis
B
$R^2 = 0.93$
Fold Increase in phospho c-Jun (18h PI)
50
40
30
20
10
(T3A)
(T3D)
(T1L)
(M)
0
20
40
60
80
100
% Apoptosis
C
$R^2 = 0.61$
JNK activity (x10³) (Imager Units)
200
100
0
20
40
60
80
% Apoptosis
D
$R^2 = 0.30$
Phospho c-Jun (Imager Units)
4
3
2
1
0
20
40
60
80
100
% Apoptosis

A

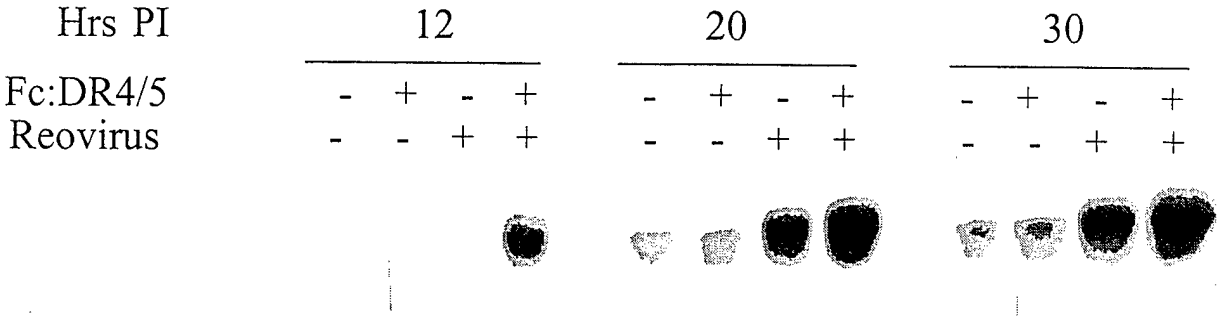
Hrs PI
12
20
30
Fc:DR4/5
- + - + - + - + - + - +
Reovirus
- - + + - - + + - - + +

B

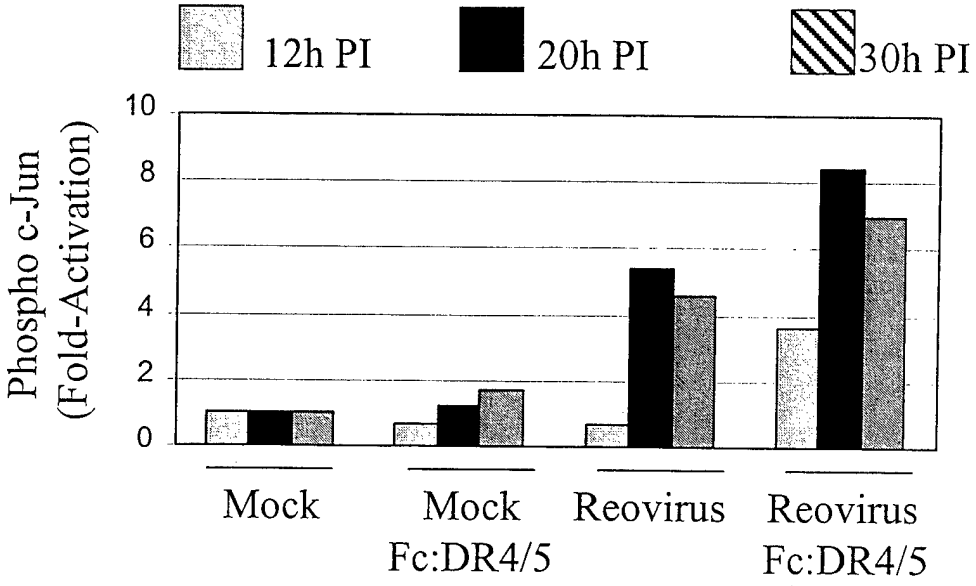
12h PI
20h PI
30h PI
Phospho c-Jun
(Fold-Activation)
10
8
6
4
2
0
Mock
Mock
Fc:DR4/5
Reovirus
Reovirus
Fc:DR4/5

C

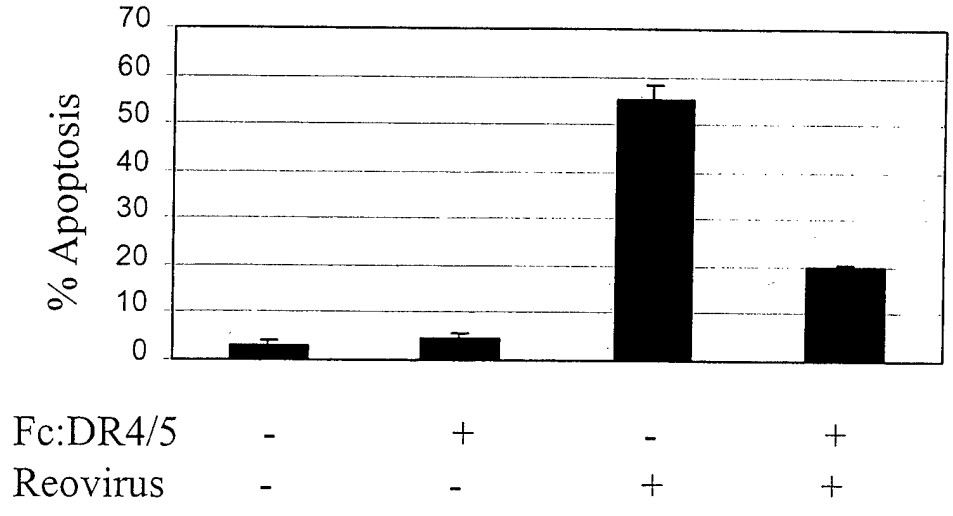
% Apoptosis
70
60
50
40
30
20
10
0
Fc:DR4/5 - + - +
Reovirus - - + +

A

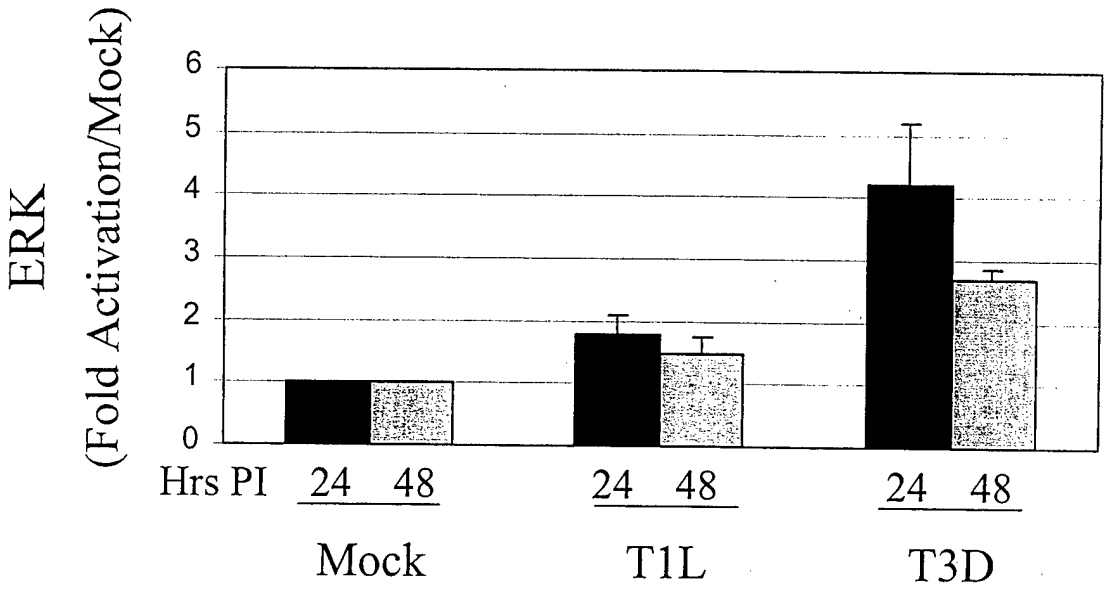
ERK
(Fold Activation/Mock)
6
5
4
3
2
1
0
Hrs PI 24 48 24 48 24 48
Mock
T1L
T3D

B

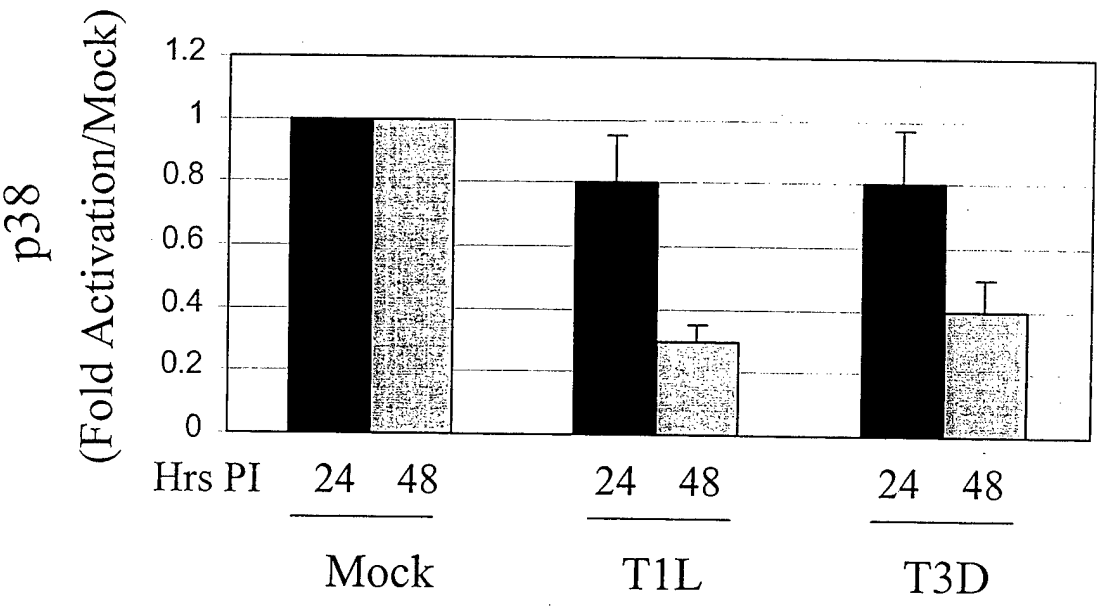
p38
(Fold Activation/Mock)
1.2
1
0.8
0.6
0.4
0.2
0
Hrs PI 24 48 24 48 24 48
Mock
T1L
T3D

C

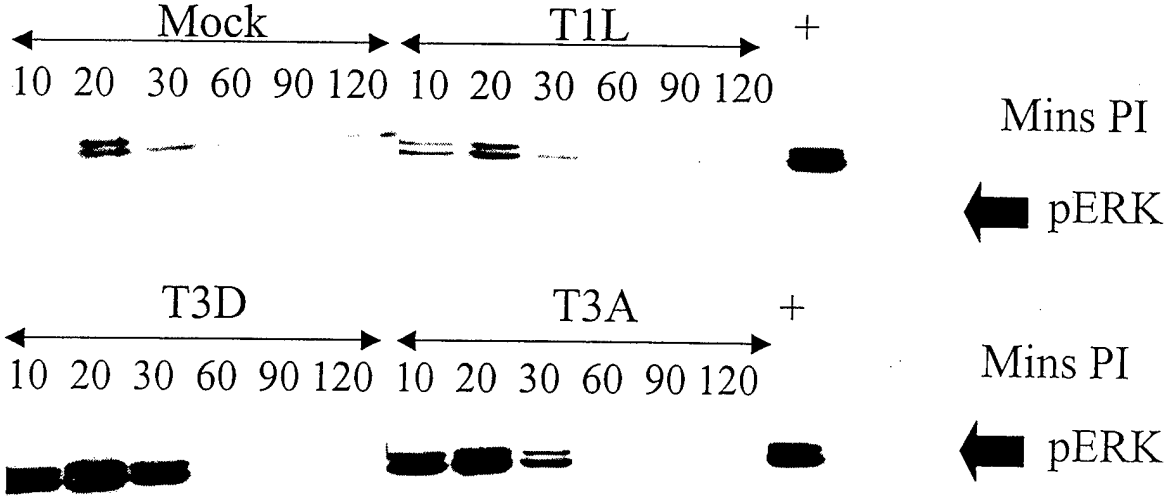
Mock
T1L
+
10 20 30 60 90 120 10 20 30 60 90 120
Mins PI
pERK
T3D
T3A
+
10 20 30 60 90 120 10 20 30 60 90 120
Mins PI
pERK

A

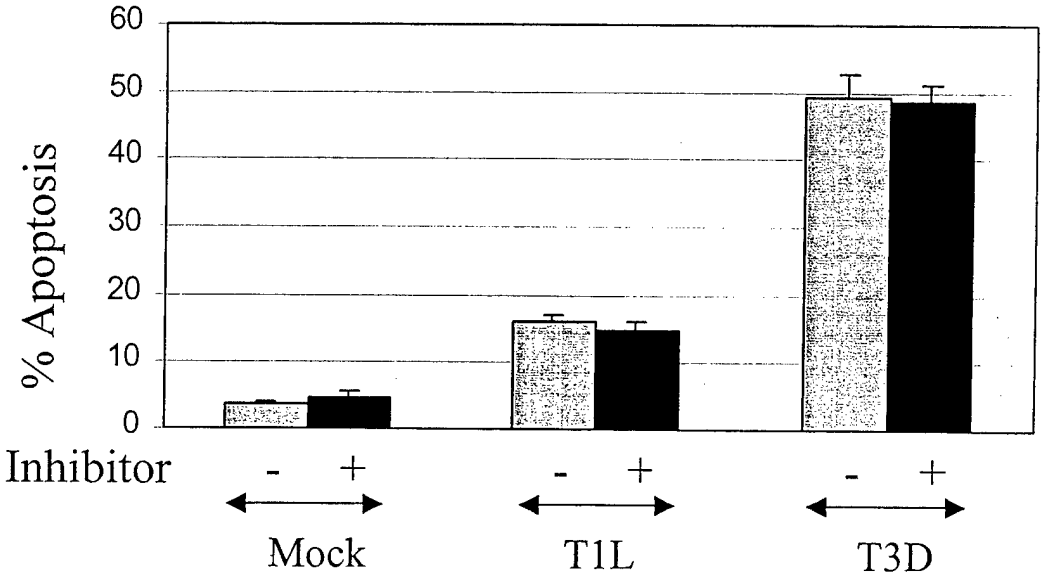
60
50
40
30
20
10
0
% Apoptosis
Inhibitor
- +
- +
- +
Mock
T1L
T3D

B

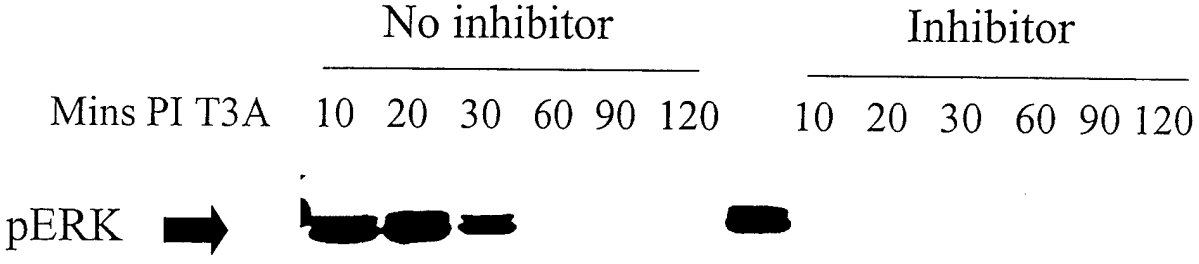
No inhibitor
Inhibitor
Mins PI T3A
10 20 30 60 90 120
10 20 30 60 90 120
pERK

Reovirus Infection Induces both Death Receptor- and Mitochondrial-Mediated Caspase-Dependent Pathways of Cell Death

Running title: Reovirus-Induced Caspase Activation

DOUGLAS J. KOMINSKY[1], RYAN J. BICKEL[1], AND KENNETH L. TYLER[1,2,3*]

Departments of Neurology[1], Medicine, Microbiology, and Immunology[2], University of Colorado Health Science Center, and Denver Veteran's Affairs Medical Center[3], Denver, Colorado 80262

*Corresponding author. Mailing address: Department of Neurology (127), Denver VA Medical Center, 1066 Clermont St., Denver, CO 80220. Phone: (303) 393-2874. Fax: (303) 393-4686. E-mail: Ken.Tyler@uchsc.edu.

Abstract

Apoptosis induction or its inhibition plays an important role in the pathogenesis of many viral infections. Apoptotic cell death can be triggered by death receptor activation, mitochondrial insult, or stress within the endoplasmic reticulum or Golgi. Virtually all apoptotic pathways involve the sequential activation of a family of cysteine proteases known as caspases. Delivery of an apoptotic stimulus to the cell triggers the activation of initiator caspases, leading to the activation of effector caspases. We have shown that reovirus-induced apoptosis involves the DR4/DR5/TRAIL cell death receptor system. We now provide the first detailed characterization of the pattern of caspase activation following reovirus infection. Reovirus infection of HEK293 cells results in the activation of the death receptor-associated initiator caspase, caspase-8. Infection induces the release of cytochrome *c* from mitochondria, leading to the activation of caspase-9. Reovirus infection is associated with caspase-8-dependent cleavage of Bid, a pro-apoptotic member of the Bcl-2 protein family. Inhibition of caspase-8 activation prevents mitochondrial release of cytochrome *c* and activation of caspase-9. Activation of initiator caspases induces the activation of effector caspases including caspase-3 and caspase-7. This activation is initiated by death receptor ligation but depends on mitochondrial amplification and can be inhibited by overexpression of Bcl-2.

Introduction

Apoptosis is a particular type of cell death that is characterized by distinctive changes in cellular morphology including cell shrinkage, zeiosis, nuclear condensation, chromatin margination and subsequent degradation that are associated with inter-nucleosomal DNA

fragmentation. Apoptosis may be initiated by a wide variety of cellular insults including death receptor stimulation, γ-radiation, and cytotoxic compounds. Induction or inhibition of apoptosis is an important feature of many types of viral infection both *in vitro* and *in vivo*.

Mammalian reoviruses induce apoptosis in a wide variety of cultured cells *in vitro* (23, 27, 38). Apoptotic cell death also plays a key role in reovirus pathogenesis. There is an excellent correlation between reovirus-induced tissue injury in the heart and the CNS and the distribution of viral antigen and the presence of apoptotic cell death (24). (23) Inhibition of apoptosis reduces the extent of reovirus-induced tissue injury *in vivo* (9).

Reovirus induced apoptosis involves the tumor necrosis factor (TNF) superfamily of cell surface death receptors, specifically DR4, DR5 and their ligand, TNF-related apoptosis-inducing ligand (TRAIL) (6), and can be inhibited by anti-TRAIL antibodies or soluble forms of DR4 or DR5 which inhibit interaction of TRAIL with DR4 and DR5 (6). Additionally, it has been shown recently that reovirus-induced apoptosis requires both sialic acid binding and interaction with junction adhesion molecule (JAM) (3). Reovirus-induced apoptosis can also be inhibited by expression of Bcl-2, suggesting that mitochondrial pathways of apoptosis also play a key role (27). However, the exact nature of the caspase cascades activated and their inter-relationship has not been previously determined.

Apoptosis induced by activation of cell surface death receptors ("extrinsic pathway") involves the formation of a death-induced signaling complex (DISC) that recruits and activates caspase-8 (reviewed in (2). Activated caspase-8 can, in turn, activate downstream effector caspases including caspases-3 and -7. Mitochondria play a central

role in an "intrinsic" pathway of apoptosis. In this pathway, apoptotic stimuli enhance mitochondrial membrane permeability and permit the translocation of cytochrome *c* and other pro-apoptotic molecules from the mitochondria into the cytosol (10, 17, 19, 32, 39). A cytosolic complex including cytochrome *c* and Apaf-1 (apoptosome) activates caspase-9 (42). Activated caspase-9, like activated caspase-8, can activate additional downstream effector caspases including caspase-3. The intrinsic and extrinsic pathways are linked by Bid, a pro-apoptotic Bcl-2 family member. Caspase-8-dependent cleavage of Bid allows this protein to translocate to the mitochondrion, where it directly or indirectly facilitates cytochrome *c* release (14, 18, 20, 40, 41). The importance of the mitochondrial apoptotic pathway in augmenting death-receptor initiated apoptosis can be assessed by studying the pattern of caspase activation and the effects of Bcl-2 expression. Death receptor-initiated, mitochondrial-dependent apoptosis is generally associated with early low level activation of caspase-8 and is inhibitable by Bcl-2 (28, 29). Conversely, mitochondrial-independent, death receptor-initiated apoptosis is associated with more robust caspase-8 activation and is not inhibited by Bcl-2 expression (28, 29).

In this paper we provide the first comprehensive characterization of the pattern of caspase activation following reovirus infection. We show that infection results in the activation of both death receptor- and mitochondrial-associated initiator caspases including caspase-8 and caspase-9. Activation of these initiator caspases is followed by activation of effector caspases including caspase-3 and caspase-7. Caspase-8-dependent cleavage of the Bid provides a linkage between the death receptor and mitochondrial pathways of apoptosis following reovirus infection. Inhibition of caspase-8 activation prevents the cleavage of Bid, and the subsequent activation of mitochondrial pathway.

The mitochondrial pathway is essential for effective apoptosis induction following reovirus infection, as inhibition of this pathway by over-expression of Bcl-2 prevents reovirus-induced effector caspase activation. Consistent with this model, cell permeable inhibitors of both group II caspases (caspase-2, -3, -7) and group III caspases (caspase-6, -8, -9) but not of group I caspases (caspase-1, -4, -5) inhibit reovirus-induced caspase-3 activation.

Materials and Methods

Reagents

Anti-cytochrome *c* (7H8.2C12) (1:1000), anti-PARP (C2-10) (1:2000), anti-caspase-6 (B93-4) (1:1000), anti-caspase-8 (B9-2) (1:2000), and anti-caspase-9 (1:1000) antibodies were purchased from Pharmingen (San Diego, California). Anti-caspase-3 (1:1000) and anti-caspase-7 (1:1000) were purchased from Cell Signaling Technology (Beverly, Massachusetts). Anti-Bid antibodies (1:1000) were from Trevigen (Gaithersburg, Maryland). Anti-actin antibodies (JLA20) (1:5000) were from Calbiochem (Darmstadt, Germany). Anti-human cytochrome *c* oxidase (subunit II) antibodies (12C4-F12) (1:1000) were from Molecular Probes (Eugene, Oregon). Anti-Fas antibody (CH-11) was from Upstate Biotechnology (Lake Placid, New York). Caspase synthetic peptide inhibitors used were caspase-3 Inhibitor I (cell permeable), caspase-8 Inhibitor I (cell permeable), and caspase-1 Inhibitor I (cell permeable) (Calbiochem, Darmstadt, Germany). ApoAlert caspase-3 fluorometric assay kit was purchased from Clontech (Palo Alto, California).

Cells, Virus, and DNA Constructs

HEK293 cells (ATCC CRL1573) were grown in Dulbecco's modified Eagle's medium (DMEM) supplemented with 100 U/ml each of penicillin and streptomycin and containing 10% fetal bovine serum. Jurkat cells were a gift of Dr. John Cohen and were grown in RPMI supplemented with 100U/ml each of penicillin and streptomycin and containing 10% fetal bovine serum. FADD-DN cells were a gift of Dr. Gary Johnson and express amino acids 80-208 of the FADD cDNA (with the addition of an AU1 epitope tag at the N-terminus) from the CMV promoter of pcDNA3 (Invitrogen, Calsbad, California). HEK 293 cells stably over-expressing Bcl-2 were provided by Dr. Gary Johnson. The cell line was constructed by cloning full-length Bcl-2 into the pLXSN vector and transfecting cells via retroviral transduction. Reovirus (Type 3 Abney, T3A) is a laboratory stock, which has been plaque purified and passaged (twice) in L929 cells (ATCC CCL1) to generate working stocks (37). All experiments were performed using an M.O.I. of 100. High M.O.I.s were chosen to insure synchronized infection of all susceptible cells, and to maximize the apoptotic stimulus.

Western Blot Analysis

Reovirus-infected cells were harvested at the indicated times, pelleted by centrifugation, washed with ice-cold phosphate-buffered saline, and lysed by sonication in 150 μl of lysis buffer (1% NP40, 0.15 M NaCl, 5.0 mM EDTA, 0.01 M Tris (pH 8.0), 1.0 mM PMSF, 0.02 mg/ml leupeptin, 0.02 mg/ml trypsin inhibitor). Lysates were cleared by centrifugation (20,000 g, 2 min), mixed 1:1 with SDS sample buffer, boiled for 5 min, and stored at −70°C. To prepare mitochondrial-free extracts, cells were pelleted, washed twice in ice-cold PBS, and incubated on ice for 30 min in buffer containing 220 mM

mannitol, 68 mM sucrose, 50 mM PIPES-KOH (pH 7.4), 50 mM KCl, 5 mM EGTA, 2 mM $MgCl_2$, 1 mM DTT, and protease inhibitors (complete cocktail, Boehringer Mannheim, Indianapolis, Indiana). Cells were lysed using 40 strokes in a Dounce homogenizer (B pestle). Lysates were centrifuged at 14,000 g for 15 min at 4°C to remove debris. Supernatants and mitochondrial pellets were prepared for electrophoresis as above. Proteins were separated by SDS-PAGE electrophoresis and transferred to Hybond-c extra nitrocellulose membrane (Amersham, Buckinghamshire, England) for immunobloting. Blots were then probed with the specified antibodies at the dilutions described above. Proteins were visualized using the ECL detection system (Amersham, Buckinghamshire, England). Densitometric analysis was performed using a FluorS MultiImager system and Quantity One software (Bio-Rad, Hercules, California).

Caspase-3 Activation Assays

Caspase-3 activation assays were performed using a kit obtained from Clontech (Palo Alto, California). Experiments were performed using 1 x 10^6 cells/ time point. Cells were centrifuged at 200 g, supernatants were removed, and the cell pellets were frozen at –70°C until all the time points were collected. Assays were performed in 96-well plates and analyzed using a fluorescent plate reader (CytoFluor 4000, PerSeptive Biosystems, Framingham, Massachusetts). Cleavage of DEVD-AFC, a synthetic caspase-3 substrate, was used to determine caspase-3 activation. Cleavage after the second Asp residue produces free AFC. The amount of fluorescence detected is directly proportional to amount of caspase-3 activity. Because all of the fluorogenic substrate assay experiments were performed at the same time, both the mock and reovirus-induced caspase-3

activation profiles are the same in all of these experiments and are included in each figure to facilitate comparisons. Results of all experiments are reported as means ± SEM.

Results

Caspase-8 is activated following reovirus infection. We have recently shown that reovirus-induced apoptosis involves the death receptors DR4 and DR5 and their cognate ligand TRAIL (6). Apoptosis initiated via TNF receptor superfamily cell death receptors involves the adaptor molecule FADD and subsequent activation of caspases, starting with the initiator caspase, caspase-8 (15). Reovirus-induced apoptosis is inhibited in HEK293 cells expressing dominant-negative FADD (FADD-DN) and in cells treated with Ac-IETD-CHO a cell permeable synthetic peptide inhibitor of caspase-8 (6). As shown in Fig. 1A, reovirus infection induces the activation of caspase-8 as evidenced by the disappearance of the full-length proenzyme (seen as a 55/54 kD doublet). The reduction in caspase-8 immunoreactivity appeared to be bi-phasic. A first phase of activation was detectable as early as 8 hrs post-infection. A second, more intense phase of activation began at 22 hrs post-infection and continued through ≥34 hrs (Fig. 1A and 1B).

Reovirus infection is associated with release of mitochondrial cytochrome *c* and activation of caspase-9. We have previously shown that stable over-expression of Bcl-2 in MDCK cells inhibits reovirus-induced apoptosis (27). Bcl-2 acts to inhibit apoptosis by preventing release of pro-apoptotic factors including cytochrome *c* from mitochondrion (1, 26). The capacity of Bcl-2 to inhibit reovirus-induced apoptosis suggested that the mitochondrial (intrinsic) pathway played a key role in reovirus-

induced apoptosis. We therefore wished to determine whether reovirus infection was associated with release of cytochrome *c* and activation of caspase-9. Mitochondria-free lysates were prepared from both mock- and reovirus-infected cells at the indicated time points and analyzed by western blot for the presence of cytosolic cytochrome *c*. Blots were probed with antisera directed against the mitochondrial integral membrane protein cytochrome *c* oxidase (subunit II) to detect potential mitochondrial contamination of the samples. Cytosolic cytochrome *c* is detected in reovirus-infected cells at ~ 10 hr post-infection (Fig. 2A). We also examined the cellular localization of mitochondrial cytochrome *c* following reovirus infection in FADD-DN expressing cells. As shown in Fig. 2B, cytochrome *c* is found at only trace levels in the cytoplasm of reovirus-infected FADD-DN expressing cells. These results indicate that caspase-8 activation occurs upstream of, and is required for, the release of cytochrome *c*. We next wished to determine whether caspase-9 was activated. Activation of caspase-9 involves the cleavage of the 46 kD pro-enzyme into a 37 kD active fragment. Activated caspase-9 was first detectable in reovirus-infected cells at 10 hrs (Fig. 3) post-infection, and was not detected in mock-infected cells. Activation increased steadily from 10 to 18 hrs and then persisted for $\geq$ 32 hrs.

Bid is cleaved following reovirus infection. Bid is a pro-apoptotic member of the Bcl-2 protein family. Activation of both Fas receptor by Fas and DR4/DR5 by TRAIL can induce caspase-8 dependent cleavage of Bid (18, 40, 41). Cleaved Bid can facilitate the release cytochrome *c* from the mitochondrion and lead to subsequent apoptosome-mediated activation of caspase-9 (20). We wished to determine whether Bid was cleaved following reovirus infection, and if this cleavage depended on caspase-8

activation. Western blot analysis revealed that while full length Bid levels remain relatively unchanged in mock-infected cells (Fig. 4A). However, following reovirus infection there was a biphasic pattern of Bid cleavage, analogous to that seen with caspase-8 (Fig. 4A). Loss of the full length immunoreactive Bid was first detected as early as 10 hrs post-infection. A second phase of Bid cleavage began at 26 hrs post-infection and continued through $\geq$ 40 hrs (Fig. 4A and 4B). In order to determine whether Bid cleavage was dependent on caspase-8 activation, we examined levels of immunoreactive Bid in cells in which caspase-8 activation was blocked by stable expression of DN-FADD. FADD-DN expression completely inhibited reovirus-induced Bid cleavage, indicating that Bid cleavage is caspase-8 dependent (Fig. 4C).

Reovirus infection is associated with activation of caspase-3 and caspase-7. Effector caspases, including caspases-3, -6 and -7, form part of the final common pathway for death receptor, mitochondrial, and ER/Golgi apoptotic pathways. Having shown that reovirus infection resulted in activation of both death receptor and mitochondrion-associated initiator caspases we next wished to determine which effector caspases were activated. Caspase-3 activation was evaluated by western blot using an antibody specific for the activated form of the enzyme. Activation of caspase-3 is associated with the appearance of specific cleavage product at ~20 kD representing the large subunit of active caspase-3. As shown in Fig. 5A, this fragment appears beginning at ~8 hrs post-infection in reovirus infected cells, but not in the mock infected controls. There is a biphasic activation profile, with the initial activation phase beginning at 8 hrs post-infection and a second, more intense activation phase beginning at 24 hrs post-infection (Fig. 5A). A similar pattern of caspase activation was seen in a fluorogenic

substrate assay using a caspase-3 specific substrate (DEVD-AFC). An initial phase of activation at 6-12 hrs was followed by a rapid activation peak 12-18 hrs (Figure 5B). Activated caspase-3 cleaves a variety of cellular substrates to induce the morphological hallmarks of apoptosis. We therefore examined the cleavage of PARP. PARP is cleaved by caspase-3 from the full-length 116 kD protein to an 85 kD inactive fragment. As shown in Fig. 5C, PARP cleavage exceeding that seen in mock-infected cells was first detectable at 14 hrs post-infection and persisted until $\geq$ 20 hrs post-infection. These experiments established that reovirus infection results in activation of the effector caspase, caspase-3 and is associated with cleavage of cellular substrates of caspase-3.

Other effector caspases may also be activated downstream of caspase-8 and caspase-9. Therefore, we examined the activation state of two other effector caspases, caspase-6 and caspase-7. We found no evidence by immunoblot of caspase-6 activation in reovirus-infected cells (data not shown). Caspase-7 is activated in infected cells as evidenced by the detection of the 20 kD large subunit of active caspase-7 (Fig. 6). However, caspase-7 activation appears to occur later than activation of caspase-3, and the amount of activation appears less.

In order to determine whether activation of effector caspases was completely dependent on the initial activation of death-receptor mediated pathways, we examined effector caspase activation in cells stably expressing DN-FADD. As shown in Fig. 7, the activation of both caspase-3 and caspase-7 is blocked in cells stably expressing DN-FADD. This suggests that activation of death-receptor initiated apoptotic signaling pathways is required for reovirus-induced effector caspase activation and apoptosis.

Bcl-2 overexpression inhibits effector caspase activation following reovirus infection. Although experiments with FADD-DN indicated that death-receptor pathways were necessary for reovirus-induced apoptosis, this process could require amplification via the mitochondrial pathway to be effective. Inhibition of apoptosis by Bcl-2 strongly supports an essential role for mitochondrial apoptotic pathways (28, 29). We have previously shown that reovirus-induced apoptosis is inhibited in MDCK cells over-expressing Bcl-2 (27). We wished to determine whether Bcl-2 expression in HEK cells inhibited caspase activation. Caspase activation was examined using both western blot analysis and fluorogenic substrate assays. As shown in Fig. 7A and 7B, activation of both caspase-3 and caspase-7 is inhibited in cells over-expressing Bcl-2. Caspase-3 activity, as measured in a fluorogenic substrate assay, is also significantly reduced in these cells (Fig. 7C). These results indicate that activation of the mitochondrial apoptotic pathway is crucial for effector caspase activation following reovirus infection.

Effects of synthetic caspase peptide inhibitors on caspase-3 activation. Caspases can be categorized into three major groups based on their pattern of substrate specificity (34, 36). Group I includes caspase-1, -4, and –5; group II includes caspase-2, -3, and –7; group III includes caspase-6, -8 and -9. Cell permeable, reversible, peptide caspase inhibitors have been developed based on these caspase substrate profiles (34, 36). We tested the capacity of three reversible cell permeable caspase inhibitors with specificity for group I (Ac-YVAD-CHO), group II (Ac-DEVD-CHO), and group III (Ac-IETD-CHO) caspases to inhibit reovirus-induced caspase-3 activation at 18 hrs post-infection. As shown in Fig. 8, the group II inhibitor Ac-DEVD-CHO completely inhibited reovirus-induced caspase-3 activity at a concentration of 10 μM. The group I inhibitor (Ac-

YVAD-CHO) had no effect on caspase-3 activation, consistent with a lack of involvement of caspases-1, -4 or -5 in reovirus-induced apoptosis. The group III inhibitor Ac-IETD-CHO achieved maximal inhibition of reovirus-induced caspase-3 activation at a concentration of 5 μM. However, the maximum degree of inhibition (65%) was not as high as that seen with the group II inhibitor. These data suggest that while the activation of group III caspases, including caspase-8 and -9, is critically important to reovirus-induced apoptosis that other as yet unidentified caspases may also contribute to caspase-3 activation. However, the fact that expression of DN-FADD was as effective as treatment with the group II inhibitor Ac-DEVD-CHO in blocking caspase-3 activation, suggests that the apical caspases that contribute to caspase-3 activation all depend on an initial death-receptor initiated caspase activation signal.

Discussion

Understanding the mechanisms of virus-induced apoptosis is crucial to understanding how viruses injure target tissues and induce disease. The exact pathways leading to virus-induced apoptosis are still incompletely understood. Since caspases play a central role in virtually all known apoptotic signaling pathways, it is not surprising that they have been implicated in virus-induced apoptosis. Pancaspase peptide inhibitors have been shown to inhibit apoptosis induced by viruses as diverse as Sindbis (16, 21), HIV-1 (4, 31), Herpes simplex virus type 1 (13), influenza (33), Sendai (5), and TGEV (11).

The events that initiate caspase activation in virus-infected cells are still incompletely understood. Activation of caspase-8 plays an important role in apoptosis induced by

HIV-1 (31), influenza (33), Sendai (5), and Sindbis (21), suggesting that death-receptor initiated processes may be important in apoptosis induced by these viruses.

Many forms of virus-induced apoptosis are inhibited by anti-apoptotic members of the Bcl-2 family (22, 25, 30, 35). One of the most thoroughly investigated mechanisms for the anti-apoptotic actions of Bcl-2 involves its inhibition of the release of cytochrome *c* from mitochondria (1, 26). Abnormalities of mitochondrial transmembrane potential and release of cytochrome *c* have been described following infection with HIV (12), TGEV (11), chicken anemia virus (8), and herpes simplex virus (13). These studies suggest that both mitochondrial and death-receptor mediated pathways may play an important role in virus-induced apoptosis.

We have used reovirus infection in HEK cells to provide a detailed characterization of the cellular pathways involved in virus-induced apoptosis. Mammalian reoviruses induce apoptosis in several cell lines *in vitro* (6, 7, 27, 38) as well as in target tissues including the heart and CNS *in vivo* (9, 23, 24). Reovirus-induced apoptosis involves the DR4/DR5/TRAIL system of cell surface death receptors (6). Over-expression of Bcl-2 inhibits reovirus-induced apoptosis in MDCK cells (27) suggesting that mitochondrial pathways also play a critical role in reovirus-induced apoptosis.

We now provide the first comprehensive characterization of the activation of caspase pathways following reovirus infection. In this study we found that caspase-8 was activated within 8 hrs of reovirus infection. The activation of caspase-8 occurs in two distinct phases, consistent with a model in which initial death-receptor mediated activation of caspase-8 is subsequently augmented by activation of caspase-9 or other caspases (discussed below). Following activation, caspase-8 cleaves Bid, a pro-

apoptotic Bcl-2 family protein. Cleaved Bid provides an essential link between reovirus-induced death-receptor mediated caspase-8 activation and activation of mitochondrial pathways. Inhibition of caspase-8 activation by over-expression of DN-FADD prevented Bid cleavage. These findings, in conjunction with our previous studies indicating that Bcl-2 expression inhibited reovirus apoptosis in MDCK cells (27) suggested that reovirus infection also activated the mitochondrial apoptotic pathway. Therefore we examined cytochrome *c* release and caspase-9 activation following reovirus infection. Cytochrome *c* was found to be present in the cytoplasm of infected cells at ~10 hr post infection. Additionally, cytochrome *c* release was blocked in FADD-DN expressing cells suggesting that this event requires caspase-8. We also examined caspase-9 activation by western blot analysis. Caspase-9 is activated at ~12 hr post infection.

Having shown that reovirus infection was associated with activation of both death-receptor and mitochondrial-associated initiator caspases we next wished to determine which effector caspases were subsequently activated. We used multiple experimental approaches to show that the effector caspase, caspase-3 is activated beginning at ~8 hrs post infection and peaking at ~18 hr post infection. Additionally, caspase-7 was activated in reovirus-infected cells, although this event occurs later than caspase-3 activation. Another effector caspase, caspase-6, was not activated in reovirus-infected cells.

There is evidence that although mitochondrial cytochrome *c* release and caspase-9 activation occur downstream of death receptor stimulation, that these events are not necessarily required for all forms of death-receptor initiated apoptosis (28, 29). In order to evaluate the contribution of the mitochondrial pathway to reovirus-induced apoptosis

we examined the effects of Bcl-2 overexpression on effector caspase activation following reovirus infection. We found that overexpression of Bcl-2 inhibits the activation of both caspase-3 and caspase-7. This provides further evidence of the importance of the mitochondrial apoptotic pathway in reovirus-induced cell death.

Caspases can be broadly grouped into three categories based on their pattern of substrate specificity (34, 36). We tested the capacity of inhibitors representing each of these groups to inhibit reovirus-induced caspase-3 activation. A group II caspase inhibitor completely blocked reovirus-induced caspase-3 activity at low concentrations. This result is consistent with the known activation of caspases-3 and -7 in reovirus infection. A group I caspase inhibitor had no effect, even at high concentrations. This suggested that caspases-1, -4 and -5 do not play a significant role in reovirus-induced apoptosis. A group III caspase inhibitor significantly reduced caspase-3 activity, but its effect was only partial when compared to the Group II inhibitor. This result was consistent with our observation that caspase-8 and -9 were involved in reovirus-induced caspase-3 activation. The lack of complete inhibition of caspase-3 activation by the group III inhibitor suggests that additional, as yet unidentified, caspases may also contribute to reovirus-induced caspase-3 activation. However, the complete inhibition of caspase-3 activation seen in cells expressing DN-FADD suggests that death receptor activation is the key initiating event in all reovirus-induced caspase activation cascades that ultimately contribute to effector caspase activation.

Acknowledgements

This work was supported by Public Health Service grant 1RO1AG14071 from the National Institute of Aging, Merit and REAP grants from the Department of Veterans Affairs, and a U.S. Army Medical Research and Material Command grant (USAMRMC98293015). Tissue culture media was obtained from the UCHSC Cancer Center Media Core.

REFERENCES

1. **Adams, J. M. and S. Cory**. 1998. The Bcl-2 protein family: arbiters of cell survival. Science **281**:1322-1326.

2. **Ashkenazi, A. and V. M. Dixit**. 1998. Death receptors: signaling and modulation. Science **281**:1305-1308.

3. **Barton, E. S., J. C. Forrest, J. L. Connolly, J. D. Chappell, Y. Liu, F. J. Schnell, A. Nusrat, C. A. Parkos, and T. S. Dermody**. 2001. Junction adhesion molecule is a receptor for reovirus. Cell **104**:441-451.

4. **Biard-Piechaczyk, M., V. Robert-Hebmann, V. Richard, J. Roland, R. A. Hipskind, and C. Devaux**. 2000. Caspase-dependent apoptosis of cells expressing the chemokine receptor CXCR4 is induced by cell membrane-associated human immunodeficiency virus type 1 envelope glycoprotein (gp120). Virology **268**:329-344.

5. **Bitzer, M., F. Prinz, M. Bauer, M. Spiegel, W. J. Neubert, M. Gregor, K. Schulze-Osthoff, and U. Lauer**. 1999. Sendai virus infection induces apoptosis through activation of caspase- 8 (FLICE) and caspase-3 (CPP32). J Virol **73**:702-708.

6. **Clarke, P., S. M. Meintzer, S. Gibson, C. Widmann, T. P. Garrington, G. L. Johnson, and K. L. Tyler**. 2000. Reovirus-Induced Apoptosis Is Mediated by TRAIL. J. Virol. **74**:8135-8139.

7. **Connolly, J. L., S. E. Rodgers, P. Clarke, D. W. Ballard, L. D. Kerr, K. L. Tyler, and T. S. Dermody**. 2000. Reovirus-induced apoptosis requires activation of transcription factor NF-kappaB. J. Virol. **74**:2981-2989.

8. **Danen-van Oorschot, A. A., A. J. Der Eb, and M. H. Noteborn**. 2000. The chicken anemia virus-derived protein apoptin requires activation of caspases for induction of apoptosis in human tumor cells. J Virol **74**:7072-7078.

9. **DeBiasi, R. L., C. L. Edelstein, B. Sherry, and K. L. Tyler**. 2001. Calpain inhibition protects against virus-induced apoptotic myocardial injury. J Virol **75**:351-361.

10. **Du, C., M. Fang, Y. Li, L. Li, and X. Wang**. 2000. Smac, a mitochondrial protein that promotes cytochrome c-dependent caspase activation by eliminating IAP inhibition. Cell **102**:33-42.

11. **Eleouet, J. F., S. Chilmonczyk, L. Besnardeau, and H. Laude**. 1998. Transmissible gastroenteritis coronavirus induces programmed cell death in infected cells through a caspase-dependent pathway. J Virol **72**:4918-4924.

12. **Ferri, K. F., E. Jacotot, J. Blanco, J. A. Este, N. Zamzami, S. A. Susin, Z. Xie, G. Brothers, J. C. Reed, J. M. Penninger, and G. Kroemer**. 2000. Apoptosis control in syncytia induced by the HIV type 1-envelope glycoprotein complex: role of mitochondria and caspases. J Exp. Med. **192**:1081-1092.

13. **Galvan, V., R. Brandimarti, J. Munger, and B. Roizman**. 2000. Bcl-2 blocks a caspase-dependent pathway of apoptosis activated by herpes simplex virus 1 infection in HEp-2 cells. J Virol **74**:1931-1938.

14. **Gross, A., X. M. Yin, K. Wang, M. C. Wei, J. Jockel, C. Milliman, H. Erdjument-Bromage, P. Tempst, and S. J. Korsmeyer**. 1999. Caspase cleaved BID targets mitochondria and is required for cytochrome c release, while BCL-XL prevents this release but not tumor necrosis factor-R1/Fas death. J Biol. Chem. **274**:1156-1163.

15. **Hu, S., C. Vincenz, J. Ni, R. Gentz, and V. M. Dixit**. 1997. I-FLICE, a novel inhibitor of tumor necrosis factor receptor-1- and CD- 95-induced apoptosis. J. Biol. Chem. **272**:17255-17257.

16. **Jan, J. T., S. Chatterjee, and D. E. Griffin**. 2000. Sindbis virus entry into cells triggers apoptosis by activating sphingomyelinase, leading to the release of ceramide. J. Virol. **74**:6425-6432.

17. **Joza, N., S. A. Susin, E. Daugas, W. L. Stanford, S. K. Cho, C. Y. Li, T. Sasaki, A. J. Elia, H. Y. Cheng, L. Ravagnan, K. F. Ferri, N. Zamzami, A. Wakeham, R. Hakem, H. Yoshida, Y. Y. Kong, T. W. Mak, J. C. Zuniga-Pflucker, G. Kroemer, and J. M. Penninger**. 2001. Essential role of the mitochondrial apoptosis-inducing factor in programmed cell death. Nature **410**:549-554.

18. **Li, H., H. Zhu, C. J. Xu, and J. Yuan**. 1998. Cleavage of BID by caspase 8 mediates the mitochondrial damage in the Fas pathway of apoptosis. Cell **94**:491-501.

19. **Li, P., D. Nijhawan, I. Budihardjo, S. M. Srinivasula, M. Ahmad, E. S. Alnemri, and X. Wang**. 1997. Cytochrome c and dATP-dependent formation of Apaf-1/caspase-9 complex initiates an apoptotic protease cascade. Cell **91**:479-489.

20. **Luo, X., I. Budihardjo, H. Zou, C. Slaughter, and X. Wang**. 1998. Bid, a Bcl2 interacting protein, mediates cytochrome c release from mitochondria in response to activation of cell surface death receptors. Cell **94**:481-490.

21. **Nava, V. E., A. Rosen, M. A. Veliuona, R. J. Clem, B. Levine, and J. M. Hardwick**. 1998. Sindbis virus induces apoptosis through a caspase-dependent, CrmA- sensitive pathway. J Virol **72**:452-459.

22. **O'Brien, V.** 1998. Viruses and apoptosis. J Gen. Virol **79 (Pt 8)**:1833-1845.

23. **Oberhaus, S. M., T. S. Dermody, and K. L. Tyler**. 1998. Apoptosis and the cytopathic effects of reovirus. Curr. Top. Microbiol. Immunol. **233 Reovir.ii**:23-49.

24. **Oberhaus, S. M., R. L. Smith, G. H. Clayton, T. S. Dermody, and K. L. Tyler.** 1997. Reovirus infection and tissue injury in the mouse central nervous system are associated with apoptosis. J. Virol. **71**:2100-2106.

25. **Razvi, E. S. and R. M. Welsh**. 1995. Apoptosis in viral infections. Adv. Virus Res. **45**:1-60.

26. **Reed, J. C.** 1998. Bcl-2 family proteins. Oncogene **17**:3225-3236.

27. **Rodgers, S. E., E. S. Barton, S. M. Oberhaus, B. Pike, C. A. Gibson, K. L. Tyler, and T. S. Dermody**. 1997. Reovirus-induced apoptosis of MDCK cells is not linked to viral yield and is blocked by Bcl-2. J. Virol. **71**:2540-2546.

28. **Scaffidi, C., S. Fulda, A. Srinivasan, C. Friesen, F. Li, K. J. Tomaselli, K. M. Debatin, P. H. Krammer, and M. E. Peter**. 1998. Two CD95 (APO-1/Fas) signaling pathways. EMBO J **17**:1675-1687.

29. **Scaffidi, C., I. Schmitz, J. Zha, S. J. Korsmeyer, P. H. Krammer, and M. E. Peter**. 1999. Differential modulation of apoptosis sensitivity in CD95 type I and type II cells. J Biol. Chem. **274**:22532-22538.

30. **Shen, Y. and T. E. Shenk**. 1995. Viruses and apoptosis. Curr. Opin. Genet. Dev. **5**:105-111.

31. **Stewart, S. A., B. Poon, J. Y. Song, and I. S. Chen**. 2000. Human immunodeficiency virus type 1 vpr induces apoptosis through caspase activation. J. Virol. **74**:3105-3111.

32. **Susin, S. A., H. K. Lorenzo, N. Zamzami, I. Marzo, B. E. Snow, G. M. Brothers, J. Mangion, E. Jacotot, P. Costantini, M. Loeffler, N. Larochette, D. R. Goodlett, R. Aebersold, D. P. Siderovski, J. M. Penninger, and G. Kroemer**. 1999. Molecular characterization of mitochondrial apoptosis-inducing factor. Nature **397**:441-446.

33. **Takizawa, T., C. Tatematsu, K. Ohashi, and Y. Nakanishi**. 1999. Recruitment of apoptotic cysteine proteases (caspases) in influenza virus-induced cell death. Microbiol. Immunol. **43**:245-252.

34. **Talanian, R. V., C. Quinlan, S. Trautz, M. C. Hackett, J. A. Mankovich, D. Banach, T. Ghayur, K. D. Brady, and W. W. Wong**. 1997. Substrate specificities of caspase family proteases. J Biol. Chem. **272**:9677-9682.

35. **Teodoro, J. G. and P. E. Branton**. 1997. Regulation of apoptosis by viral gene products. J Virol **71**:1739-1746.

36. **Thornberry, N. A., T. A. Rano, E. P. Peterson, D. M. Rasper, T. Timkey, M. Garcia-Calvo, V. M. Houtzager, P. A. Nordstrom, S. Roy, J. P. Vaillancourt, K. T. Chapman, and D. W. Nicholson**. 1997. A combinatorial approach defines specificities of members of the caspase family and granzyme B. Functional relationships established for key mediators of apoptosis. J Biol. Chem. **272**:17907-17911.

37. **Tyler, K. L., M. K. Squier, A. L. Brown, B. Pike, D. Willis, S. M. Oberhaus, T. S. Dermody, and J. J. Cohen**. 1996. Linkage between reovirus-induced apoptosis and inhibition of cellular DNA synthesis: role of the S1 and M2 genes. J. Virol. **70**:7984-7991.

38. **Tyler, K. L., M. K. Squier, S. E. Rodgers, B. E. Schneider, S. M. Oberhaus, T. A. Grdina, J. J. Cohen, and T. S. Dermody**. 1995. Differences in the capacity of reovirus strains to induce apoptosis are determined by the viral attachment protein sigma 1. J. Virol. **69**:6972-6979.

39. **Verhagen, A. M., P. G. Ekert, M. Pakusch, J. Silke, L. M. Connolly, G. E. Reid, R. L. Moritz, R. J. Simpson, and D. L. Vaux**. 2000. Identification of DIABLO, a mammalian protein that promotes apoptosis by binding to and antagonizing IAP proteins. Cell **102**:43-53.

40. **Yamada, H., S. Tada-Oikawa, A. Uchida, and S. Kawanishi**. 1999. TRAIL causes cleavage of bid by caspase-8 and loss of mitochondrial membrane potential resulting in apoptosis in BJAB cells. Biochem. Biophys. Res. Commun. **265**:130-133.

41. **Yin, X. M., K. Wang, A. Gross, Y. Zhao, S. Zinkel, B. Klocke, K. A. Roth, and S. J. Korsmeyer**. 1999. Bid-deficient mice are resistant to Fas-induced hepatocellular apoptosis. Nature **400**:886-891.

42. **Zou, H., Y. Li, X. Liu, and X. Wang**. 1999. An APAF-1.cytochrome c multimeric complex is a functional apoptosome that activates procaspase-9. J. Biol. Chem. **274**:11549-11556.

Figure Legends

Fig. 1. **Reovirus infection induces the activation of caspase-8.** HEK 293 lysates were prepared at the indicated times points from mock-infected or reovirus-infected cells and probed with anti-caspase-8 antibodies and anti-actin antibodies (A). Control lanes represent Jurkat cell lysates untreated (-) or treated (+) with activating anti-Fas antibody and harvested at 8 hr post treatment. The graph displays densitometric analysis of the virus-infected western blot analysis (B). Values are expressed as arbitrary densitometric units.

Fig. 2. **Cytochrome *c* is present in the cytosol of reovirus infected cells.** HEK 293 cell lysates (A) and FADD-DN expressing HEK 293 cells lysates (B) were prepared at the indicated time points as described (see Materials and Methods) and resolved using SDS-PAGE. Western blot analysis was performed using anti-cytochrome *c* antibodies and anti-cytochrome *c* oxidase (subunit II).

Fig. 3. **Caspase-9 is activated in reovirus-infected cells.** HEK 293 cell lysates were prepared from mock-infected or reovirus-infected cells at the indicated time points and resolved by SDS-PAGE. Western blot analysis was performed using anti-caspase-9 antibodies.

Fig. 4. **Reovirus infection leads to cleavage of full length Bid.** Lysates were prepared at the indicated time points from mock-infected or reovirus-infected HEK 293 cells (A) and reovirus infected FADD-DN expressing HEK 293 cells (C) and probed with anti-Bid antibodies and anti-actin antibodies. The graph displays densitometric analysis of the virus-infected western blot analysis (B). Values are expressed as arbitrary densitometric units.

Fig. 5. **Reovirus infection leads to activation of caspase-3.** Western blot analysis was performed using HEK 293 lysates harvested at the indicated time points from mock-infected and reovirus-infected cells and probed with anti-caspase-3 antibodies (A) or anti-PARP antibodies (C). Control lanes represent Jurkat cell lysates untreated (-) or treated (+) with activating anti-Fas antibody and harvested at 8 hr post treatment. Fluorogenic substrate assays (B) were performed in triplicate. Error bars represent standard error of the mean. Fluorescence is expressed as arbitrary units.

Fig. 6. **Caspase-7 is activated following reovirus infection.** Western blot analysis was performed using HEK 293 lysates harvested at the indicated time points from mock-infected and reovirus-infected cells and probed with anti-caspase-7 antibodies. Control lanes represent Jurkat cell lysates untreated (-) or treated (+) with activating anti-Fas antibody and harvested at 8 hr post treatment.

Fig. 7. **Effector caspase activation in inhibited in FADD-DN expressing cells.** Western blot analysis was performed using cell lysates prepared from reovirus-infected cells at the indicated time points and probed with anti-caspase-3 antibodies and anti-caspase-7 antibodies (A). Control lanes represent Jurkat cell lysates untreated (-) or treated (+) with activating anti-Fas antibody and harvested at 8 hr post treatment. Fluorogenic substrate assays (B) were performed in triplicate. Error bars represent standard error of the mean. Fluorescence is expressed as arbitrary units.

Fig. 8. **Effector caspase activation is inhibited in Bcl-2 overexpressing cells.** Western blot analysis was performed using cell lysates prepared from reovirus-infected cells at the indicated time points and probed with anti-caspase-3 antibodies and anti-caspase-7

antibodies (A). Control lanes represent Jurkat cell lysates untreated (-) or treated (+) with activating anti-Fas antibody and harvested at 8 hr post treatment. Fluorogenic substrate assays (B) were performed in triplicate. Error bars represent standard error of the mean. Fluorescence is expressed as arbitrary units.

Fig. 9. **Synthetic peptide inhibition of DEVD-specific caspase activation.** HEK 293 cells were pretreated with the synthetic peptide inhibitors at the concentrations shown for 1 hr prior to reovirus infection (M.O.I. 100). Fluorogenic substrate assays were performed at 18 h post infection. Values are expressed as percent inhibition where untreated reovirus-infected cells represent 0% inhibition and mock-infected cells repesent 100% inhibition.

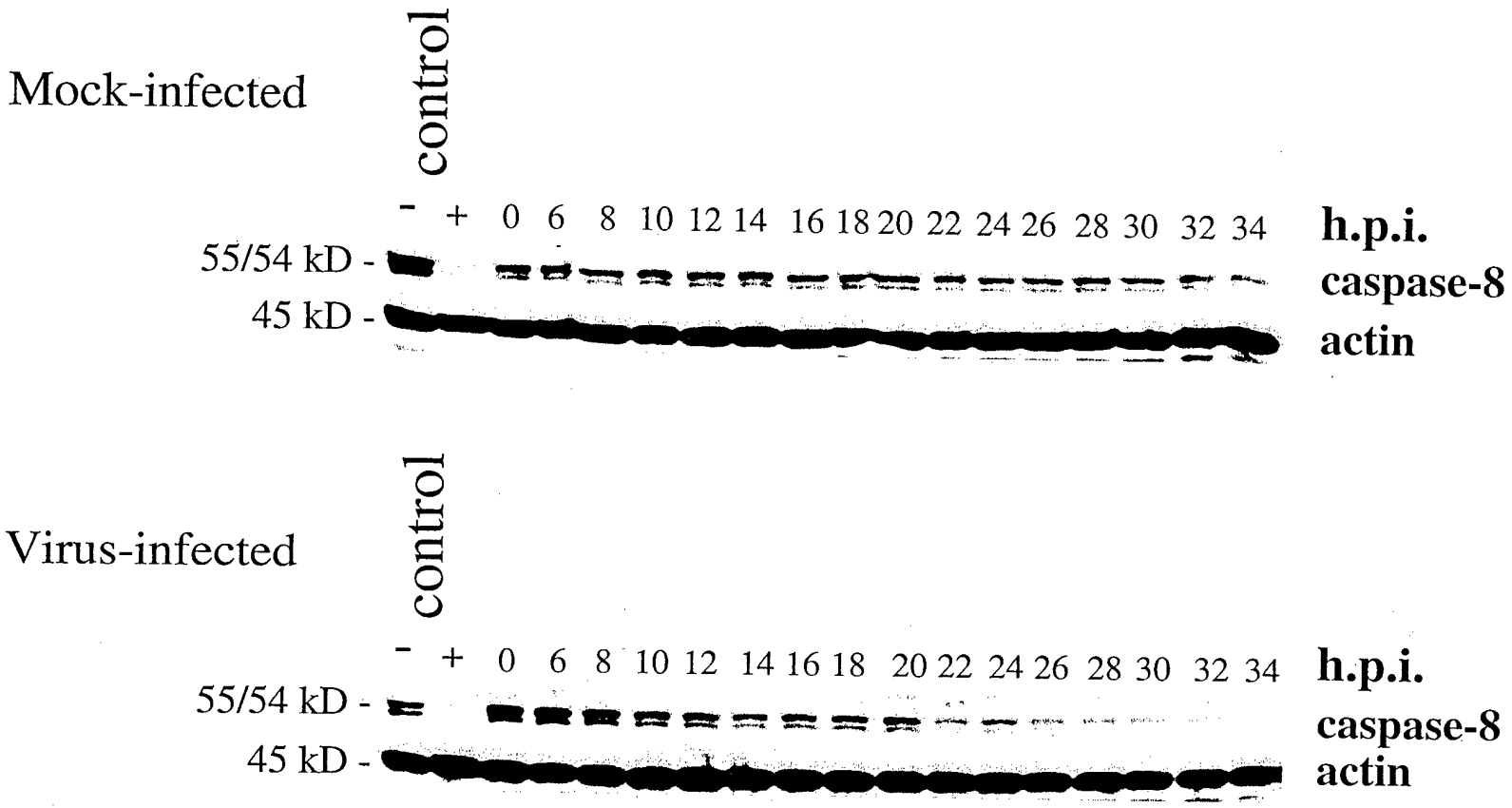
Mock-infected
control
- + 0 6 8 10 12 14 16 18 20 22 24 26 28 30 32 34
h.p.i.
55/54 kD -
caspase-8
45 kD -
actin
Virus-infected
control
- + 0 6 8 10 12 14 16 18 20 22 24 26 28 30 32 34
h.p.i.
55/54 kD -
caspase-8
45 kD -
actin

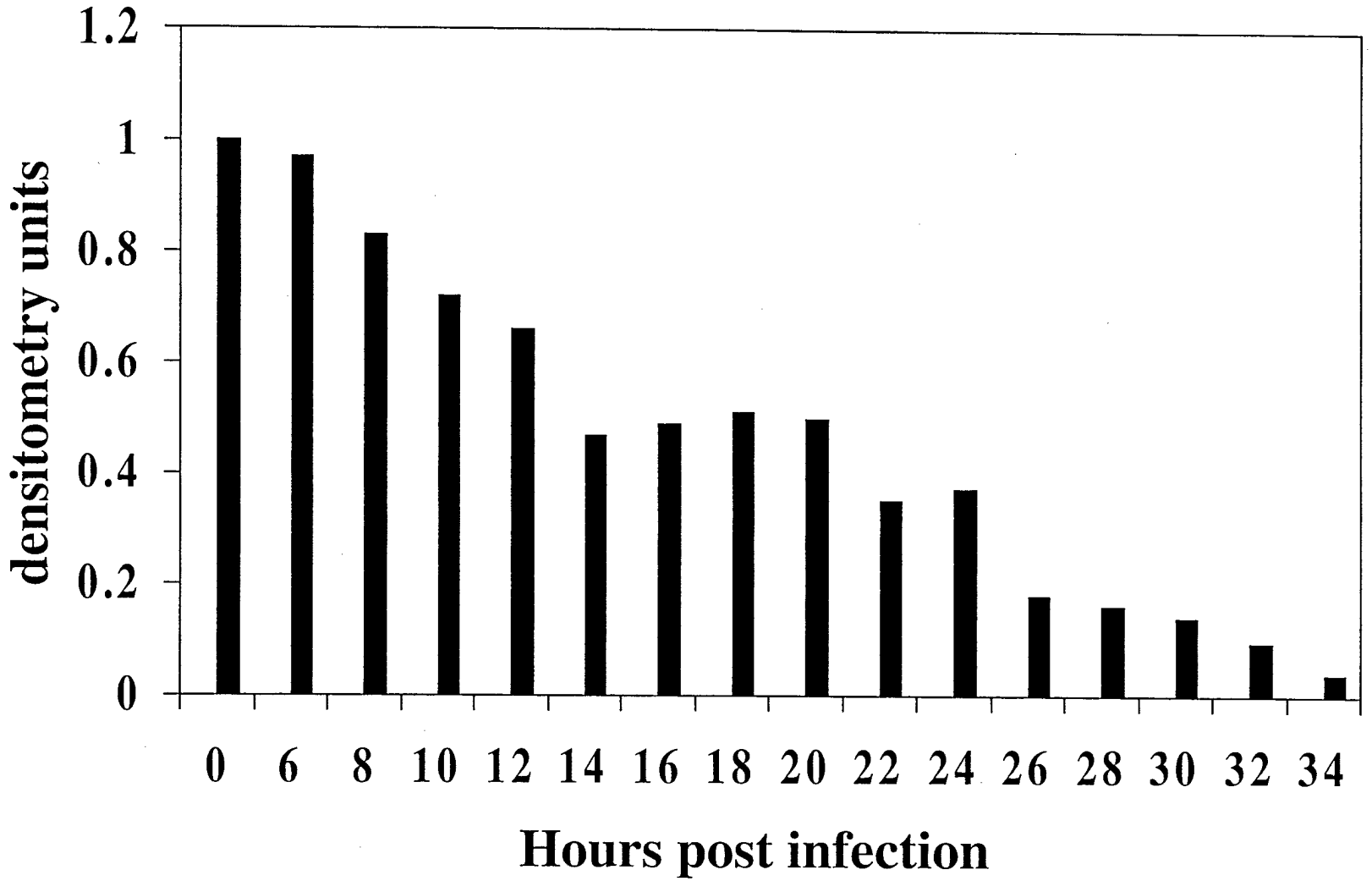
densitometry units
1.2
1
0.8
0.6
0.4
0.2
0
0 6 8 10 12 14 16 18 20 22 24 26 28 30 32 34
Hours post infection

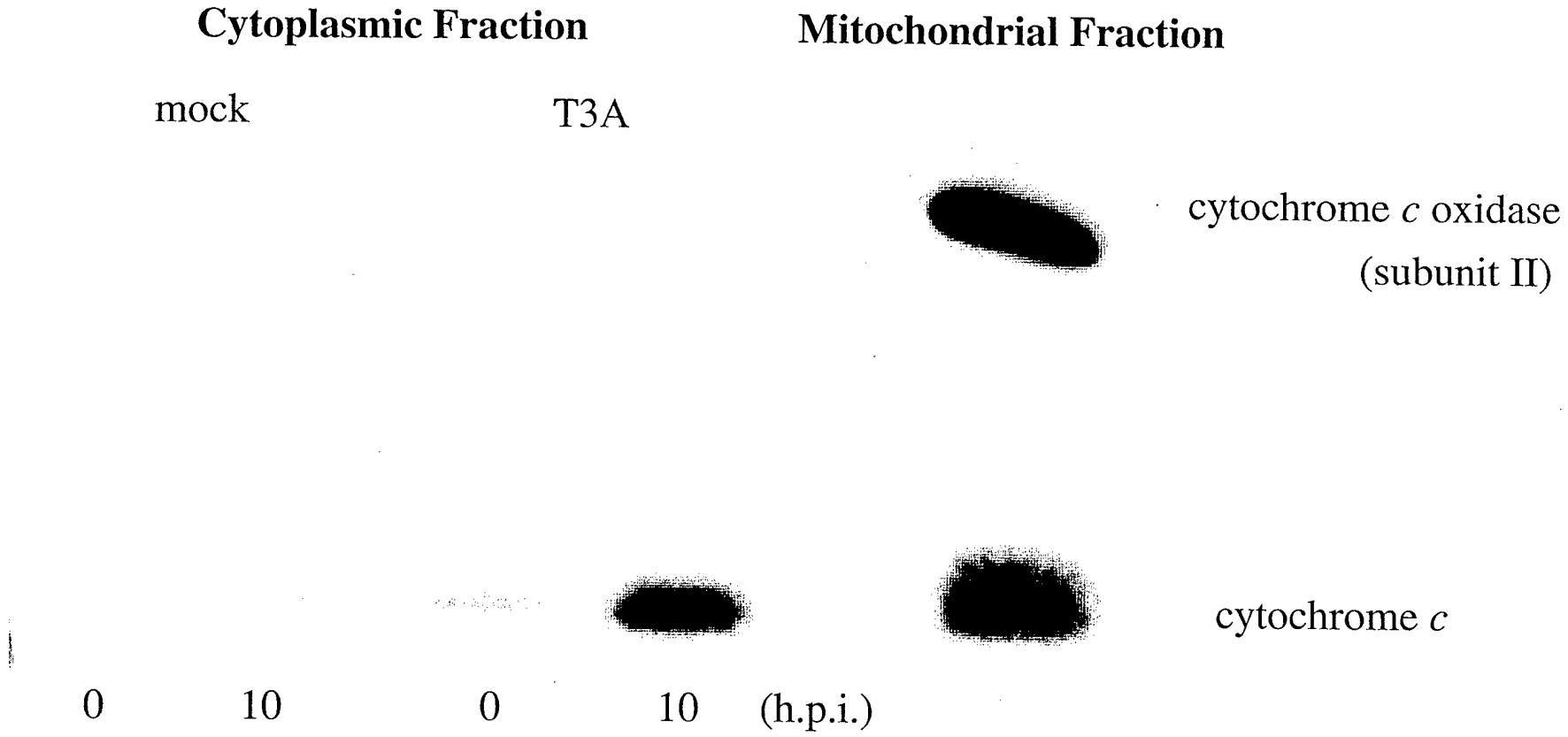
Cytoplasmic Fraction
Mitochondrial Fraction
mock
T3A
cytochrome c oxidase
(subunit II)
cytochrome c
0
10
0
10
(h.p.i.)

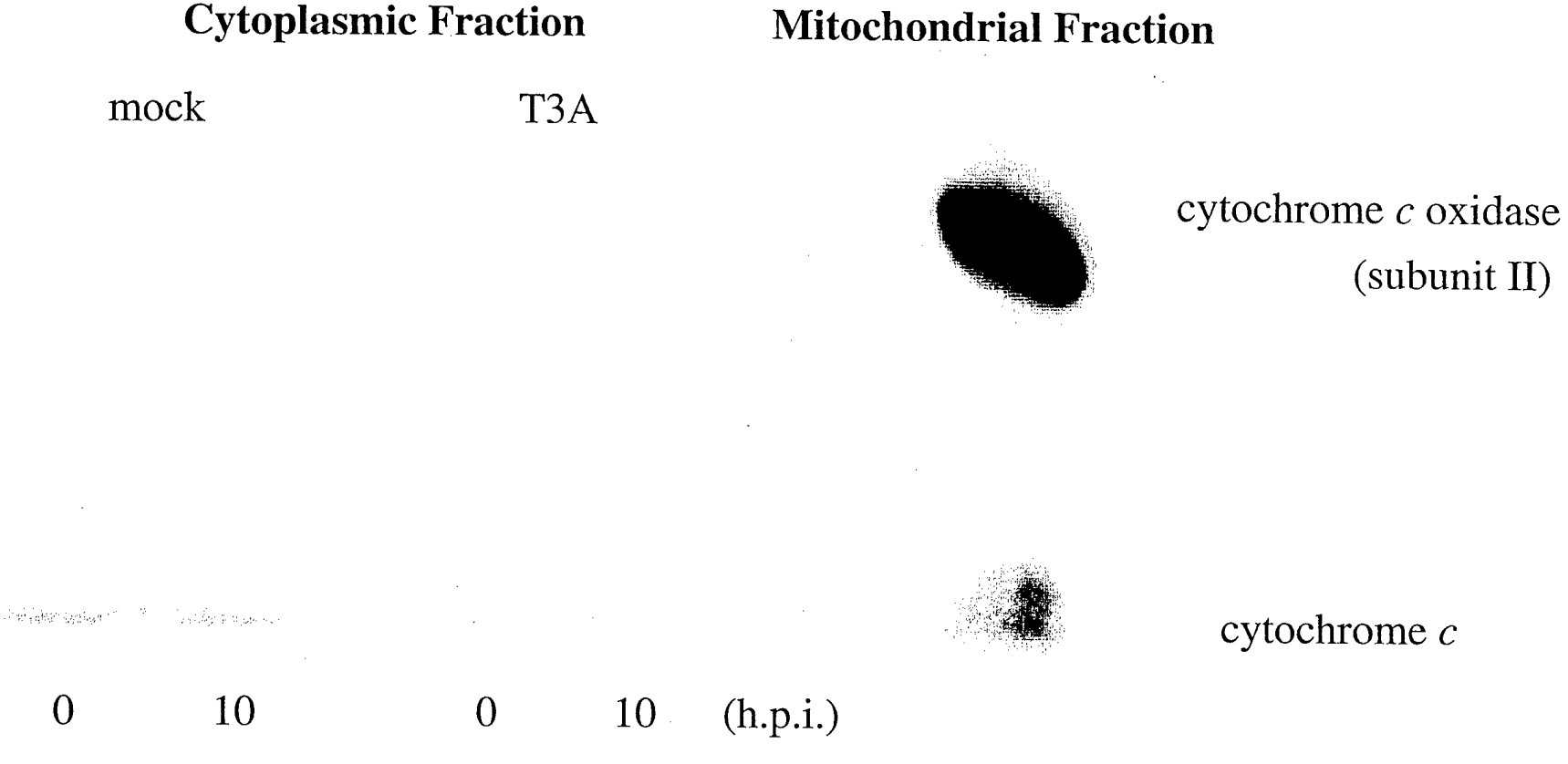
Cytoplasmic Fraction
Mitochondrial Fraction
mock
T3A
cytochrome c oxidase
(subunit II)
cytochrome c
0
10
0
10
(h.p.i.)

Mock-infected

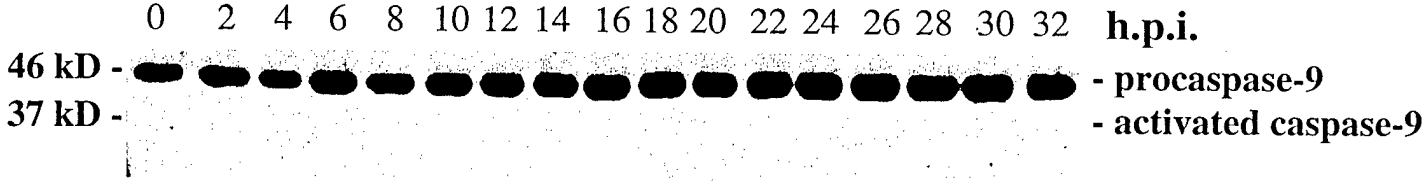

Virus-infected

Mock-infected

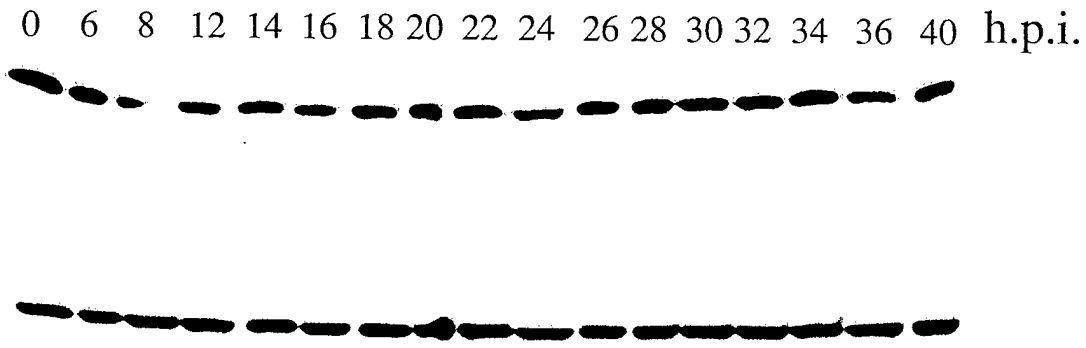

Virus-infected

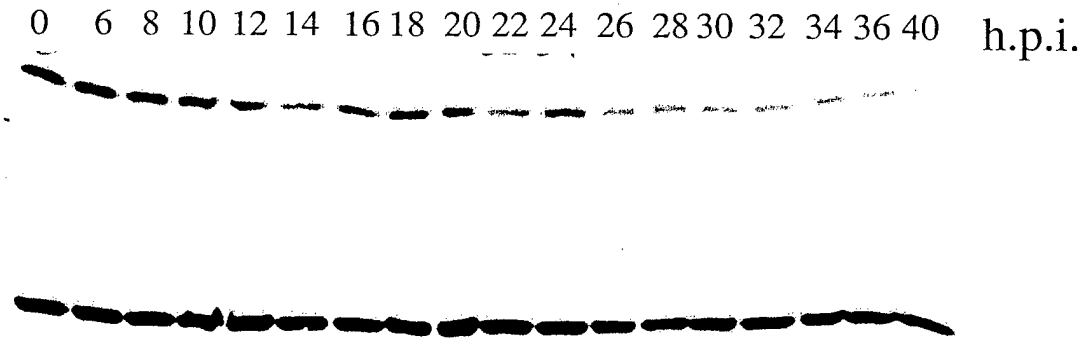

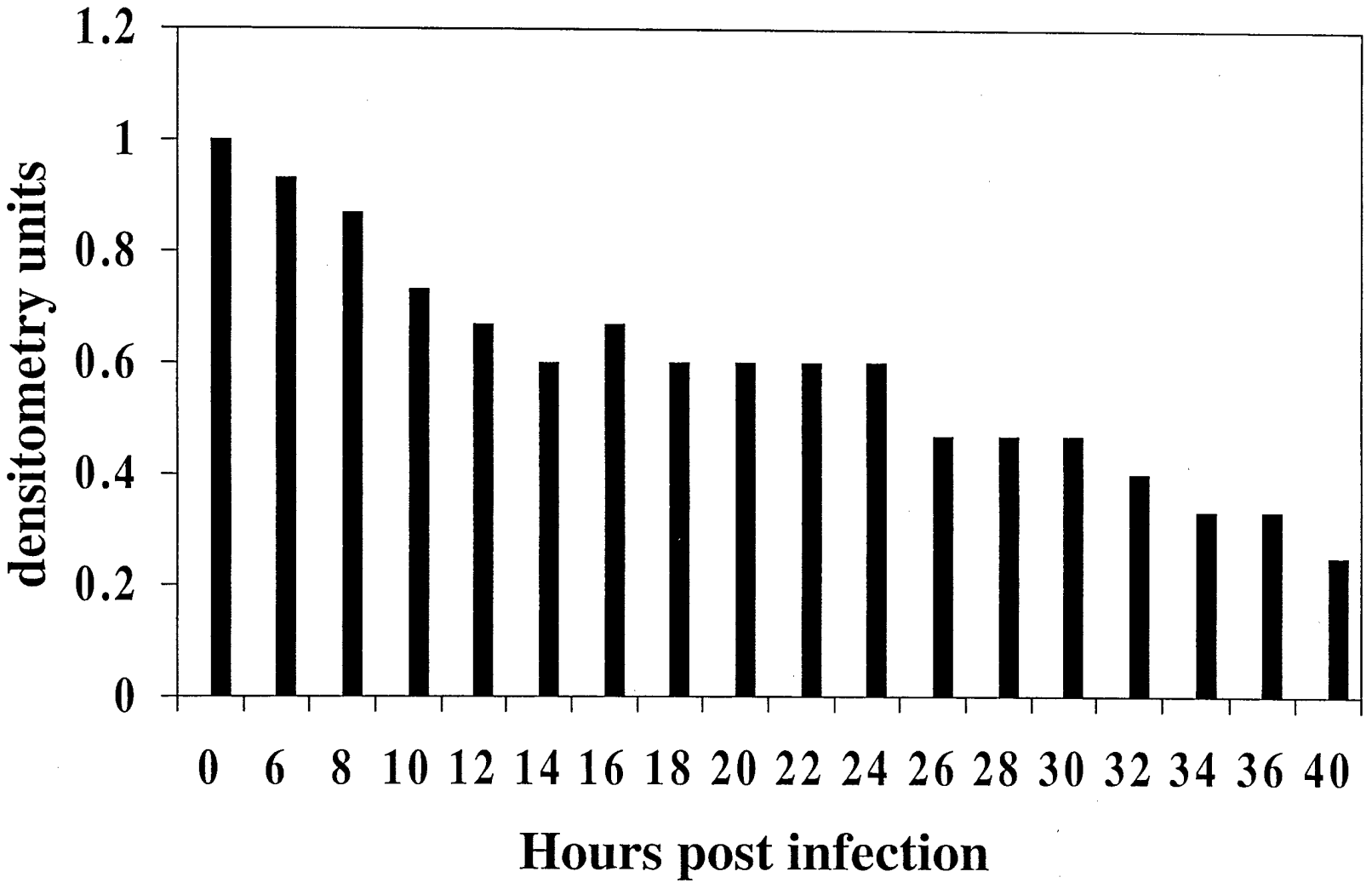
densitometry units
1.2
1
0.8
0.6
0.4
0.2
0
0 6 8 10 12 14 16 18 20 22 24 26 28 30 32 34 36 40
Hours post infection

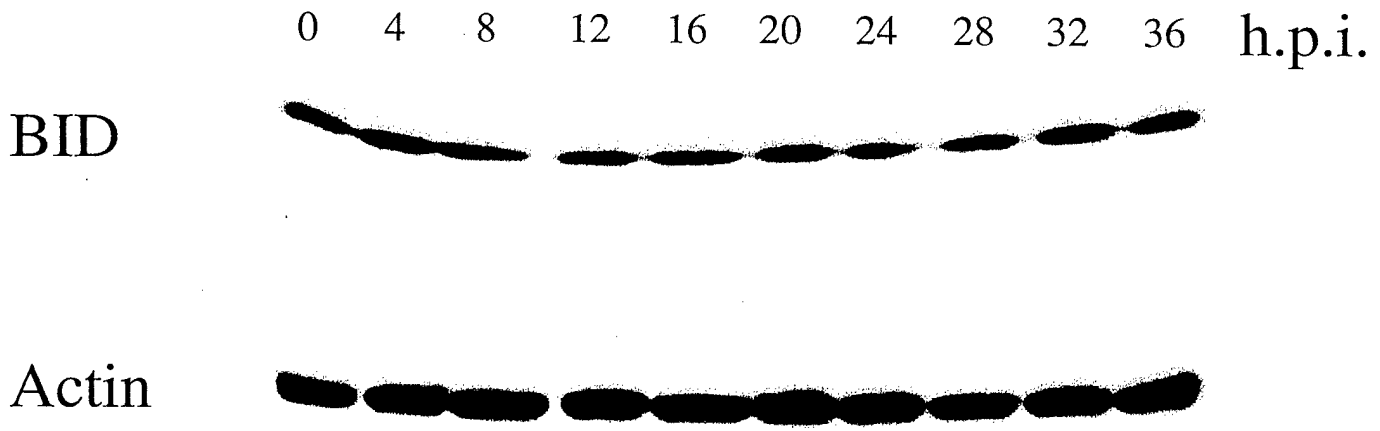
0 4 8 12 16 20 24 28 32 36 h.p.i.
BID
Actin

Mock-infected

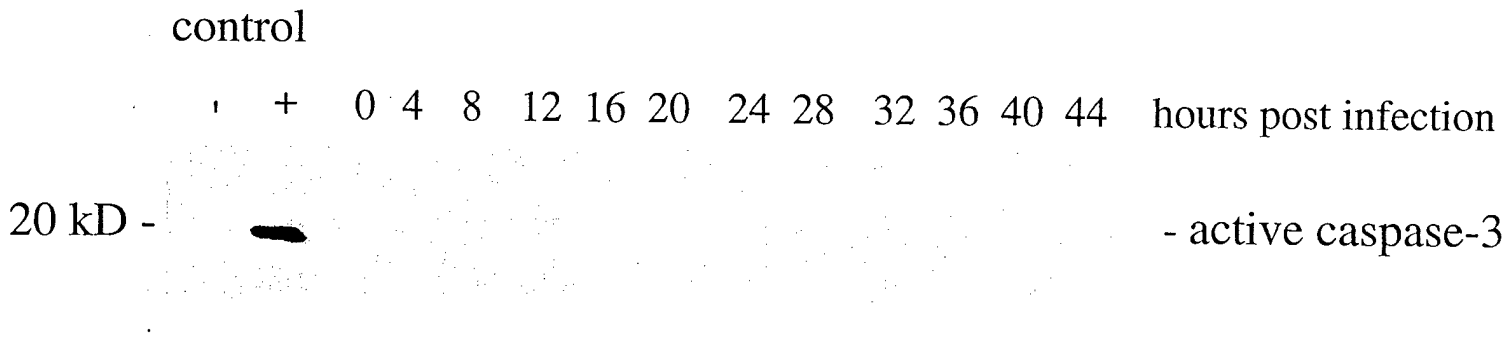

Virus-infected

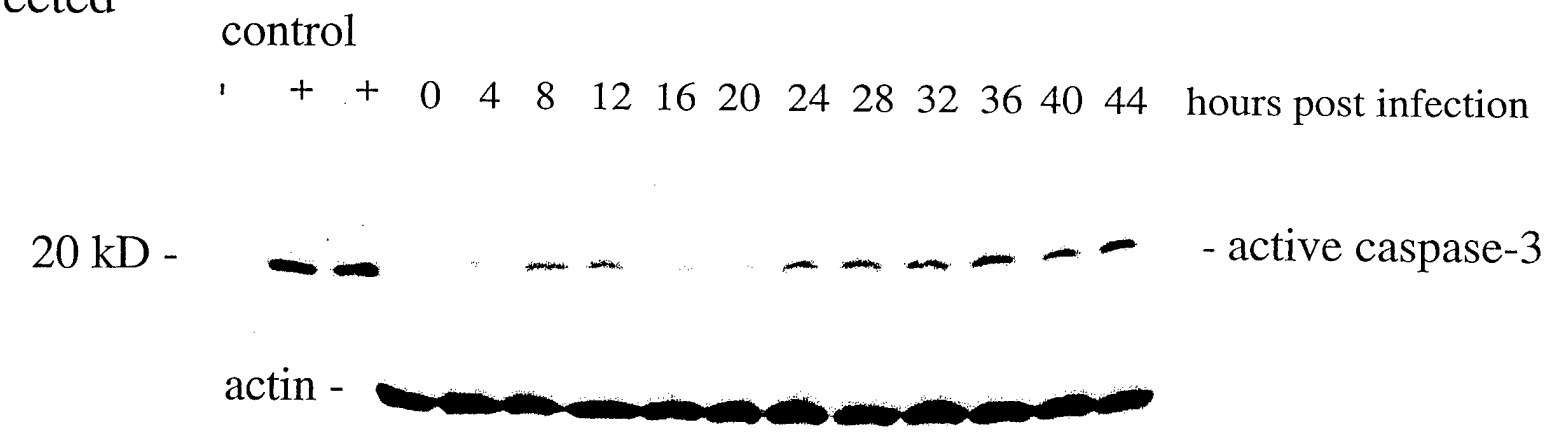

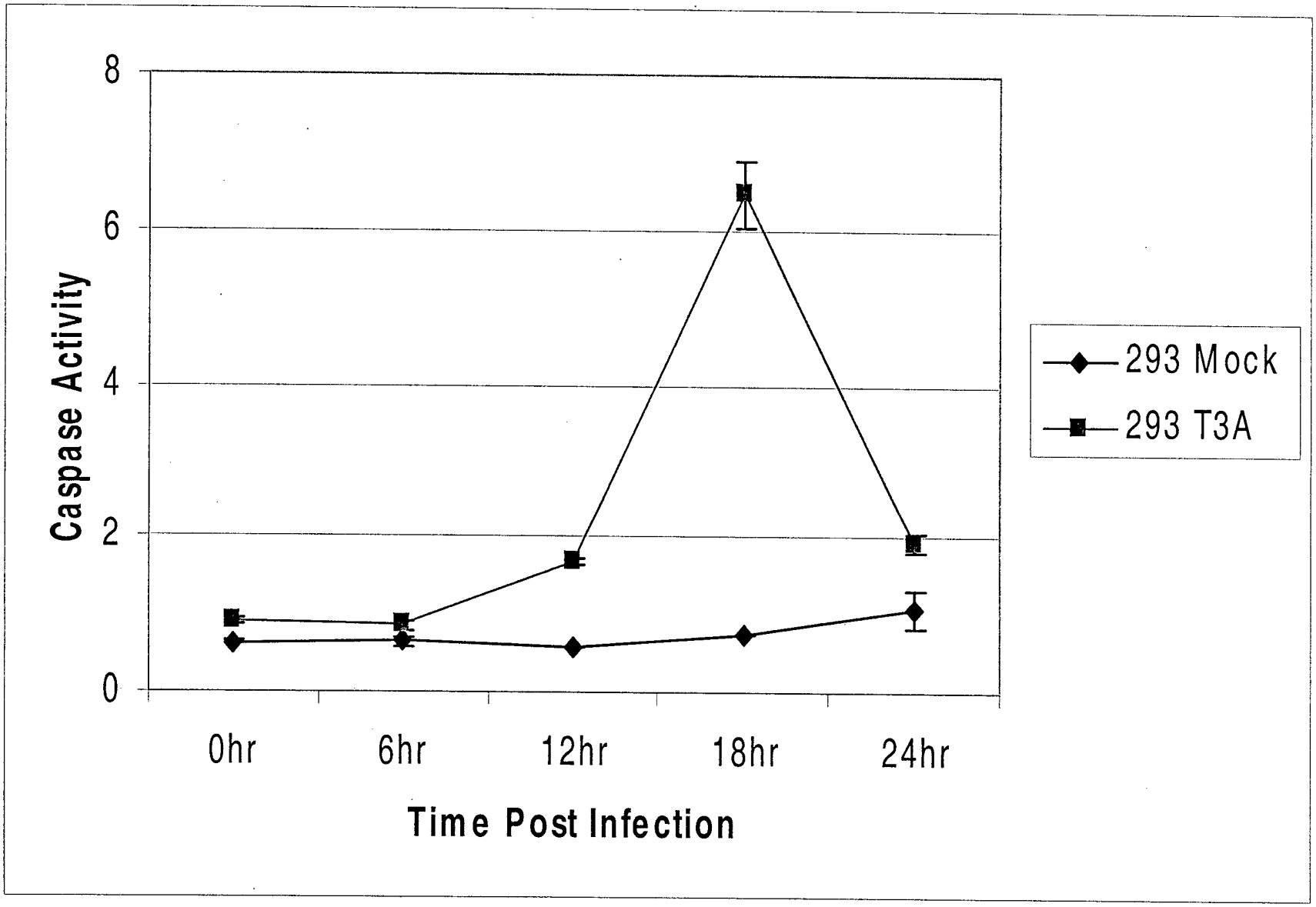
8
6
4
2
0
Caspase Activity
0hr
6hr
12hr
18hr
24hr
Time Post Infection
293 Mock
293 T3A

Mock-infected

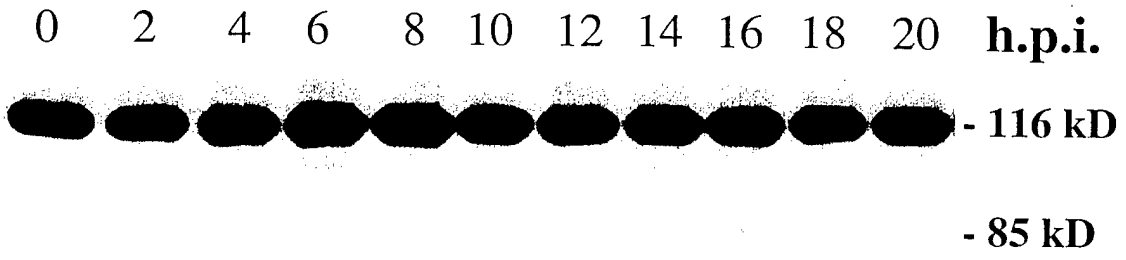

Virus-infected

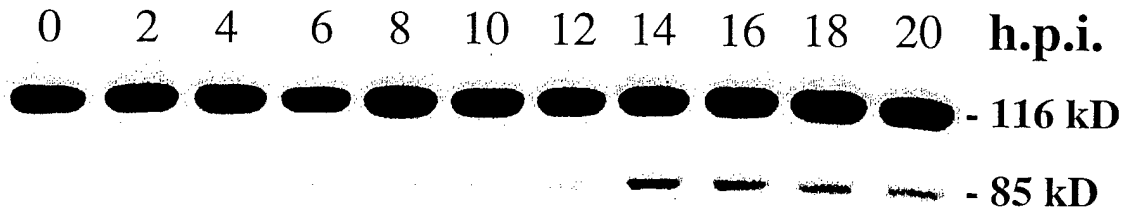

Mock-infected

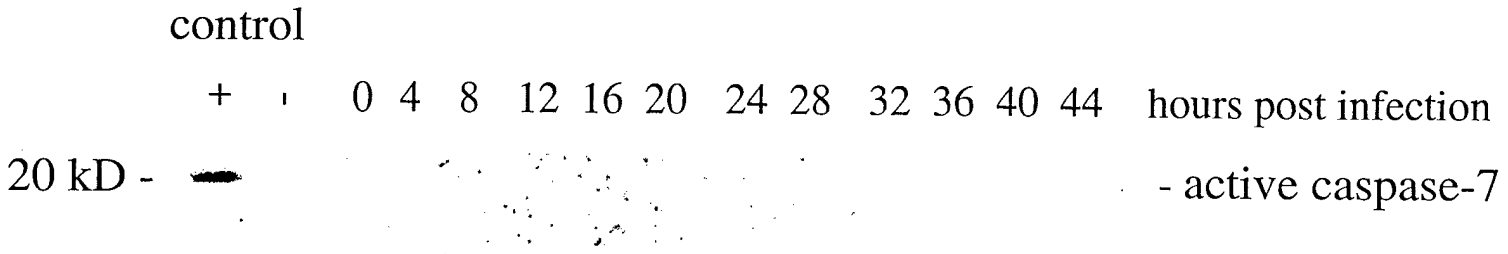

Virus-infected

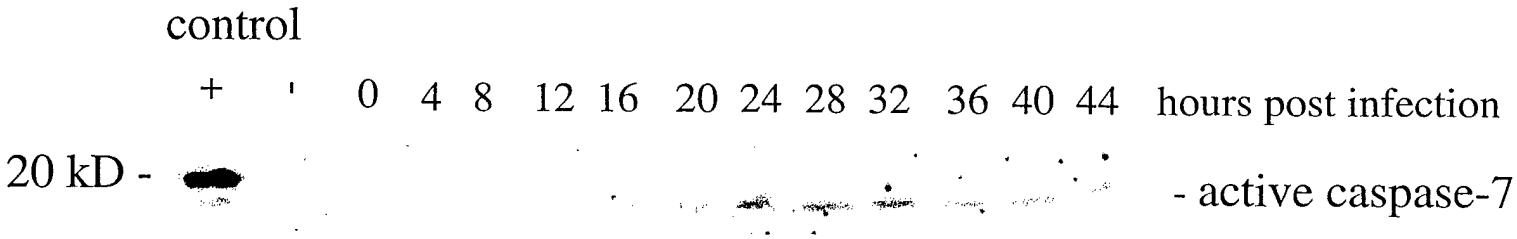

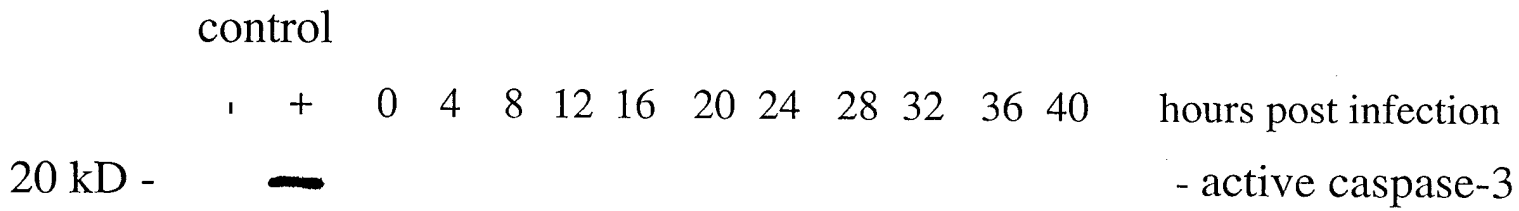
control
- + 0 4 8 12 16 20 24 28 32 36 40 hours post infection
20 kD -
- active caspase-3

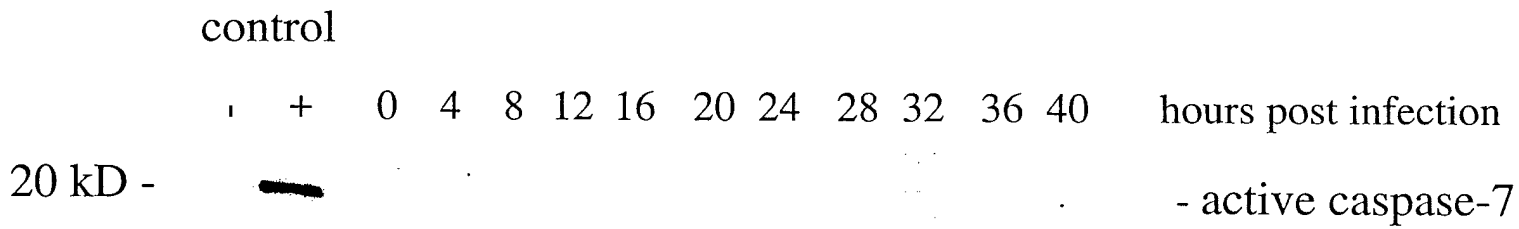
control
- + 0 4 8 12 16 20 24 28 32 36 40 hours post infection
20 kD -
- active caspase-7

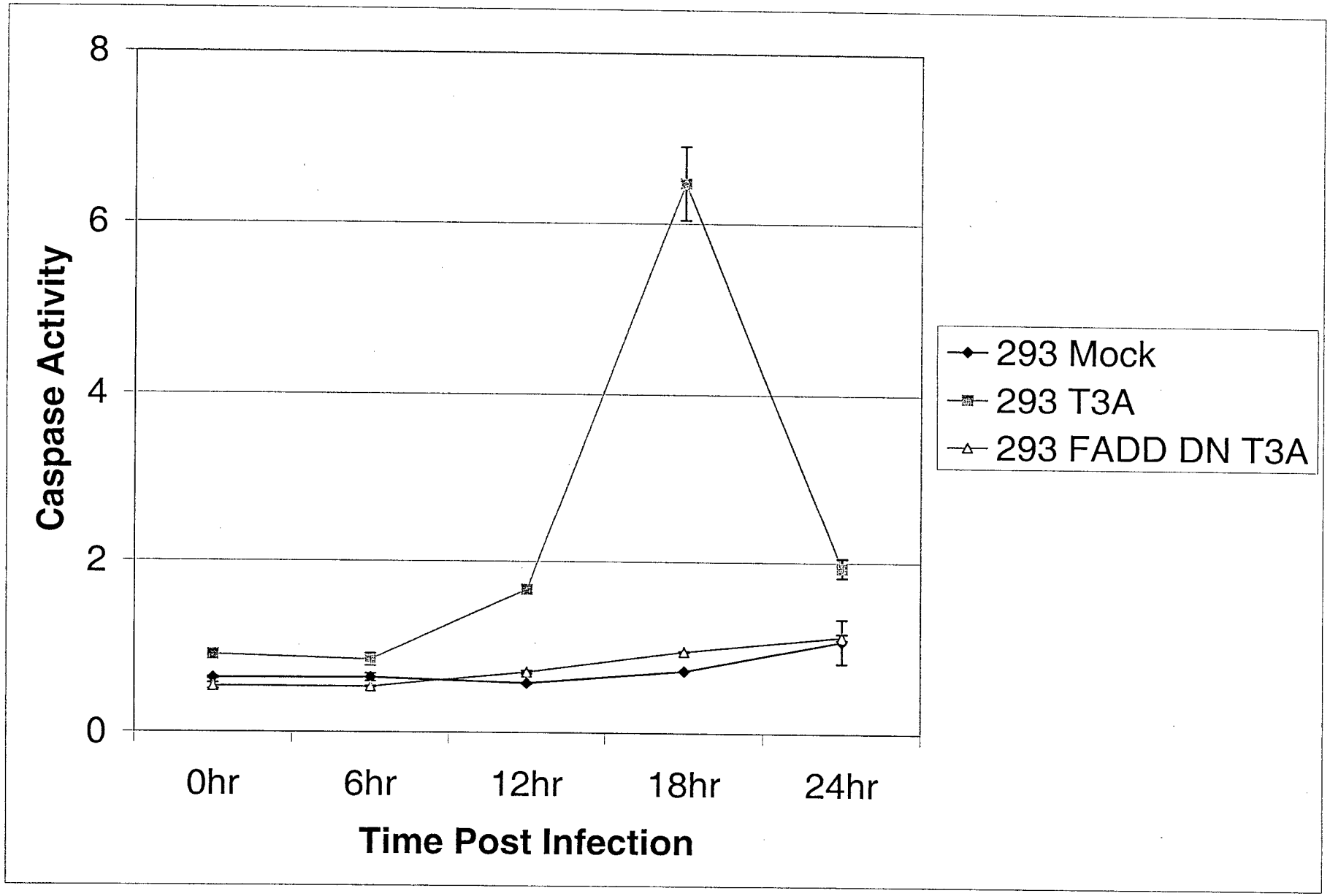
8
6
4
2
0
Caspase Activity
0hr
6hr
12hr
18hr
24hr
Time Post Infection
293 Mock
293 T3A
293 FADD DN T3A

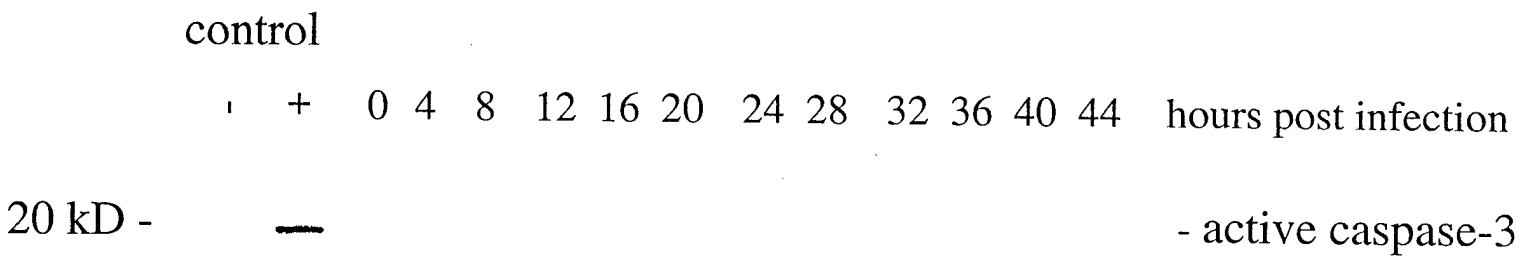
control
- + 0 4 8 12 16 20 24 28 32 36 40 44 hours post infection
20 kD -
- active caspase-3

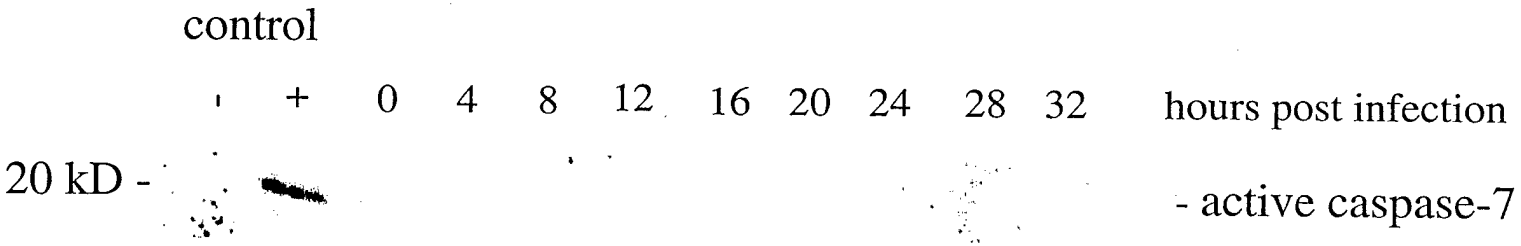
control
- + 0 4 8 12 16 20 24 28 32 hours post infection
20 kD -
- active caspase-7

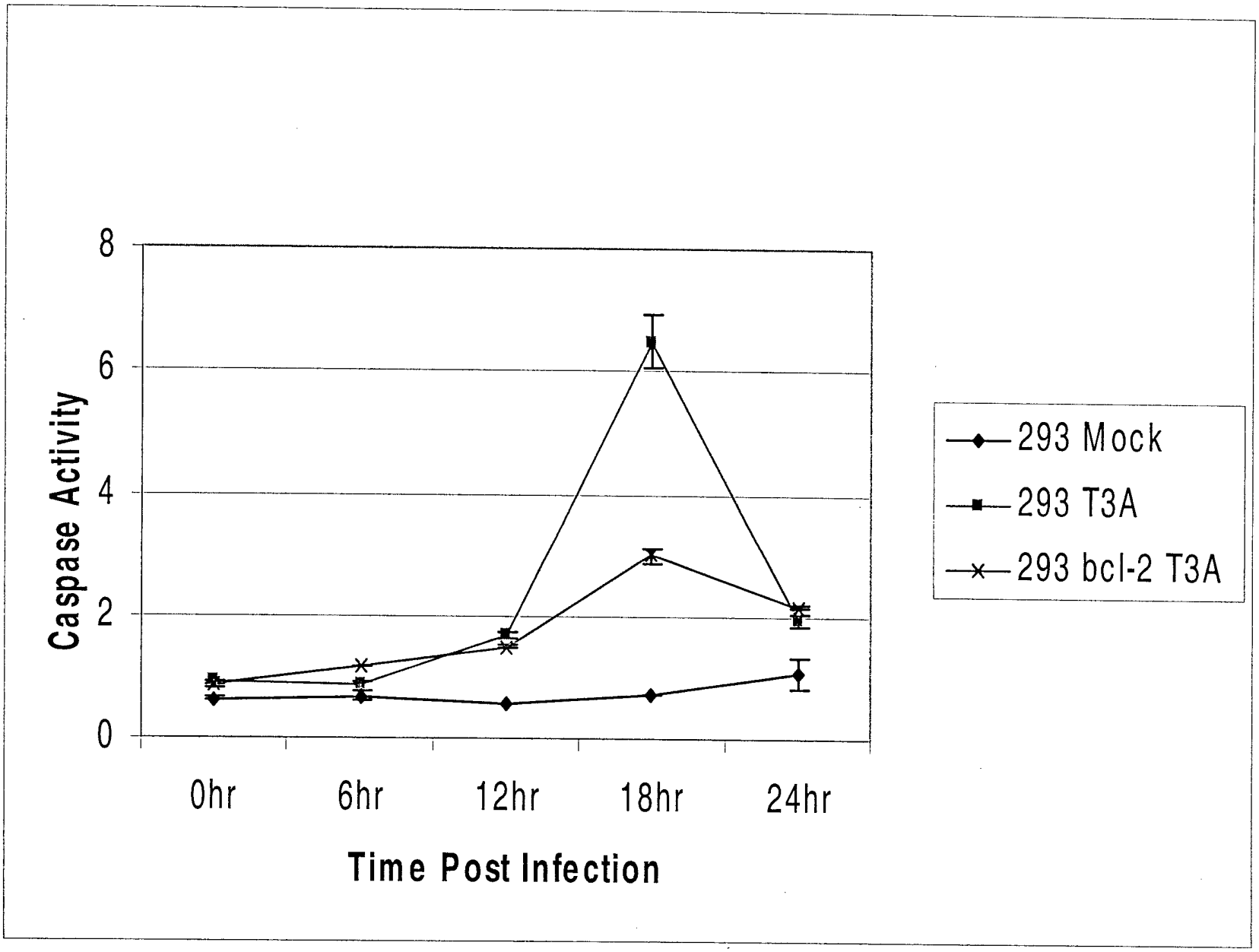
8
6
4
2
0
Caspase Activity
0hr
6hr
12hr
18hr
24hr
Time Post Infection
293 Mock
293 T3A
293 bcl-2 T3A

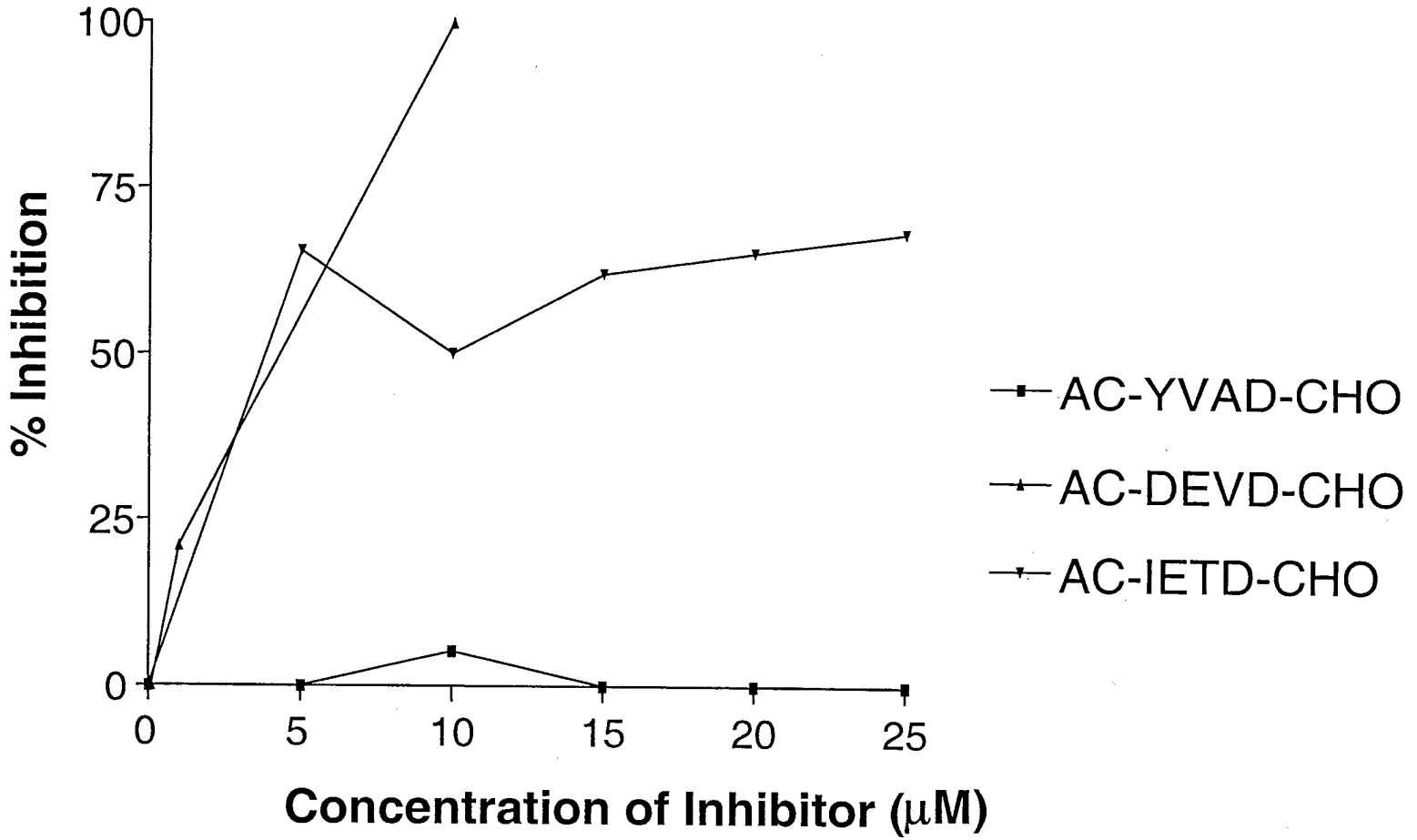
100
75
50
25
0
% Inhibition
0
5
10
15
20
25
Concentration of Inhibitor (μM)
AC-YVAD-CHO
AC-DEVD-CHO
AC-IETD-CHO

Reovirus-induced transcriptional alteration of genes related to cell cycle regulation

GEORGE J. POGGIOLI,[1‡] ROBERTA DEBIASI,[2,3‡] RYAN BICKEL,[3] ROBERT JOTTE,[4,5] AARON SPALDING,[4] GARY L. JOHNSON,[4,6,7] AND KENNETH L. TYLER[1,3,8,9,10*]

‡ These authors contributed equally to this work.

Departments of Neurology,[3] Pediatrics,[2] Medicine,[8] Hematology and Oncology,[5] Microbiology,[1] Pharmacology,[4] and Immunology,[9] University of Colorado Health Sciences Center, and Neurology Service, Denver Veterans Affairs Medical Center,[10] Denver, Colorado 80220 and Program in Molecular Signal Transduction[6] and Division of Basic Sciences, [7] National Jewish Center for Immunology and Respiratory Medicine, Denver, Colorado 80206

*Corresponding author. Mailing address: Department of Neurology (B-182), University of Colorado Health Sciences Center, 4200 E. 9th Ave., Denver, CO 80262. Phone (303) 393-2874. Fax: (303) 393-4686. E-mail: Ken.Tyler@UCHSC.edu

ABSTRACT

Mammalian reovirus infection results in perturbation of host cell cycle progression. Since reovirus infection is known to activate cellular transcription factors, we investigated alterations in cell cycle related gene expression following HEK293 cell infection using the Affymetrix U95A microarray. Serotype 3 reovirus infection results in differential expression of 10 genes classified as encoding proteins that function at the G_1 to S transition, 11 genes classified as encoding proteins that function at G_2 to M transition, and 4 genes classified as encoding proteins that function at the mitotic spindle checkpoint. Serotype 1 reovirus infection results in differential expression of 4 genes classified as encoding proteins that function at the G_1 to S transition, 3 genes classified as encoding proteins that function at G_2 to M transition, and does not alter any genes classified as encoding proteins that function at the mitotic spindle checkpoint. We have previously shown that serotype 3, but not serotype 1, reovirus infection induces a G_2 to M transition arrest resulting from inhibition in cdc2 kinase activity. Of the differentially expressed genes encoding proteins regulating the G_2 to M transition, chk1, wee1, and GADD45 are known to inhibit cdc2 kinase activity. A hypothetical model describing serotype 3 reovirus-induced inhibition of cdc2 kinase is presented, and reovirus-induced perturbation of the G_1 to S, G_2 to M and mitotic spindle checkpoints are discussed.

INTRODUCTION

Perturbation of cell cycle regulation is a characteristic of infection by viruses belonging to a diverse group of viral families. The reasons viruses stimulate proliferation or induce cell cycle arrest are not completely understood. In some cases, virus replication may depend on the availability of host cell precursors, whose abundance varies in a cell cycle specific manner. In other cases, kinases critical in regulating cell cycle progression may be essential for phosphorylating viral proteins (reviewed in 58).

Reoviruses infect a variety of mammalian hosts and serve as an important experimental system for studying the molecular bases of viral pathogenesis (reviewed in 80). Reoviruses also provide a valuable model for studying virus-induced perturbations in cell cycle regulation, since reovirus infection has been associated with G_1 arrest, G_2/M arrest, and disruption of the mitotic spindle apparatus (see below). Inhibition of host cell DNA synthesis is one of the earliest cytopathic effects observed following serotype 3 reovirus infection in cultured cells (reviewed in 53). It was originally suggested that serotype 3 reovirus-induced inhibition of cellular proliferation resulted from inhibition in the initiation of DNA replication (14, 27, 68). However, the degree of cell culture synchronization prior to infection was either incomplete or not specified in these studies, impeding accurate identification of the cell cycle phase affected (14, 68).

Serotype 3 prototype strains type 3 Dearing (T3D) and type 3 Abney (T3A) inhibit cellular DNA synthesis to a greater extent than the serotype 1 prototype strain type 1 Lang (T1L) in a variety of cell lines (20, 23, 75, 82). Studies using T1L × T3D and T1L × T3A reassortant viruses indicate that the serotype 3 S1 gene is the primary determinant of differences in the capacity of reovirus strains to inhibit DNA synthesis

(75, 82). The reovirus S1 gene segment is bicistronic, encoding the viral attachment protein, σ1, and a non-virion associated protein, σ1s, from overlapping, alternative open reading frames (53).

Studies using purified recombinant serotype 3 σ1 protein, and an anti-idiotype antibody (87.92.6) generated against the T3D σ1-specific monoclonal antibody 9BG5 suggest that inhibition of DNA synthesis in some cells may result from engagement of a cell surface receptor by σ1 (23, 70-72). For example, treatment of R1.1 thymoma cells with purified T3D σ1 results in a reversible G_1 to S transition arrest (70, 71). The mechanism for T3D σ1-induced G_1 to S arrest is not clear, but may involve inhibition of $p21^{ras}$ (Ha-ras), since overexpression of Ha-ras prevents T3D σ1-induced G_1 to S transition arrest (71, 72).

We have shown that reovirus infection inhibits cellular proliferation by inducing a G_2/M phase cell cycle arrest in a variety of cell types (63). T3A and T3D induce G_2/M phase cell cycle arrest to a greater extent than T1L (63). Like strain specific differences in the capacity of reovirus to inhibit DNA synthesis (82), strain-specific differences in the capacity of reovirus to induce G_2/M phase cell cycle arrest is determined by the serotype 3 S1 gene (63). The S1 encoded σ1s protein is both necessary and sufficient to induce G_2/M arrest since a σ1s-deficient reovirus mutant fails to induce G_2/M arrest and inducible expression of σ1s results in accumulation of cells in the G_2/M phase of the cell cycle (63).

G_2 to M transition requires the formation and activation of the $p34^{cdc2}$/cdk1 (cdc2)-cyclin B heterodimeric complex (reviewed in 38, 55). Activation of the cdc2-cyclin B complex is regulated by inhibitory phosphorylation of cdc2 (76). We showed

that cdc2 kinase activity is inhibited following serotype 3, not serotype 1, reovirus infection (62). Inhibition of cdc2 kinase activity is, in part, due to serotype 3 σ1s-dependent phosphorylation of cdc2 (62). However, the pathway(s) leading to cdc2 kinase inhibition following serotype 3 reovirus infection remains unclear.

Since G_2 phase arrest cannot easily be distinguished from M phase arrest by flow cytometry using DNA intercalating dyes, it is possible that both G_2 to M checkpoint arrest and mitotic spindle checkpoint arrest contribute to reovirus-induced G_2/M phase cell cycle arrest. Electron microscopic studies have shown that reovirus particles align along parallel arrays of microtubules and have the capacity to bind microtubules *in vitro* (3). Serotype 3 reovirus particles associate with microtubules of the mitotic spindle apparatus in infected cells (15), and require microtubule stability for fast axonal transport (81). In addition to association with microtubules, reovirus infection results in progressive disruption and reorganization of the vimentin (intermediate) filament network (74). The binding of reovirus to microtubules and the disruption of vimentin filaments may lead to changes in microtubule tension or binding to the kinetochore. Reovirus-induced disruption of the microtubule-kinetochore association could lead to activation of the mitotic spindle checkpoint and M phase cell cycle arrest (2, 78).

Serotype 3 reovirus infection activates the cellular transcription factors NF-κB (4, 13) and c-jun (P. Clarke, personal communication). Activation of transcription factors following reovirus infection suggests that gene expression is critical in reovirus-induced pathogenesis. To identify potential pathways leading to serotype 3 reovirus-induced inhibition of proliferation, we conducted experiments to investigate the transcriptional response following serotype 3 and serotype 1 reovirus infection. High-throughput

screening of over 12,000 genes using oligonucleotide microarrays has identified potential reovirus-induced signaling pathways regulating cell cycle control. Of the genes differentially expressed following reovirus infection, several encode regulators of the critical G_2 to M transition kinase cdc2.

MATERIALS AND METHODS

Infection. Human embryonic kidney (HEK293) cells (ATCC CRL1573) were plated in T75 flasks (Becton Dickinson, Franklin Lakes, NJ) at a density of 5×10^6 cells per flask in a volume of 12 ml Dulbecco's modified Eagle's medium (DMEM) supplemented to contain 10% heat-inactivated fetal bovine serum, 2 mM L-glutamine (Gibco-BRL, Gaithersburg, MD), 1 mM sodium pyruvate (Gibco-BRL) and 100 U of penicillin per ml and 100 μg of streptomycin per ml (Gibco-BRL). After 24 h of incubation, when cells were 60-70% confluent, the medium was removed, and cells were infected with viral strain T3A at a multiplicity of infection (MOI) of 100 PFU per cell in a volume of 2 ml at 37°C for 1 h. High MOI was used to ensure that all susceptible cells were infected, and studies in our laboratory indicate that high MOI enhances the reproducibility of gene expression studies. Following infection, 10 ml of DMEM was added and flasks were incubated at 37°C. Control infections were inoculated with a virus-free cell lysate control. In order to identify differentially regulated transcripts important for serotype 3 reovirus-induced cell cycle perturbation, an identical experiment using T1L was performed.

cRNA target preparation and hybridization. Cells were harvested at 6, 12 and 24 h post-infection, washed with PBS, and total RNA was isolated using the RNeasy Mini Kit (Qiagen, Valencia, CA). 10 μg of RNA was converted to cDNA using SuperScript Choice (Gibco-BRL) substituting HPLC purified T7-oligo-$d(T)_{24}$ for random primers. Second strand synthesis was performed using T4 DNA polymerase and cDNA was isolated by phenol/chloroform extraction using phase lock gels. Isolated cDNA was *in vitro* transcribed using the BioArray High Yield RNA Transcript Labeling Kit (Enzo

Biochem, New York, New York) supplied with biotin labeled UTP and CTP to produce biotin labeled cRNA. Labeled cRNA was isolated using an RNeasy Mini Kit column (Qiagen), and quantified for purity and yield. cRNA was fragmented in 100 mM potassium acetate, 30 mM magnesium acetate and 40 mM Tris-acetate, pH 8.1 for 35 min at 94°C and hybridization performance was analyzed using Test 2 arrays (Affymetrix, Santa Clara, CA). Target cRNA was hybridized to the U95A microarray (Affymetrix) as per Affymetrix protocols. Briefly, 15 μg of fragmented cRNA was hybridized for 16 h at 45°C with constant rotation (60 rpm). Microarrays were washed and stained with streptavidin conjugated phycoerythrin (SAPE) using the Affymetrix GeneChip® Fluidic Station 400 (Affymetrix). Staining intensity was antibody amplified using a biotinylated anti-streptavidin antibody at a concentration of 3 μg per ml followed by a second SAPE stain and visualized at 570 nm. All hybridization steps were performed at the UCHSC Cancer Center Microarray Facility.

Data analysis. Each gene on the U95A array is represented by 20 different 25 base cDNA oligonucleotides complementary to a cRNA target transcript (perfect match). As a hybridization specificity control, an oligonucleotide containing a single base substitution corresponding to each perfect match cDNA oligonucleotide (mismatch) is represented on the array. The combination of perfect match and mismatch cDNA oligonucleotides for each gene is termed a probe set. Using Affymetrix-defined absolute mathematical algorithms describing perfect match and mismatch intensities, each gene was defined as absent or present and assigned a value. Binding intensity values were scaled to evaluate differential expression following reovirus infection. Using Affymetrix-defined comparison mathematical algorithms, a reovirus-induced transcript

was classified as not changed, marginally increased, marginally decreased, increased or decreased, and a fold change in expression was calculated. Nucleotide accession numbers for transcripts that were not changed and cited in the text appear in Table 2. Since each condition was performed in duplicate, we used two additional criteria to classify a gene as significantly up or downregulated following reovirus infection: (1) Reovirus-induced expression of a gene at each timepoint must be classified as increased/marginally increased (or decreased/marginally decreased) in each virus-infected condition compared to each mock-infected condition. (2) The mean fold change in reovirus-induced gene expression must be greater than 2. Mean transcriptional expression of a gene at a timepoint was calculated by the sum of the fold change in gene expression for each virus-infected condition compared to each mock-infected condition divided by four. Standard errors indicate standard errors in mean transcriptional expression of a gene.

RT-PCR. HEK293 cells were infected as described above. Cells were harvested at 12 and 24 h post-infection, washed with PBS, and RNA was isolated. 5 μg of RNA was converted to cDNA using the SuperScript Preamplification System (Gibco-BRL) supplied with oligo-d$(T)_{12-18}$ primer. Reverse transcription was performed at 42°C for 1 h. PCR was performed using primers generated against chk1 (AF016582) (forward: 5′-CTG AAG AAG CAG TCG CAG TG-3′; reverse: 5′-TTC CAC AGG ACC AAA CAT CA-3′), wee1 (U10564) (forward: 5′-AAC CTC AAT CCC AAA TGC TG-3′; reverse: 5′-TTG CCA TCT GTG CTT TCT TG-3′), GADD45 (M60974) (forward: 5′-TGC GAG AAC GAC ATC AAC AT-3′; reverse: 5′-TCC CGG CAA AAA CAA ATA AG-3′), and β-actin (BC004251) (forward: 5′-GAA ACT ACC TTC AAC TCC ATC-3′; reverse: 5′-

CGA GGC CAG GAT GGA GCC GCC-3′), yielding product sizes of 495, 506, 200, and 219 base pairs, respectively. PCR cycle conditions were 94°C for 30 s, 55°C for 30 s and 72°C for 1 min for 25 cycles. Dilutions of cDNA were performed to determine the linear range for each primer pair. PCR products were resolved on a 2% agarose gel containing ethidium bromide and visualized with UV light. Densitometric analysis was performed using a FluorS MultiImager System and Quantity One software (Biorad, Hercules, CA).

RESULTS

Reovirus-induced alterations in transcription. Previous work has established that serotype 3, not serotype 1, reovirus infection induces perturbations in cell cycle regulation. To identify potential pathways exploited by serotype 3 reovirus to deregulate host cell cycle, we evaluated the profile of HEK293 cellular transcription following T3A infection at 6, 12 and 24 h using the Affymetrix U95A microarray. We found that serotype 3 reovirus infection induced significant changes in the expression of 25 genes encoding proteins regulating cell cycle progression. Ten genes (40%) were classified as encoding proteins that function at the G_1 to S transition, 11 genes (44%) were classified as encoding proteins that function at the G_2 to M transition, and 4 genes (16%) were classified as encoding proteins that function at the mitotic spindle checkpoint (Table 1). Twenty cell cycle related transcripts were increased following serotype 3 reovirus infection and 5 transcripts were decreased. Four of the 5 downregulated genes were classified as transcripts encoding proteins regulating G_2 to M transition. No cell cycle related genes were differentially expressed at 6 h post-infection. At 12 h, 5 cell cycle related genes were found to be differentially expressed following serotype 3 reovirus infection, 2 were upregulated and 3 were downregulated. Four of the 5 genes altered at 12 h post-infection were classified as transcripts encoding proteins regulating G_2 to M transition. At 24 h post-infection, 23 cell cycle related genes were found to be differentially expressed, 19 were upregulated and 3 were downregulated. One transcript found to be upregulated and one found to be downregulated at 12 h post-T3A infection were increased and decreased at 24 h post-infection, respectively. Histone H1, histone H2A and wee1 were represented twice on the array, and histone H2B was represented 6

times. Fold changes in gene expression for replicates and for multiple representations of a gene were highly reproducible.

To identify differentially regulated transcripts important for serotype 3 reovirus induced cell cycle perturbation, we compared the profile of HEK293 cellular transcription following T1L infection at 24 h post-infection using the Affymetrix U95A microarray. We found that serotype 1 reovirus infection induced significant changes in the expression of 6 genes encoding proteins regulating cell cycle progression. Three genes (50%) were classified as encoding proteins that function at the G_1 to S transition, and 3 genes (50%) were classified as encoding proteins that function at the G_2 to M transition (Table 1). T1L infection did not alter any genes classified as encoding proteins that function at the mitotic spindle checkpoint at 24 h post-infection (Table 1). Each cell cycle related transcript differentially regulated following serotype 1 reovirus infection was increased. T1L infection resulted in differential regulation of 23% of transcripts differentially regulated by T3A at 24 h post-infection. The transcript encoding E2F6 was the only cell cycle related transcript differentially regulated by T1L infection that was not differentially regulated by T3A infection. Of the 9 T3A regulated transcripts encoding proteins that function at the G_1 to S transition at 24 h post-infection, 2 (22%) were differentially regulated by T1L. Of the 9 T3A regulated transcripts encoding proteins that function at the G_2 to M transition at 24 h post-infection, 3 (33%) were differentially regulated by T1L. These results indicate that serotype 3 reovirus infection perturbs the differential expression of genes encoding proteins that regulate the G_1 to S, G_2 to M and mitotic spindle checkpoints, and that T1L infection results in differential regulation of a subset of these transcripts. In addition, the earliest detectable changes in transcription

following T3A infection were genes encoding G_2 to M regulatory proteins, suggesting that deregulation of the G_2 to M transition is an early event following serotype 3 reovirus infection.

Reovirus-induced alterations in genes encoding proteins that regulate G_1 to S progression. Treatment of specific cell types, including R1.1 thymoma cells, with purified T3D-σ1 protein leads to a reversible G_1 to S transition arrest that depends upon the inhibition of Ha-ras (70-72). Ten genes encoding proteins that function at the G_1 to S transition were altered following serotype 3 reovirus infection. The level of Ha-ras transcription was not changed following reovirus infection. The expression of the gene encoding N-ras was also not inhibited and, was, in fact, increased 2.1 ± 0.2 fold in serotype 3 reovirus-infected cells at 24 h post-infection (Table 1).

The G_1 to S transition requires activation of cyclin dependent kinases (cdk) (57). Cdk2, 4 and 6 kinase activity results in phosphorylation of the retinoblastoma protein (pRb) and the pRb related proteins, p107 and p130. Phosphorylation of pRb leads to activation of the transcription factor E2F (31). The level of cdk4 transcription was not changed following reovirus infection (Table 2). Cdk2 and 6 were not represented on the U95A microarray. The levels of pRb, p107, p130, E2F1, 2, 4, 5, and 6 transcription were not changed following reovirus infection (Table 2), except for the transcript encoding E2F6, which was upregulated 2.1 ± 0.1 fold following T1L infection (Table 1). Activation of cdk2, 4 or 6 requires binding to cyclin E or cyclin D (31). Cyclin E expression was reduced 2.8 ± 0.1 fold in serotype 3 reovirus-infected cells. However, the level of cyclin E2, a cyclin E isoform, gene expression was increased 2.1 ± 0.2 fold in

serotype 3 reovirus-infected cells (Table 1). The levels of cyclin D1, 2, and 3 expression were not changed following reovirus infection (Table 2).

Activation of cdk2 depends upon its phosphorylation state (57). The level of protein phosphatase 2C (PP2C) transcription at 24 h post-infection with T3A was 5.3 ± 0.4 greater than a mock-infected control. Cdk-cyclin complex activity is known to be inhibited by cyclin dependent kinase inhibitors (CDKI) (29, 31). The levels of CDKI expression, including $p21^{WAF1/CIP1}$, $p27^{KIP1}$, $p57^{KIP2}$, $p16^{INK4a}$, $p15^{INK4b}$, and $p19^{INK4d}$ were not changed following reovirus infection (Table 2). Since active cdk2, 4 or 6 kinase results in E2F dependent transcription, the transcriptional level of E2F responsive genes necessary for G_1 to S transition, including cyclin E, cyclin A, cdc2, cdc25C, $p21^{WAF1/CIP1}$, c-myc, B-myb, p107, E2F1, E2F2, dihydrofolate reductase, thymidine kinase, DNA polymerase α, histone H2A and cdc6, serve as a measure of cdk2, 4 or 6 kinase activity (26). The level of these E2F responsive transcripts were not changed following reovirus infection except for cyclin E, c-myc, and DNA polymerase α, which were downregulated 2.8 ± 0.1, 2.0 ± 0.0, and 2.5 ± 0.2 fold following serotype 3 reovirus infection, respectively, and histone H2A and cdc2, which were upregulated 2.0 ± 0.1 or 2.2 ± 0.1 and 1.8 fold in serotype 3 reovirus compared to mock-infected cells. The failure to detect a coherent pattern of gene expression encoding key G_1 to S checkpoint control proteins is consistent with our observation that reovirus infection does not induce G_1 arrest in HEK293 cells. However, we did find changes in expression of genes encoding histones, cyclin E and E2, and some E2F responsive transcripts following serotype 3 reovirus infection.

Reovirus-induced alterations in genes encoding proteins that regulate G_2 to M progression. We have previously shown that serotype 3 reovirus-induced G_2/M phase cell cycle arrest is due to inhibitory phosphorylation of cdc2 (62). Eleven genes encoding proteins that function at the G_2 to M transition were altered following serotype 3 reovirus infection. These changes were among the earliest changes in gene expression identified in serotype 3 reovirus-infected cells. The level of cdc2 transcription at 24 h post-infection with T3A was 1.8 fold greater than a mock-infected control. We have not reproducibly detected changes in levels of cdc2 protein in reovirus-infected cells, however we have consistently found an increase in the proportion of hyperphosphorylated cdc2 following serotype 3 reovirus infection (62). An increase in cdc2 phosphorylation could result from an increase in wee1 kinase activity, which directly phosphorylates and inactivates cdc2 (60). wee1 was determined to be upregulated at 24 h post-infection using the U95A microarray (Table 1). The level of wee1 transcription at 24 h post-infection with T3A was 2.4 ± 0.1 (for accession number U10564) and 2.5 ± 0.1 (for accession number X62048) fold greater than a mock-infected control. The increase in wee1 transcription following T3A infection was confirmed by RT-PCR and was 1.8 ± 0.1 fold greater than a mock-infected control at 24 h post-infection (Fig. 1A). The level of wee1 transcription at 24 h post-infection with T1L was 1.9 ± 0.1 (for accession number U10564) and 2.0 ± 0.1 (for accession number X62048) fold greater than a mock-infected control. Increased levels of wee1 kinase may result in inhibitory phosphorylation of cdc2 following serotype 3 reovirus infection, but increases in wee1 is not sufficient for serotype 3 reovirus-induced phosphorylation of cdc2 since T1L infection results in similar increases in wee1 transcription.

Increased inhibitory phosphorylation of cdc2 following reovirus infection could also result from inactivation of the cdc2 specific phosphatase cdc25C (reviewed in 38). Following reovirus infection, the level of cdc25C transcription was not changed (Table 2). The kinase chk1 can enhance wee1 kinase activity (56) and inhibit cdc25C phosphatase activity (22). The level of chk1 transcription at 24 h post-infection with T3A was 3.2 ± 0.1 fold greater than a mock-infected control (Table 1). The increase in chk1 transcription following T3A infection was confirmed by RT-PCR and was 1.6 ± 0.1 fold greater than a mock-infected control at 24 h post-infection (Fig. 1B). This suggests that increased levels of chk1 kinase may result in inhibitory phosphorylation of cdc25C on ser-216 and activation of wee1 following serotype 3 reovirus infection.

In addition to the inhibition of cdc2 by phosphorylation, serotype 3 reovirus-induced G_2/M phase cell cycle arrest could result from dissociation of cdc2 from cyclin B. The level of cyclin B transcription was not changed following reovirus infection (Table 2), consistent with our studies suggesting that changes in the level of cyclin B protein are not responsible for reovirus-induced G_2 to M transition arrest (62).

The growth arrest and damage inducible protein 45 (GADD45) is known to inhibit cdc2 kinase activity by physically dissociating cdc2 kinase from cyclin B (87). To determine whether GADD45 could be responsible for reovirus-induced inactivation of cdc2, we analyzed the transcriptional expression of GADD45 following serotype 3 reovirus infection. The level of GADD45 transcription at 12 and 24 h post-infection with T3A was 3.3 ± 0.2 and 4.9 ± 0.1 fold greater than a mock-infected control, respectively (Table 1). The increase in GADD45 transcription following T3A infection was confirmed by RT-PCR and was 1.6 fold greater than a mock-infected control at 24 h post-

infection (Fig. 1C). The level of GADD45 transcription at 24 h post-infection with T1L was 4.4 ± 0.1 fold greater than a mock-infected control. This suggests that increased levels of GADD45 may result in inhibition of cdc2 by physically dissociating cdc2 from cyclin B following serotype 3 reovirus infection, but increases in GADD45 is not sufficient for serotype 3 reovirus-induced phosphorylation of cdc2 since T1L infection results in a similar increase in GADD45 transcription. Thus, we found that reovirus infection induces changes in levels of gene expression encoding key proteins regulating cdc2 kinase activity, including wee1, chk1 and GADD45, which is consistent with our previous studies suggesting a central role for cdc2 inhibition in serotype 3 reovirus-induced G_2/M phase cell cycle arrest (63).

Reovirus-induced alterations in genes encoding proteins that regulate mitotic spindle checkpoint signaling. Reovirus particles are capable of binding microtubules, and infection results in progressive disruption of vimentin filaments. Changes in microtubule tension or binding to the kinetochore could lead to reovirus-induced mitotic arrest. Four genes encoding proteins that function at the mitotic spindle checkpoint were altered following reovirus infection. The transcriptional level of mitotic spindle checkpoint components that monitor spindle abnormalities, including MAD2, 3 and BUB1, were not changed following reovirus-infection (Table 2). The level of BUB3 transcription at 24 h post-infection with T3A was 2.2 ± 0.1 fold greater than a mock-infected control (Table 1). Activation of the mitotic spindle checkpoint leads to inhibition of the anaphase promoting complex (APC) and M phase cell cycle arrest (2, 78). Nuc2, an APC component, transcription was 2.1 ± 0.2 fold greater than a mock-

infected control (Table 1). These results suggest that serotype 3 reovirus-induced alterations in gene transcription may induce M phase cell cycle arrest.

DISCUSSION

The use of DNA microarray technology following reovirus infection has identified several genes encoding proteins that may play a role in serotype 3 reovirus-induced disruption of the cell cycle. The results presented here provide a comprehensive overview of alterations in gene expression encoding proteins that regulate cell cycle progression following reovirus infection.

G_1 to S checkpoint: Reovirus-induced alterations in G_1 to S restriction checkpoint control. Treatment with purified T3D-σ1 protein leads to a reversible G_1 to S phase transition arrest in R1.1 thymoma cells that is dependent upon Ha-ras inhibition (70-72). However, G_1 to S arrest is not a universal feature of reovirus infection and does not occur in reovirus-infected HEK293 cells (63). We were unable to detect changes in expression of $p21^{ras}$-related genes involved in G_1 to S regulation, and found that transcription of the $p21^{ras}$ isoform, N-ras, was selectively increased following serotype 3 reovirus infection.

G_1 to S transition arrest following serotype 3 reovirus infection could result from inactivation of the G_1 to S cyclin dependent kinases cdk2, 4, or 6 by the protein phosphatase PP2C-α. PP2C-α is known to dephosphorylate activating phosphates on cdk2 (9), which may result in abrogation of cdk2 kinase activity. Decreased expression of the cdk2 regulatory cyclin, cyclin E, was counterbalanced by an increase in the expression of the cyclin E isoform, cyclin E2, suggesting that G_1 cyclin expression does not play a significant role in regulating serotype 3 reovirus-induced G_1 to S progression. Alterations in histone synthesis and alterations in the relative levels of histone proteins could alter G_1 to S progression considering the onset of DNA synthesis, but no clear

model has been elucidated (19). Collectively, these findings indicate that serotype 3 reovirus-induced alterations in gene expression is not consistent with G_1 to S arrest in HEK293 cells.

G_2 to M checkpoint: Reovirus-induced inhibition of cdc2 by phosphorylation. Serotype 3 reovirus-induced G_2/M phase cell cycle arrest results from a reduction in cdc2 kinase activity due to inhibitory phosphorylation (62). An increase in hyperphosphorylated cdc2 could be due to either increases in cdc2-specific kinase activity and/or decreases in cdc2-specific phosphatase activity. The kinases wee1 and myt1, and the phosphatase cdc25C regulate the phosphorylation state of cdc2 (reviewed in 38). Following serotype 3 reovirus infection, wee1 transcription is elevated, suggesting that this kinase may play a role in inhibiting cdc2 (Fig. 2). However, an elevation in wee1 transcript is not sufficient for serotype 3 reovirus-induced inhibitory phosphorylation of cdc2 since the transcript encoding wee1 kinase is similarly upregulated following T1L infection. The activity of the cdc2-specific phosphatase cdc25C is regulated by phosphorylation. Hyperphosphorylation of cdc25C results in active phosphatase activity capable of removing inhibitory phosphates from cdc2 kinase (reviewed in 38). Following reovirus infection, cdc25C is inhibited by dephosphorylation (62). It is suggested that HIV vpr protein can inhibit cdc2 kinase activity (30, 64) through mechanisms requiring wee1 and involving the inactivation of cdc25C (35, 48).

Protein phosphatase 2A (PP2A) or PP2A-like activity is capable of negatively regulating cdc25C by removing activating phosphates (12, 42, 45). HIV vpr is reported to inactivate cdc25C by physically targeting PP2A to the nucleus and enhancing the

recruitment and dephosphorylation of cdc25C though association with the PP2A-B55 regulatory subunit (35). Following serotype 3 reovirus infection, we found selective decreased expression of the PP2A-B56-β regulatory subunit. Since the B56-β regulatory subunit is known to localize PP2A to the cytoplasm (50), downregulation of B56-β production may lead to increased nuclear localization of PP2A following reovirus infection (Fig. 2). Furthermore, upregulation of SG2NA (S/G_2 nuclear antigen) may target PP2A to the nucleus following serotype 3 reovirus infection since SG2NA is known to both localize to the nucleus (52) and interact with the C subunit of PP2A (51). However, an elevation in SG2NA transcript is not sufficient for serotype 3 reovirus-induced dephosphorylation of cdc25C since the transcript encoding SG2NA is similarly upregulated following T1L infection. Nonetheless, it is possible that reovirus-induced nuclear localization of PP2A could inhibit cdc25C, which is consistent with cdc2 hyperphosphorylation and G_2/M phase cell cycle arrest found following serotype 3 reovirus infection.

Cdc25C activity is also inhibited following phosphorylation by the kinases chk1 and chk2 (22, 69). Phosphorylation of cdc25C on ser-216 by chk1 or chk2 leads to 14-3-3 protein binding, which results in sequestration of cdc25C into the cytoplasm (47, 61). Export to the cytoplasm physically separates cdc25C from cdc2 kinase. We have found that reovirus infection is associated with increased expression of chk1, suggesting that this kinase plays a role in reovirus-induced inhibition of cdc25C (Fig. 2). Chk1 kinase activity is also suggested to regulate wee1 sub-cellular localization, such that cdc2 kinase is phosphorylated and inactivated (56) (Fig. 2). This suggests that serotype 3 reovirus

infection may selectively increase the level of chk1 kinase activity to modulate the activity of kinases and phosphatases directly responsible for regulating cdc2 activity.

G_2 to M checkpoint: Reovirus-induced inhibition of cdc2 by physical dissociation from cyclin B. An alternative mechanism for cdc2 inhibition is by physical interaction with the growth arrest and DNA damage inducible protein, GADD45. GADD45 inhibits cdc2 kinase by physically dissociating cdc2 from cyclin B (83, 87). Physical dissociation of cdc2 kinase from its regulatory cyclin results in abrogation of cdc2 kinase activity and G_2 to M checkpoint arrest (24, 55). Serotype 3 reovirus induces an increase in GADD45 expression suggesting that GADD45 plays a role in reovirus-induced G_2 to M checkpoint arrest (Fig. 2). However, an elevation in GADD45 transcript is not sufficient for serotype 3 reovirus-induced inhibition of cdc2 kinase activity since the transcript encoding GADD45 is similarly upregulated following T1L infection. Interestingly, it is possible that GADD45-induced inhibition of cdc2 kinase activity results in accumulation of cells in the G_2/M phase of the cell cycle following infection with a Herpes Simplex Virus (HSV) restricted to expressing the infected cell polypeptide ICP0 since this virus induces an increase in GADD45 protein levels (34). The capacity of GADD45 to regulate cdc2 activity is a function of protein concentration (83). GADD45 transcription is regulated by p53 (41, 87) and Brca1 (28, 39). We have preliminary data suggesting that serotype 3 reovirus infection may result in increased expression of Brca1 protein. Reovirus-induced increase in Brca1 activity may result from changes in the activity of ATM or ATM-related kinases (46). Although we did not detect changes in expression of the gene encoding ATM, the expression of FRP1, a

kinase with significant homology to ATM kinases (11), was selectively increased following serotype 3 reovirus infection.

The data presented in this manuscript and our previous studies are consistent with a model in which reovirus-induced phosphorylation of cdc2 results in G_2/M phase cell cycle arrest that is dependent upon σ1s expression (63). σ1s is a highly basic protein (16, 17) that is present in the nucleus of serotype 3 infected cells (7, 67) where it could directly interact with cdc2 or proteins regulating cdc2 kinase activity. However, the role for σ1s in serotype 3 reovirus-induced G_2/M phase cell cycle arrest is not yet determined.

Mitotic spindle checkpoint: Reovirus-induced alterations in spindle checkpoint signaling. Reovirus-induced disruption of the microtubule-kinetochore association may contribute to G_2/M arrest by activating the mitotic spindle checkpoint, which inhibits the APC and results in M phase arrest (2, 78). Selective expression of several genes encoding proteins with putative roles in regulating the mitotic spindle checkpoint were altered following serotype 3 reovirus infection. For example, Bub3 is an integral component of mitotic spindle checkpoint signaling, localizes to unattached kinetochores, and phosphorylates and complexes with Bub1 (6, 40, 66, 79). The functions of MPP11 and HZWINT1 are not completely understood, but have been speculated to contribute to mitotic spindle checkpoint regulation since they localize to mitotic structures, including kinetochores (49, 65, 77). These results suggest that deregulation of mitotic spindle checkpoint proteins may also contribute to serotype 3 reovirus-induced G_2/M phase cell cycle arrest.

Other proteins functioning in G_2 or M. Several genes encoding proteins that influence both the G_2 to M and the mitotic spindle checkpoints were selectively differentially

regulated following serotype 3 reovirus infection. For example, polo-like kinase activity is important in regulating G_2 to M transition events by activating cdc25C, and M phase events including APC regulation, centrosome maturation and bipolar spindle formation (25, 54). SAK, a polo-like kinase (36), was found to be upregulated following serotype 3 reovirus infection however, the role of SAK in cell cycle regulation is not clear. Interestingly, expression of murine SAK-a is cell cycle regulated with levels peaking in M phase, which is consistent with a role in the latter portion of the cell cycle (21). This suggests that serotype 3 reovirus may perturb both the G_2 to M transition and mitotic spindle checkpoint to ensure host cell cycle arrest in the G_2/M phase.

Serotype 3 reovirus infection also selectively altered expression of genes encoding proteins with cdc2-related serine/threonine kinase activity, including C-2k (5) and PCTAIRE-2 (33). This suggests that serotype 3 reovirus may require cdc2-like kinase activity to post-translationally modify a viral protein in a similar fashion to the phosphorylation of varicella–zoster virus glycoprotein gI (84), Epstein-Barr virus EBNA-LP (43), hepatitis E virus ORF3 (86), and herpes simplex virus ICP0 (1) by cdc2. Alternatively, cdc2-like kinase activity may be responsible for alterations in cytoskeletal structure following serotype 3 reovirus infection. As discussed earlier, reovirus infection leads to disruption and reorganization of vimentin filaments into viral inclusions. Vimentin organization is regulated by cdc2-related kinase activity (10). PCTAIRE-2 kinase activity may regulate cytoskeletal protein distribution (33). Thus, alterations in PCTAIRE-2 and Trap (tudor repeat associator with PCTAIRE-2 (32)) following reovirus infection may lead to cytoskeletal changes necessary for viral inclusion formation. These

results suggest that the reovirus life cycle may require modulation of cdc2-like kinase activity.

In conclusion, reovirus infection alters a limited subset of transcripts encoding proteins that function to regulate cell cycle progression. Transcripts encoding proteins that function at the G_1 to S, G_2 to M, and mitotic spindle checkpoints were altered following serotype 3 reovirus infection. Of this group, genes encoding proteins regulating G_2 to M cell cycle transition were among the earliest to show changes in expression. This is consistent with our previous studies indicating that serotype 3 reovirus infection of HEK293 cells induces a G_2/M phase cell cycle arrest (63). We recently showed that G_2/M arrest results from inhibition of the key G_2 to M transition kinase cdc2 (62). Consistent with these findings, we found changes in expression of kinases, phosphatases, and GADD proteins that directly and indirectly influence cdc2 kinase activity. These results have enabled us to provide a hypothetical model for modulating cdc2 kinase activity in serotype 3 reovirus-infected cells.

ACKNOWLEDGMENTS

This work was supported by Public Health Service award AG14071 from the National Institute of Aging, Merit and REAP grants from the Department of Veterans Affairs, and a U.S. Army Medical Research Acquisition Activity Grant (DAMD17-98-1-8614) (K.L.T.), and an Infectious Diseases Society of America Young Investigator Award (R.D.B).

REFERENCES

1 **Advani, S. J., R. R. Weichselbaum, and B. Roizman.** 2000. The role of cdc2 in the expression of herpes simplex virus genes. Proc. Natl. Acad. Sci. U.S.A. **97**:10996-11001.

2 **Amon, A.** 1999. The spindle checkpoint. Curr. Opin. Genet. Dev. **9**:69-75.

3 **Babiss, L. E., R. B. Luftig, J. A. Weatherbee, R. R. Weihing, U. R. Ray, and B. N. Fields.** 1979. Reovirus serotypes 1 and 3 differ in their *in vitro* association with microtubules. J. Virol. **30**:863-874.

4 **Barton, E. S., J. C. Forrest, J. L. Connolly, J. D. Chappell, Y. Liu, F. J. Schnell, A. Nusrat, C. A. Parkos, and T. S. Dermody.** 2001. Junction adhesion molecule is a receptor for reovirus. Cell **104**:441-451.

5 **Best, J. L., D. H. Presky, R. A. Swerlick, D. K. Burns, and W. Chu.** 1995. Cloning of a full-length cDNA sequence encoding a cdc2-related protein kinase from human endothelial cells. Biochem. Biophys. Res. Commun. **208**:562-568.

6 **Brady, D. M. and K. G. Hardwick.** 2000. Complex formation between Mad1p, Bub1p and Bub3p is crucial for spindle checkpoint function. Curr. Biol. **10**:675-678.

7 **Ceruzzi, M. and A. J. Shatkin.** 1986. Expression of reovirus p14 in bacteria and identification in the cytoplasm of infected mouse L cells. Virology **153**:35-45.

8 **Chen, P. L., Y. C. Ueng, T. Durfee, K. C. Chen, T. Yang-Feng, and W. H. Lee.** 1995. Identification of a human homologue of yeast nuc2 which interacts with the retinoblastoma protein in a specific manner. Cell Growth Differ. **6**:199-210.

9 **Cheng, A., P. Kaldis, and M. J. Solomon.** 2000. Dephosphorylation of human cyclin-dependent kinases by protein phosphatase type 2C α and β 2 isoforms. J. Biol. Chem. **275**:34744-34749.

10 **Chou, Y. H., J. R. Bischoff, D. Beach, and R. D. Goldman.** 1990. Intermediate filament reorganization during mitosis is mediated by $p34^{cdc2}$ phosphorylation of vimentin. Cell **62**:1063-1071.

11 **Cimprich, K. A., T. B. Shin, C. T. Keith, and S. L. Schreiber.** 1996. cDNA cloning and gene mapping of a candidate human cell cycle checkpoint protein. Proc. Natl. Acad. Sci. U.S.A. **93**:2850-2855.

12 **Clarke, P. R., I. Hoffmann, G. Draetta, and E. Karsenti.** 1993. Dephosphorylation of cdc25-C by a type-2A protein phosphatase: specific regulation during the cell cycle in *Xenopus* egg extracts. Mol. Biol. Cell **4**:397-411.

13 **Connolly, J. L., S. E. Rodgers, P. Clarke, D. W. Ballard, L. D. Kerr, K. L. Tyler, and T. S. Dermody.** 2000. Reovirus-induced apoptosis requires activation of transcription factor NF-κB. J. Virol. **74**:2981-2989.

14 **Cox, D. C. and J. E. Shaw**. 1974. Inhibition of the initiation of cellular DNA synthesis after reovirus infection. J. Virol. **13**:760-761.

15 **Dales, S.** 1963. Association between the spindle apparatus and reovirus. Proc. Natl. Acad. Sci. U.S.A. **50**:268-275.

16 **Dermody, T. S., M. L. Nibert, R. Bassel-Duby, and B. N. Fields**. 1990. Sequence diversity in S1 genes and S1 translation products of 11 serotype 3 reovirus strains. J. Virol. **64**:4842-4850.

17 **Duncan, R., D. Horne, L. W. Cashdollar, W. K. Joklik, and P. W. Lee**. 1990. Identification of conserved domains in the cell attachment proteins of the three serotypes of reovirus. Virology **174**:399-409.

18 **Endl, E. and J. Gerdes**. 2000. The Ki-67 protein: fascinating forms and an unknown function. Exp. Cell Res. **257**:231-237.

19 **Ewen, M. E.** 2000. Where the cell cycle and histones meet. Genes Dev. **14**:2265-2270.

20 **Fajardo, E. and A. J. Shatkin**. 1990. Expression of the two reovirus S1 gene products in transfected mammalian cells. Virology **178**:223-231.

21 **Fode, C., C. Binkert, and J. W. Dennis**. 1996. Constitutive expression of murine Sak-a suppresses cell growth and induces multinucleation. Mol. Cell Biol. **16**:4665-4672.

22 **Furnari, B., N. Rhind, and P. Russell**. 1997. Cdc25 mitotic inducer targeted by chk1 DNA damage checkpoint kinase. Science **277**:1495-1497.

23 **Gaulton, G. N. and M. I. Greene** . 1989. Inhibition of cellular DNA synthesis by reovirus occurs through a receptor-linked signaling pathway that is mimicked by antiidiotypic, antireceptor antibody. J. Exp. Med. **169**:197-211.

24 **Gautier, J., J. Minshull, M. Lohka, M. Glotzer, T. Hunt, and J. L. Maller**. 1990. Cyclin is a component of maturation-promoting factor from *Xenopus*. Cell **60**:487-494.

25 **Glover, D. M., I. M. Hagan, and A. A. Tavares**. 1998. Polo-like kinases: a team that plays throughout mitosis. Genes Dev. **12**:3777-3787.

26 **Grana, X., J. Garriga, and X. Mayol**. 1998. Role of the retinoblastoma protein family, pRB, p107 and p130 in the negative control of cell growth. Oncogene **17**:3365-3383.

27 **Hand, R. and I. Tamm**. 1974. Initiation of DNA replication in mammalian cells and its inhibition by reovirus infection. J. Mol. Biol. **82**:175-183.

28 **Harkin, D. P., J. M. Bean, D. Miklos, Y. H. Song, V. B. Truong, C. Englert, F. C. Christians, L. W. Ellisen, S. Maheswaran, J. D. Oliner, and D. A. Haber**. 1999. Induction of GADD45 and JNK/SAPK-dependent apoptosis following inducible expression of BRCA1. Cell **97**:575-586.

29 **Harper, J. W.** 1997. Cyclin dependent kinase inhibitors. Cancer Surv. **29**:91-107.

30 **He, J., S. Choe, R. Walker, P. Di Marzio, D. O. Morgan, and N. R. Landau.** 1995. Human immunodeficiency virus type 1 viral protein R (vpr) arrests cells in the G_2 phase of the cell cycle by inhibiting $p34^{cdc2}$ activity. J. Virol. **69**:6705-6711.

31 **Herwig, S. and M. Strauss.** 1997. The retinoblastoma protein: a master regulator of cell cycle, differentiation and apoptosis. Eur. J. Biochem. **246**:581-601.

32 **Hirose, T., M. Kawabuchi, T. Tamaru, N. Okumura, K. Nagai, and M. Okada.** 2000. Identification of tudor repeat associator with PCTAIRE 2 (Trap). A novel protein that interacts with the N-terminal domain of PCTAIRE 2 in rat brain. Eur. J. Biochem. **267**:2113-2121.

33 **Hirose, T., T. Tamaru, N. Okumura, K. Nagai, and M. Okada.** 1997. PCTAIRE 2, a Cdc2-related serine/threonine kinase, is predominantly expressed in terminally differentiated neurons. Eur. J. Biochem. **249**:481-488.

34 **Hobbs, W. E. and N. A. DeLuca.** 1999. Perturbation of cell cycle progression and cellular gene expression as a function of herpes simplex virus ICP0. J. Virol. **73**:8245-8255.

35 **Hrimech, M., X. J. Yao, P. E. Branton, and E. A. Cohen.** 2000. Human immunodeficiency virus type 1 vpr-mediated G_2 cell cycle arrest: vpr interferes with cell cycle signaling cascades by interacting with the B subunit of serine/threonine protein phosphatase 2A. EMBO J. **19**:3956-3967.

36 **Hudson, J. W., L. Chen, C. Fode, C. Binkert, and J. W. Dennis**. 2000. Sak kinase gene structure and transcriptional regulation. Gene **241**:65-73.

37 **Iijima, M., Y. Kano, T. Nohno, and M. Namba**. 1996. Cloning of cDNA with possible transcription factor activity at the G_1-S phase transition in human fibroblast cell lines. Acta Med. Okayama **50**:73-77.

38 **Jackman, M. R. and J. N. Pines**. 1997. Cyclins and the G_2/M transition. Cancer Surv. **29**:47-73.

39 **Jin, S., H. Zhao, F. Fan, P. Blanck, W. Fan, A. B. Colchagie, A. J. Fornace, and Q. Zhan**. 2000. BRCA1 activation of the GADD45 promoter. Oncogene **19**:4050-4057.

40 **Kalitsis, P., E. Earle, K. J. Fowler, and K. H. Choo**. 2000. Bub3 gene disruption in mice reveals essential mitotic spindle checkpoint function during early embryogenesis. Genes Dev. **14**:2277-2282.

41 **Kastan, M. B., Q. Zhan, W. S. el Deiry, F. Carrier, T. Jacks, W. V. Walsh, B. S. Plunkett, B. Vogelstein, and A. J. Fornace**. 1992. A mammalian cell cycle checkpoint pathway utilizing p53 and GADD45 is defective in ataxia-telangiectasia. Cell **71**:587-597.

42 **Kinoshita, N., H. Ohkura, and M. Yanagida**. 1990. Distinct, essential roles of type 1 and 2A protein phosphatases in the control of the fission yeast cell division cycle. Cell **63**:405-415.

43 **Kitay, M. K. and D. T. Rowe.** 1996. Cell cycle stage-specific phosphorylation of the Epstein-Barr virus immortalization protein EBNA-LP. J. Virol. **70**:7885-7893.

44 **Kumada, K., S. Su, M. Yanagida, and T. Toda.** 1995. Fission yeast TPR-family protein nuc2 is required for G_1-arrest upon nitrogen starvation and is an inhibitor of septum formation. J. Cell Sci. **108 (Pt 3)**:895-905.

45 **Lee, T. H., M. J. Solomon, M. C. Mumby, and M. W. Kirschner.** 1991. INH, a negative regulator of MPF, is a form of protein phosphatase 2A. Cell **64**:415-423.

46 **Li, S., N. S. Ting, L. Zheng, P. L. Chen, Y. Ziv, Y. Shiloh, E. Y. Lee, and W. H. Lee.** 2000. Functional link of BRCA1 and ataxia telangiectasia gene product in DNA damage response. Nature **406**:210-215.

47 **Lopez-Girona, A., B. Furnari, O. Mondesert, and P. Russell.** 1999. Nuclear localization of Cdc25 is regulated by DNA damage and a 14-3-3 protein. Nature **397**:172-175.

48 **Masuda, M., Y. Nagai, N. Oshima, K. Tanaka, H. Murakami, H. Igarashi, and H. Okayama.** 2000. Genetic studies with the fission yeast *Schizosaccharomyces pombe* suggest involvement of wee1, ppa2, and rad24 in induction of cell cycle arrest by human immunodeficiency virus type 1 vpr. J. Virol. **74**:2636-2646.

49 **Matsumoto-Taniura, N., F. Pirollet, R. Monroe, L. Gerace, and J. M. Westendorf.** 1996. Identification of novel M phase phosphoproteins by expression cloning. Mol. Biol. Cell **7**:1455-1469.

50 **McCright, B., A. M. Rivers, S. Audlin, and D. M. Virshup**. 1996. The B56 family of protein phosphatase 2A (PP2A) regulatory subunits encodes differentiation-induced phosphoproteins that target PP2A to both nucleus and cytoplasm. J. Biol. Chem. **271**:22081-22089.

51 **Moreno, C. S., S. Park, K. Nelson, D. Ashby, F. Hubalek, W. S. Lane, and D. C. Pallas**. 2000. WD40 repeat proteins striatin and S/G2 nuclear autoantigen are members of a novel family of calmodulin-binding proteins that associate with protein phosphatase 2A. J. Biol. Chem. **275**:5257-5263.

52 **Muro, Y., E. K. Chan, G. Landberg, and E. M. Tan**. 1995. A cell-cycle nuclear autoantigen containing WD-40 motifs expressed mainly in S and G_2 phase cells. Biochem. Biophys. Res. Commun. **207**:1029-1037.

53 **Nibert, M. L., L. A. Schiff, and B. N. Fields**. 1996. Reoviruses and their replication, p. 1557-1596. *In* B. N. Fields, D. M. Knipe, and P. M. Howley (eds.), Fields Virology. Lipincott-Raven Press, NY.

54 **Nigg, E. A.** 1998. Polo-like kinases: positive regulators of cell division from start to finish. Curr. Opin. Cell Biol. **10**:776-783.

55 **Nurse, P.** 1990. Universal control mechanism regulating onset of M-phase. Nature **344**:503-508.

56 **O'Connell, M. J., J. M. Raleigh, H. M. Verkade, and P. Nurse**. 1997. Chk1 is a wee1 kinase in the G_2 DNA damage checkpoint inhibiting cdc2 by Y15 phosphorylation. EMBO J. **16**:545-554.

57 **O'Connor, P. M.** 1997. Mammalian G_1 and G_2 phase checkpoints. Cancer Surv. **29**:151-182.

58 **Op, D. B. and P. Caillet-Fauquet**. 1997. Viruses and the cell cycle. Prog. Cell Cycle Res. **3**:1-19.

59 **Page, A. M. and P. Hieter**. 1997. The anaphase promoting complex. Cancer Surv. **29**:133-150.

60 **Parker, L. L., S. Atherton-Fessler, and H. Piwnica-Worms**. 1992. $p107^{wee1}$ is a dual-specificity kinase that phosphorylates $p34^{cdc2}$ on tyrosine 15. Proc. Natl. Acad. Sci. U. S. A **89**:2917-2921.

61 **Peng, C. Y., P. R. Graves, R. S. Thoma, Z. Wu, A. S. Shaw, and H. Piwnica-Worms**. 1997. Mitotic and G_2 checkpoint control: regulation of 14-3-3 protein binding by phosphorylation of Cdc25C on serine-216. Science **277**:1501-1505.

62 **Poggioli, G. J., T. S. Dermody, and K. L. Tyler**. 2001. Reovirus-induced σ1s dependent G_2/M cell cycle arrest results from inhibition of $p34^{cdc2}$. J. Virol. **Accepted**.

63 **Poggioli, G. J., C. Keefer, J. L. Connolly, T. S. Dermody, and K. L. Tyler**. 2000. Reovirus-induced G_2/M cell cycle arrest requires σ1s and occurs in the absence of apoptosis. J. Virol. **74**:9562-9570.

64 **Re, F., D. Braaten, E. K. Franke, and J. Luban.** 1995. Human immunodeficiency virus type 1 vpr arrests the cell cycle in G_2 by inhibiting the activation of $p34^{cdc2}$-cyclin B. J. Virol. **69**:6859-6864.

65 **Resto, V. A., O. L. Caballero, M. R. Buta, W. H. Westra, L. Wu, J. M. Westendorf, J. Jen, P. Hieter, and D. Sidransky.** 2000. A putative oncogenic role for MPP11 in head and neck squamous cell cancer. Cancer Res. **60**:5529-5535.

66 **Roberts, B. T., K. A. Farr, and M. A. Hoyt.** 1994. The *Saccharomyces cerevisiae* checkpoint gene BUB1 encodes a novel protein kinase. Mol. Cell Biol. **14**:8282-8291.

67 **Rodgers, S. E., J. L. Connolly, J. D. Chappell, and T. S. Dermody.** 1998. Reovirus growth in cell culture does not require the full complement of viral proteins: identification of a σ1s-null mutant. J. Virol. **72**:8597-8604.

68 **Roner, M. R. and D. C. Cox.** 1985. Cellular integrity is required for inhibition of initiation of cellular DNA synthesis by reovirus type 3. J. Virol. **53**:350-359.

69 **Sanchez, Y., C. Wong, R. S. Thoma, R. Richman, Z. Wu, H. Piwnica-Worms, and S. J. Elledge.** 1997. Conservation of the Chk1 checkpoint pathway in mammals: linkage of DNA damage to Cdk regulation through Cdc25. Science **277**:1497-1501.

70 **Saragovi, H. U., A. Bhandoola, M. M. Lemercier, G. K. Akbar, and M. I. Greene**. 1995. A receptor that subserves reovirus binding can inhibit lymphocyte proliferation triggered by mitogenic signals. DNA Cell Biol. **14**:653-664.

71 **Saragovi, H. U., N. Rebai, G. M. Di Guglielmo, R. Macleod, J. Sheng, D. H. Rubin, and M. I. Greene**. 1999. A G_1 cell cycle arrest induced by ligands of the reovirus type 3 receptor is secondary to inactivation of $p21^{ras}$ and mitogen-activated protein kinase. DNA Cell Biol. **18**:763-770.

72 **Saragovi, H. U., N. Rebai, E. Roux, M. Gagnon, X. Zhang, B. Robaire, J. Bromberg, and M. I. Greene**. 1998. Signal transduction and antiproliferative function of the mammalian receptor for type 3 reovirus. Curr. Top. Microbiol. Immunol. **233 Reovir.i**:155-166.

73 **Scholzen, T. and J. Gerdes**. 2000. The Ki-67 protein: from the known and the unknown. J. Cell Physiol **182**:311-322.

74 **Sharpe, A. H., L. B. Chen, and B. N. Fields**. 1982. The interaction of mammalian reoviruses with the cytoskeleton of monkey kidney CV-1 cells. Virology **120**:399-411.

75 **Sharpe, A. H. and B. N. Fields**. 1981. Reovirus inhibition of cellular DNA synthesis: role of the S1 gene. J. Virol. **38**:389-392.

76 **Solomon, M. J., M. Glotzer, T. H. Lee, M. Philippe, and M. W. Kirschner**. 1990. Cyclin activation of $p34^{cdc2}$. Cell **63**:1013-1024.

77 **Starr, D. A., R. Saffery, Z. Li, A. E. Simpson, K. H. Choo, T. J. Yen, and M. L. Goldberg**. 2000. HZwint-1, a novel human kinetochore component that interacts with HZW10. J. Cell Sci. **113 (Pt 11)**:1939-1950.

78 **Straight, A. F.** 1997. Cell cycle: checkpoint proteins and kinetochores. Curr. Biol. **7** :R613-R616.

79 **Taylor, S. S., E. Ha, and F. McKeon**. 1998. The human homologue of Bub3 is required for kinetochore localization of Bub1 and a Mad3/Bub1-related protein kinase. J. Cell Biol. **142**:1-11.

80 **Tyler, K. L. and B. N. Fields**. 1996. Reoviruses, p. 1597-1623. *In* B. N. Fields, D. M. Knipe, and P. M. Howley (eds.), Fields Virology. Lipincott-Raven Press, NY.

81 **Tyler, K. L., D. A. McPhee, and B. N. Fields**. 1986. Distinct pathways of viral spread in the host determined by reovirus S1 gene segment. Science **233**:770-774.

82 **Tyler, K. L., M. K. Squier, A. L. Brown, B. Pike, D. Willis, S. M. Oberhaus, T. S. Dermody, and J. J. Cohen**. 1996. Linkage between reovirus-induced apoptosis and inhibition of cellular DNA synthesis: role of the S1 and M2 genes. J. Virol. **70**:7984-7991.

83 **Wang, X. W., Q. Zhan, J. D. Coursen, M. A. Khan, H. U. Kontny, L. Yu, M. C. Hollander, P. M. O'Connor, A. J. Fornace, Jr., and C. C. Harris**. 1999. GADD45 induction of a G_2/M cell cycle checkpoint. Proc. Natl. Acad. Sci. U.S.A. **96**:3706-3711.

84 **Ye, M., K. M. Duus, J. Peng, D. H. Price, and C. Grose.** 1999. Varicella-zoster virus Fc receptor component gI is phosphorylated on its endodomain by a cyclin-dependent kinase. J. Virol. **73**:1320-1330.

85 **Yoshida, Y., S. Matsuda, N. Ikematsu, J. Kawamura-Tsuzuku, J. Inazawa, H. Umemori, and T. Yamamoto.** 1998. ANA, a novel member of Tob/BTG1 family, is expressed in the ventricular zone of the developing central nervous system. Oncogene **16**:2687-2693.

86 **Zafrullah, M., M. H. Ozdener, S. K. Panda, and S. Jameel.** 1997. The ORF3 protein of hepatitis E virus is a phosphoprotein that associates with the cytoskeleton. J. Virol. **71**:9045-9053.

87 **Zhan, Q., M. J. Antinore, X. W. Wang, F. Carrier, M. L. Smith, C. C. Harris, and A. J. Fornace, Jr.** 1999. Association with cdc2 and inhibition of cdc2/cyclin B1 kinase activity by the p53-regulated protein GADD45. Oncogene **18**:2892-2900.

FIGURE LEGENDS

Figure 1. wee1, chk1 and GADD45 transcription is increased following reovirus infection. HEK293 cells were mock-infected or infected with T3A at an MOI of 100 PFU per cell. mRNA was collected at 12 and 24 h post-infection, and analyzed for wee1 (A), chk1 (B), and GADD45 (C) transcription by RT-PCR to confirm microarray analyses. β-actin was used as a control in each RT-PCR. Results for wee1 and chk1 are representative of 4 and 3 independent experiments, respectively.

Figure 2. Proposed model for serotype 3 reovirus-induced G_2 to M transition arrest. cdc2 kinase activity is required for entry into mitosis. Active cdc2 kinase is complexed with cyclin B and dephosphorylated at Thr14/Tyr15. Following reovirus infection cdc2 is inhibited, in part, by phosphorylation. The increase in phosphorylated cdc2 may be due to upregulation of the kinases chk1 and wee1 and/or localization of the phosphatase PP2A to the nucleus, which can inhibit the cdc2 activating phosphatase cdc25C. cdc2 kinase activity may also be inhibited by dissociation of cyclin B by GADD45. Arrows indicate activation and blunted lines indicate inhibition.

Table 1. Reovirus-induced transcriptional alterations in genes known to regulate the cell cycle[a]

Gene	Accession Number[b]	Fold Change in Expression Post-Infection (h)[c,d]		
		T3A		T1L
		12	24	24
G_1-S Checkpoint				
N-Ras	X02751		2.1 ± 0.2	
cyclin E	M73812		-2.8 ± 0.1	
cyclin E2	AF091433		2.1 ± 0.2	
PP2C-α	AF070670		5.3 ± 0.4	
C-1[e]	U41816		2.2 ± 0.1	
ANA[f]	D64110		2.9 ± 0.1	2.5 ± 0.1
E2F6	AF041381			2.1 ± 0.1
Histone H1	X03473[g]		2.7 ± 0.1 3.1 ± 0.2	2.3 ± 0.2 2.1 ± 0.2
Histone H2A	L19779[h] AI885852		2.0 ± 0.1 2.2 ± 0.1	
Histone H2B	X00088[h] Z80782 Z80780 Z80779 AA873858		2.0 ± 0.1 2.8 ± 0.1 3.1 ± 0.3 3.2 ± 0.2 5.8 ± 0.6	
Histone H4	X00038	4.7 ± 0.5		
G_2-M Checkpoint				
wee-1	U10564[h] X62048		2.4 ± 0.1 2.5 ± 0.1	1.9 ± 0.1[i] 2.0 ± 0.1
chk-1	AF016582		3.2 ± 0.1	
GADD45	M60974	3.3 ± 0.2	4.9 ± 0.1	4.4 ± 0.1
B56-β subunit of PP2A	L42374	-3.1 ± 0.3		
SG2NA	U17989		2.4 ± 0.2	2.5 ± 0.2
FRP1	U49844		-2.1 ± 0.1	
PCTAIRE-2	X66360		2.6 ± 0.1	
Trap	AB025254[j]		2.0 ± 0.3	
C-2K	X80230	-2.1 ± 0.1		
SAK	Y13115		3.8 ± 0.5	
Ki-67 antigen[k]	X65550	-1.9 ± 0.0	-2.3 ± 0.2	
Mitotic Spindle Checkpoint				
BUB-3	AF047472		2.2 ± 0.1	
MPP11	X98260		2.0 ± 0.1	
HZWINT1	AF067656		2.6 ± 0.0	
Nuc-2[l]	S78234		2.1 ± 0.2	

[a] A blank cell represents no change, and genes that are not addressed in the text are referenced in the table legend.
[b] Corresponds to the nucleotide accession number assigned to the Affymetrix probe set on the U95A microarray.
[c] A negative number indicates that the transcript was downregulated.
[d] ± indicates the standard error of the mean from two independent experiments.
[e] A possible transcription factor with activity at the G_1 to S transition (37).
[f] Overexpression leads to retardation of cell cycle progression trough the G_1 phase (85).
[g] Represented twice on the U95A microarray.
[h] Represented multiple times on the U95A microarray.
[i] Gene was not defined as upregulated as defined in the Materials and Methods since it was found to be increased in 3 of 4 analyses.
[j] Affymetrix assigned GenBank accession number refers to partial coding sequence for Trap. Complete coding sequence is at AB030644.
[k] General marker of proliferation and may be regulated by cdc2 (reviewed in 18, 73).
[l] An APC component (reviewed in 59) and may also play a role in G_1 to S transition (8, 44).

Table 2. Nucleotide accession numbers for genes that were not changed following T3A or T1L infection and mentioned in the text

Gene	Accession number[a]
ATM	U26455
B-myb	X13293
BUB1	AF053305
cdc25C	M34065
cdc6	U77949
cdk4	U37022
cyclin A	X51688, U66838[b]
cyclin B	M25753
cyclin D1	M64349
cyclin D2	X68452
cyclin D3	M92287
Dihydrofolate reductase	J00146, J00140, J00139[b]
E2F1	U47677, M96577[b]
E2F2	L22846
E2F4	S75174
E2F5	U15642
E2F6	AF041381
Ha-ras	J00277
MAD2	AJ000186, U65410[b]
MAD3	AF053306
pRb	M15400, L49219, L49229, L41913, L41870[b]
p107	L14812
p130	X74594, X76061[b]
$p15^{INK4b}$	AF004819, L36844[b]
$p16^{INK4a}$	U26727
$p19^{INK4d}$	U40343
$p21^{WAF1/CIP1}$	U03106
$p27^{KIP1}$	U10906
$p57^{KIP2}$	D64137, U22398[b]
thymidine kinase	K02581, M15205, U80628[b]

[a] Corresponds to the nucleotide accession number assigned to an Affymetrix probe set on the U95A microarray.

[b] Represented multiple times on the U95A microarray.

A

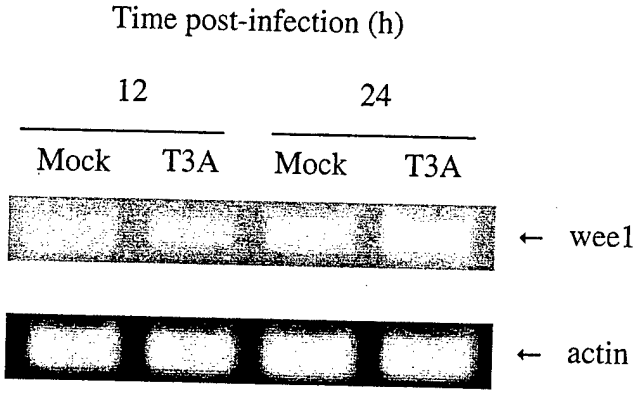
Time post-infection (h)
12
24
Mock
T3A
Mock
T3A
← wee1
← actin

B

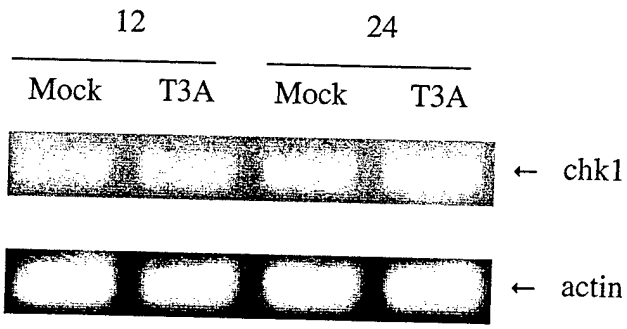
Time post-infection (h)
12
24
Mock
T3A
Mock
T3A
← chk1
← actin

C

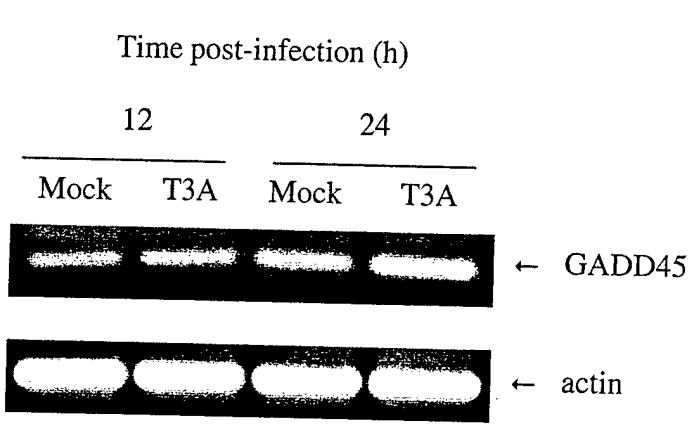
Time post-infection (h)
12
24
Mock
T3A
Mock
T3A
← GADD45
← actin

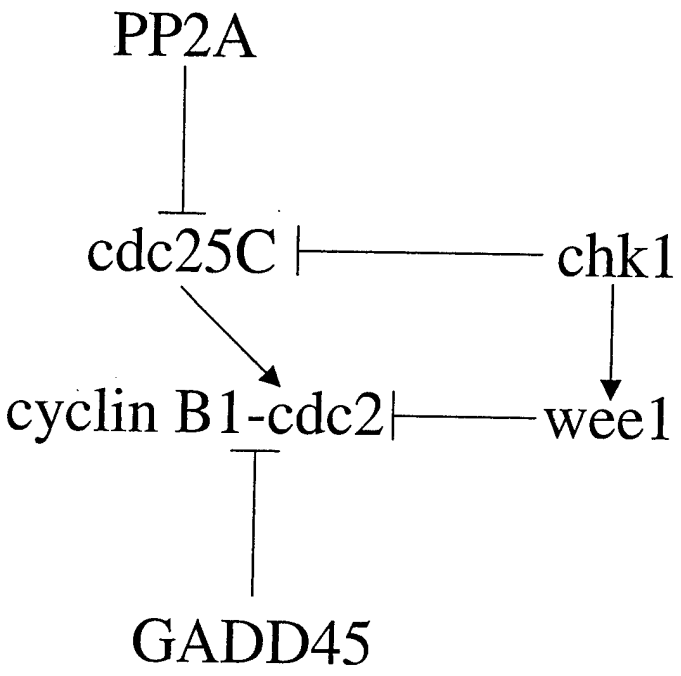
PP2A
cdc25C
chk1
cyclin B1-cdc2
wee1
GADD45